LEABHARLANN CHOLÁISTE NA TRÍONÓIDE, BAILE ÁTHA CLIATH | TRINITY COLLEGE LIBRARY DUBLIN
Ollscoil Átha Cliath | The University of Dublin

Terms and Conditions of Use of Digitised Theses from Trinity College Library Dublin

Copyright statement

All material supplied by Trinity College Library is protected by copyright (under the Copyright and Related Rights Act, 2000 as amended) and other relevant Intellectual Property Rights. By accessing and using a Digitised Thesis from Trinity College Library you acknowledge that all Intellectual Property Rights in any Works supplied are the sole and exclusive property of the copyright and/or other IPR holder. Specific copyright holders may not be explicitly identified. Use of materials from other sources within a thesis should not be construed as a claim over them.

A non-exclusive, non-transferable licence is hereby granted to those using or reproducing, in whole or in part, the material for valid purposes, providing the copyright owners are acknowledged using the normal conventions. Where specific permission to use material is required, this is identified and such permission must be sought from the copyright holder or agency cited.

Liability statement

By using a Digitised Thesis, I accept that Trinity College Dublin bears no legal responsibility for the accuracy, legality or comprehensiveness of materials contained within the thesis, and that Trinity College Dublin accepts no liability for indirect, consequential, or incidental, damages or losses arising from use of the thesis for whatever reason. Information located in a thesis may be subject to specific use constraints, details of which may not be explicitly described. It is the responsibility of potential and actual users to be aware of such constraints and to abide by them. By making use of material from a digitised thesis, you accept these copyright and disclaimer provisions. Where it is brought to the attention of Trinity College Library that there may be a breach of copyright or other restraint, it is the policy to withdraw or take down access to a thesis while the issue is being resolved.

Access Agreement

By using a Digitised Thesis from Trinity College Library you are bound by the following Terms & Conditions. Please read them carefully.

I have read and I understand the following statement: All material supplied via a Digitised Thesis from Trinity College Library is protected by copyright and other intellectual property rights, and duplication or sale of all or part of any of a thesis is not permitted, except that material may be duplicated by you for your research use or for educational purposes in electronic or print form providing the copyright owners are acknowledged using the normal conventions. You must obtain permission for any other use. Electronic or print copies may not be offered, whether for sale or otherwise to anyone. This copy has been supplied on the understanding that it is copyright material and that no quotation from the thesis may be published without proper acknowledgement.

The Role of the *Salmonella* PagN Protein in Adhesion and Invasion

Samantha E. Paré

2015

Declaration

I declare that this thesis has not been submitted as an exercise for a degree at this or any other university and it is entirely my own work.
I agree to deposit this thesis in the University's open access institutional repository or allow the library to do so on my behalf, subject to Irish Copyright Legislation and Trinity College Library conditions of use and acknowledgement.

Signed,
Samantha Pare
10 June, 2015

10/06/15

THESIS
10869

50564197

PhD in Medi

TRINITY COLLEGE
0 6 OCT 2015
LIBRARY DUBLIN
Thesis 10869

Summary

Salmonella, an important genus of Gram-negative enteric bacteria, is the causative agent of many different diseases including Typhoid Fever and Gastroenteritis. *Salmonella* utilises multiple methods of invading mammalian cells, the best characterised is the Type Three Secretion System (T3SS). In addition to the T3SS, *Salmonella* express a multitude of fimbrial and non-fimbrial adhesins to facilitate attachment to and invasion of the epithelial layer lining the intestinal mucosa.

A high-throughput fluorescent assay was developed and optimised for use in determining bacterial adherence to and invasion of mammalian cells. Bacteria were rendered fluorescent using GFP expressed from plasmid pCM01. Mammalian cells and extracellular bacteria were distinguished using nucleic acid dyes and antibody labelling.

Previously, our laboratory has characterised the PagN outer membrane protein of *Salmonella* Typhimurium. PagN was discovered in *S.* Typhi in 2011 and implicated as a bacterial adhesin and potential vaccine candidate (129). The structure of the *S.* Typhi PagN ($PagN_{STY}$) was determined and its function compared with that of the *S.* Typhimurium protein ($PagN_{STM}$).

The main aim of this study was to further characterise the structure and function of the $PagN_{STM}$ protein. A *pagN*-constitutive expression plasmid was created for ease of use. The *pagN*$_{STM}$ gene was cloned under the control of the P_{hek} promoter to create plasmid pSP8. The homologous Hek protein of *Escherichia coli* has been shown to mediate autoaggregation, however this was not seen for $PagN_{STM}$-expressing bacteria (103, 203). Autoaggregation was measured for bacteria expressing either Hek or $PagN_{STM}$ to determine whether the phenotype was due to overexpression via the P_{hek} promoter or through the action of the protein itself. $PagN_{STM}$-expressing bacteria were unable to autoaggregate above levels seen by the vector plasmid. $PagN_{STM}$-mediated attachment to and invasion of the CHO-K1 epithelial cell line was also abolished for bacteria expressing $PagN_{STM}$ using the constitutive expression pSP8 plasmid.

The four extracellular loops of the PagN protein have been demonstrated as necessary to mediate invasion of epithelial cells (204). These mutants were tested for their adherence to and invasion of CHO-K1 and HT-29 epithelial cells in a high-throughput manner. Deletion of any one of the extracellular loops led to a complete abolishment of association with either cell type. The loop-deletions were created at the membrane-surface interface, and this may affect the ability of the protein to mediate attachment. New, smaller loop-deletion mutants were created to further

determine the role they play in mediating invasion of epithelial cells. Again, each of these loop-deletion mutants was unable to promote adherence to or invasion of the CHO-K1 and HT-29 cell lines.

As PagN shares significant sequence homology with the Hek protein, and research has indicated that specific charged residues in Loop two of Hek are involved in invasion (101), the conserved residues in PagN (R71, D75, K77, and D81) were mutated to a neutral alanine residue. High-throughput invasion assays were performed to determine the ability of the mutant forms of PagN to promote adhesion and invasion of CHO-K1 and HT-29 cells. The R71A mutant showed a statistically significant increase in both adhesion and invasion of CHO-K1 cells, and this was not seen for HT-29 cells. There was no statistically significant difference seen for any of the other mutant forms of the protein.

Deletion of the *pagN* gene in *S.* Typhimurium has been shown to affect bacterial adhesion/invasion (160, 205, 259, 357). Strains of wild-type *S.* Typhimurium and strains lacking the *pagN* gene were tested for adherence to and invasion of CHO-K1 and HT-29 cells. Bacteria grown in L-broth did not show any difference in adhesion/invasion of either cell line upon the loss of *pagN.* The *pagN* gene is under the control of the PhoP/Q two-component system. Bacteria were grown overnight in PhoP-inducing media and the high-throughput assay was repeated. Again, no differences were seen in cell association or invasion of either cell line.

Finally, PagN interacts with heparan sulphate proteoglycans expressed on the surface of mammalian cells (204). In human cells, there are two xylosyltransferases, XT-I and XT-II, present to catalyse the rate-limiting step in proteoglycan biosynthesis. XT-II is expressed in many different cell-types while XT-I is less expressed. siRNA knockdown methodology was used to decrease expression of *xylt-2* in the human HT-29 colonic cell line. A high-throughput assay was performed to investigate PagN-mediated invasion of these cells. There was no difference in invasion of siRNA-knockdown as compared with those cells exposed to a scrambled siRNA.

Acknowledgements

First and foremost, I would like to thank Stephen not only for the opportunity to study with him for the past three years, but also for all of the guidance he has given me. I have learned a lot the last few years and have grown and developed as an independent researcher. Thank you for everything Stephen.

To Clodagh, thank you so much for being my lab-partner in crime. Thank you for listening to me whine when things weren't going well and for helping to celebrate my successes. You were always available to help me troubleshoot, or even to just listen to me as I tried to work things out for myself. Helen, I honestly can't thank you enough. You've play such a massive role in helping me through my PhD from start to finish. Thank you for the countless hours you spent proof-reading my thesis and for all of the times you were there to buoy my confidence when things weren't going well for me. And to all of the other members of SPD: Míchael, Geraldine, Emma, Katie and everyone else, thank you for both the helpful chats and the necessary distractions. To Mark, thank you for sharing all of your expertise in siRNA knockdowns and qPCR. Thank you for the chats, troubleshooting sessions, and of course the reagents!

I'd like to thank my family (and Liz) for all of the help and support they've given me over the years. Mum and Dad have pushed me to never give up and to constantly challenge myself. Thank you both for everything that you've done for me. Finally I'd like to thank Mary, without whom I would have lost my mind and subsisted on a diet of tears and pizza for the last 4 months. Thank you for always being a shoulder to cry on, an ear to bend, and a partner in every sense of the word. Thank you for all of the support you've given me from the start of my PhD to the finish. You can have 10 % of my doctorate.

Table of Contents

List of Figures

List of Tables

List of Abbreviations

Abbreviation	Full Name
ANOVA	Analysis of Variance
ATc	Anhydrotetracycline
Car	Carbenecillin
Cm	Cloramphenicol
CHO-K1	Chinese hamster ovary cells
CS	Centisome
DMEM	Dulbecco's modified Eagle medium
DMSO	N,N-dimethylsulphoxide
EDTA	Ethylenediaminetetraacetic acid
GAPDH	Glyceraldehyde-3-phosphate dehydrogenase
GFP	Green fluorescent protein
GPA	Gentamicin protection assay
GPI	Glycosylphosphatidylinositol
HCA	High content assay
IPTG	Isopropyl β-D-1-thiogalactopyranoside
LB	L-Broth
LPS	Lipopolysaccharide
NMR	Nuclear magnetic resonance
OD	Optical density
PBS	Phospho-buffered saline
PIPES	Piperazine-1,4-bis(2-ethansulphonic acid)
PVDF	Polyvinylidene difluoride
qRT-PCR	Quantitative real-time PCR
SCV	*Salmonella* containing vacuole
SDS	Sodium dodecylsulphate
SDS-PAGE	Sodium dodecylsulphate – polyacrylamide gel electrophoresis
siRNA	Small-interfering RNA
SPI	*Salmonella* pathogenicity island
TBE	Tris-borate EDTA buffer
X-gal	5-bromo-4-chloro-3-indoyl-β-D-galactoside
XT-I	Xylosyltransferase-I
XT-II	Xylosyltransferase-II

Chapter 1 Introduction

1.1 *Salmonella*: an introduction

The genus *Salmonella*, a close relative of the *Escherichiae*, is comprised of Gram-negative, pathogenic, rod-shaped and motile bacteria of the family *Enterobacteriaceae*. In 1885, the genus *Salmonella* was discovered by Daniel Elmer Salmon and his assistant Theobald Smith in their search for the causative agent of common hog cholera. Strains were originally differentiated based on their reaction to sera, each new serotype corresponding to a new species. It is now generally accepted that the genus *Salmonella* is divided into two species, *Salmonella bongori* and *Salmonella enterica*. *S. enterica* can be further divided into 6 subspecies comprised of numerous serovars (173, 333).

The species *S. bongori* is considered to be phylogenetically older than *S. enterica* and is most commonly associated with cold-blooded vertebrates in the environment. *S. enterica* are capable of infecting a range of animal hosts including poultry, cattle, pigs, mice and humans (264). Almost all *Salmonella* organisms that cause disease in humans and domestic animals belong to *S. enterica* subspecies *enterica* (I) (107, 206). *Salmonella enterica* serovar Typhimurium (hereafter referred to as *S.* Typhimurium) is a facultative anaerobe and is distinguishable from other enteric bacteria on the basis of its biochemical properties. *S.* Typhimurium is distinguishable from *Escherichia coli* and the *Shigellae* as it can utilise citrate as a carbon source, is urease negative and unable to metabolise lactose (320). Lack of lysine decarboxylase production is also characteristic of the genus *Salmonella*.

Salmonella are of importance as an on-going concern in world-wide public health services, due to the emergence of antimicrobial drug resistance mechanisms (60, 98, 347). *Salmonella* have also served as a

paradigm for the study of the mechanisms of bacterial pathogenesis. Since the turn of the millennium, the genomes of multiple *S.* Typhimurium strains and *S.* Typhi strains including *S.* Typhimurium LT2 and *S.* Typhi CT18 have been sequenced (236, 267).

1.2 Salmonellosis: the key features

Salmonellosis is a major public health burden representing a sizeable cost to society in both developing and developed nations (224, 301). The principle diseases associated with *Salmonella* infection are typhoid fever and gastroenteritis. *Salmonella enterica* serovars Typhi and Paratyphi, are exclusively human pathogens and are the causative agents of Typhoid Fever. *S.* Typhi and *S.* Paratyphi are prevalent in developing countries and are responsible for more than 21 million illnesses per year and more than 200,000 deaths worldwide (69). The clinical manifestations of typhoid include fever, headache, abdominal pain, and transient diarrhoea or constipation. Infection can produce fatal respiratory, hepatic, spleen and/or neurological damage (43, 326). Without treatment, the mortality is 10-20% decreasing to <1% among patients treated with antibiotics (264, 268).

Salmonella enterica serovars Typhimurium and Enteritidis are the leading causes of gastroenteritis in the developing and the developed world. It is estimated that there are more than 94 million cases of non-typhoidal salmonellosis (NTS) each year; of these, 155,000 people will die (224). In developing countries, children and HIV-infected individuals experiencing NTS are also susceptible to septicaemia with a fatality rate of greater than 25% (173). Initial symptoms include nausea and vomiting, which are followed by abdominal pain and diarrhoea. The nature and severity of the disease is largely dependent on the *Salmonella* serovar and host species involved (77).

1.3 *Salmonella* Pathogenesis

Salmonellae are normally ingested in contaminated food and/or drinking water. The bacteria can withstand the drastic change in temperature and pH between the gut and the environment. As *Salmonella* pass through the digestive system, they are exposed to environmental stresses such as osmotic shock, oxygen starvation, and bile salts produced by the liver. As the immune system targets extracellular bacteria for degradation, it is imperative that *Salmonella* spp. invade the epithelial mucosa to evade detection. The bacteria have evolved several mechanisms for attachment to epithelial cells including numerous fimbriae (18), outer membrane proteins, such as Rck (156, 158), and OmpD (149), and a type three secretion system encoded on the *Salmonella* pathogenicity island-1 (SPI-1). The bacteria that pass through the epithelial cells lining the lumen, are phagocytosed by immune cells such as macrophages, dendritic cells, neutrophils, monocytes, and B and T cells (359). Within these immune cells, bacteria experience a number of conditions such as acid pH, reactive oxygen species, and limiting amounts of magnesium, iron, and phosphate. A schematic of *Salmonella* pathogenesis can be seen in Fig. 1.1.

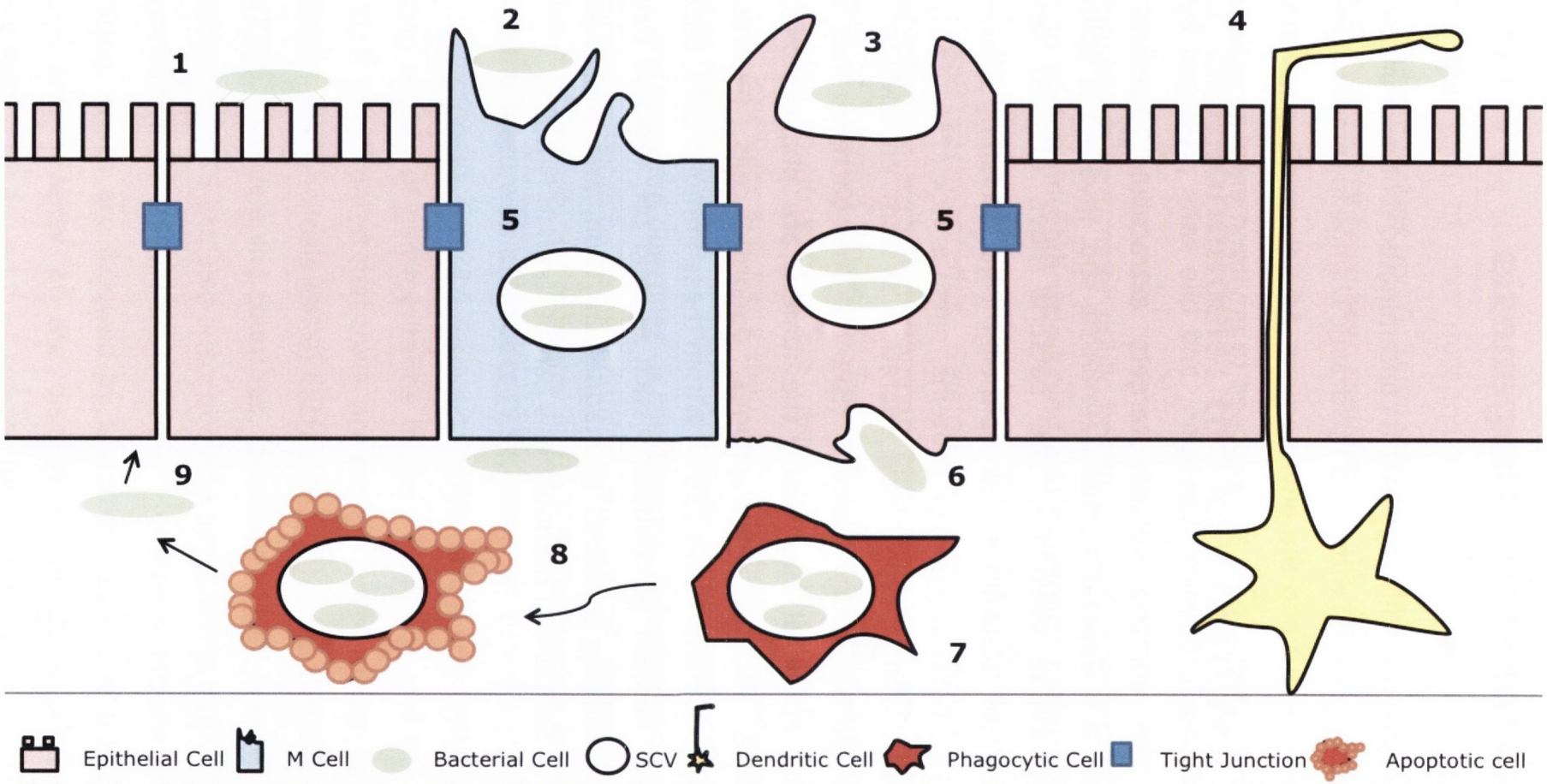

FIG. 1.1. *Salmonella* invasion of epithelial cells. *S.* Typhimurium cross the epithelial barrier by first adhering to the cells (1) and inducing actin polymerization, membrane ruffling and uptake (3). Once inside the epithelial cells, *Salmonella* are contained within *Salmonella* containing vacuoles (SCVs) (5). The bacteria are able to escape the vacuole and the cell (6). Professional phagocytic cells such as macrophages engulf the bacteria (7), however, *Salmonella* are able to induce apoptosis (8) and invade the monolayer from the basolateral surface (9). *Salmonella* are also able to invade M cells which sample the gut environment (2). Dendritic cells also disrupt tight junctions to capture bacteria (4).

1.4 Genetic Virulence Determinants of *Salmonella*

In order to facilitate bacterial invasion as discussed above, *Salmonella* employ many different virulence strategies to interact with host innate and acquired immune responses. The majority of the genes involved in pathogenesis are located within highly conserved laterally acquired pathogenicity islands termed *Salmonella* pathogenicity islands (SPIs). Other genes are located on a virulence plasmid pSLT or within the chromosome. Thus far, five SPIs (SPI-1 to SPI-5) along with the *spv* operon located on the pSLT plasmid, and a number of adhesins, flagella, and factors contributing to biofilm development have been clearly implicated in *S.* Typhimurium virulence (61, 181, 228).

1.4.1 SPI-1

The SPI-1 locus, the best characterised of the SPIs, is ~40-kb in size and is located at centisome (cs) 63 (228). SPI-1 has an overall G+C content of 42% and is flanked by *flhA* and *mutS*. More than 35 genes are contained within SPI-1 (Fig. 1.2) (95). SPI-1 forms a coordinated unit involved in promoting bacterial uptake within epithelial cells. Contained within SPI-1, are all of the genes necessary to form a functional type three secretion system (T3SS) apparatus (Section 1.5.6.), several effector proteins, and its cognate regulators, HilA, HilC, HilD, and InvF (95). The *prg/org* and *inv/spa* operons encode the needle complex of the T3SS, while the *sic/sip* operons encode the effector proteins and the translocon. Other injected effectors are encoded elsewhere on the chromosome. For example, SopB is encoded within SPI-5 at 25 cs (354) and the gene encoding SopE is located

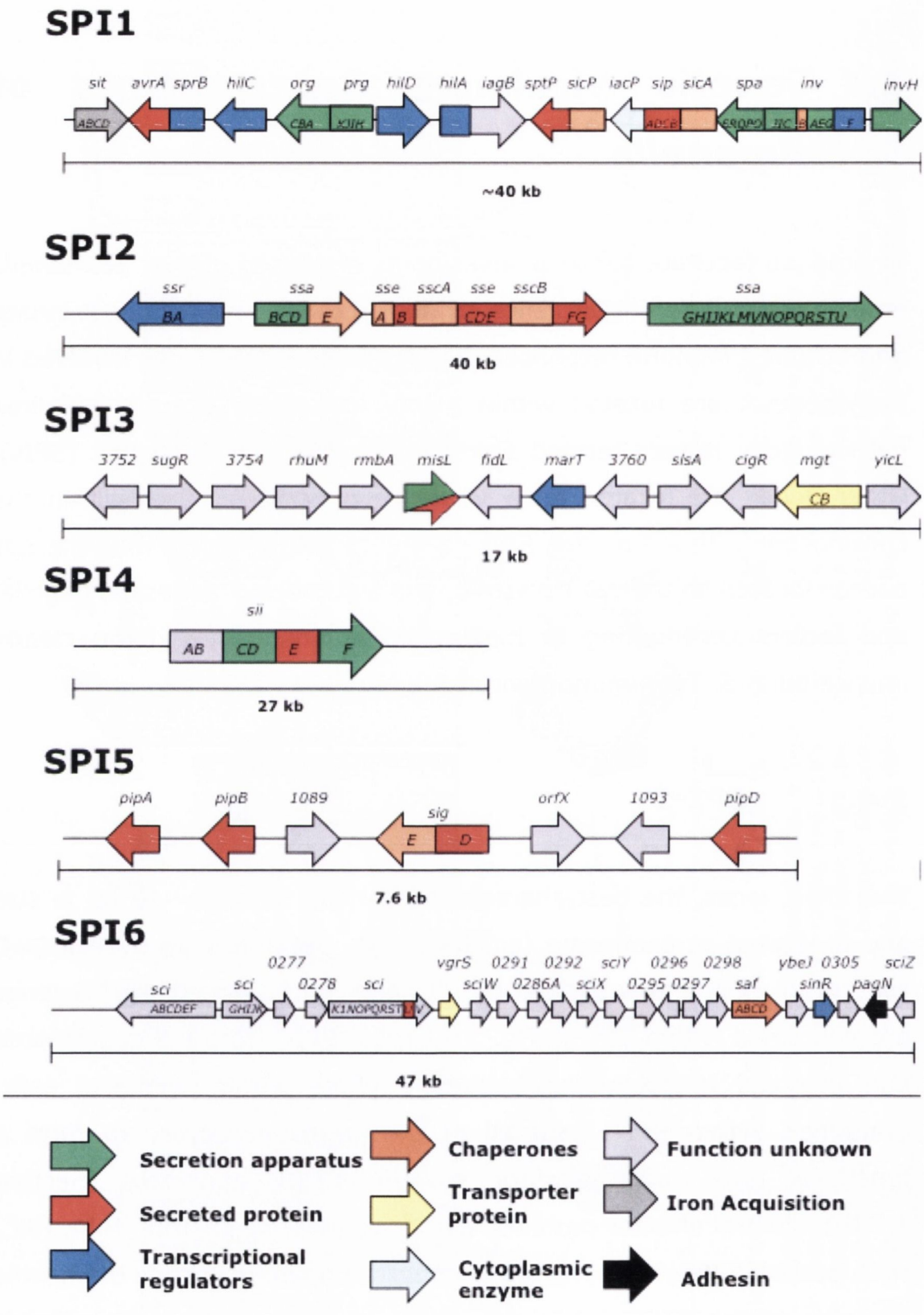

FIG. 1.2. Schematic representation of the genes of SPI-1 through SPI-6 and their putative functions.

within the integrated P2-like phage SopEΦ at 60 cs (151). Several chaperone proteins are also encoded within SPI-1 and protect the effector proteins from degradation, prevent premature interactions, or mediate recognition by the T3SS.

Injection of the T3SS effector molecules into the host cell promotes cytoskeletal rearrangements resulting in membrane ruffling and traversal of the intestinal epithelium by *S.* Typhimurium (Section 1.5.6.1). SPI-1-defective *S.* Typhimurium are attenuated for virulence in a mouse model when inoculated orally but not intraperitoneally (121, 180). This suggests that SPI-1 is necessary for the colonisation of intestinal epithelia, while other virulence determinants were acquired to allow for systemic spread of the bacteria.

1.4.2 SPI-2

SPI-2, located at 32 cs, is a 40-kb virulence determinant inserted adjacent to the $tRNA^{Val}$ gene (263, 306). The 42 ORFs of SPI-2 are utilised *S.* Typhimurium for intracellular replication within host cells, and for persistent, systemic infection after internalisation (Fig. 1.2) (164, 263). When compared with wild-type *Salmonella,* SPI-2-defective mutants are severely attenuated regardless of whether they are infected orally, intraperitoneally or intravenously (167, 263, 306).

The SPI-2 locus can be divided into two separate segments, which may have been obtained in two distinct horizontal transfer events (166). The smaller 14.5-kb region of SPI-2 is found in both *S. enterica* and *S. bongori* and was most likely acquired first. This region, together with seven ORFs of unknown function, harbours a cluster of *ttr* genes involved in anaerobic tetrathionate reduction (165). This arm of SPI-2 is flanked by ORF 242 and *pykF* at 30.5 cs and is not required for virulence (166).

The larger 25.3-kb portion of SPI-2, located between $tRNA^{Val}$ gene at 31 cs and *ssrB* of SPI-2 is restricted to *S. enterica* and may present a more recent insertion (166).

The larger region of SPI-2 harbours the genes necessary to mediate virulence including a T3SS, as well as regulatory, chaperone and effector proteins. The SPI-2 encoded T3SS functions to secrete its effector proteins from within an intracellular environment (164). Four operons termed regulatory, structural I, structural II and effector/chaperone encode the 31 genes that comprise the T3SS and associated proteins (58, 166, 306). These genes were named to reflect the function of the products they encoded: regulatory proteins were designated *ssr* (secretion system regulator), components of the T3SS were designated *ssa* (secretion system apparatus), while substrate proteins and their cognate chaperones were designated *sse* (secretion system effector), and *ssc* (secretion system chaperone) respectively (168).

After further functional analyses, several SPI-2 encoded genes have been re-annotated. The putative effector protein SseA was further characterised to reveal that it acts as a chaperone for SseB and SseD, two of the translocon components (291, 365). SsaB was also incorrectly labelled as a component of the T3SS apparatus and has since been relabelled SpiC as it has been shown to inhibit phagosome-lysosome fusion and interfere with intracellular trafficking (338).

A more thorough exploration of the role of the SPI-2 encoded T3SS and effector proteins in *Salmonella* pathogenesis is presented in Section 1.6.

1.4.3 SPI-3

SPI-3 is a 17-kb insertion located at the *selC* tRNA locus at centisome 82. Within SPI-3, there are ten ORFs encoded within 6 transcriptional units, only four of which have been studied (Fig. 1.2). This island encodes proteins with no functional relationship to one another and analysis of the G+C content of SPI-3 reveals a mosaic structure indicating that it evolved in a multi-step process (33). One of the SPI-3 operons, *mgtCB*, encodes the macrophage survival protein MgtC and the high-affinity Mg^{2+} transporter MgtB (314). Transcription of the *mgtCB* operon is induced under conditions of low Mg^{2+} by the PhoP-PhoQ two-component signal transduction system (33, 313). None of the other SPI-3 genes are PhoP-regulated nor are they required for survival in macrophage, or for invasion of epithelial cells. Of the other ORFs, one, encoding a membrane insertion and secretion protein, MisL exhibits sequence similarity to the AIDA-I adhesin of enteropathogenic *E. coli* (24), and is involved in binding of fibronectin and in intestinal persistence in mice (85). Another ORF, MarT (for membrane-associated regulator) displays 43% identity at the C-terminal end to the ToxR transcriptional regulator from *Vibrio cholerae* (245). The function of the remaining ORFs is undefined but as their distribution varies between serovars of *Salmonella* it is postulated they contribute to host specificity or chronic infection (9).

1.4.4 SPI-4

SPI-4, located at 92 cs, is a 27-kb genetic element flanked by putative tRNA genes, which contains a previously identified locus required for survival in murine macrophages (Fig. 1.2) (106, 353). An initial description of SPI-4 suggested there were 18 putative ORFs encoded in the pathogenicity island (353). However, upon publication of the

complete genome of *Salmonella* Typhimurium LT2, the operon was reorganised into 6 ORFs labelled STM4257-62 (236, 250). The SPI-4 encoded genes have since been renamed *siiABCDEF* for *Salmonella* intestinal infection after SPI-4 was shown to be important for the colonisation and infection of calves (250). SPI-4 mutants have since been shown to be attenuated relative to wild-type bacteria during systemic infection of mice (209). Data published by Gerlach *et al.* demonstrated invasion of the intestinal epithelia from the apical side requires the cooperation of the SPI-1 encoded T3SS with a giant adhesin termed SiiE (128). SiiE is discussed in more detail in Section 1.5.3.

1.4.5 SPI-5

Located at 25 cs of the *S.* Typhimurium chromosome, SPI-5 is flanked by *serT* and *copR* with an overall G+C content of 43.6% (Fig. 1.2), and has been characterised in detail in *S.* Dublin (175, 354). SPI-5 has also been identified in several other *Salmonella* spp. including *S.* Typhimurium (175, 354). SPI-5, like SPI-1, is involved in traversal of the intestinal epithelium (354). SPI-5 encodes the SopB effector protein (Section 1.5.6.1.1.1), which is secreted through the SPI-1-encoded T3SS, and thought to be responsible for inducing fluid secretion from host epithelial cells (175, 190, 269). It is not thought to be associated with systemic disease, although two genes, *pipD* encoding a cysteine protease homologue, and *copS,* encoding a histidine kinase, have been implicated in systemic infection (189).

1.4.6 SPI-6

SPI-6 is relatively uncharacterised. Located at 7 cs of the *S.* Typhimurium chromosome next to the $tRNA^{asp}$ gene, it is 47-kb in size (113, 114). In 2002, Folkesson *et al.* demonstrated that SPI-6 is necessary to mediate entry of *S.* Typhimurium into HEp-2 cells (114). Klumpp *et al.* also demonstrated that several genes located within SPI-6 are necessary to mediate survival within J774A.1 macrophages (188). 44 genes are encoded within SPI-6, though many of them have not been characterised (Fig. 1.2) (194). The genes encoding a type-6 secretion system, the fimbrial gene cluster *safABCD*, and the adhesin/invasin *pagN* are all located within SPI-6 (113, 205, 275). PagN will be discussed in more detail in Section 1.5.5.

1.4.7 The *Salmonella* virulence plasmid

Pathogenic, non-typhoidal *Salmonella* serovars carry a large, low-copy-number virulence plasmid required for systemic disease (139, 289). The *Salmonella* virulence plasmid is present at 2.75 copies per cell and varies in size depending on the serovar from 50-kb in size (for *S.* Choleraesuis) to 95-kb in size (for *S.* Typhimurium) (57, 236). The *S.* Typhimurium virulence plasmid contributes to systemic infection in mice by increasing the growth rate of the bacteria inside host cells (141). A region of 8-kb is highly conserved throughout. This region encodes five genes *spvRABCD* (designated *Salmonella* plasmid virulence (*spv*) genes) and is sufficient to restore virulence to plasmid-cured bacteria (140).

The *spv* locus encodes four structural genes, *spvABCD*, as well as the gene for a transcriptional regulatory protein, *spvR*. SpvR is a transcriptional activator of the LysR family, which activates expression from both the P_{spvR} and P_{spvA} promoters. The SpvB protein is a mono(ADP-ribosyl)transferase that modifies actin, destabilising the

cytoskeleton of infected cells (214, 331). SpvC is a phosphothreonine lyase that has been reported to remove phosphate groups and thus inactivate extracellular signal-regulated kinase (ERK), a mitogen-activated protein kinase (MAPK) signalling pathway required for *Salmonella*-induced inflammation. Both SPI-1 T3SS and SPI-2 T3SS are able to deliver SpvC into the host cell cytoplasm (146, 235). SpvC was reported to be required for systemic infection (234); however, recent evidence indicates that mice infected with *spvC* mutant bacteria show pronounced colitis compared to those infected with wild-type bacteria. SpvC reduces expression of proinflammatory cytokines (IL-8 and TNF-α) and decreases inflammation and neutrophil infiltration at infection sites during the early stages of infection (146, 235).

The *spv* genes are induced during the stationary phase of bacterial growth in mice and macrophages (160, 230, 285). In addition to SpvR, the expression of the *spv* locus is regulated by the stationary phase sigma factor RpoS, the nucleoid-associated proteins H-NS (262), and IHF (231), the leucine-responsive regulatory protein Lrp (231), and the cAMP receptor protein CRP (261).

Outside of this conserved region are several loci including the plasmid encoded fimbrial operon *pef*, the *rck* operon (Section 1.5.2.1), and the *rsk* loci which is thought to play a role in regulation of *S.* Typhimurium virulence (289, 341). Recently, it was demonstrated that the *rck* operon is up-regulated by SdiA, in an *N*-acyl homoserine lactone-dependent manner in actively migrating swarmer populations of *S.* Typhimurium (187). SdiA is a component of a cell-cell signalling system coupled to swarmer differentiation in *S.* Typhimurium (1). Swarming refers to the tendency of almost all members of the *Salmonella* genus to differentiate and migrate on semisolid surfaces in a coordinated population. It is thought to be relevant to the differentiation state displayed within an animal host (187).

1.5 Intestinal invasion by *Salmonella*

1.5.1 The fimbriae of *Salmonella*

As mentioned above, fimbrial adhesins mediate attachment to the epithelial mucosa, initiating the first step in the invasion process (18-20). Fimbriae were first discovered in 1958 (88); it is generally accepted that there are 4 kinds of *Salmonella* fimbriae, encoded by four separate operons. They have been categorised as Type I (59), Long Polar (17), Plasmid-encoded (117), and Thin aggregative fimbriae (64). Fimbrial adhesins are thought to mediate attachment to the intestinal epithelial surface. Experiments performed *in vitro* have shown that the fimbriae expressed by *S.* Typhimurium promote attachment to various cell lines with each fimbrial operon promoting attachment to and invasion of an individual cell type (18). This points to fimbriae as a major factor in aiding *S.* Typhimurium to distinguish various cell types. Fimbriae may provide host specificity as there are several fimbriae present in strains of *S.* Typhimurium that are required for attachment to bovine rather than murine Peyer's patches (335).

1.5.2 Afimbrial adhesins

1.5.2.1 Rck

Outer membrane proteins can also promote adhesion to the intestinal epithelium. One such outer membrane protein is Rck, the gene for which is encoded on the *S.* Typhimurium virulence plasmid. Rck belongs to a family of related 17- to 19-kDa outer membrane proteins including PagC from *S.* Typhimurium (243), Ail from *Yersinia enterocolitica* (244), and OmpX in *E. coli* (239). Rck is a β-barrel protein composed of 8 anti-

parallel β-sheets that give rise to 4 surface-exposed loops (156). It has been shown that Rck provides high-level serum resistance by interfering with the formation of polymerised C9 tubular membrane attack complexes (157). Rck, when expressed exogenously in strains of non-invasive *E. coli* can promote adhesion to and invasion of mammalian cell cultures *in vitro* (158). The Rck protein induces bacterial binding to extracellular matrix (ECM) component laminin (67).

1.5.2.2 OmpD

Another important outer membrane protein is encoded by the *ompD* gene. OmpD is a 34-kDa porin that displays sequence similarity to the major porins OmpC, OmpF, and PhoE as well the NmpC and Lc porins of *E. coli* K-12 (183, 310, 311). The abundance of OmpD in the outer membrane is determined at the transcriptional level. Levels of OmpD increase in response to anaerobic shock and decrease in response to low pH (296). Dorman *et al.* originally reported that *S.* Typhimurium strains harbouring an *ompD* mutation were less virulent in BALB/c mice (84). However, it has also been reported that there is no difference in virulence between wild-type *S.* Typhimurium and the *ompD* mutant (241). However, *ompD* mutants display lower levels of macrophage and epithelial cell binding *in vitro*, this suggests that OmpD is involved in the recognition of *S.* Typhimurium by human macrophages and intestinal epithelial cells (149).

1.5.3 SiiE

Encoded within SPI-4, the *siiE* gene forms an operon with *siiABCDF*. SiiC, SiiD, and SiiF form a type-1 secretion system (T1SS) with SiiF acting as the ATPase subunit, SiiD acting as the periplasmic adaptor protein, and SiiC as the outer membrane pore (16). SiiE is the substrate of the T1SS where it is secreted and surface retained during cultivation (344). Recent work suggests that SiiAB form a proton channel similar to MotA and MotB of the flagellar motor and function to regulate SiiE surface retention and release (350). SiiE is the largest protein of the *Salmonella* proteome at 595-kDa (128, 208). SiiE is composed of 53 BIg domains (127, 344). The N-terminus possesses one coiled-coil domain flanked by two β-sheet domains while the C-terminus contains the signal sequence for secretion (344). Electron microscopy has revealed that SiiE is a linear molecule approximately 175 ± 5 nm in length (344). SiiE was shown to bind to GlcNAc and α2,3 linked sialic acid containing structures expressed on the apical side of polarized epithelial cells (344). Maximal surface retention of SiiE was demonstrated at 3.5 hours of growth in rich media, which is also when SPI-1 T3SS mediated invasion was also observed, indicating that SiiE may play a role in mediating initial attachment prior to the interaction of the epithelial cell with the T3SS needle complex (344)

1.5.4 BapA

Salmonellae possess the ability to form surface-attached biofilms on both biological and non-biological surfaces. Biofilms are thought to cause up to 60% of all human infections (319). Biofilms are also highly resistant to killing by anti-bacterials (4, 62, 80, 221, 319). In rich medium at room temperature, *S.* Enteritidis bacteria form a pellicle composed of curli fimbriae and cellulose at the air-broth interface (315,

364). In 2005, Latasa *et al.* discovered a large secreted protein that they termed BapA that is required for biofilm formation and host colonisation in *S.* Enteritidis strains (208). In late 2010, Biswas *et al.* confirmed the presence of the *bapA* gene in 67 *Salmonella* isolates belonging to 34 different serotypes including *S.* Typhi and Paratyphi, Typhimurium, Dublin, Enteritidis, and Gallinarium (32).

The *bapA* gene (*stm2689*) was first annotated as a large pseudogene with a frameshift in position 6969 in the genome of *S.*Typhimurium LT2 (236). Latasa *et al.*, however, found that this truncation did not occur in either the laboratory strain *S.* Typhimurium LT2 or the clinical isolate *S.* Enteritidis 3934 during PCR-amplification of DNA fragments encompassing this region of the genome (208). The *bapA* gene gives rise to a 386-kDa protein. The BapA protein contains three regions; region A encompasses amino acids 1-360, region B contains 29 tandem repeats (amino acids 159-3003), and region C encompasses amino acids 3003-3824. Loss of the *bapA* gene in both *S.* Enteritidis and *S.* Typhimurium 14028 abrogated the ability of the bacterium to produce the pellicle at the air-broth interface in liquid L-broth. Overproduction of curli fimbriae, however was shown to overcome the biofilm deficiency in this mutant strain (208).

Latasa *et al.* also demonstrated that BapA plays a role in the pathogenesis of *S.* Enteritidis (208). In their experiments, BALB/c mice were orally and intraperitoneally inoculated with wild-type and *bapA* deficient bacteria. At 5-11 days post infection, mice inoculated with wild-type bacteria showed 100% mortality rate, while those inoculated with the Δ*bapA* strain did not begin to die until 8 days post-infection, and 55% of those infected survived until 24 days post infection (208). Latasa *et al.* also showed that bacteria harbouring a *bapA* deletion, were unable to effectively adhere to and invade the intestinal epithelium in a ligated ileal loop (208). These results indicate that BapA is involved in intestinal colonisation during invasion and in biofilm formation.

1.5.5 PagN

First annotated as IviVI-A (160), the PagN protein is an outer membrane adhesin that is required for bacterial survival and virulence in BALB/c mice (160, 358). The PagN protein is predicted to comprise eight amphipathic β-strands, giving rise to four surface-exposed extracellular loops. PagN shares 54% homology with the Tia and Hek invasins found in enterotoxigenic *E. coli* and neonatal meningitic *E. coli*, respectively (101, 103, 112). Together, PagN, Hek, and Tia form the PATH family of adhesins/invasins.

The *pagN* gene is conserved between all *S.* Typhimurium strains. Recently, Ghosh *et al.* showed that the PagN protein is also conserved in several clinical strains of *S.* Typhi and Paratyphi (129). The PagN protein of *S.* Typhi ($PagN_{STY}$) shares 96% sequence homology with the PagN protein of *S.* Typhimurium ($PagN_{STM}$). There are two amino acid substitutions in transmembrane portions of the $PagN_{STY}$, and two amino acid substitutions D20E and D69Q in extracellular loops 1 and 2 respectively. While $PagN_{STM}$ recognises heparin-sulphate molecules expressed on the surface of host cells, $PagN_{STY}$ mediates adhesion to the extracellular matrix component, laminin (129, 204). $PagN_{STY}$ is also crucial for *S.* Typhi pathogenesis as deletion of the *pagN* gene leads to a 10-fold greater LD_{50} for mice (129). Ghosh *et al.* proposed PagN as a potential vaccine candidate for *Salmonella* Typhi as mice that had been immunized using recombinant $PagN_{STY}$ were able to survive for up to 7 days after being challenged with 5×10^7 C.F.U./ml bacteria (129). Recently, Yang *et al.* have also proposed $PagN_{STM}$ as a potential vaccine candidate (358). In this study, mice were immunized with recombinant $PagN_{STM}$ and challenged with 1×10^6 C.F.U./ml bacteria; 60% of immunized mice survived past day 20, while 100% of naïve mice died by day 11 (358).

The *pagN* gene is part of the PhoP/Q activated-gene regulon, discussed more in depth in Section 1.7.1 (22). It has been proposed that

PhoP/Q can be activated by a mild acidic pH (6, 11). Previous studies have shown that *pagN* is expressed when bacteria are grown in minimal media at pH 5.8 (205), however, a more recent study has shown that PagN expression can be activated by growth to late stationary phase in a rich media at pH 5.8 (358). *pagN* expression is also highly up-regulated when bacteria are grown in minimal media that is starved of magnesium, or when bacteria are grown in a SPI-2 inducing media (259). Nunez-Hernandez *et al.* also showed that *pagN* expression is highly up-regulated during invasion of fibroblast cells (259).

Previous studies have demonstrated that PagN is a conserved outer membrane protein necessary to mediate efficient invasion of mammalian cells (160, 161, 203, 205, 357). However, there is a serious gap in the literature with respect to the specific mammalian cell receptor recognised by the PagN protein as well as the amino-acid residues involved in mediating these interactions.

1.5.6 The SPI-1 Type Three Secretion System of *Salmonella*

Salmonella encode two distinct virulence-associated T3SSs involved with different stages of the infection process (177). The SPI-1 T3SS is required for epithelial cell invasion and enteric pathogenesis while the SPI-2 encoded T3SS, is associated with intracellular survival (167, 177). These secretion systems provide a channel for the direct transport of effector molecules from the cytoplasm of the bacterium to the host cell. T3SSs are considered the most complex secretion systems in bacteria comprising more than 20 proteins. The main components of the apparatus seem to be generally conserved in many Gram-negative species, while the arsenal of effector proteins they deliver is specific to each system (122).

The SPI-1-encoded T3SS is generally considered central for entry to the intestinal epithelium. It is composed of a supramolecular structure called the needle complex (NC), which shares sequence homology with proteins of the flagellar export machinery (196). The NC consists of a multi-ring base that is required to anchor the structure to the bacterial envelope with a filamentous needle-like projection (composed of PrgI) that protrudes ~50 nm from the bacterial surface. InvG, PrgH and PrgK form the base of the NC in a ratio of 1:1:1 (196, 229). The base features four distinct rings, two associated with the outer membrane (OR1 and OR2) and two contacting the inner membrane (IR1 and IR2) (Fig. 1.3 (a)) (229). The base is traversed by a cylindrical inner rod (PrgJ) connecting the needle to a socket substructure, stabilised by InvJ, at the neck of the inner rings. Surface renderings of the structures of the base and needle complex are displayed in Fig. 1.3(b).

The assembly of the apparatus is a multi-step process with the base complex being constructed prior to the addition of the inner rod, socket and needle components (197, 229). Once fully assembled, the base substructure (InvG, PrgH and PrgK) begins to function as a secretion apparatus devoted to transport of factors required to assemble the needle and inner rod substructures. Upon completion of the NC, the specificity of the machine changes and it becomes concerned with the export of effector proteins (63, 197).

The diameter of the needle complex forces effector proteins to pass through in an unfolded state. There also seems to be some semblance of a hierarchy regarding the order in which the effectors are secreted (63, 273, 356). It is therefore thought that a complex substrate-recognition system exists, involving multiple signals and accessory proteins (317). All known T3SS effector proteins possess signal sequences within the first 20 – 30 amino acids, which are

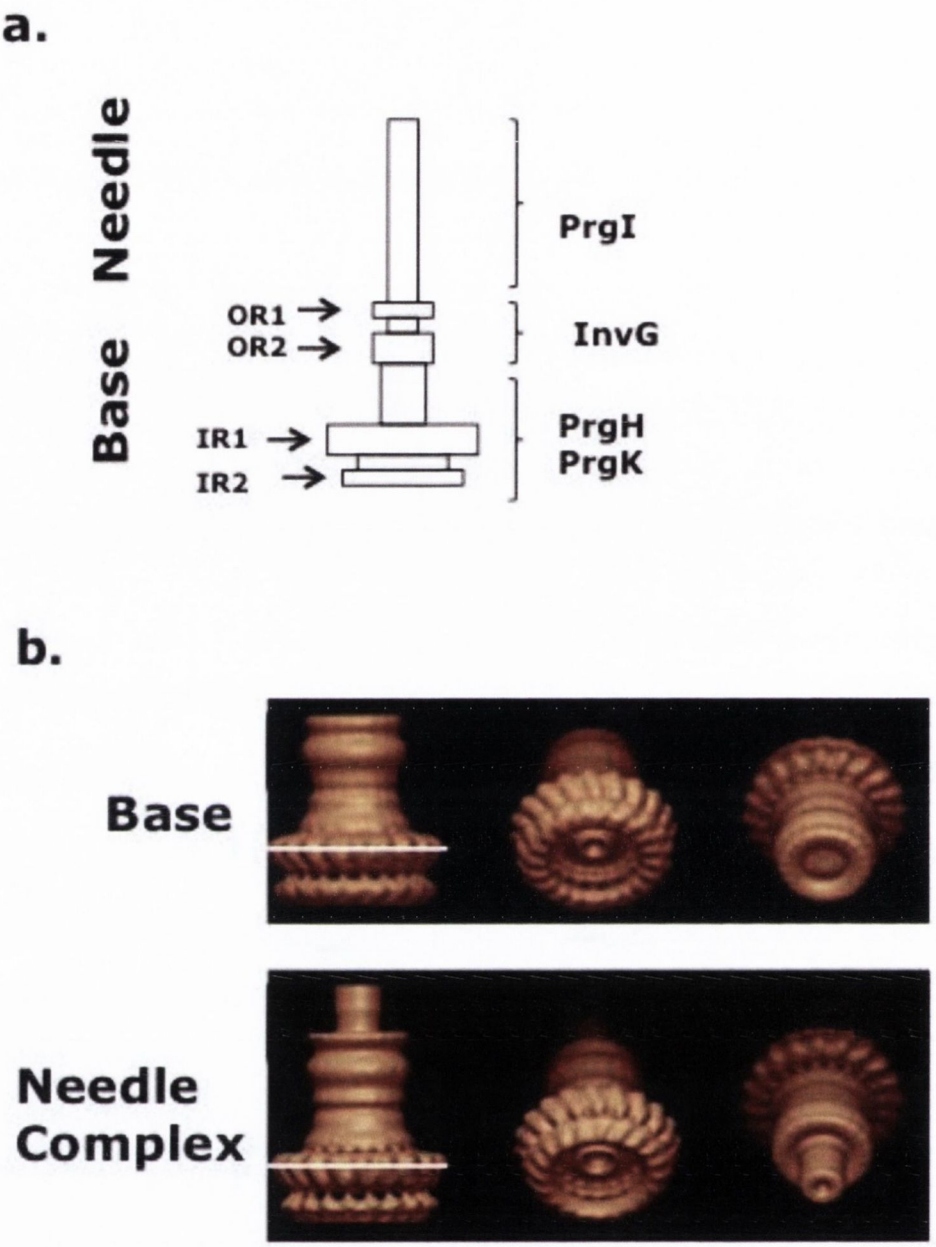

FIG. 1.3. The needle complex and base of the SPI-1 encoded T3SS. The needle complex is divided into two substructures. The base, embedded in the membrane, and the extracellular needle filament (a). The outer membrane associated rings (OR1 and OR2) are composed of the InvG protein, while the inner membrane-associated rings (IR1 and IR2) are composed of the PrgH and PrgK proteins. PrgI comprises the needle filament. Panel b displays surface renderings of the base and needle complex. The individual subunits within the inner rings are displayed while the outer rings appear smooth. The white bar in panel b indicates 208 Å. Reproduced and adapted from (229).

thought to be involved in their targeting to the secretion apparatus (305, 318). Upon secretion, these sequences remain unprocessed and attached to the mature protein. The stringency of substrate-specificity within the T3SS, the subject of much debate, seems to be supplied by somewhat generic signal sequences, made specific by the addition of chaperones and accessory proteins. These T3SS-associated chaperones are small, acidic, dimeric proteins, which unlike other chaperones lack ATP-binding or hydrolysing capabilities (105). In general, these chaperones bind a ~15 - 100 amino acid domain immediately downstream of the effector protein signal sequence (105). The proteins function to stabilise and target the effector to the translocation apparatus (118, 175, 213). Most chaperones are specific for a single effector, but some can facilitate the secretion of more than one effector protein (38, 89, 171, 337). An ATPase located at the base of the NC not only drives the export process, but also facilitates the release of effectors from chaperones before transport (3).

Finally, the effector proteins must be delivered into the host cell. A model was proposed in which the needle complex punctured the target cell membrane and injected proteins directly into the host cytosol (174). It has since been established that T3SSs need a set of effectors termed translocators, which insert into the target cell's membrane forming a channel through the membrane and a "dock" for the needle to complex with (142, 328). The needles of several T3SSs are thought to interact with this dock via an accessory structure at the tip, consisting of one protein. In 2009, Lara-Tejero *et al.* demonstrated that the SPI-1 effectors SipB, SipC, and SipD are required for the intimate association of *S.* Typhimurium strains with Henle-407 cells, indicating that these proteins form the translocase (207).

1.5.6.1 Bacterial-promoted endocytosis

Entry of *S.* Typhimurium into cultured epithelial cells is achieved through actin cytoskeletal reorganization, membrane ruffling, and bacterial internalization by macropinocytosis (65-70). These ruffles are brought about through the actions of at least five different effector proteins delivered by the SPI-1 T3SS. Unlike other bacterial toxins that modify target host cell proteins in a non-reversible manner, T3SS effectors seem to act by mimicking the function of host cell proteins (321). Many of the bacterial effector proteins do not share any sequence or structural similarity to their eukaryotic counterparts. The function of the main T3SS effector proteins including the *Salmonella* outer proteins (Sop) SopE, SopE2, SopB, the secreted protein tyrosine phosphatase SptP, and the *Salmonella* invasion proteins (Sip), SipA and SipC will be discussed below.

1.5.6.1.1 Indirect manipulation of the actin cytoskeleton

The effector proteins SopE, SopE2 and SptP are capable of activating (SopE and SopE2) and inactivating (SptP) Cdc42 and Rac-1, members of the Rho-family of low-molecular-weight GTPases. Rho GTPases have two peptide regions, called Switch I and II that undergo conformational changes depending on the nucleotide bound (143). SopE and SopE2 are guanine nucleotide exchange factors that catalyse exchange of GDP to GTP (15, 41, 290, 325, 355). Upon translocation into the host cell, SopE binds and activates both Cdc42 and Rac-1. SopE2, however, has significant activity only towards Cdc42 and not Rac-1 (116). When GTP is bound, Rho GTPases are in an active state with Switch I and II in a conformation such that they can bind signalling molecules. This activation leads to recruitment of downstream effectors such as Wiskott-

Aldrich Syndrome protein (WASP) family members N-WASP and WAVE, which mediate Arp2/3-dependent actin nucleation (339). Such remodelling of host actin near the cell surface produces the characteristic membrane ruffles that accompany bacterial entry.

1.5.6.1.1.1 SopB/SigD

SopB, also termed SigD for *Salmonella* invasion gene D (123, 175), stimulates Cdc42 and RhoG indirectly by inducing changes in phosphoinositol metabolism through its inositol phosphate phosphatase activity (116, 150, 269, 325, 360).

There is a general requirement for phosphatidylinositol-4,5-bisphosphate [PtdIns(4,5)P_2] depletion at sites of phagocytosis and endocytosis (36, 182). It has been established that SopB is responsible for the elimination of PtdIns(4,5)P_2 at the base of membrane ruffles (329). Patel *et al.* have demonstrated that activation of RhoG by SopB occurs by a cellular exchange factor called SGEF (269). SGEF has a phosphoinositide-binding pleckstrin homology domain that is activated by the phosphoinositide fluxes that arise from the enzymatic action of SopB. Activation of Rho GTPases then results in the activation of the WASP family members N-WASP and WAVE2 which leads to recruitment of the actin-related protein-2/3 (Arp2/3) complex to sites of membrane ruffles and stimulation of actin polymerization (68, 307, 325, 339).

1.5.6.1.1.2 SptP

The activity of effector proteins delivered by the SPI-1 T3SS is tightly coordinated in a temporal manner, allowing for the delivery of proteins with antagonistic functions (195). SptP is a GTPase activating protein (GAP), which catalyses the loss of the γ-phosphate, during hydrolysis of GTP to GDP thus inactivating the Rho GTPases Cdc42 and Rac-1 (185).

This enzymatic activity reverses the cytoskeletal changes induced during internalisation of *Salmonella*, restoring normal actin architecture at the site of bacterial entry (119). To facilitate regulation of actin assembly and disassembly, *Salmonella* exploit the host cell ubiquitin-mediated proteasome degradation pathway. The N-terminal secretion and translocation domain found in each protein determines the stability of each effector protein. SopE, for example, is ubiquitinated and rapidly degraded upon entry into host cells, while SptP is much more stable and persists (195). The relatively short-life of SopE as compared with the longevity of SptP ensures that SopE-induced actin rearrangements at the bacterial entry site can be restored to normal.

1.5.6.1.2 Direct manipulation of the actin cytoskeleton

In addition to the indirect reorganisation of actin by SopE/SopE2/SopB, *Salmonella* secrete effector proteins that can modulate actin dynamics directly. SipC and SipA proteins (also known as *Salmonella* secreted proteins, SspC and SspA) are two such effectors. These factors function in a cooperative manner to manipulate the processes of actin nucleation and polymerisation, which are required for membrane ruffling during bacterial invasion (237, 238).

1.5.6.1.2.1 SipC

SipC is a 42-kDa protein involved in early bacterial entry of epithelial cells. SipC forms an essential portion of the translocon and is involved in the translocation of other effector proteins into the mammalian cell cytoplasm (120, 355). It is itself secreted into host cells and becomes inserted in the epithelial plasma membrane (304). The SipC protein is multi-functional with individual functions being attributed to particular domains of the protein. The protein can be divided into three regions:

the N-terminal domain, which is involved in F-actin bundling, a C-terminal domain that directly nucleates actin *in vitro* and a middle hydrophobic, transmembrane region that is thought to form an integral part of the translocation apparatus pore (155). It has been reported that the C-terminal domain can be further divided into two regions: residues 201-220 are essential for actin nucleation while residues 321-409 are required for effector translocation (48).

1.5.6.1.2.2 SipA

The SipA protein, like SopE/E2 and SopB, is responsible for tight junction disruption during *Salmonella* infection (37). SipA is involved in many different processes. It stabilises actin filaments by inhibiting their depolymerization at early stages of infection (184, 362). SipA also enhances SipC-induced actin nucleation and bundling (238), and is capable of binding to F-actin (238, 363) and G-actin, reducing the minimal concentration for G-actin polymerisation (363). It also promotes the actin-bundling activity of host T plastin at the site of bacterial/host contact (361). Furthermore, SipA locally inhibits ADF/cofilin- and gelsolin-directed actin-depolymerisation (75, 237) thus stabilising the activities of other effector proteins. In addition, SipA contributes to bacterial localization in clusters in the invasion area, thereby facilitating bacterial uptake (362).

1.6 Intracellular survival of *Salmonella*

When foreign bodies, such as bacteria, viruses and protozoa enter mammalian cells they become encased in a lipid-based phagosome. *Salmonella* that have been successful in invasion, reside within a vacuolar compartment named the spacious phagosome (5). The

spacious phagosome shrinks over the course of several min to several hours to form an adherent membrane around one or more bacteria termed the *Salmonella* containing vacuole (SCV). SCV-contained bacteria trigger events to maintain the SCV by preventing the delivery of antimicrobial host factors (e.g. free-radical generating complexes) through the modification of the host cell cytoskeleton and by impairing vesicular transport (198, 281, 338).

Phagosomes undergo biochemical changes inducing maturation and direction to the centriole of the host cell. Lysosomes are also trafficked to the centriole where they collide with the phagosomes, thereby killing the intra-phagosomal bacteria (40). *Salmonella*, however, have the ability to prevent phagosomal maturation and thus avoid lysosomal killing (40, 346).

Typical phagosomal maturation starts with the acquisition of the small GTPase Rab5 (286). Rab5 directs the stimulation of a phosphatidyl-inositol 3-kinase (PI3K), the enzyme responsible for the generation of phosphatidyl-inositol 3-phosphate (PI3P), which is required for phagosomal maturation (115). This enzyme in turn binds EEA1 (early endosome-associated protein) and Hrs, which are responsible for bridging vesicles and forming multi-vesicle bodies, respectively (115, 280). Hrs also interacts with ubiquitylated proteins and triggers inner budding of vesicles in a process involving ESCRT (endosomal sorting complex required for transport) complexes (279). Maturation of phagosomes is accompanied by the accumulation of LBPA (lyso-*bis*phosphatidic acid), and lysosomal glycoproteins LAMP-1 and -2 (40). In the final stage of maturation, Rab5 and EEA1 dissociate from the phagosome and are replaced by another GTPase, Rab7, which interacts with RILP (Rab-interacting lysosomal protein) (44, 343). RILP bridges Rab7-containing vesicles with a dynein motor complex that powers the trafficking of phagosomes along microtubules to the centriole (44, 152). This physical translocation facilitates the collision and fusion of phagosomes with lysosomes (152).

The SCV has been shown to interact transiently with the early endocytic pathway and quickly gain and lose early endocytic markers, such as EEA1, and the early endocytic trafficking GTPases Rab5 and Rab11 (312, 322). The SCV displays many of the markers of phagosome maturation, however, SCVs undergo repeated cycles of PI3P formation and depletion (271). Several late endosomal markers are commonly associated with the SCV at later time points, including the GTPase Rab7, LAMP1, LAMP2, LAMP3 and the vacuolar ATPase (87, 124, 240, 322). There is conflicting data concerning the occurrence of M6PR (mannose-6-phosphate receptor), LBPA and the lysosomal hydrolase, cathepsin D, on the SCV (40, 70, 124, 126, 153). Cholesterol has also been reported to accumulate on the SCV (40, 46). The presence or absence of different markers on the persistent SCV may indicate that they are variably detected rather than reflect whether or not the SCV has matured through a normal endocytic pathway.

Studies using various cell types have shown that the SCV acidifies, though this acidification can be delayed in both macrophages and epithelial cells (5, 87, 232, 284). Samonellae sense the acidic environment of the SCV, resulting in the induction of several different regulatory systems to promote intracellular survival. Some systems are involved in surface remodelling of the protein, carbohydrate, and membrane components of the bacterial envelope (5). These regulatory systems include OmpR/EnvZ, PhoP/PhoQ, RpoS/RpoE, PmrA/PmrB, Cya/Cyp and cyclic diGMP, all of which confer resistance to antimicrobial peptides and oxidative stress (74, 104, 160, 172, 211, 243, 257, 330).

Various studies have indicated that the phagosomal environment is acidic, with a pH range of <5 to 5.5 and a calcium/magnesium concentration of ~1 mM (5, 232, 284). The SCV also contains antimicrobial peptides and oxygen and nitrogen radicals that can damage the bacterial cell (5, 232, 284). Various studies have indicated that both pH and antimicrobial peptides are important signatures of the

phagosomal environment and such conditions activate many of the regulators that are implicated in *Salmonella* virulence (10, 21, 242, 277).

1.6.1 Survival within macrophages and systemic dissemination

Internalisation of the infecting *Salmonella* within the SCV is followed by systemic spread through other target organs such as the spleen and liver. Several bacterial strategies have been reported to contribute to this systemic stage of the disease. *Salmonella* induces epithelial cell death featuring the morphological changes of apoptosis including: maintenance of an intact plasma membrane to prevent release of inflammatory intracellular contents. Membrane-bound apoptotic bodies can be taken up by phagocytes or neighbouring cells, allowing for degradation of cellular components in a generally noninflammatory process. This event is induced after prolonged exposure, at least 12 hours after *in vitro* infection (108). Induction of apoptosis in epithelial cells involves caspase-3 as well as the SPI-2 encoded T3SS (108). The effector SpvB is reported to induce epithelial cell death as a result of the actin depolymerization activity expressed by this plasmid-encoded protein, though the mechanism remains to be elucidated (201).

Another *Salmonella* effector, SlrP, has been reported to contribute to epithelial cell death (242). SlrP was initially characterised as a leucine-rich repeat protein involved in *in vivo* colonisation of mice (335). More recent studies, however, have demonstrated that SlrP promotes cell death by two complementary interactions with Trx and with Erdj3 (26). SlrP is an E3 ubiquitin ligase, which interacts with mammalian thioredoxin-1 (Trx), a protein involved in stimulating cell growth and inhibiting apoptosis. SlrP has also been reported to interact with Erdj3,

a member of the Hsp40/DnaJ family of chaperones. This interaction is thought to promote accumulation of unfolded proteins, a process that can eventually induce apoptosis (26).

When *S.* Typhimurium cross the basolateral membrane of intestinal epithelial cells, they are met by neutrophils and macrophages. These professional phagocytes engulf the *Salmonella*, encasing them in a SCV; this time composed of macrophage/neutrophil membrane. It is the ability of *S.* Typhimurium to survive with murine macrophages that leads to bacterial dissemination and systemic infection. *Salmonella* can cause macrophage death in several different ways (340). This effect is thought to enable bacterial systemic dissemination throughout infected organs by incoming uninfected macrophages engulfing either infected dying cells or bacteria released by these cells into the extracellular space (138). This process is termed pyroptosis and is dependent on the inflammasome, a multiprotein complex that mediates activation of caspase-1, which in turn leads to proteolytic activation of IL-1β and IL-18. These two cytokines play central roles in acute and chronic inflammation and potently stimulate recruitment of immune cells, contributing to the inflammatory outcome of programmed cell death (108).

SipB, a member of the SPI-1 encoded T3SS translocon system, mediates early pyroptosis. SipB binds to caspase-1 and acts as a cytotoxic effector (170, 297). In macrophage cells deficient in caspase-1 production, rapid cell death does not occur and takes as long as 3 h (169). This caspase-1 independent programmed cell death is also dependent upon SipB (169). The effector is thought to bring about cell death as a consequence of its ability to induce autophagy by damaging macrophage mitochondria (169).

In the absence of a functional SPI-1, *S.* Typhimurium is still capable of promoting caspase-1-dependent macrophage killing through the use of the SPI-2 and *spv* loci in a process that takes up to 24 h (39, 248, 340). This delayed form of *Salmonella*-induced cell death also requires

the protein kinase PKR and activation of Toll-like receptor 4 on macrophages by bacterial LPS (176). PKR is required for the promotion of bacterial-induced apoptosis (178). The SPI-2-encoded T3SS is essential to push this balance in favour of apoptosis, however, the effector proteins involved remain poorly characterised.

1.7 Coordinate Regulation of virulence

To survive each stage of invasion, *Salmonella* must adapt to a series of ecological pressures. Each new environment encountered can be defined in terms of specific parameters including temperature, nutrient availability, osmotic pressure, oxygen status, and pH. The bacterium must sense its environment and then communicate this information to the DNA. The cell modulates its gene expression profiles in a manner that enhances the fitness of the bacterium within that specific environment. This requires the coordinated control of the expression of a large number of genes using complex regulatory networks.

Regulatory networks interact and overlap to switch distinct sets of genes on and off in response to the environmental stimuli present. As discussed, *S. enterica* encode two distinct T3SSs, operating at different steps of the infection cycle. The expression of these systems is, therefore, differentially regulated. The SPI-1 T3SS is stimulated by environmental queues present in the intestinal tract (high osmolarity, low O_2 levels), whereas the expression of the SPI-2 T3SS is stimulated by conditions present within host cells (low Mg^{2+} concentration and acidic pH) (14, 125, 212).

The extremely complex regulation of SPI-1 genes depends on the balance between the interactions of the regulators encoded both inside and outside of the island (218, 219). Four transcriptional regulators, HilD, HilC, HilA and InvF are encoded within SPI-1 and act in an ordered fashion to activate expression of the SPI-1 T3SS (13, 90, 303).

Expression of the *hilA* gene is controlled by the combined action of three AraC-like transcriptional activators (303). *hilC* and *hilD* are encoded within SPI-1, while *rtsA* is encoded within an independent island (94, 303). Each activator can bind to the *hilA* promoter and activate its expression and can also significantly induce its own expression as well as activate the other regulators (34, 93). HilC and HilD can also activate a subset of SPI-1 genes independently of their positive regulation of *hilA* (2). HilD can also induce expression of the SPI-2 genes by direct binding of the *ssrAB* promoter (the most important and essential regulatory system required for SPI-2 gene expression) (42). HilC, HilD, and RtsA can also activate InvF expression in a *hilA*-independent manner by direct interaction with an alternative *invF* promoter (34, 94).

HilA plays the central role in invasion not only because all of the regulatory systems and environmental signals affect its expression, but also because a deletion of *hilA* has been shown to be phenotypically equivalent to a deletion of the entire SPI-1 locus (7, 14, 93, 95). HilA activates all of the operons encoding the functional SPI-1 T3SS including the *prg/org* and *inv/spa* operons which are activated by a direct binding of HilA to their promoters, and the *sic/sop* operons which are induced via the activation of InvF (13, 14, 76). HilA also activates expression of the *sii* operon of SPI-4 (Section 1.5.3) as well as the *sigD* operon of SPI-5 (128, 189, 223, 332). A schematic of some of the virulence regulatory networks is displayed in Fig. 1.4.

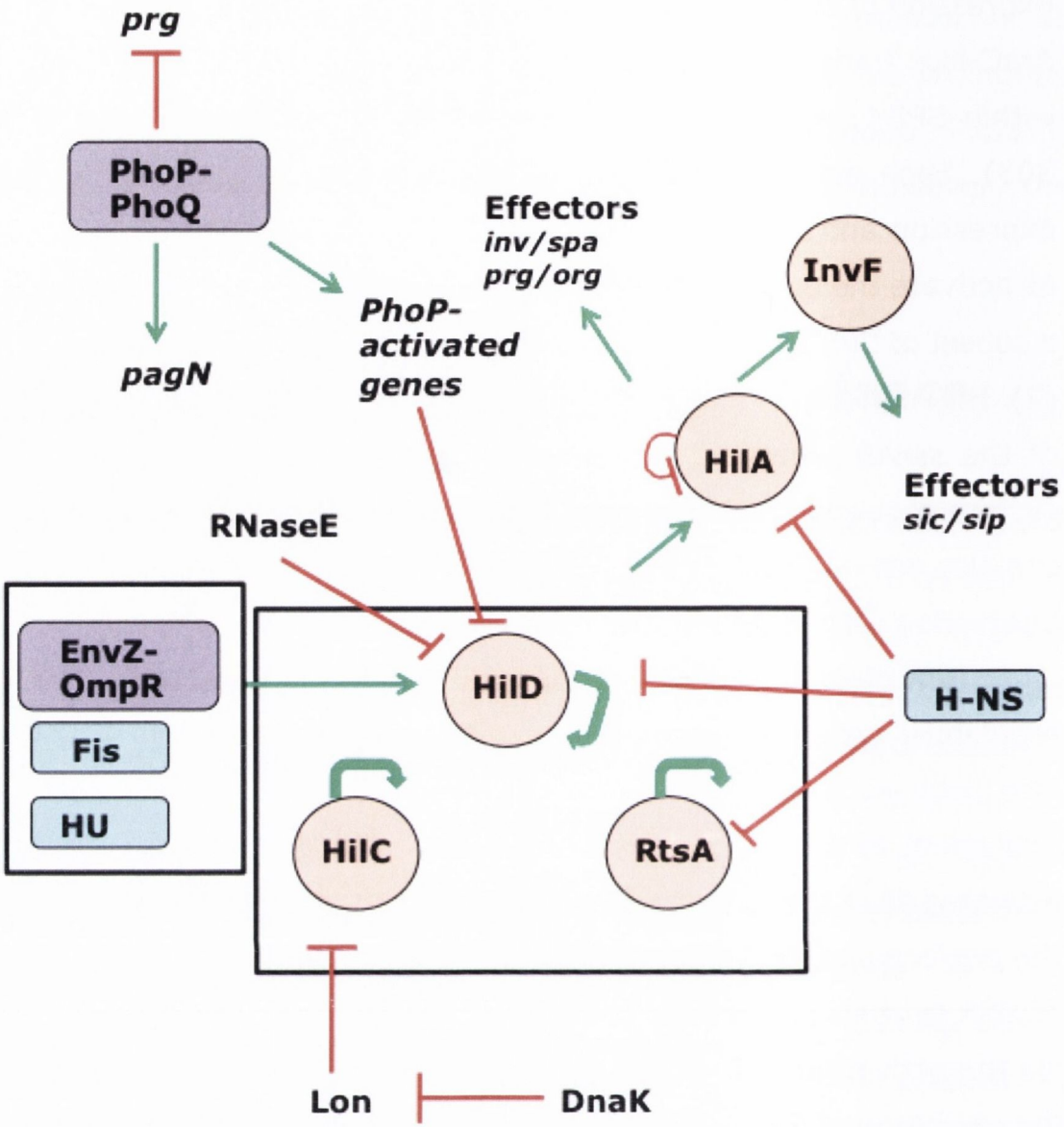

FIG. 1.4. Diagram of some of the virulence regulatory networks of *Salmonella*. Green arrows indicate activation or autoactivation while the red blunt arrows indicate repression. The blue boxes display nucleoid associated proteins, while the peach circles surround regulators that play a major role in invasion. The purple boxes indicate two-component regulatory systems. PhoP/Q activates expression of a number of genes involved in systemic virulence, including *pagN*. Adapted from (218).

1.7.1 The PhoP/PhoQ Two-Component System

The PhoP/Q two-component system is required for intracellular survival within both macrophages and epithelial cells (29, 106, 135). The genes *phoP* and *phoQ* form an operon encoding a two-component regulatory system consisting of a membrane-located sensor/kinase domain (PhoQ) and a cytoplasmically located response regulator (PhoP) (136, 243). In response to specific signals PhoQ, the membrane-located sensor, adjusts the phosphorylation state of the cytoplasmically-located DNA-binding protein PhoP, thereby increasing its DNA-binding capabilities (45, 47, 249). Three different cues have been proposed to activate the PhoP/Q system inside macrophages: a mild acidic pH (6, 11, 277), antimicrobial peptides (11), and low Mg^{2+} (134). In the presence of high Mg^{2+} concentrations the system is switched off, while at lower levels, such as those found within macrophages, the system is switched on and regulates the expression of over 100 genes in *S.* Typhimurium, representing ~4% of the *Salmonella* genome (366). Genes that are activated are referred to as *pags* (PhoP-activated genes) while those that are repressed are called *prgs* (PhoP-repressed genes).

PhoP/Q controls virulence determinants both directly and indirectly by regulating the expression of several transcriptional factors required for *S.* Typhimurium virulence, such as PhoP/Q itself (316), SsrB (29), SlyA (258), PmrA (193), RpoS (336), and HilA (14). SsrB is the response regulator of the SsrA/B two-component system and as such is responsible for the activation of SPI-2 encoded genes. PhoP/Q indirectly controls expression of SPI-2 as PhoP binds to the *ssrB* promoter thereby activating transcription. PhoP/Q also activates the transcriptional regulator, SlyA (258, 308). SlyA belongs to the MarA family of transcription factors. These homodimeric, winged-helix transcription factors control their DNA binding activity via interactions with small

molecules within a cleft formed at the junction between the subunits (133). SlyA induces transcription of the SsrA sensor kinase by binding to the *ssrA* promoter (265). SlyA-regulated genes such as *pagC*, *pagD*, *ugtL*, *mig-14*, *virK*, *phoN*, *pgtE*, *pipB2*, *sopD2*, *pagJ* and *pagK* are also controlled by the PhoP/Q system (255).

1.8 Overview of thesis

The *Salmonella*-specific gene *pagN* has been somewhat characterised at the DNA level in the context of the *Salmonella* chromosome and at the protein level. The aim of this thesis is to further characterise the PagN proteins of *S.* Typhimurium and *S.* Typhi. Functional studies were performed to determine the contributions of each of the extracellular loops of the protein to adhesion and invasion of epithelial cells such as Chinese hamster ovary (CHO-K1) and human HT-29 colonic cancer cells. Several charged amino acids located in the second extracellular loop of the protein were mutated to a neutral alanine residue to determine their involvement in promoting PagN-mediated phenotypes. Adhesion and invasion of mammalian cell monolayers was monitored using the gentamicin protection assay (GPA) and through a high-throuput fluorescent microscopy assay developed and optimised for this thesis. Initial work was also completed to characterise the cell-surface receptor to which PagN binds using siRNA techniques to knockdown expression of the proposed PagN receptor molecule followed by monitoring of expression levels through qRT-PCR and finally detecting invasion via the HCA.

Chapter 2 Materials and Methods

2.1 General Methods

2.1.1 Bacterial strains and culture conditions

2.1.1.1 Bacterial strains

All bacterial strains used in this study were derivatives of *S. enterica* serovar Typhimurium strain SL1344, and *Escherichia coli* strain K-12 and are listed in Table 2.1. Permanent stocks were maintained in L broth supplemented with 8.7% (v/v) DMSO and stored at −80 °C.

Table 2.1. Bacterial strains used in this study.

Strains	Relevant details	Reference or source
S. Typhimurium		
SL1344	Wild-type mouse-virulent strain, Str^R	ATCC
ML5	SL1344 *invA*::*cat*, Cm^R	(203)
ML6	SL1344 *pagN*::*spc*, Spc^R	(203)
Escherichia coli		
DH5α	F′ *endA1 hsdR17* ($r_k^- m_k^+$) *glnV44 thi-1 recA1 gyrA* (Nal^r) *relA1 Δ(lacIZYA-argF)U169 deoR (Φ80dlacΔ (lacZ)M15)*	Invitrogen
DH5αZ1	P_{lacI^q}, $P_{N25\text{-}tetR}$, *deoR*, *supE44*, *Δ(lacIZYA-argF)U169*, *(Φ80dlacΔ (lacZ)M15)*,	(220)

	hsdR17(rK- mK+), recA1, F′ *endA1, thi-1 recA1 gyrA96* (Nal^r) *relA1*	
XL-1 Blue	*recA1 endA1 gyrA96 thi-1 hsdR17 supE44 relA1 lac* [F′ *proAB lac^{q}ZΔM15* Tn*10* (Tet^r)]	Stratagene
MC4100	F′ *araD139*Δ(*argF-lac*)*U169 rspL150 relA1 flbB5301 fruA25 deoC1 ptsF25*	(272)
LT004	CFT073 *cobS::f(PLtetO-1-gfp+),* Cm^R	(35)

2.1.1.2 Bacterial growth media

All media were prepared using Millipore 18 MΩcm^{-1} grade water and chemicals obtained from Sigma-Aldrich. Media were sterilised by autoclaving at 120 °C for 20 min prior to use. Additives not suitable for autoclaving were sterilised by filtration through 0.2 μm Millex filters (Millipore). The quantities listed below are sufficient for 1 litre of medium.

Lennox L broth and agar:

L broth and agar were used throughout this study for the routine culturing of all Gram-negative bacterial strains except where otherwise stated.

L broth: 10 g tryptone, 5 g yeast extract, 5 g NaCl

L agar: 10 g tryptone, 5 g yeast extract, 5 g NaCl, 15 g bacteriological agar

Minimal Media 5.8 (MM5.8):

MOPS [3-(N-morpholino)propanosulfonic acid] minimal medium, adjusted to pH 5.8 with HCl (MM 5.8), is a low pH, minimal medium adapted from media previously described by Neidhardt *et al.* (256) and Kox *et al.*. (193). It is used to simulate conditions inside a macrophage and has been shown to activate transcription of SPI-2 and PhoP-activated genes (193).

10X MOPS solution: 83.7 g MOPS, 7.2 g Tricine, 0.03 g $FeSO_4.7H_2O$, 5 g NH_4Cl, 0.5 g K_2SO_4, 1 ml $CaCl_2$ (50 mM), 73.05 g NaCl, 10 ml micronutrients (see below), adjust to 1 L with dH_2O.

Micronutrients: $(NH_4)_5(MO_7)_{24}$, 3 μM; H_3BO_3, 400 μM; $CoCl_2$, 30 μM; CuSO4, 10 μM; $MnCl_2$, 80 μM; $ZnSO_4$, 10 μM

MM 5.8: 100 ml 10X MOPS, 0.23 g K_2HPO_4, 20 ml glycerol, 1 g Casamino acids, adjust volume to 1 L with dH_2O.

The solution was adjusted to pH 5.8 with HCl (1 M)

After filter-sterilisation, 50 μl of filter-sterilised $MgCl_2$ (1M) was added.

2.1.1.3 Bacterial culture conditions

Bacteria were routinely grown on L agar plates and in aerobic liquid cultures shaken at 200 rpm at 37 °C, except where otherwise stated. Liquid cultures were inoculated by transferring single colonies from agar plate cultures into an appropriate volume of L broth and grown overnight. Where mid-logarithmic cultures were required, overnight cultures were diluted in fresh media to an optical density of 0.05 at 600 nm and grown to the appropriate phase.

2.1.1.4 Antibacterials and media additions

All media additives including stock antibacterials were filter sterilised using an 0.2 µm Millex filter (Millipore) and stored at -20 °C. Where appropriate, antibacterials were added to media at the following concentrations: Carbenicillin (Car) 50 µg/ml, Kanamycin (Kan) 50 µg/ml, Chloramphenicol (Cm) 30 µg/ml, and Spectinomycin (Spc) 100 µg/ml. Anhydrous-tetracycline (Sigma-Aldrich) at a concentration of 0.2 µg/ml was added to cultures of *E. coli* to induce expression of *gfp*+ from the $P_{LtetO-1}$ promoter. The *lac* operon inducer IPTG was prepared as a 100 mM stock and used at a concentration of 1 mM.

2.1.2 Eukaryotic cell lines and growth conditions

2.1.2.1 Eukaryotic cell lines

All eukaryotic cell lines used were obtained from Sigma-Aldrich (United Kingdom). The mammalian cell lines used were CHO-K1 (ECACC 85051005) and HT29 (ECACC 91072201). Stocks of all cell lines were maintained in cell freezing medium/DMSO (Sigma-Aldrich) under liquid nitrogen.

2.1.2.2 Cell growth conditions

CHO-K1 cell lines were grown in a 1:1 mixture of DMEM/Ham's F12K medium with 2 mM L-glutamine adjusted to contain 1.5 g/L sodium bicarbonate, supplemented with 10% (v/v) heat-inactivated foetal bovine serum (Sigma-Aldrich). HT-29 cells were grown in McCoy's 5a medium with 2 mM L-glutamine supplemented with 10% (v/v) heat-inactivated fetal bovine serum (Sigma-Aldrich). Cells were routinely

cultured in 75 cm^2 flasks at 37 °C in 5% CO_2. Confluent monolayers were disrupted by treatment with a trypsin/EDTA solution (Sigma-Aldrich) and diluted into fresh medium.

2.1.3 Plasmids and oligonucleotides

2.1.3.1 Plasmids

All plasmids used in this study are listed in Table 2.2 along with relevant descriptions and sources. For plasmids constructed during this study the details of construction are described in the relevant chapters.

TABLE 2.2. Plasmids used in this study

Plasmid	Relevant Details	Source or Reference
pACYC177	Empty vector, Km^R Ap^R	New England BioLabs
pBSKII	ColE1 replicon, Ap^R	Stratagene
pCM01	pACYC177 plasmid containing $P_{LtetO-1}$-*gfp*$^+$*cmR* inserted in the *bla* gene	(253)
pD103A	Ap^r *pagN* (D103A) ORF in pTrc99a	(203)
pD97A	Ap^r *pagN* (D97A) ORF in pTrc99a	(203)
pET19b	N-terminal His-tag, T7 promoter, Ap^R	Novagen
pHek6	866 bp of RS218 DNA carrying the *hek* gene cloned into pBSKII,Ap^R	(103)
pK99A	Ap^r *pagN* (K99A) ORF in pTrc99a	(203)

pKM001	pZep08 plasmid derivative containing $P_{LtetO-1}$-*gfp*$^{+}$*cmR*	(35)
pLoop1$_{\Delta 16-45}$	Ap^{r} Derivative of pML1 with the DNA sequence corresponding to the first loop of the PagN protein replaced with CGCGCG	(204)
pLoop1$_{\Delta 18-42}$	*pagN*$_{STM}$ gene in pTrc99a, the DNA sequence corresponding to the first loop of the PagN protein replaced with CGCGCG, Ap^{r}	This study
pLoop2$_{\Delta 71-96}$	Ap^{r} Derivative of pML1 with the DNA sequence corresponding to the second loop of the PagN protein replaced with CGCGCG	(204)
pLoop2$_{\Delta 74-96}$	*pagN*$_{STM}$ gene in pTrc99a, the DNA sequence corresponding to the second loop of the PagN protein replaced with CGCGCG, Ap^{r}	This study
pLoop3$_{\Delta 127-153}$	Ap^{r} Derivative of pML1 with the DNA sequence corresponding to the third loop of the PagN protein replaced with CGCGCG	(204)
pLoop3$_{\Delta 131-150}$	*pagN*$_{STM}$ gene in pTrc99a, the DNA sequence corresponding to the third	This study

	loop of the PagN protein replaced with CGCGCG, Ap^r	
$pLoop4_{\Delta 182-207}$	Ap^r Derivative of pML1 with the DNA sequence corresponding to the fourth loop of the PagN protein replaced with CGCGCG	(204)
$pLoop4_{\Delta 184-205}$	$pagN_{STM}$ gene in pTrc99a, the DNA sequence corresponding to the fourth loop of the PagN protein replaced with CGCGCG, Ap^r	This study
pML1	$pagN_{STM}$ gene in pTrc99a	(205)
pML4	Ap^r *pagN* ORF inserted into pBSKII	(205)
pR93A	Ap^r *pagN* (R93A) ORF in pTrc99a	(203)
pSP1	$pagN_{STY}$ ORF in pTrc99a	This study
pSP4	pTrc99a containing $P_{LtetO-1}$-gfp^+cmR inserted in the *bla* gene	This study
pSP5	pML1 containing $P_{LtetO-1}$-gfp^+cmR inserted in the *bla* gene	This study
pSP8	$pagN_{STM}$ ORF in pBSKII, under the constitutive P_{hek} promoter	This study
pTrc99a	Empty vector plasmid containing an IPTG inducible promoter, Ap^R	(8)

2.1.3.2 Oligonucleotides

The sequences of all oligonucleotides used in this study are listed in Table 2.3. All oligonucleotides were synthesised by Metabion, Martinsried, Germany.

TABLE 2.3. Oligonucleotide primers used in this study

Primer	Sequence
GAPDHfwd	5′ – CTC TGC TCC TGT TCG AC – 3′
GAPDHrev	5′ – TGA AGG GGT CAT TGA TGG CA – 3′
Loop1Fwd	5′ – Pho – GCA GGC GTT TTT GGC GGG GTT G – 3′
Loop1Rev	5′ – Pho – GCG GAC ATT GAC TAC GGA TGT CCC C – 3′
Loop2Fwd	5′ – Pho – GCA CAG GTC CGA ATG ACC ACT TAC – 3′
Loop2Rev	5′ – Pho – GCG ACC TCT GAA AGT GGT ATC CAG – 3′
Loop3Fwd	5′ – Pho – GCA AAC TTT GCC TGG GGC GCA GG – 3′
Loop3Rev	5′ – Pho – CGC CTT CAC ATG AGC GAG GCC – 3′
Loop4Fwd	5′ – Pho – GCA GCC TCC AAT GAC TTC ATG CTC – 3′
Loop4Rev	5′ – Pho – GCG TAC TTT GCC AGC ATT AAT GTA T – 3′
pHek6 Inverse Fwd	5′ – CAT TTC AAT TAT CTC CAT TAT TGT ATC – 3′
pHek6 Inverse Rev	5′ – GAC ACT GCT CCT GAA CGA TAT CGA ATT C – 3′
PagNdATG Fwd	5′ – AAA AAC TTT TTC GCA GTC TG – 3′
PagNHis fwd	5′ – Pho – CAT TAA GGC TCC TCT AGA GTC GAC – 3′
PagNHis rev	5′ – Pho – ATG AAA GGC GTA AGT AAT GCC GAG – 3′
Phek fwd	5′ – GTA AAG CTT GAG GCT GCC TTT ACT CCG – 3′
Phek rev	5′ – CGC CCA TGG TTC AAT TAT CTC C – 3′
Phek NcoI fwd	5′ – ATA ATG GAG ATA ATT GCC ATG GAT AAG GTT TTT GTT TCA GTG – 3′

Phek NcoI rev	5′ – CAC TGA AAC AAA AAC CTT ATC CAT GGC AAT TAT CTC CAT TAT – 3′
P1CobKM	5′ – GTG ACG GGG GGC GCA CGG AGC GGG AAG AGT GCG CAC GCA AGC CTG GGG TAA TGA CTC TCT AG – 3′
P2CobKM	5′ – CAG CGT ATC GCC CGT TTG CGC GCC CAG CGT ACG TTT GAG ACG TCA TTT CTG CCA TTC ATC – 3′
p1gfp	5′ – GCC TGG GGT AAT GAC TCT CTA GC – 3′
p2gfp	5′ – CGT CAT TCC TGC CAT TCA TCC – 3′
T2544Fwd	5′ – CGC CCC ATG GAA AAC TTT TTC GCA – 3′
T2544Rev	5′ – GGC GTG GAT CCT TAA AAG GCG TAA GTA ATG C – 3′
XYLT2Fwd	5′ – GCT CTA AGG CCC GAA CA – 3′
XYLT2Rev	5′ – CCT GGA AAC TCT GCA TGG GT – 3′

2.2 Nucleic acid methodologies

2.2.1 Transformation of *Salmonella* and *E. coli* strains

Two distinct strategies were used to introduce foreign DNA including plasmids and PCR products into bacterial cells. Cells were made competent either by repeated washing in an ice-cold calcium chloride solution or ice-cold sterile water and then transformed by heat-shock (226) or electroporation (86), respectively. Significantly greater transformation efficiencies were achieved using the electroporation method. The calcium chloride method was used to transform plasmids that had been PCR amplified using the QuikChange II Site-Directed Mutagenesis Kit (Agilent Technologies).

2.2.1.1 Transformation of *E. coli* strains using calcium chloride method

A 5 ml culture of the strain to be made chemically competent was inoculated from a single colony into L broth and incubated overnight with shaking. This culture was sub-inoculated to an OD_{600nm} of 0.05 in 100 ml of fresh L broth containing suitable antibiotic. Bacteria were grown to an OD_{600nm} of 0.4 to 0.6 at 37 °C with shaking. The cultures were then incubated on ice for 20 min and the bacteria were harvested by centrifugation at 6,000x *g* for 10 min. The pellet was resuspended in 20 ml of cold $CaCl_2$ solution (60 mM $CaCl_2$, 15% (v/v) glycerol, 10 mM PIPES, pH 7) and harvested by centrifugation as before. This pellet was resuspended in 20 ml ice-cold $CaCl_2$ solution and incubated on ice for 30 min before harvesting the bacteria as before. The pellet was then resuspended in a final volume of 4 ml of cold $CaCl_2$ and incubated overnight on ice before aliquoting 100 µl volumes and stored at –80 °C.

Competent bacterial cells (100 μl) were mixed with between 50 ng and 1 μg of plasmid DNA and incubated on ice for 10 min. The cells were then transferred to a 42 °C water bath and incubated for 90 s, thus inducing the uptake of the DNA. Cells were immediately transferred to ice. Following a 1 min incubation on ice the cells were mixed with 1 ml of pre-warmed SOC broth or L broth and incubated at 37 °C for 1 h to allow expression of plasmid-borne antibiotic resistance genes. Aliquots of 1 μl, 10 μl, 100 μl and 889 μl of the transformation mixture were spread on selective L agar plates and transformants were single colony purified onto fresh L agar plates following growth overnight at 37 °C.

2.2.1.2 Transformation of *E. coli* and *S.* Typhimurium strains by electroporation

A 5 ml culture of the strain to be made electrocompetent was inoculated from a single colony into L broth and incubated overnight with shaking. This culture was then sub-inoculated to an OD_{600nm} of 0.05 in 100 ml of fresh L broth containing the requisite antibiotic. Bacteria were grown to an OD_{600nm} of 0.4 to 0.6 at 37 °C with shaking. The cultures were then incubated on ice for 20 min. Bacteria were harvested by centrifugation at 6,000x *g* for 20 min. The pellet was resuspended in 20 ml sterile ice-cold water. Bacteria were harvested as before, resuspended in 10 ml ice-cold water, and harvested again. The pellet was resuspended in sterile ice-cold 10% (v/v) glycerol, harvested at 6,000x *g* for 10 min and resuspended again in ice-cold 10% (v/v) glycerol to a final volume of 200 μl. 50 μl aliquots were stored at -80 °C.

Electro-competent bacteria (50 μl) were mixed with between 50 ng and 2 μg of DNA (in a volume not exceeding 4 μl) and immediately transferred into a cold electroporation cuvette (BioSmith, 0.2 cm electrode width). The electroporation was carried out in a Bio-Rad gene pulser at 12.5 $kVcm^{-1}$, 25 μF and 200Ω. The bacteria were quickly mixed with 1 ml of pre-warmed SOC broth or L broth and incubated at 37 °C

for 1 h to allow expression of plasmid-borne antibiotic resistance markers. Aliquots of 1 μl, 10 μl, 100 μl and 889 μl of the transformation mixture were spread on selective L agar plates and transformants were single colony purified onto fresh L agar plates following growth overnight at 37 °C.

2.2.2 λ Red-mediated allele replacement

The inactivation of chromosomal genes involved a two-step process whereby mutated alleles were constructed *in vitro* and transferred to the bacterial chromosome using an allele-replacement system based on the gene products of the λ phage red operon (78). This system is based on the ability of the *gam*, *bet* and *exo* gene products to inhibit the Exonuclease V activity of RecBCD thereby allowing the transformation of linear DNA fragments and promoting homologous recombination at regions of homology between the chromosome and the transformed linear DNA fragment. The λ-phage *redγβα* operon used was located on the pKD46 (51) plasmid under the control of the L-arabinose-inducible P_{BAD} promoter. This plasmid has a temperature sensitive replicon, which permits plasmid replication at 30 °C but not at higher temperatures. The plasmid also confers resistance to the antibiotic carbenicillin.

2.2.2.1 λ Red- mediated allele replacement in *E. coli*

E. coli XL-1 Blue bacteria lack a functional *recA* gene. The lack of a *recA* gene makes this strain less receptive to the Red system. The *E. coli* strain MC4100 does not contain the *recA* mutation, and is easier to manipulate using this system. Briefly, bacteria harbouring the plasmid pKD46 were grown to an OD_{600nm} of 0.2 - 0.4 at 30 °C in the presence of 50 μg/ml carbenicillin. Expression of the Red α, β and γ proteins was induced by addition of 0.2% L-arabinose. The induced bacteria were

grown for a further 2 h and made electrocompetent (Section 2.2.1.2). These electrocompetent bacteria were then transformed with 500 ng - 1 μg of purified linear DNA comprised of the PCR amplified gene and antibiotic resistance cassette along with 35 nt corresponding to the flanking region of the gene to be disrupted. After electroporation, bacteria were subsequently incubated for 1 h at 37 °C to allow recovery of the bacteria, expression of the antibiotic resistance markers, and to promote loss of the pKD46 plasmid. Cells were spread on L agar plates containing the appropriate antibiotic. All subsequent steps were carried out at 37 °C in the absence of carbenicillin to ensure rapid loss of the pKD46 plasmid. Putative mutants were single-colony purified and then screened for the presence of the novel mutant allele by PCR. Loss of the pKD46 plasmid was confirmed by testing for carbenicillin sensitivity on agar containing the antibiotic.

2.2.3 Purification of plasmid and chromosomal DNA

2.2.3.1 Small-scale purification of plasmid DNA

The GenElute Plasmid Miniprep kit (Sigma-Aldrich) was used for the routine purification of plasmid DNA from overnight bacterial cultures. Purification was carried out according to the manufacturer's instructions using a modified alkaline lysis method. Briefly, bacteria from a 5 ml overnight culture were harvested by centrifugation and resuspended in a buffer containing RNase A to degrade RNA before being lysed using an alkaline SDS-lysis solution to degrade proteins, chromosomal DNA, and plasmid DNA. The solution is rapidly neutralized which causes the plasmid DNA to reanneal while the chromosomal DNA forms a white precipitate. The lysate was cleared by centrifugation to remove cellular debris and chromosomal DNA. The soluble plasmid DNA was adsorbed onto silica in the presence of high-salts. Contaminants were removed by

a spin-wash step and the bound DNA was finally eluted in water or Tris-EDTA buffer.

2.2.3.2 Large-scale purification of DNA

The Qiagen Plasmid Midi kit was used to purify plasmid DNA from 100 ml overnight cultures of *E. coli* according to the manufacturer's instructions. Purification was carried out using a modified alkaline lysis similar to that described above. Bacteria were lysed as before, and the cleared lysate was passed through a cation-exchange column to bind the re-natured plasmid DNA. The column with bound DNA was washed repeatedly and the DNA was eluted in a high-salt buffer. The DNA was further purified and desalted by precipitation with isopropanol and resuspended in ddH_2O.

2.2.4 *in vitro* manipulation of DNA

2.2.4.1 Restriction endonuclease digestion of DNA

All restriction digests were carried out using enzymes supplied by New England Biolabs (NEB) according to the manufacturer's instructions. Briefly, 10 ng to 2 μg of purified DNA was incubated with 10 U of restriction enzyme in the appropriate NEB buffer for 1 h at 37 °C. Digests with multiple enzymes were carried out in the recommended double digest buffer or in an appropriate buffer in which all enzymes had 100% activity. Where no suitable buffer was available sequential digests were performed.

2.2.4.2 Purification of DNA fragments

Following digestion with restriction endonucleases or PCR amplification, linear DNA fragments were purified directly from solution or from an agarose gel slice using the GenElute Gel Extraction Kit or GenElute PCR Clean-up kit (Sigma-Aldrich). To purify PCR amplified DNA fragments from solution, 5 volumes of Binding Solution were added to 1 volume of the PCR reaction mixture and mixed by vortexing. The solution was then added to a spin column where the DNA fragments bound to a silica matrix. Salts, enzymes and unincorporated nucleotides were removed in 2 subsequent wash steps. Purified DNA was eluted from the column in Tris-EDTA buffer.

Purification from an agarose gel slice used a similar protocol. The gel slice was first melted at 56 °C in 3 gel volumes of gel solubilisation solution. One gel volume of isopropanol was added prior to binding of the DNA. DNA was bound, washed, and eluted as before.

2.2.4.3 Ligation of DNA fragments

The T4 DNA Ligase was used to catalyse the formation of a phosphodiester bond between the exposed 5′ phosphate and 3′ hydroxyl groups of linear DNA fragments in an ATP-dependent fashion (97). These ligations were carried out using the Quick Ligation kit (NEB) and were routinely used for the cloning of DNA fragments into appropriate plasmid vectors.

50 ng of digested vector DNA was mixed with a three-fold molar excess of digested insert in a total volume of 20 µl, and mixed with 2 µl of 10 x Quick Ligation Reaction Buffer. 1 µl of Quick T4 DNA Ligase was added, and the reaction was incubated at room temperature for 20 min. The ligated DNA molecules were then transformed into either calcium-chloride or electrocompetent *E. coli* XL-1 Blue or DH5α cells. Where calcium-chloride competent cells were used, the whole ligation reaction was directly transformed. For electrocompetent cells, the ligated DNA

was concentrated by pellet-paint precipitation (Section 2.2.4.5) prior to electroporation.

2.2.4.4 Agarose gel electrophoresis

DNA samples were visualized following separation on a 1 - 2% agarose gel, depending on the size of the DNA. Briefly, for a 1% gel, agarose (1 g) was added to 100 ml of 0.5X TBE buffer (44.5 mM tris borate, pH 8.3, 1 mM EDTA) and heated to 100 °C to dissolve the agarose. Safe View nucleic acid stain (Bi-Med, Malahide, Ireland) was added to a final concentration of 1 μg/ml, and the molten gel was poured into a gel mould and allowed to set. DNA samples were prepared by adding an appropriate volume of 5x sample loading buffer (25 mM Tris HCl pH 7.6, 30% (v/v) glycerol, 0.125% (w/v) bromophenol blue) and these samples were electrophoresed through the gel at 120 V for 60 min in 0.5X TBE buffer.

2.2.4.5 Purification of DNA samples from solution by Pellet Paint and ethanol precipitation

For concentrating dilute DNA samples, Pellet Paint® Co-Precipitant was routinely used. Pellet Paint® Co-Precipitant is a visible dye-labelled carrier formulated specifically for use in alcohol precipitation of nucleic acids. 6 μl of Pellet Paint® Co-Precipitant was added to DNA solution followed by 0.1 volumes of 10 x Reaction Buffer and 2.5 volumes of ice cold 85% ethanol. The samples were vortexed briefly and incubated at -20 °C for 20 min. Precipitated DNA was collected by centrifugation at 12,100x *g* for 10 min. DNA was subsequently washed with 70% ethanol, harvested as before, and dried for 5 min at 37 °C. The dried DNA pellet was resuspended in an appropriate volume of ddH_2O.

2.2.5 Polymerase chain reaction

Polymerase chain reaction (PCR) was used for the amplification of specific DNA fragments for use in cloning reactions, and for the confirmation of constructed plasmids and mutant alleles. PCR is based on the ability of certain thermostable DNA polymerases to synthesize a new DNA strand complementary to a provided single-stranded, denatured DNA template, when primed with specific complementary oligonucleotides (293). The procedure involves successive rounds of thermal denaturation of a double-stranded DNA template, hybridization of two complementary oligonucleotides (primers) and synthesis of the new DNA strand by the DNA polymerase. The primers are designed to be complementary to opposite strands at either end of the fragment to be amplified and orientated such that their 3′ ends face each other. The new DNA strand is synthesized from provided dNTPs by the DNA polymerase in the presence of Mg^{2+}. Each new strand acts as a template in further rounds of amplification and the procedure thus results in exponential amplification of the desired DNA fragment.

2.2.5.1 Amplification of DNA by PCR

Where a high degree of sequence fidelity was required, for example to generate DNA fragments for cloning reactions, Q5® High-Fidelity DNA Polymerase was used (NEB). Q5 Polymerase is a high-fidelity, thermostable DNA polymerase with 3′→ 5′ exonuclease activity, fused to a processivity-enhancing Sso7d domain. The 3′ → 5′ exonuclease activity is necessary for proof-reading as it results in a significant decrease in the rate of nucleotide misincorporation. Q5 polymerase has an error rate > 100-fold lower than that of *Taq* DNA Polymerase and 12-fold lower than that of *Pyrococcus furiosus* (*Pfu*) DNA Polymerase.

Q5 PCR reactions were carried out according to the manufacturer's instructions in an MJ Research PTC-200 peltier thermal cycler. Briefly, 10 µl of 5X Q5 buffer was mixed with 10 mM dNTPs, 10 µM of each

primer, 50 ng of template DNA, 1 U of Q5 High-Fidelity polymerase and ddH_2O to a final volume of 50 μl.

2.2.5.2 Inverse PCR

Inverse PCR works on the same principles as a normal PCR reaction. However, primers are synthesised such that the forward primer binds to the top strand of DNA while the reverse primer binds to the bottom strand. The extension continues in opposing directions, thus amplification of DNA located between the 5' ends of the primers does not occur. To introduce flexibility into the protein sequences decoded in the deleted loop DNA, a CGC codon (encoding arginine) is incorporated into the sequence of the top strand while a GCG codon (for alanine) is added to the bottom strand. Ligation of the linear plasmid results in the arginine/alanine substituting the deleted loop. Partial gene deletions were performed in this manner. After PCR amplification, parental plasmid DNA was digested using *Dpn*I, isolated and purified from an agarose gel (Section 2.2.4.2), and the ends were ligated using T4 DNA Ligase (Section 2.2.4.3). The ligated plasmid was concentrated by Pellet Paint®-precipitation (Section 2.2.4.5) and transformed into electrocompetent cells (Section 2.2.1.2). Plasmids were purified from putative clones and sent for sequencing.

2.2.6 siRNA knockdown in human epithelial cells

Recent advances in molecular biology have shown that gene expression can be effectively silenced in a highly specific manner through the addition of double stranded RNA (dsRNA) (109, 148, 254). The term RNA interference (RNAi) was coined to describe this phenomenon and, while the mechanism was originally observed in plants and later in the worm *Caenorhabditis elegans*, subsequent studies have shown that RNAi

is present in a wide variety of eukaryotic organisms including mammals (30, 91, 266). Once dsRNA enters the cell, it is cleaved by an RNase III-like enzyme, Dicer, into double stranded small interfering RNAs (siRNA) 21 – 23 nucleotides in length that contain 2 nucleotide overhangs on the 3' ends (28, 92, 145). In an ATP-dependent step, the siRNAs become integrated into a multi-subunit protein complex, commonly known as the RNAi induced silencing complex (RISC), which guides the siRNAs to the target RNA sequence (260). The siRNA duplex unwinds, and the antisense strand remains bound to RISC and directs degradation of the complementary mRNA sequence by a combination of endo- and exo-nucleases (233). siRNA methodology was used to decrease expression of XYLT-2 in the human colon cancer cell line HT-29. XYLT-2 is a xylosyltransferase that catalyses the rate-limiting step of proteoglycan biosynthesis (130).

2.2.6.1 Reverse Transfection of HT-29 cells

Reverse transfections of cells using a validated SilencerSelect XYLT-2 siRNA (s34495, Life Technologies) or scrambled siRNA were performed as per the manufacturer's instructions. Briefly, the lipid reagent Lipofectamine RNAiMAX (Life Technologies) was diluted in low-serum media such as Opti-MEM media (Life Technologies). The siRNA or scrambled siRNA was prepared as a 10 µM solution and diluted to 20 nM in Opti-MEM media. The siRNA or scrambled siRNA was added to the diluted Lipofectamine RNAiMAX in a 1:1 ratio. The resulting mixture was incubated at room-temperature for 5 min. The siRNA-lipid complex was added to the wells of a 24-well or 96-well tissue culture plate to give a final siRNA/scrambled siRNA concentration of 10 nM.

HT-29 cells were prepared for transfection as follows. Confluent monolayers of cells were disrupted using trypsin/EDTA solution and harvested by centrifugation at 1200 rpm for 3 min. Cells were seeded on top of the siRNA-lipid complex at a density of 1.7×10^6 cells/well in

24-well tissue culture plates or 5.2 x 10^4 cells/well in 96-well high-content plates. After 24 hours, the media was removed and fresh media was added to the cells. After a further 24 hours, the total RNA was extracted (Section 2.2.6.2), cDNA was synthesized (Section 2.2.6.3), and qRT-PCR (Section 2.2.6.4) was performed to determine the efficiency of the siRNA knockdown. High-throughput invasion assays were also performed (Section 2.4.3.2).

2.2.6.2 Total RNA extraction

RNA was extracted from the mammalian cell line HT-29 for use in quantitative real-time PCR reactions. The method used for RNA extraction and purification was first published by Chomczynski *et al.* (56). This method involves cell lysis, phase separation, RNA precipitation and wash, and redissolving the RNA pellet. TRI Reagent (Sigma-Aldrich) contains a mixture of guanidine thiocyanate and phenol in a monophase solution, and was used to dissolve DNA, RNA, and protein during lysis of the mammalian cells. Briefly, 1 ml of TRI Reagent was added to each well in a 12-well cell culture plate containing HT-29 cells at 60 - 80% confluency. The resulting mixture was pipetted into a 1.5 ml Eppendorf, which could be frozen at -80 °C for up to 1 month. For RNA separation, chloroform was added at 1/5 of the volume of TRI Reagent and the mixture was incubated for 2 - 15 min at room-temperature. The different phases were separated by centrifugation at 12,000x *g* for 15 min at 4 °C. Centrifugation separates the mixture into 3 phases: an upper aqueous phase containing the RNA, the interphase containing DNA, and an organic phase containing proteins. The RNA containing phase was removed to a clean mini-centrifuge tube and isopropanol (1/2 TRI Reagent volume) was added. The RNA-isopropanol mixture was incubated for 10 min at room-temperature before the RNA was pelleted by centrifugation as before. The RNA pellet was then washed once in 70% ethanol and once in 100% ethanol, and the RNA was pelleted by

centrifugation at 12,000x *g* for 10 min at 4 °C. The pellet was allowed to air-dry and finally, redissolved in 50 - 100 µL of ddH_2O. RNA was stored at -80 °C.

2.2.6.3 cDNA synthesis

cDNA was synthesized using the SuperScript Vilo cDNA Synthesis kit (Invitrogen) as per the manufacturer's instructions. Briefly, 5x VILO Reaction mix was added to 10x SuperScript Enzyme mix, 1 µg of RNA, and ddH_2O to 20 µl. The mixture was incubated at 25 °C for 10 min, followed by incubation at 42 °C for 60 min, and finally reaction termination at 85 °C for 5 min. cDNA was stored at -20 °C until use. Prior to use in qRT-PCR experiments, cDNA was thawed on ice and diluted 1:10 in ddH_2O.

2.2.6.4 Quantitative real-time PCR (qRT-PCR)

qRT-PCR was used to monitor the gene expression for a target gene (*XYLT2*) in mammalian cells in real time after RNA extraction and cDNA synthesis. For comparative C_T experiments, cells exposed to a scrambled siRNA were used as a reference sample, while the housekeeping gene, *GAPDH* was used as an endogenous control to show targeted siRNA knockdown. Samples were tested in quadruplicate with negative controls tested in triplicate.

qRT-PCR reactions were carried out using the SensiMix SYBR Low-ROX kit (Bioline) according to the manufacturer's instructions in a 7500 Fast Thermal Cycler. Briefly, 10 µl of 2x SensiMix SYBR Low-Rox was mixed with 0.5 - 0.8 µM of each primer, 50 ng of template cDNA, and ddH_2O to a final volume of 20 µl.

2.3 Analysis and manipulation of proteins

2.3.1 SDS-PAGE

Proteins were separated on discontinuous denaturing polyacrylamide gels by the method of Laemmli (202). Using this method, proteins are denatured in SDS and β-mercaptoethanol, and separated based on their size as they travel through a polyacrylamide gel towards the anode. SDS binds to most proteins in a constant weight ratio, masking their natural charge with its own negative charge and giving each protein a similar mass:charge ratio allowing separation on the basis of size rather than charge. The discontinuous gel is formed using buffers of differing composition and pH to firstly focus the separating proteins into narrow well-defined bands, and then separate these focused proteins on the basis of their size.

2.3.1.1 Preparation of total cellular extract for SDS-PAGE analysis

The OD_{600nm} of an overnight culture was measured and 1 ml of the culture was then harvested by centrifugation at 15,800x *g* for 1 min. The pelleted bacteria were then resuspended in an appropriate volume of Laemmli buffer (75 mM tris-HCl, pH 6.8, 20% (v/v) glycerol, 2% (w/v) SDS, 2% (v/v) β-mercaptoethanol, 10 μg/ml bromophenol blue) such that the final concentration was 10 OD_{600nm} units/ml. The samples were boiled at 100 °C for 5 min and stored at −20 °C. Prior to use, samples were thawed and boiled again to facilitate complete denaturation.

2.3.1.2 Sarcosyl enrichment of outer membrane proteins

Bacterial lysates were enriched for outer-membrane proteins as previously described (81). This procedure is based on the ability of the detergent N-laurylsarcosine (sarcosyl) to disaggregate and solubilise protein and lipid components of the bacterial cytoplasmic membrane while, due to its similar charge density to LPS, leaving the LPS-containing outer-membranes intact and insoluble.

Overnight cultures of bacteria were sub-inoculated in 10 ml fresh LB to an OD_{600nm} of 0.05. Bacteria were allowed to grow to mid-logarithmic phase and protein expression was induced with 1 mM isopropyl β-D-1-thiogalactopyranoside (IPTG). The bacteria were allowed to grow and express protein for a further 3 h. After 3 h, the OD_{600nm} was measured and 12 OD units/ml of bacteria was harvested by centrifugation at 6,000x *g* for 10 min. The pellet of bacteria was resuspended in 600 µl sonication buffer (10% sucrose, 50 mM TrisHCl (pH 7.5), 100 mM NaCl, 1mM EDTA) and stored at -20 °C.

Lysis was achieved through sonication. Samples were sonicated in 15 sec bursts for up to 2 min. Cellular debris was removed by centrifugation at 12,000x *g* for 10 min. The supernatant was incubated with 0.5% sarkosyl solution for 30 min at room temperature with shaking. The outer membrane was harvested by centrifugation at 21,000x *g* for 30 min. The supernatant was removed and the pellet was resuspended in 100 µl Laemmli buffer. Samples were stored at -20 °C and boiled for 5 min at 100 °C prior to use.

2.3.1.3 Electrophoresis and staining of protein samples

Protein samples were separated on discontinuous 12% SDS-polyacrylamide gels using a Bio-Rad Power Pack basic at 200 V for 45 min. Gels were stained using Coomassie brilliant blue R-250 (0.25% Coomassie brilliant blue R-250, 45% (v/v) methanol, 10% (v/v) acetic acid) and destained using Coomassie destain solution (45% (v/v)

methanol, 10% (v/v) acetic acid) or transferred to polyvinylidene difluoride (PVDF) membranes for use in Western immunoblottings.

2.3.2 Western Immunoblotting

2.3.2.1 Development of an anti-PagN antiserum

An antibody was required to detect PagN expressed exogenously in *E. coli* and from its native promoter in *Salmonella*. Eurogentec (Belgium) generated an anti-PagN peptide antibody via immunization with a peptide coupled to Keyhole Limpet haemolysin (KLH). The peptide sequence, AGDEHTAYDADTKAA, located in the exposed loop 4 of the protein was chosen. This peptide was chosen as it is surface exposed and the antibody would be able to recognise full-length PagN protein. The peptide-KLH carrier was injected into a rabbit several times over the course of 28 days. After 28 days, the rabbit was sacrificed and antibody was purified from the serum. An ELISA assay was performed to determine the affinity of the antibody to the peptide and the resulting anti-PagN antibody was dispatched.

2.3.2.2 Electro-transfer of separated proteins

Proteins were transferred to PVDF membranes (Biotrace) using an Insight Maxi Semi Dry Electroblotter transfer apparatus (Galileo Bioscience). Briefly, the SDS gel was equilibrated in transfer buffer (25 mM tris, 192 mM glycine, 20% (v/v) methanol) while the PVDF membrane was activated in methanol for 10 sec. Blotting was carried out according to the manufacturer's instructions at 80 mA for 30 min. Following transfer, all membranes were stained with Ponceau S stain to visualise proteins. Excess Ponceau S stain was removed by washing in Millipore purified water. Membranes were incubated in blocking buffer (5% non-fat powdered milk in PBS containing 0.01% Tween-20) at 4 °C overnight or for 1 h at room temperature with shaking.

2.3.2.3 Detection of bound proteins

Blocked membranes were incubated with anti-PagN antiserum diluted 1:1000 in blocking buffer for 1 h at room temperature with shaking. The membrane was then washed three times for 10 min in PBS containing 0.01% Tween-20 and incubated with an HRP-linked anti-rabbit antibody diluted 1:10,000 in blocking buffer for 30 min. The blot was washed as before and proteins were visualized using the SuperSignal West Pico Chemiluminescent HRP substrate (Thermo Scientific). Chemiluminescence was detected using an LAS-4000 Luminescent Image Analyser. Typical exposure length was 10 sec – 5 min.

Membranes that were used as a control for protein expression were blocked as before and washed three times for 5 min in PBS containing 0.01% Tween-20. Following washing, membranes were incubated with monoclonal anti-MBP antibody HRP conjugate diluted 1:2,000 in blocking buffer for 1 hour. Membranes were washed and proteins were visualized as before.

2.4 Phenotypic Assays

2.4.1 Haemagglutination assay

The ability of bacteria to agglutinate erythrocytes was determined using a 1% suspension of human type O^+ erythrocytes. Sterile human blood was diluted 1:10 in PBS to give a 10% suspension of blood, and intact erythrocytes were pelleted by centrifugation at 6,000x *g* for 10 sec. The pellet was resuspended in the same volume of PBS. This process of washing was repeated 3 times, or until the supernatant was clear. The final resuspension of blood was in PBS containing 100 mM mannose. The 10% blood suspension was then diluted 1:10 in mannose-PBS to give a 1% erythrocyte suspension. Mannose was used to inhibit agglutination of erythrocytes mediated by type 1 fimbriae. The OD_{600nm} of overnight cultures of bacteria was measured, and bacteria were sub-cultured in 5 ml fresh L broth to an OD_{600nm} of 0.05. Bacteria were allowed to grow to mid-logarithmic phase and protein expression was induced with 1 mM IPTG. Bacteria were allowed to grow and express protein for a further 3 h. After 3 h of growth, the OD_{600nm} of cultures was measured, and 1 ml of bacteria was centrifuged at 15,800x *g* for 1 min. The supernatant was removed and bacteria were resuspended in an appropriate volume of PBS to a concentration of 10 OD units/ml. The bacteria were 2-fold serially diluted with PBS in a 96-well microtitre plate to give a final volume of 50 µl per well. 50 µl of the 1% erythrocyte suspension was added to each well and the plates were incubated overnight at 4 °C to allow unagglutinated erythrocytes to settle out of suspension.

For bacteria harbouring constitutive expression plasmids, the OD_{600nm} of overnight cultures was measured and 1 ml of bacteria was centrifuged at 15,800x *g* for 1 min. The protocol continued as before.

2.4.2 Autoaggregation assays

The Hek protein has been shown to promote auto-aggregation of bacteria (102). Assays were carried out to ascertain if the same holds true for PagN. Briefly, overnight cultures (30 ml) of *E. coli* XL-1 expressing Hek, or PagN, were grown in L broth, harvested by centrifugation, and resuspended in 5 ml PBS. The OD_{600nm} were measured and adjusted to approximately 4.0 by the addition of PBS. 3 ml of each culture was then transferred to a Kahn tube, a 100 µl sample was taken and the OD_{600nm} measured again to determine the starting OD for each culture (T=0). Further 100 µl samples were taken from the surface of the cultures every 30 min and the OD_{600nm} was measured as before. Assays were performed three times and the rate of autoaggregation was determined by the decrease in optical density over time.

2.4.3 Adhesion, cell association and invasion assays

2.4.3.1 Quantitative cell association and invasion assays

CHO-K1 cells were seeded into 12-well tissue culture plates at a density of 3.4×10^4 cells/well 3 days prior to invasion. HT-29 cells were seeded at a density of 2.5×10^5 cells/well and allowed to grow over four nights at 37 °C in 5% CO_2. One day prior to invasion, the cells were fed. On the day of invasion, the OD_{600nm} of overnight cultures of bacteria was measured, and bacteria were inoculated in 5 ml fresh L broth to an OD_{600nm} of 0.05. Bacteria were allowed to grow to mid-logarithmic phase and protein expression was induced with 1 mM IPTG. Bacteria were allowed to grow and express protein for a further 3 h. Prior to invasion bacteria were diluted 1:500 in warm tissue culture media. The mammalian cell monolayer was washed once in warm PBS, and 1 ml of

bacteria-containing medium was added to each well. In order to initiate contact between the bacteria and the mammalian cells, the plates were centrifuged at 600x *g* for 5 min. Plates containing the bacteria and mammalian cells were incubated at 37 °C in 5% CO_2 for 1 h to allow the bacteria time to adhere to and invade the monolayer. During this time, samples of the medium containing bacteria were diluted and spread on L agar plates to determine the initial inoculum. The infected cells were then washed 5 times with warm PBS to remove any non-adherent bacteria. To determine the total number of cell-associated bacteria, the monolayer was disrupted by treatment with 0.1% Triton X-100 and the released bacteria were enumerated by spreading dilutions on L agar. To determine the number of invasive bacteria, a standard gentamicin protection assay was performed (179). Following the 1 h incubation, the monolayer was washed thrice in warm PBS to remove any non-adherent bacteria. The cells were then incubated with gentamicin (100 µg/ml) for 90 min at 37 °C in 5% CO_2 to kill any extracellular bacteria, washed twice in PBS to remove dead bacteria and gentamicin, and the mammalian cell membrane was disrupted using 0.1% Triton X-100. Bacteria were enumerated as before.

2.4.3.2 Quantitative high-throughput invasion assays

To determine the ability of PagN-expressing bacteria to invade a mammalian cell monolayer in a more quantitative manner, a high-throughput invasion assay was developed based on the previously described method (324). Briefly, CHO-K1 cells were seeded into 96-well Perkin Elmer view plates at a density of 1.0×10^6 cells/plate and allowed to grow over two nights at 37 °C in 5% CO_2. HT-29 cells were seeded at a density of 5.0×10^6 cells/plate and allowed to grow over three nights at 37 °C in 5% CO_2. Overnight cultures of bacteria were sub-inoculated in 5 ml fresh L broth to and OD_{600nm} of 0.1 and allowed to grow for 3 hours. Expression of GFP from pCM01 was induced using 0.2 µg/ml

anhydrotetracycline 30 min prior to the start of invasion. *Salmonella* strains lack the TetR repressor protein leading to constitutive GFP expression. Bacterial cultures were harvested by centrifugation and resuspended in 1 ml of warm cell culture media. Prior to the addition of the bacteria, the mammalian cells were washed in warm PBS. To each well, 50 µl of warm tissue culture media containing bacteria was added. The plates were incubated at 37 °C in 5% CO_2 for 30 min to allow the bacteria to invade the monolayer. The cells were then washed thrice in warm PBS to remove any non-adherent bacteria. A 4% paraformaldehyde solution was added to fix the bacteria and cells. After 30 min, the fixative was removed and 100 µl of PBS was added to each well. Plates were stored overnight at 4 °C.

2.4.3.2.1 Staining of quantitative high-throughput invasion assays for use with the GE Incell Analyzer 2000

Prior to imaging, the extracellular bacteria and the mammalian cells must be stained. The staining protocol was adapted from Steinberg *et al.* (222). The cells were first incubated for 30 min in a blocking solution composed of 0.2% BSA in PBS. The blocking solution was removed and the primary antibody, either mouse monoclonal anti-*Salmonella* LPS antibody or anti-*E. coli* vesicle antibody (P. Owen), was diluted 1:200 in blocking buffer and added to each well. The plates were incubated for a further 1 h. After incubation with the primary antibody, the cells were washed thrice in PBS and the secondary antibody, Alexa fluor 350 goat anti-mouse IgG, was diluted 1:200 in PBS and added to each well. The cells were incubated with the secondary antibody in the dark for 30 min. After incubation with the secondary antibody, the cells were washed thrice in PBS and the nuclear and cytoplasmic stain, Draq5 (Biostatus), was diluted 1:250 in PBS and added to each of the wells. The cells were incubated with the cytoplasmic stain in the dark for at least 30 min. Prior to imaging, the Draq5 was decanted and 100 µl of PBS was added to

each of the wells. Plates were imaged using the GE Incell Analyser, and data was analysed using the Incell analyser software. 10 fields per well were imaged at an average of 40 – 80 mammalian cells per field.

2.4.3.2.2 Staining of quantitative high-throughput invasion assays for use with the Scan^R IX81 (Olympus)

The staining protocol for use with the Olympus microscope was again adapted from Steinberg *et al.* (222). The cells were incubated for 1 h with the primary antibody, either mouse monoclonal anti-*Salmonella* LPS antibody (Abcam) or rabbit polyclonal anti-vesicle antibody (P. Owen), diluted 1:200 in blocking buffer. After incubation with the primary antibody, the cells were washed thrice in PBS and the secondary antibody, Alexa fluor 568 goat anti-mouse IgG or Alexa fluor 568 donkey anti-rabbit, was diluted 1:250 or 1:500 in PBS, and added to each well. The cells were incubated with the secondary antibody in the dark for 30 min. After incubation with the secondary antibody, the cells were washed thrice in PBS and the nucleic acid stain Hoechst (Life Technologies), was diluted 1:5000 in PBS and added to each of the wells. The cells were incubated with the nucleic acid stain in the dark for 20 min. Prior to imaging, the Hoechst was decanted, and 50 µl of PBS was added to each of the wells. Plates were imaged using the Olympus IX81 fluorescent microscope with the Scan^R acquisition programme, and data were analysed using the Columbus Image Data Storage and Analysis System (Perkin Elmer). 12 fields per well were imaged at an average of 100 mammalian cells per field.

2.5 *in silico* Analyses

2.5.1 *in silico* predictions of secondary structure

The secondary structure of the PagN proteins of both *Salmonella* Typhimurium and *Salmonella* Typhi was elucidated using several online tools. The signal sequence of the proteins were analysed using SignalP 4.1 (23). The discrimination score cut-off was calculated to be 0.570, while the score given for the proposed signal sequence was 0.724, indicating that both PagN proteins contain a signal sequence.

In addition to the signal sequence analysis, the online programme PRED-TMBB was used to determine whether the PagN protein of *S.* Typhi was located in the outer-membrane and whether it formed a β-barrel the threshold value was set at 2.965 (12). Finally, the secondary structure of the PagN protein of *S.* Typhi was determined using the web-based Phyre2 modelling programme (186). The model chosen showed 92% of the amino acid residues were modeled at >90% confidence.

Chapter 3 Generation and Optimisation of a high content assay for analysis of invasion

3.1 Introduction

Traditionally, bacterial invasion of mammalian cells is measured by the gentamicin protection assay (GPA) (96). This assay relies on the inability of the aminoglycoside antibiotic gentamicin to penetrate the mammalian cell membrane (342). Bacteria which successfully invade the mammalian cell monolayer are protected from killing, while those that remain extracellular are killed by gentamicin. Intracellular bacteria can be released from the mammalian cells by incubating the monolayer with a low concentration of a non-ionic detergent such as Triton-X-100. The lysates are then diluted, plated on solid media, and subsequently, colonies are counted after incubation. The amount of bacteria recovered is then indexed against the inoculum. Whilst the GPA is a much utilised assay, it can be a cumbersome method for analysing bacterial invasion. Each GPA is carried out with three biological as well as two technical replicates. This makes testing large numbers of samples particularly cumbersome. In addition, the Miles and Misra method, which is often used to enumerate surviving bacteria is inherently variable due to pipetting error caused by infrequently calibrated pipettes. A considerable amount of culture media and other materials are required for the GPA. In addition to the material constraint, the assay is time consuming. Each assay takes up to 5 days to complete from the first seeding of the mammalian cells to the enumeration of bacteria. It is also not possible to simultaneously determine the number of bacteria associating with or invading the mammalian cell monolayer. The GPA also falls short when trying to determine bacterial numbers interacting with or invading

individual cells. Thus, a miniaturised assay that is amenable to higher throughput is desirable. High-throughput assays (using the Cellomics platform) of phagocytosis, phagosome maturation, and bacterial invasion in the context of *Salmonella* were first developed in 2006 by Steinberg *et al.* (323). Previously, experimental procedures had included labour intensive microscopy, whereby each cell or organelle had to be individually observed in a time-consuming process that limited the number of experimental conditions that could be tested.

Fluorescent microscopy has become a useful tool in measuring bacterial invasion (217, 227, 246, 324). The principles behind this assay are much the same as with the GPA; bacteria (albeit fluorescently-labelled) are added to a mammalian cell monolayer and allowed to invade, non-adherent or loosely-adherent bacteria are then removed via several steps of washing, and the monolayer containing bacteria is fixed using paraformaldehyde. Finally, extracellular bacteria are distinguished from those residing within the mammalian cells through the use of an anti-*E. coli* or anti-*Salmonella* primary antibody and a fluorophore-conjugated secondary antibody. Only bacteria that are extracellular are detected with the primary and secondary antibodies.

In this work, two separate microscopes and associated software were used, the GE Incell Analyzer 2000 with Analyzer software, and the Olympus IX81 microscope with Scan^R acquisition and Columbus analysis software.

Both the GE Incell Analyzer and the Olympus microscopes are fluorescent microscopes linked to image analysis systems, which take high resolution images of fluorescent entities (159, 334). High-throughput fluorescent microscopy offers several advantages, including the ability to analyse multiple isolates simultaneously with minimal extra work and the ability to analyse other cellular parameters involved in bacterial cell adhesion and invasion. This chapter describes the development and optimisation of a high-throughput assay using both the GE Incell Analyzer and the Olympus microscope. Two similar but

separate staining methodologies were utilised. This study sought to develop and optimise a high-throughput invasion assay in several different ways:

- GFP labelling of bacteria by allelic replacement.
- GFP labelling of bacteria by over expression.
- Optimisation of the time of invasion.
- Analysis of the optimal bacterial inocula.
- Development of a staining protocol for extracellular bacteria.

3.1.1 Statistical Analyses Utilised

All data presented within tables and graphs in this chapter reflect the mean plus or minus the standard error. When the number of strains tested reached three or more, a one way analysis of variance test was used. The Dunnett post-test analysis was used to compare all means to a control mean as indicated in the text. Statistical significance was described for values where $p < 0.05$.

3.2 Results

3.2.1 Cloning and expression of a *gfp* gene in *Escherichia coli* and *Salmonella*

3.2.1.1 Introduction of a chromosomal *gfp* gene in *E. coli* MC4100

To facilitate visualisation of invasive and non-invasive bacteria using fluorescence microscopy, it was first necessary to render bacteria fluorescent. The strategy taken was to transfer an inducible *gfp*+ gene into the non-essential *cobS* gene of *E. coli*. Allelic exchange was accomplished using the λ red recombinase system (79). *E. coli* strain MC4100 was utilised as it contains a functional *recA* gene making it more amenable to the λ red recombinase system. Furthermore, this strain is non-invasive. Plasmid pKM001 was obtained from Mansson *et al.* (227). This plasmid contains the *gfp*+ gene and chloramphenicol resistance cassette under the control of the tetracycline promoter ($P_{LtetO-1}$). In bacterial strains that lack the Tet repressor, constitutive expression of the *gfp*+ gene is observed.

Briefly, the *gfp*+ gene, chloramphenicol resistance cassette, and $P_{LtetO-1}$ promoter were PCR-amplified from pKM001 along with flanking sequences corresponding to the *cobS* locus on the *E. coli* chromosome using primers P1CobKM and P2CobKM (Table 2.3). The *cobS* gene encodes the cobalamin coenzyme B12 in both *E. coli* and *Salmonella*. The *cobS* gene was chosen as Mansson *et al.* have shown that replacement of this gene with the *gfp*+ gene did not affect bacterial fitness in *E. coli* CFT073 (227). The linear PCR-amplified fragment was then digested with *Dpn*I to remove parental plasmid DNA, purified from an agarose gel and 1 - 2 µg of DNA were transformed into electrocompetent MC4100 containing pKD46. Plasmid pKD46 was

eliminated from transformants by culture at 37 °C without ampicillin. Putative mutants were single colony purified twice and then screened for the presence of the novel mutant allele by PCR. The successful GFP-expressing strain was named SPD1.

Initial high-throughput fluorescent invasion experiments using the GE Incell Analyzer suggested that SPD1 was not sufficiently fluorescent for use in this assay. It was proposed that although the *gfp*+ gene is constitutively expressed in SPD1, it is only expressed as a single copy within the *E. coli* genome meaning that the level of fluorescence produced is not sufficiently intense to permit detection. A control strain expressing GFP from a multi-copy plasmid was visible using the fluorescent microscope. In order to facilitate enhanced expression of GFP and thus permit detection, plasmids expressing GFP as well as the protein of interest, e.g. PagN, were generated.

3.2.1.2 Cloning of the *gfp* gene into the *bla* locus of plasmids pML1 and pTrc99a

In order to increase the copy number of the *gfp*+ gene within the bacteria, the gene was inserted into the *bla* locus, encoding ampicillin resistance, of plasmids containing a gene of interest, e.g. *pagN*, as well as the empty vector plasmid. The *bla* locus for β-lactam resistance was chosen as it would enable rapid screening of colonies that are rendered ampicillin sensitive and chloramphenicol resistant. Primers P1GFP and P2GFP (Table 2.3) were designed to amplify the *gfp*+ gene, chloramphenicol resistance cassette, and $P_{LtetO-1}$ promoter in pKM001 as before. The blunt-end PCR product containing restriction endonuclease *Sca*I sites was purified. Plasmids pML1 (containing the *pagN* gene) and pTrc99a (vector plasmid) were digested with *Sca*I (NEB) and agarose gel purified. Digested vectors were ligated with the PCR product using T4 DNA Ligase (NEB), concentrated using pellet-paint, then transformed into NEB5α High-efficiency electrocompetent cells. Plasmids were

extracted from the bacteria and the orientation of the *gfp*+ gene was assessed by digestion with *Hind*III (NEB) followed by separation on an agarose gel (Fig. 3.1). Plasmids containing the correct *gfp*+ orientation were transformed into electrocompetent *E. coli* XL-1 cells, and re-named pSP4 (*pagN* and *gfp*+) and pSP5 (vector and *gfp*+), respectively. A schematic of plasmid generation can be seen in Fig. 3.2.

3.2.1.3 GFP expressed from plasmid pSP4 and pSP5 affects invasion of CHO-K1 cells

Production of GFP is a costly process in terms of bacterial fitness (282). Since *E. coli* strains XL-1 Blue and DH5α, which were used in previous GPA assays, lack the TetR repressor protein, they constitutively express GFP. Therefore, it was important to determine whether the constant synthesis and expression of GFP presented a large enough fitness cost to the bacterium to affect invasion of a mammalian cell monolayer.

Chinese hamster ovary (CHO-K1) cells display typical epithelial cell morphology and are a useful tool for the study of bacterial adhesion and invasion as there are a number of mutant cell lines available that are lacking various cell-surface components (288). These cells are easily cultured and are readily invaded by strains of pathogenic *S.* Typhimurium (83) and *E. coli* (110). To investigate whether the overproduction of GFP prevents epithelial cell invasion, standard gentamicin protection assays were performed as described in Section 2.4.3.1. *E. coli* XL-1 carrying plasmid pML1, the parent plasmid to the *gfp*+ expressing pSP4, were included as a positive control.

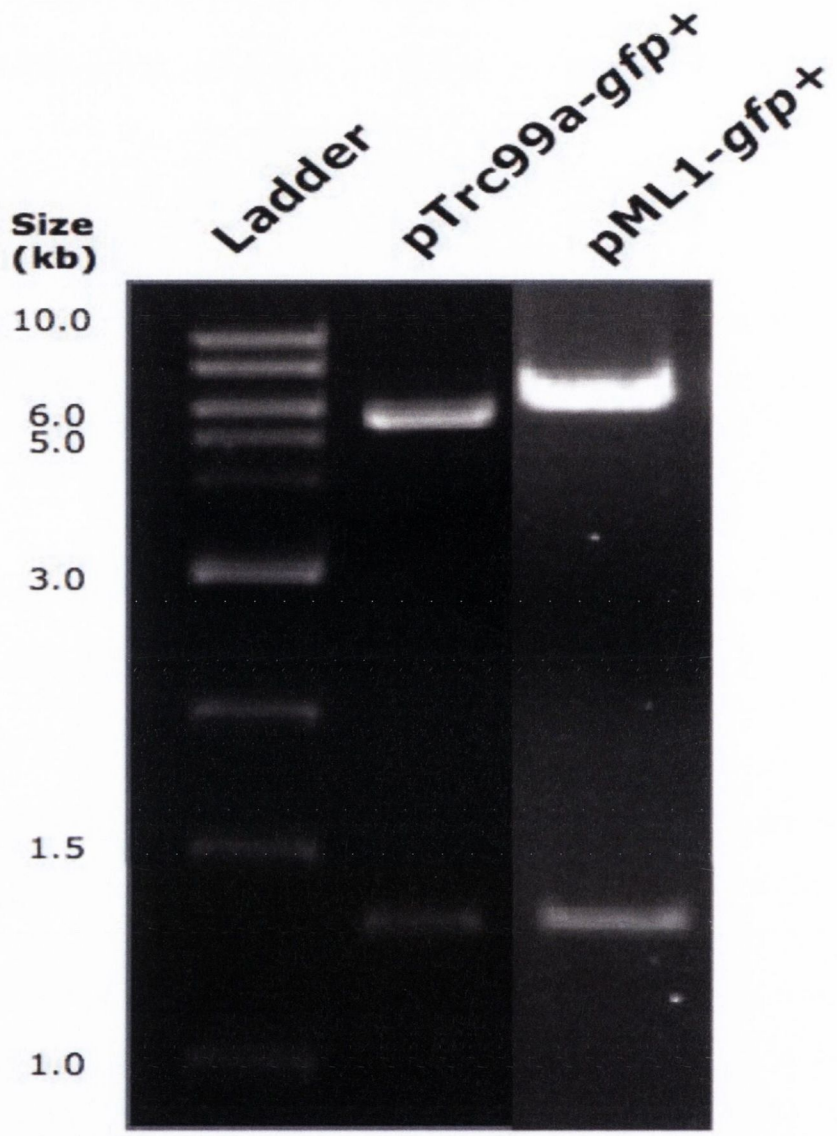

FIG. 3.1. Confirmation of the correct orientation of the *gfp*+ gene in plasmids pSP4 and pSP5. Plasmids pTrc99a-*gfp*+ (pSP4) and pML1-*gfp*+ (pSP5) were digested with *Hind*III and the resulting fragments were separated on a 1% agarose gel. Lane 1 contains a 1 kbp DNA ladder. Several putative clones were electrophoresed using the same agarose gel; for clarity, only the clones used in high throughput assays are shown.

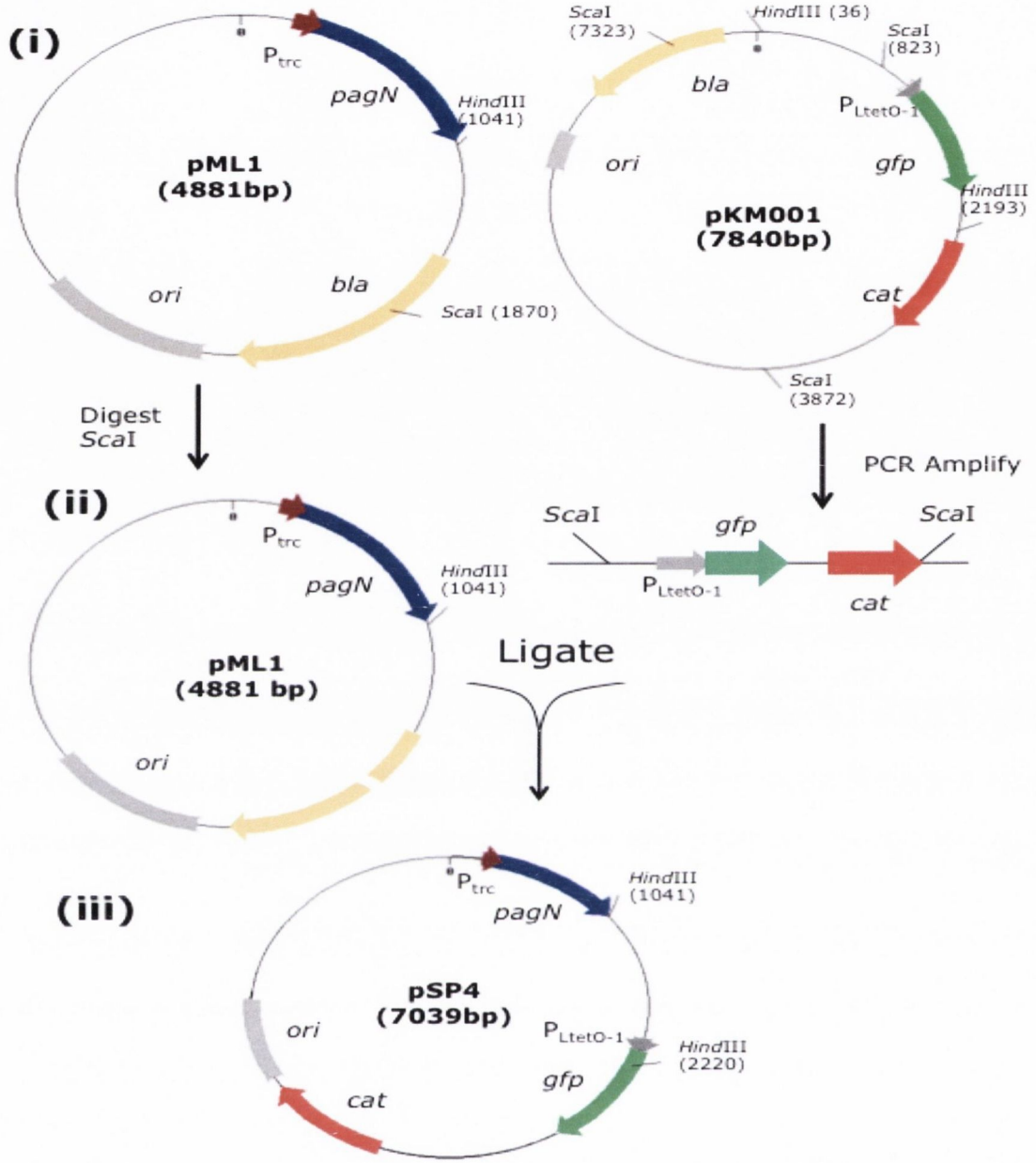

FIG. 3.2. Schematic of the construction of plasmid pSP4. (i) plasmid pML1 containing the *pagN* gene under the control of the P_{trc} promoter was digested with *Sca*I to disrupt the *bla* gene. The *gfp* and *cat* genes as well as the $P_{LtetO-1}$ promoter were amplified from plasmid pKM001 by PCR. (ii) The ~2.2 kb *gfp*-containing fragment was ligated into the digested pML1 plasmid giving rise to (iii) plasmid pSP4. The positions of the *pagN*, *bla*, *gfp*, and *cat* genes are indicated. Restriction endonuclease sites used in the construction of the plasmid, and those used for diagnostic tests are marked.

Table 3.1. Interaction of *E. coli* K-12 expressing PagN or PagN and GFP with CHO-K1 cells

Protein Expressed	Percentage Invasion
PagN	64.18 ± 19.44
None	0.07 ± 0.01**
PagN-GFP	10.52 ± 4.13 *
GFP	0.002 ± 0.001**

Percentage invasion refers to the percentage of bacteria that were successful in invasion when compared with the number of bacteria present in the initial inoculum. $n = 3$. * indicates $p < 0.05$, ** indicates $p < 0.001$. Data were analysed using the one way analysis of variance with the Dunnett post test to compare all means to the bacteria expressing PagN only.

When PagN was over expressed in *E. coli* K-12 strain XL-1, more than 60% of the inoculum expressing PagN were internalised by, CHO-K1 cells (Table 3.1). Large-scale uptake of bacteria into the non-phagocytic CHO-K1 monolayer took place. When compared with bacteria expressing both PagN and GFP, the PagN-only expressing bacteria were significantly more invasive ($p < 0.05$). Of the initial inocula of PagN-only expressing bacteria, 64.2% were able to invade the CHO-K1 cell monolayer, while only 10.5% of bacteria expressing both PagN and GFP were invasive. These data indicate that the overproduction of GFP by *E. coli* dampens bacterial invasion.

GFP production was imperative for the visualisation of internalised bacteria in the high-throughput fluorescent assay, and as such it became necessary to obtain a separate low-copy number (~15 copies per cell) GFP expressing plasmid that is compatible with pTrc99a and pBlueScriptII derived plasmids. Thus, pCM01 was used to visualize bacteria.

The low copy-number plasmid pCM01 was created by Clodagh Murphy (253) to counteract the decreased invasion observed by the over expression of GFP. A map of plasmid pCM01 is shown in Fig. 3.3.

3.2.1.4 GFP induction does not affect bacterial invasion

As shown in Table 3.1, the constant overproduction of GFP produces enough of a fitness burden to the bacterium to impede epithelial cell invasion. A new level of control of GFP expression was obtained using *E. coli* K-12 strain, DH5αZ1 (220). The DH5αZ1 strain is distinct from its parent, DH5α, in that it contains the gene for the TetR repressor protein. In strains containing the *tetR* gene, the translated protein binds to operator sequences thereby blocking gene transcription. Addition of exogenous tetracycline (Tc), or tetracycline derivatives, relieves gene repression by TetR by dissociating TetR from the operator DNA sequence (25). In the DH5αZ1 strain, GFP synthesis is turned off until addition of anhydrotetracycline (ATc). ATc is a synthetic derivative of tetracycline that has lost its antibiotic ability while still displaying a high affinity for TetR (210).

Growth of *E. coli* DH5αZ1 expressing GFP from the inducible tetracycline promoter was tested in the presence of ATc/GFP and for invasion of CHO-K1 cells. To determine the effect of GFP on bacterial viability, overnight cultures of DH5αZ1 or DH5αZ1 pCM01 were sub-inoculated to an OD_{600nm} of 0.05 and grown at 37 °C with shaking for up to 5 hours. Every 30 min, the OD_{600nm} was measured and a sample of the culture was taken, serially diluted, and spread on agar plates for enumeration. ATc was added at a final concentration of 0.2 µg/ml after 3 hours of incubation. The results are shown in Fig. 3.4.

After the addition of ATc, bacteria expressing GFP continue to grow normally for 60 min, after which there is a sharp decline in the number of viable bacteria (Fig. 3.4 panel b); however, this decline in the viable count is not represented in the OD_{600nm}.

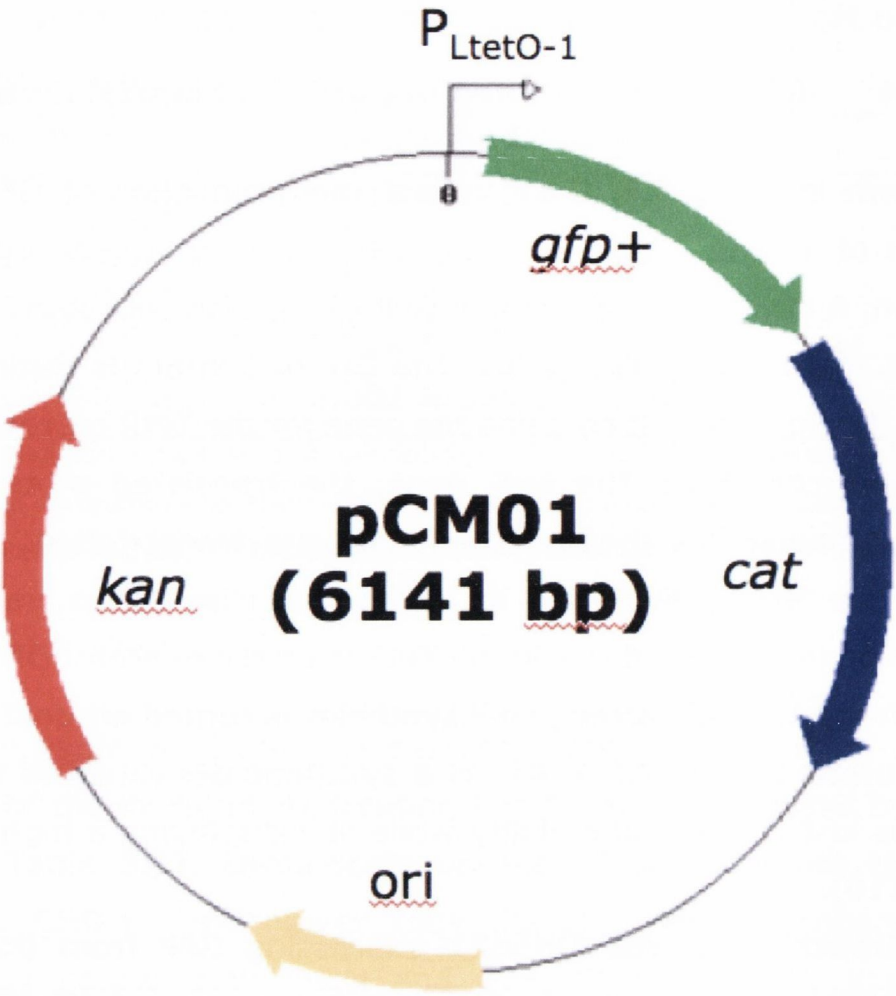

FIG. 3.3. Map of the plasmid pCM01. The positions of the *gfp+*, *kan*, and *cat* genes are indicated as is the $P_{LtetO-1}$ promoter for tetracycline resistance. The origin of replication is indicated which gives rise to a copy number of ~15 plasmids/cell.

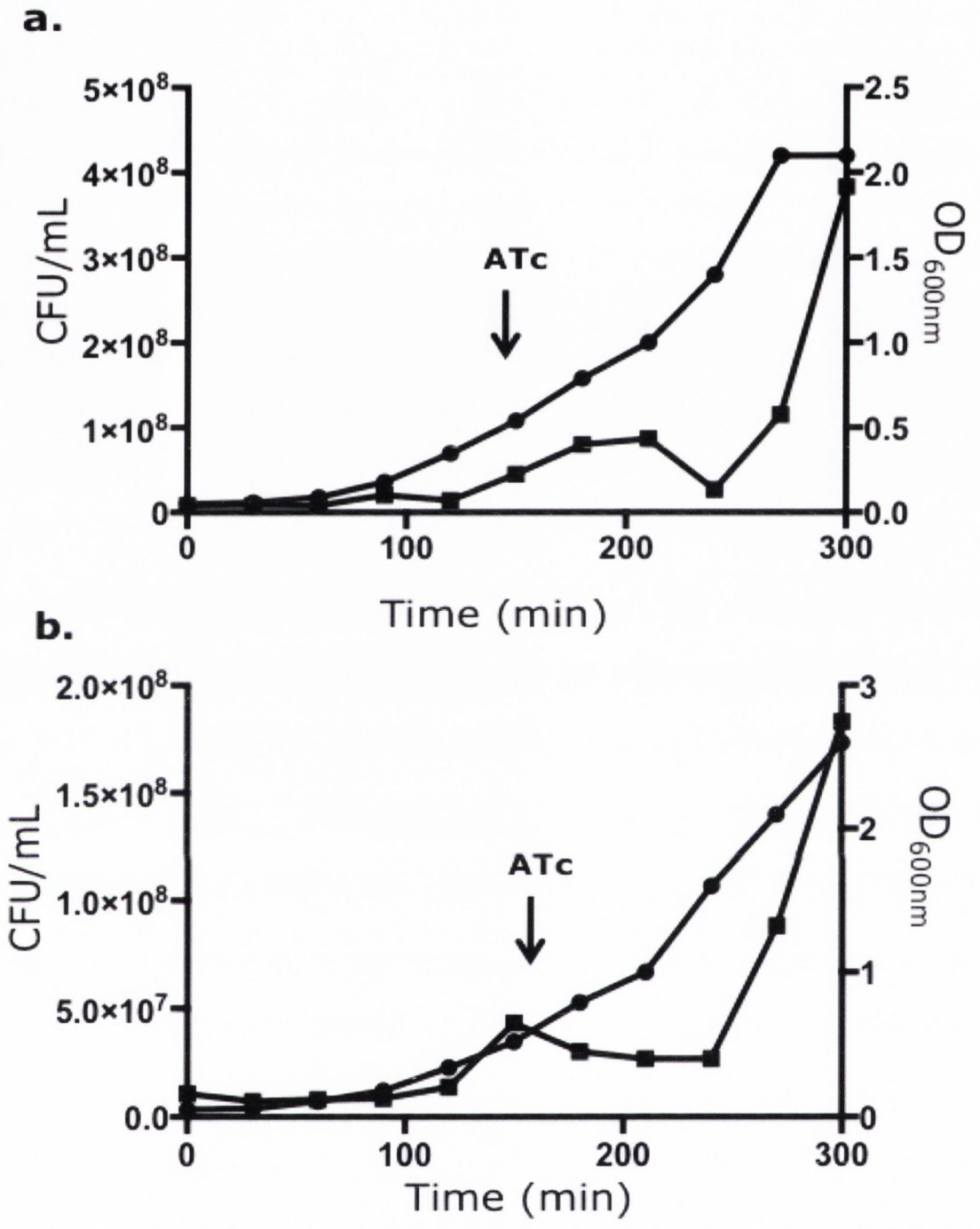

FIG. 3.4. Growth of *E. coli* DH5αZ1 expressing *gfp*+ over time. Overnight cultures of bacteria harbouring plasmid pCM01 were sub-inoculated to an OD_{600nm} of 0.05, samples were taken and dilutions were plated on solid agar. Every hour, the OD_{600nm} of the culture was measured and a viable count was performed. Panel a depicts the CFU/mL and OD_{600nm} of DH5αZ1 while panel b displayed the same for DH5αZ1 harbouring pCM01. The circles represent the OD_{600nm} of the bacteria while the squares represent the CFU/mL. ATc was added after 180 minutes.

When this experiment was performed with *E. coli* XL-1 Blue (which lack *tetR*), bacteria became unable to effectively divide, instead forming long aggregates, which can account for the increase in the optical density of the bacteria while the viable count decreased (data not shown). This, however, is not the case for DH5αZ1 bacteria. There is also a decrease in viable count seen after the addition of ATc to cultures of DH5αZ1 that are unable to produce GFP. The decrease seen in non-*gfp*+ expressing cells coupled with the fact that when viewed under a microscope, bacteria do not appear to be growing aberrantly, point towards a different reason for the decrease in viable count. In both cases, the bacteria are able to rebound and the viable count reaches more than 1.0 x 10^8 CFU/ml by 5 hours incubation.

In order to determine whether the decrease in the number of viable bacteria as a result of ATc induction of GFP affected the ability of the bacteria to invade mammalian cells, a GPA was performed. In this assay, DH5αZ1 bacteria expressing either PagN from pML1 or PagN and GFP from pML1 and pCM01, respectively, were tested for mammalian cell invasion by GPA. DH5αZ1 bacteria were also tested to determine whether they possess an innate ability to invade mammalian cells (Table 3.2).

Table 3.2. Interaction of *E. coli* DH5αZ1 expressing PagN or PagN and GFP with CHO-K1 cells

Protein Expressed	Percentage Invasion
None	0.07 ± 0.09**
PagN	3.06 ± 0.291
PagN and GFP	10.7 ± 1.95 *
GFP	0.05 ± 0.07**

Percentage invasion refers to the percentage of bacteria that were successful in invasion when compared with the number of bacteria present in the initial inoculum. $n = 3$. * indicates $p < 0.05$, ** indicates $p < 0.001$, Data were analysed using the one way analysis of variance with the Dunnett post test to compare all means to the bacteria expressing PagN only.

When PagN was over expressed in *E. coli* K-12 strain DH5αZ1, 3% of the inoculum expressing PagN bound to, and were internalised by, CHO-K1 cells (Table 3.2). When compared with bacteria expressing both PagN and GFP, the PagN-only expressing bacteria were significantly less invasive ($p < 0.05$). Only 3% of the initial inocula of PagN-only expressing bacteria were able to invade the CHO-K1 cell monolayer, while 10.7% of bacteria expressing both PagN and GFP were invasive. The presence of GFP appears to be beneficial for bacterial invasion of mammalian cells; however this is only true for bacteria expressing both PagN and GFP. Bacteria that expressed GFP only were unable to effectively invade the CHO-K1 cell monolayer (<1% invasion). As all bacteria used in the high-throughput fluorescence assay expressed GFP from plasmid pCM01, relative defects in invasion and adhesion could still be accurately measured.

There are many pathogenic strains of *E. coli* that are capable of invasion. It was important to determine whether *E. coli* DH5αZ1 was intrinsically invasive in the absence of adhesins such as PagN. Less than 1% of DH5αZ1 were able to invade the mammalian cell monolayer. This is significantly lower than bacteria expressing PagN ($p < 0.0002$). These

data indicate that the controlled production of GFP by *E. coli* does not interfere with invasion; instead, it provides an unexpected invasion advantage.

3.2.2 Development of a high content invasion assay for *E. coli* and *Salmonella* using the GE Incell Analyzer 2000

3.2.2.1 Determination of the optimal time of invasion

The first step in the development and optimisation of a high content invasion assay involved testing several different invasion times. *Salmonella* possess the ability to modify vacuoles within the host cell to prevent acidification and subsequent death. It is imperative to stop the invasion via fixation with paraformaldehyde prior to the start of intracellular replication as failure to stop the assay at the appropriate time leads to skewing of the results. For *E. coli*, however, bacterial intracellular multiplication is less of a problem.

The main advantage of the high-content assay is the ability to rapidly compare invasion and adhesion of bacteria in half of the time required for the GPA. A high-throughput invasion assay comprising of *E. coli* DH5α expressing GFP from pCM01 and PagN from pML1 was performed as described in Section 2.4.3.2 to determine whether bacteria began replicating intracellularly within the 60 minute invasion time, as well as determining whether there was a difference in adhesion or invasion when the assay was allowed to progress from between 5 and 60 min. Extracellular bacteria were not distinguished from those that had invaded the monolayer, and the results given in Table 3.3 indicate bacteria that have either invaded or adhered to the mammalian cell monolayer the mammalian cell monolayer.

Table 3.3. Characterisation of *E. coli* DH5α association with CHO-K1 cells using the GE Incell Analyzer microscope.

Time (min)	Average number of bacteria per CHO cell
5	2.04 ± 0.13
10	3.28 ± 0.65
15	3.62 ± 0.57
20	5.81 ± 1.10
25	5.81 ± 1.10
30	6.26 ± 0.62
40	7.57 ± 1.03
60	11.82 ± 0.49

Cell association indicates the number of bacteria that have either invaded or are adherent to the mammalian cell monolayer. $n = 1$.

As this assay was performed without the use antibody labelling, it was impossible to distinguish intracellular versus extracellular bacteria and thus invasive versus adherent bacteria. For the following optimisation steps, an invasion time of between 20 and 25 min was chosen as the number of bacteria interacting with the CHO cell monolayer stayed constant during this time.

A second high-throughput invasion assay comprising of *S.* Typhimurium SL1344 harbouring pCM01 was also performed as described in Section 2.4.3.2. Again, extracellular bacteria were not distinguished from those that had invaded the monolayer, and the results given in Table 3.4 indicate bacteria that are associated with the mammalian cell monolayer.

Table 3.4. Characterisation of *Salmonella* association with CHO-K1 cells over time.

Time (min)	Average number of bacteria per CHO cell
10	0.540 ± 0.17
15	1.47 ± 0.24
20	2.72 ± 0.41
30	3.38 ± 0.69
40	4.63 ± 0.27
60	7.15 ± 1.81

Cell association indicates the number of bacteria that have either invaded or are adherent to the mammalian cell monolayer. $n = 1$.

As described for the high-throughput assay for *E. coli* invasion, this assay was performed without the use of antibody labelling, and an invasion time of 30 min was chosen for ease of use.

3.2.2.2 Analysis of the change in bacterial invasion and adhesion in a dose dependent manner

Once the optimal time of invasion was determined, it was necessary to find the optimal quantity of bacteria or multiplicity of infection to add to the mammalian cell monolayer. High content invasion assays utilising *E. coli* DH5α (pCM01 pML1) were performed as before, and several different multiplicities of infection (MOIs) were tested. Briefly, overnight cultures of bacteria were sub-inoculated to OD_{600nm} 0.05. Cultures were then grown to mid-logarithmic phase at which point IPTG (1 mM) was added to induce expression of *pagN.* Following a further 3 hours of growth, 1 ml of culture was harvested by centrifugation and the bacteria were resuspended in 1 ml of pre-warmed cell-culture media. 50 µL of media were maintained on the mammalian cell monolayer at all times,

meaning for inocula of less than 50 µL, sterile DMEM was added to make up the difference. The changes in invasion and adhesion of bacteria to the monolayer are shown in Table 3.5.

Table 3.5. M.O.I. and Relative adherence to and invasion of CHO-K1 cells by PagN-expressing *E. coli*.

MOI	Invasive	Adherent
10	0.099 ± 0.013	0.015 ± 0.003
30	0.25 ± 0.030	0.027 ± 0.004
40	0.27 ± 0.009	0.023 ± 0.005
55	0.40 ± 0.023	0.023 ± 0.007
70	0.72 ± 0.065	0.044 ± 0.014
80	1.25 ± 0.157	0.035 ± 0.011
100	2.20 ± 0.255	0.044 ± 0.007
140	2.49 ± 0.762	0.058 ± 0.009

The average number of bacteria per CHO-K1 cell are indicated above. M.O.I. indicates the multiplicity of infection. Standard error is given. $n = 1$.

The average number of invasive bacteria was quite low (2.49 bacteria/CHO-K1 cell for an MOI of 140). However, when compared with an initial inocula of 10 bacteria/CHO, the increase in invasion appears much larger. The observed increase in adhesion and invasion corresponds to the addition of an excess of bacteria. An M.O.I. of 140 was chosen.

3.2.2.3 Optimisation of the detection of extracellular bacteria

The protocol for bacteria and CHO-K1 cell staining was adapted from Steinberg *et al.* in their 2007 paper on phagosome maturation and bacterial invasion (330). In that paper, extracellular bacteria were distinguished from those that had invaded the human HeLa cell line using a rabbit anti-*Salmonella* antibody diluted 1:250 in PBS and a Cy2-

conjugated donkey anti-rabbit secondary antibody (324). As a commercially unavailable anti-*E. coli* vesicle antibody raised in rabbits (provided by Prof. P. Owen) was used, it was necessary to determine not only the optimal concentration of the secondary antibody, but also whether it was necessary to pre-incubate the mammalian cell monolayer with a blocking buffer composed of 0.2% BSA in PBS.

To determine the optimal staining procedure, a final high-throughput invasion assay was performed using *E. coli* DH5α harbouring pML1 and pCM01. Bacteria were incubated with the CHO-K1 cell monolayer for 30 min before non-adherent and loosely adherent bacteria were removed via 3 washes in PBS and fixed in 4% paraformaldehyde. A range of blocking times from no blocking to 30 or 60 min incubation in blocking buffer was tested. The primary antibody concentration was kept static at 1:200 diluted in blocking buffer, while secondary antibody concentrations of 1:100 or 1:200 (in PBS) were tested. The data shown in Fig. 3.5 indicates the average number of extracellular bacteria per CHO-K1 cell. The wells treated with no prior incubation with blocking buffer and a secondary antibody concentration of 1:100 yielded the highest number of visible extracellular bacteria with an average of ~0.2 bacteria per CHO cell. Data were analysed using the one way ANOVA method. A post-test Dunnett test was performed to compare all means to the the wells containing bacteria exposed to the highest concentration of antibody with the lowest blocking time. No significant differences in the number of bacteria detected per CHO-K1 cell were observed between the staining protocols.

The same assay and staining procedure was performed for *S.* Typhimurium SL1344 pCM01, however, instead of using the anti-vesicle primary antibody, a mouse monoclonal anti-*Salmonella* LPS primary antibody was used at 1:200 concentration. As with *E. coli*, the wells treated with no prior incubation with blocking buffer and a secondary antibody concentration of 1:100 yielded the highest number of visible

extracellular bacteria with an average of ~ 1 bacterium per CHO cell (Fig. 3.6).

While initial experiments carried out using the GE Incell Analyzer microscope were valuable in determining the optimal time of invasion and the optimal concentration of bacteria, it became apparent that the equipment would not suit the needs of this study. The staining of extracellular bacteria was extremely difficult as the wavelengths emitted by the mammalian cell stain DRAQ5 and GFP forced the secondary antibody emission wavelength close to ultraviolet in the spectrum of light. The GE Incell Analyzer was unable to accurately and easily discern the wavelength emitted by the secondary antibody, forcing a move to the Olympus IX81 platform. A typical set of images generated by the GE Incell Analyzer is displayed in Fig. 3.7.

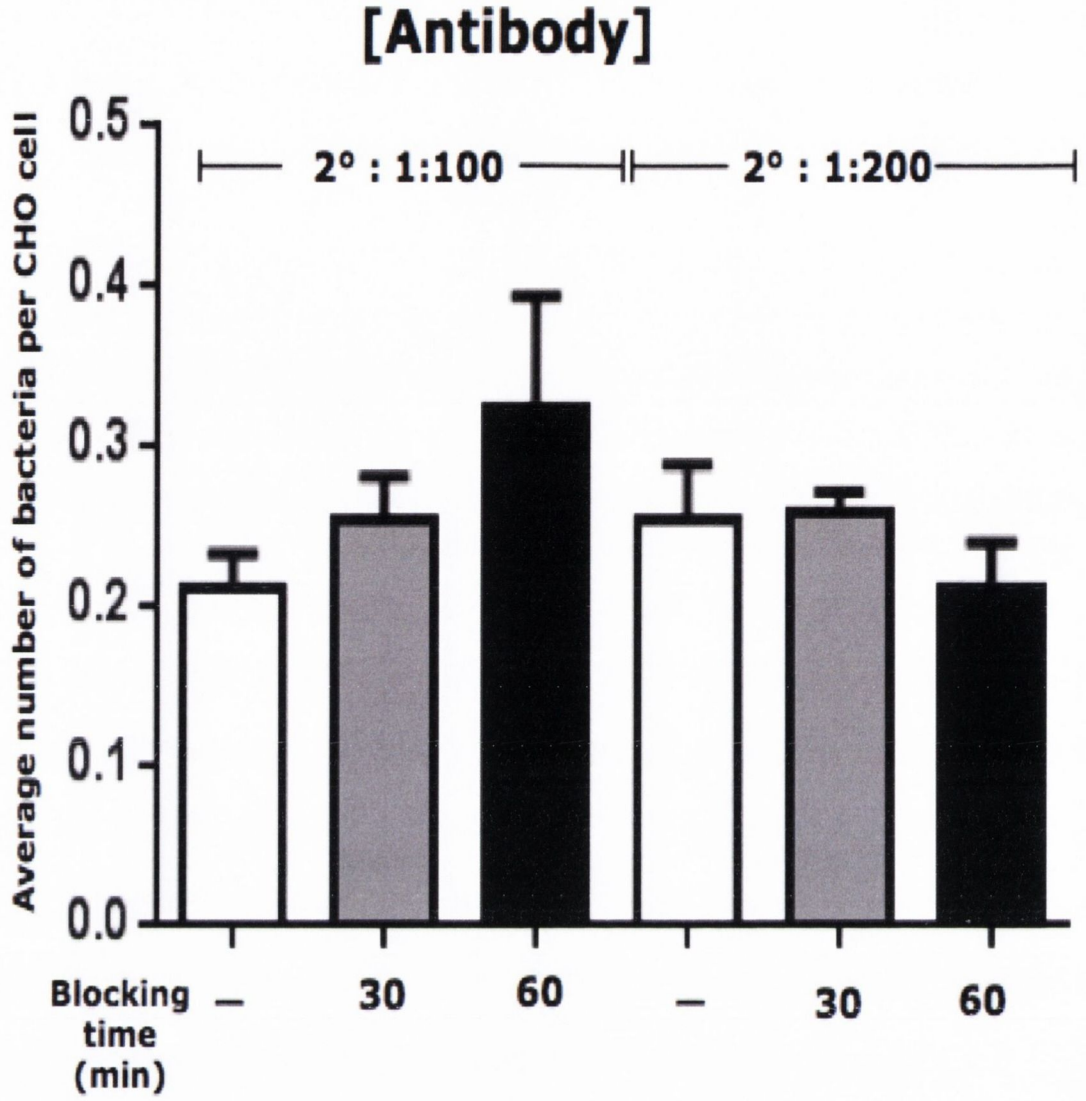

FIG 3.5. Optimisation of the staining of extracellular *Escherichia coli* in a high-throughput assay. The average number of *E. coli* DH5α expressing *pagN* from plasmid pML1 and *gfp+* from plasmid pCM01 adhering to CHO-K1 cells was calculated. A range of staining procedures were tested and standard error bars are shown. – indicates no blocking while some wells were incubated for 30 or 60 minutes of blocking in 0.2% BSA prior to the addition of the primary anti-vesicle antibody. Secondary antibody at a concentration of 1:100 or 1:200 was also tested. $n = 3$. Data were analysed using the one way ANOVA method. A post-test Dunnett test was performed to compare all means to the the wells containing bacteria exposed to the highest concentration of antibody with the lowest blocking time. Statistical significance was determined for $p < 0.05$.

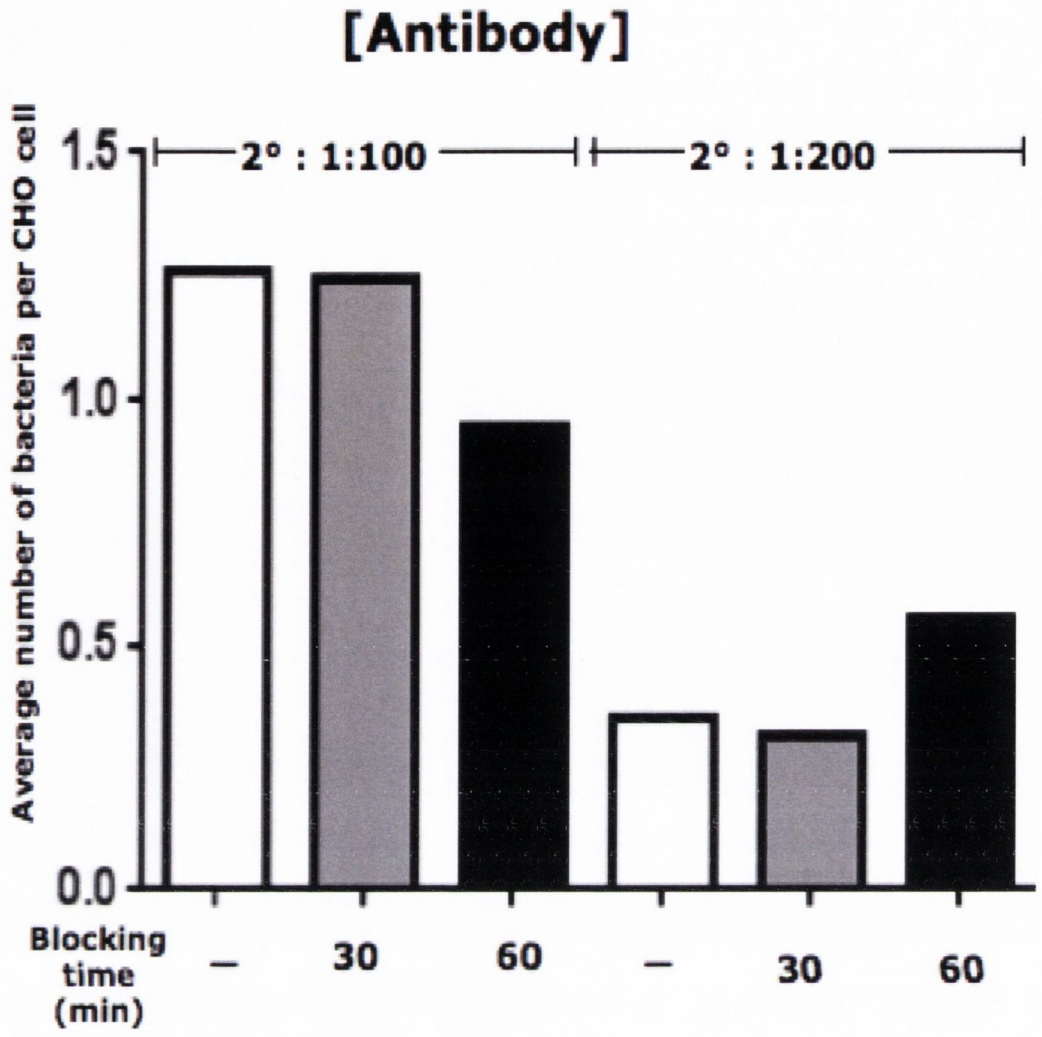

FIG 3.6. Optimisation of the staining of extracellular *Salmonella* in a high-throughput assay. The average number of *S.* Typhimurium SL1344 expressing *gfp+* from plasmid pCM01 adhering to CHO-K1 cells was calculated. A range of staining procedures were tested and standard error bars are shown. – indicates no blocking while some wells were incubated for 30 or 60 minutes of blocking in 0.2% BSA prior to the addition of the primary anti-vesicle antibody. Secondary antibody at a concentration of 1:100 or 1:200 were also tested. $n = 1$.

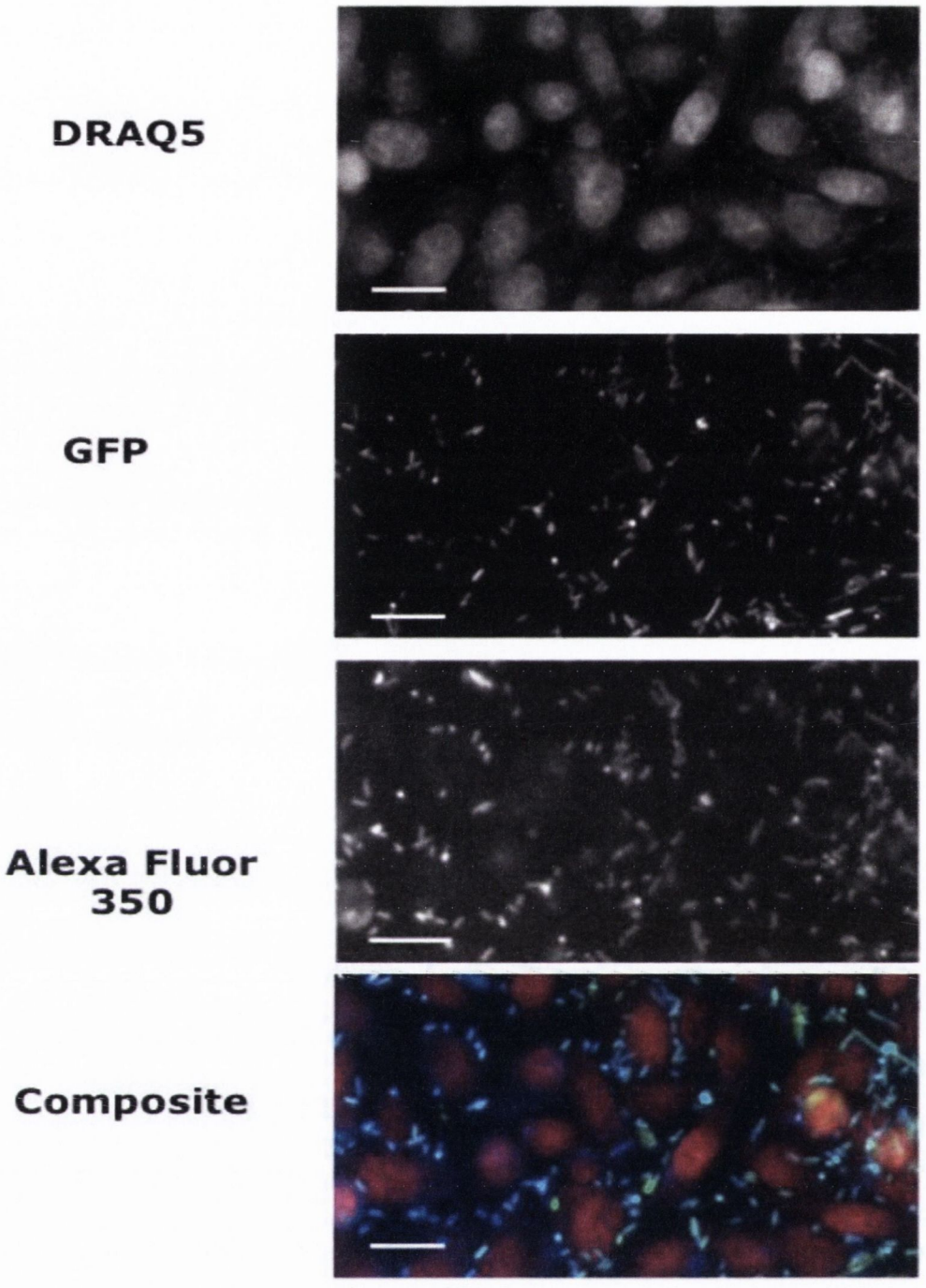

FIG. 3.7. Images of *E. coli* generated using the GE Incell Analyzer. CHO-K1 mammalian cells were stained using DRAQ5, bacteria express GFP from plasmid pCM01, and extracellular bacteria were stained using an anti-vesicle primary antibody and the Alexa fluor 350 secondary antibody. The white bar indicates 20 μm.

3.2.3 Development of a high content invasion assay for *E. coli* and *Salmonella* using the Olympus IX81 microscope

3.2.3.1 Determination of the optimal time of invasion

As discussed in Section 3.2.2.1, it was necessary to determine the optimal time of invasion for the high content platform. A high-throughput invasion assay comprising of *E. coli* DH5αZ1 containing pCM01 was performed in triplicate as described in Section 2.4.3.2. In contrast to experiments performed with the GE Incell Analyzer, extracellular bacteria were distinguished from those that had invaded the mammalian cell monolayer, and the results given in Table 3.6 indicate bacteria that are either adherent to the mammalian cell monolayer or those that were successful in invasion.

Table 3.6. Characterisation of *E. coli* DH5αZ1 expressing PagN associated with CHO-K1 cells.

Time (min)	Invasion	Adhesion
10	8.56 ± 1.37	1.20 ± 0.41*
15	6.94 ± 1.69	2.64 ± 0.26
20	6.03 ± 0.10*	2.63 ± 0.18
25	7.04 ± 0.24	2.18 ± 0.06*
30	6.68 ± 0.08	2.94 ± 0.27
40	7.63 ± 0.52	3.25 ± 0.31
50	9.15 ± 0.54	3.50 ± 0.28
60	9.93 ± 0.05	3.26 ± 0.11

Cell association and invasion levels are given as the average number of bacteria per CHO-K1 cell. $n = 3$. * indicates $p < 0.05$ as measured using the one-way ANOVA

method with the Dunnett post-test to compare all means to the 60 minute time point. 60 minutes was chosen as this is the normal length of invasion used in the GPA.

There was no significant difference in bacterial invasion of CHO-K1 cells between 60 min invasion and 10 min invasion ($p = 0.477$). For adhesion, however, there was a statistically significant increase in bacterial adhesion when the experiment is allowed to progress for between 10 and either 25 or 60 min ($p < 0.05$, measured using the one-way ANOVA method with the Dunnett post-test to compare the means to the 60 minute time point).

One of the major drawbacks of the GPA is the time required to complete the assay, from the first hour long incubation with bacteria to the 90 minute long incubation with gentamicin. Since there was no significant difference between an invasion time of 30 min or 60 min, the 30 minute invasion time was chosen.

A second high-throughput invasion assay comprising of *S.* Typhimurium SL1344 pCM01 was also performed. Again, for this assay, extracellular bacteria were distinguished from those that had invaded the monolayer, and the results given in Table 3.7 indicate bacteria that have successfully invaded the mammalian cell monolayer or those which are adherent to the cells.

Table 3.7. Characterisation of *Salmonella* association with CHO-K1 cells over time.

Time (min)	Invasion	Adhesion
10	1.48 ± 0.15*	0.92 ± 0.05*
15	1.61 ± 0.13*	1.22 ± 0.10*
20	1.34 ± 0.13*	1.08 ± 0.13*
25	1.55 ± 0.13*	1.40 ± 0.05*
30	1.63 ± 0.26 *	1.42 ± 0.07*
40	2.67 ± 0.54	1.89 ± 0.12*
50	2.72 ± 0.15	2.57 ± 0.18*
60	2.94 ± 0.21	3.02 ± 0.08

Cell association and invasion levels are given as the average number of bacteria per CHO-K1 cell. $n = 3$. * indicates $p < 0.05$ as measured using the one-way ANOVA method with the Dunnett post-test to compare all means to the 60 minute time point. 60 minutes was chosen as this is the normal length of invasion used in the GPA.

For *Salmonella*, there was a significant difference in bacterial invasion of CHO-K1 cells between 10, 15, 20, 25, 30 and 60 min invasion ($p < 0.005$). As *Salmonella* are able to modify the *Salmonella* containing vacuole (SCV) within epithelial cells to allow for bacterial replication, and the bacteria have an average doubling time of 25 min, it is possible that after 30 min of invasion, the bacteria begin replicating intracellularly, which leads to skewing of the results and the statistically significant increase in invasion after 30 min. To combat this misrepresentation, an invasion time of 30 min was chosen because the bacteria are able to efficiently invade the monolayer but have not yet begun intracellular replication.

3.2.3.2 Dose dependent bacterial invasion and adhesion

As before, it was necessary to find the optimal quantity of bacteria to add to each well. High content invasion assays utilising *E. coli* DH5αZ1 pCM01 pML1 were performed, and a range of bacterial concentrations were tested from a multiplicity of infection (MOI) of 10 to an MOI of 90. The changes in invasion and adhesion of bacteria to the monolayer are shown in Table 3.8, which represent the average of triplicate cultures tested in quadruplicate.

Table 3.8. Analysis of the change in PagN expressing *E. coli* adherence to and invasion of CHO-K1 cells.

MOI	Invasion	Adhesion
10	3.90 ± 0.24	1.39 ± 0.17*
20	3.68 ± 0.07	2.26 ± 0.07
30	3.66 ± 0.13	2.45 ± 0.08
35	3.45 ± 0.16	2.32 ± 0.04
45	3.29 ± 0.01	2.32 ± 0.18
50	3.34 ± 0.29	2.56 ± 0.25
70	3.22 ± 0.10	2.51 ± 0.08
90	3.38 ± 0.23	2.72 ± 0.32

Cell adhesion and invasion levels are given as the average number of bacteria per CHO-K1 cell. M.O.I. indicates the multiplicity of infection. $n = 3$. * indicates $p < 0.05$ * indicates $p < 0.05$ as measured using the one-way ANOVA method with the Dunnett post-test to compare all means to an MOI of 90.

The average number of invasive bacteria was slightly increased compared to the previous optimisation step (3.38 bacteria/CHO versus 2.49 bacteria/CHO for the GE Incell Analyzer). The difference in perceived invasivity was due to the change in staining procedure and the greater sensitivity of the Olympus microscope. There was no significant increase in the number of invasive *E. coli* interacting with the CHO-K1 cell monolayer when the initial inoculum was increased from an MOI of 10 to 90 as measured using a one-way ANOVA method and

Dunnett post-test to compare all MOIs to an MOI of 90; however, there was an increase in bacterial adhesion when an MOI of 10 was compared with an MOI of 90 (when measured as described above). It is possible that the bacteria behave cooperatively to facilitate adhesion, indicating that the higher initial inoculum provides more bacteria to mediate attachment to the mammalian cell monolayer. For ease of use, an M.O.I. of 90 was chosen.

A similar assay was performed with *Salmonella* Typhimurium SL1344 harbouring pCM01. The changes in invasion and adhesion of *Salmonella* to the monolayer are shown in Table 3.9.

Table 3.9. Analysis of the change in *S.* Typhimurium SL1344 adherence to and invasion of CHO-K1 cells in a dose dependent high-throughput assay.

MOI	Invasion	Adhesion
1	0.56 ± 0.06*	0.43 ± 0.08*
2	0.51 ± 0.08*	0.51 ± 0.09*
3	0.53 ± 0.12*	0.59 ± 0.08*
4	0.55 ± 0.09*	0.59 ± 0.07*
5	0.66 ± 0.13*	0.67 ± 0.11*
7	1.19 ± 0.19	1.00 ± 0.04*
10	1.69 ± 0.00	1.02 ± 0.07

Cell adhesion and invasion levels are given as the average number of bacteria per CHO-K1 cell. $n = 3$. * indicates $p < 0.05$ as measured using the one-way ANOVA method with the Dunnett post-test to compare all means to an MOI of 10.

There was a significant increase in adhesion when an MOI of 10 bacteria/CHO is used when compared with an MOI of 1, 2, 3, 4, or 5 ($p < 0.05$). It is possible that once one bacterium has invaded a given CHO cell, the cell becomes more receptive to attachment by other bacteria meaning that the higher the multiplicity of infection, the more bacteria available to invade CHO cells, and the greater the number of adherent

bacteria. It is also possible that in the wells treated with a low MOI, many bacteria were located in sections of the well where there were few mammalian cells while in other areas, there was a surplus of mammalian cells when compared with the number of bacteria present leading to the low level of adhesion and invasion seen in Table 3.9. In this assay, an M.O.I. of 10 was used.

3.2.3.3 Optimisation of the detection of extracellular bacteria

A final high-throughput invasion assay was performed to determine the optimal staining procedure for use with the Olympus microscope. In this assay, *E. coli* DH5αZ1 harbouring pML1 and pCM01 were used. As before, bacteria were incubated with the CHO-K1 cell monolayer for 30 min, before non-adherent and loosely adherent bacteria were removed via 3 washes in PBS and fixed in 4% paraformaldehyde. The same range of blocking times from no blocking to 30 or 60 min incubation in blocking buffer was tested. The primary antibody concentration was again kept static at 1:200 diluted in blocking buffer, while secondary antibody concentrations of 1:250 or 1:500 (in PBS) were tested. The data shown in Fig. 3.8 indicates the average number of extracellular bacteria per CHO-K1 cell. The assay was performed with three biological and four technical replicates. The wells treated with no prior incubation with blocking buffer and a secondary antibody concentration of 1:500 yielded the highest number of visible extracellular bacteria with an average of ~5 bacteria per CHO cell. Data were analysed using the one way ANOVA method. A post-test Dunnett test was performed to compare all means to the the wells containing bacteria exposed to the highest concentration of antibody with the lowest blocking time. No significant differences in the number of bacteria detected per CHO-K1 cell were observed between the staining protocols. The images generated during the secondary antibody staining procedure can be seen in Fig. 3.9.

The same assay was performed for *S.* Typhimurium SL1344 pCM01 and bacteria were stained following an identical procedure as for *E. coli*. The mouse monoclonal anti-*Salmonella* LPS primary antibody was added at 1:200 concentration while secondary antibody concentrations of 1:250 or 1:500 (in PBS) were tested. This assay was performed with three biological replicates in quadruplicate wells. The wells treated with no prior incubation with blocking buffer and a secondary antibody concentration of 1:250 yielded the highest number of visible extracellular bacteria (average of ~5 bacteria per CHO cell) with the lowest standard error (Fig. 3.10). Data were analysed as described previously for *E. coli* interactions with CHO-K1 cells. No significant differences in the number of bacteria detected per cell were observed between the staining protocols.

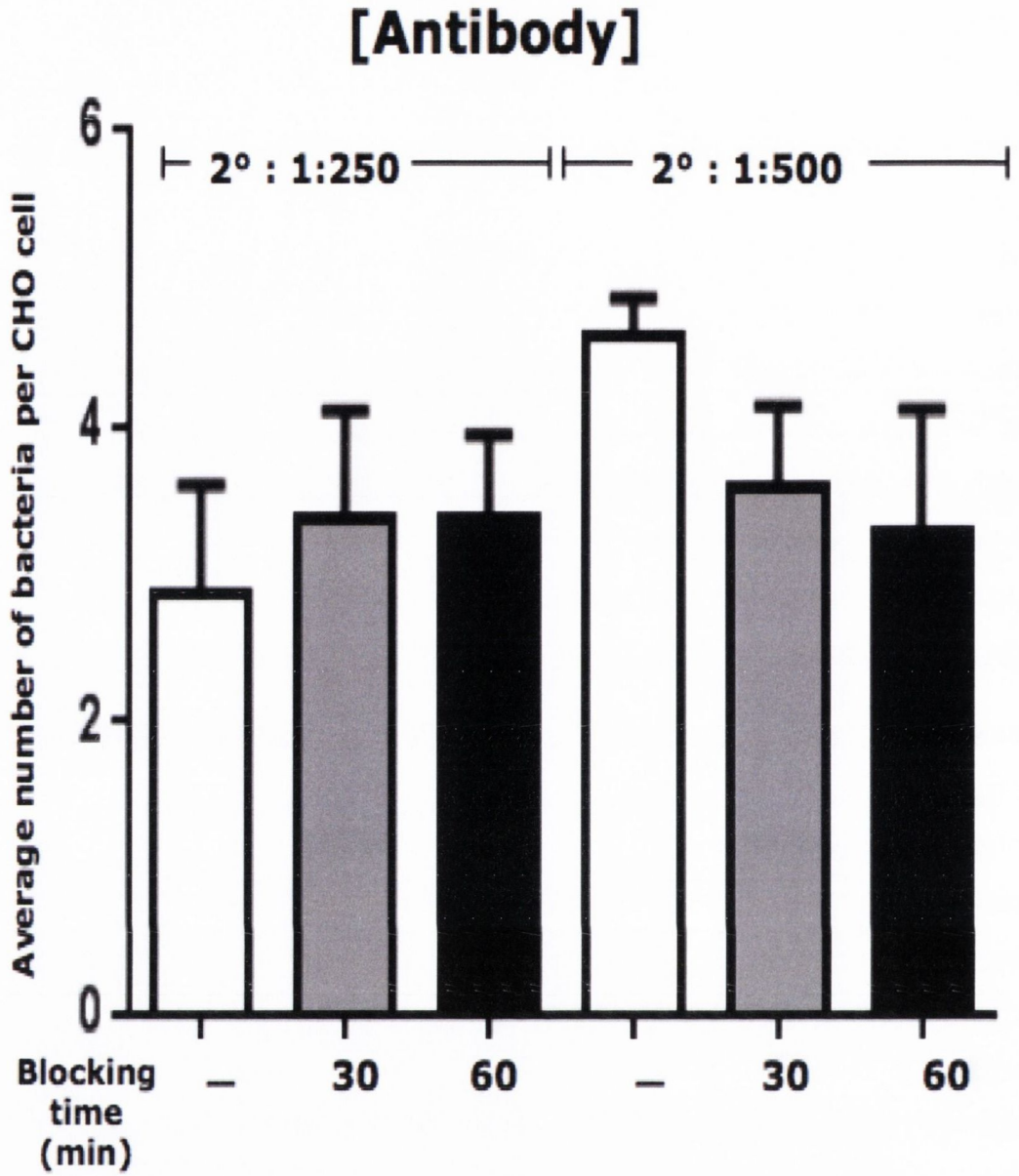

FIG 3.8. Optimisation of the staining of extracellular *E. coli* in a high-throughput assay. The average number of *E. coli* DH5α expressing *pagN* from plasmid pML1 and *gfp*+ from plasmid pCM01 adhering to CHO-K1 cells was calculated. A range of staining procedures were tested and standard error bars are shown. – indicates no blocking while some wells were incubated for 30 or 60 minutes in 0.2% BSA prior to the addition of the primary anti-vesicle antibody. Secondary antibody at a concentration of 1:250 or 1:500 were also tested. $n = 3$. Data were analysed using the one way ANOVA method. A post-test Dunnett test was performed to compare all means to the the wells containing bacteria exposed to the highest concentration of antibody with the lowest blocking time. Statistical significance was determined for $p < 0.05$.

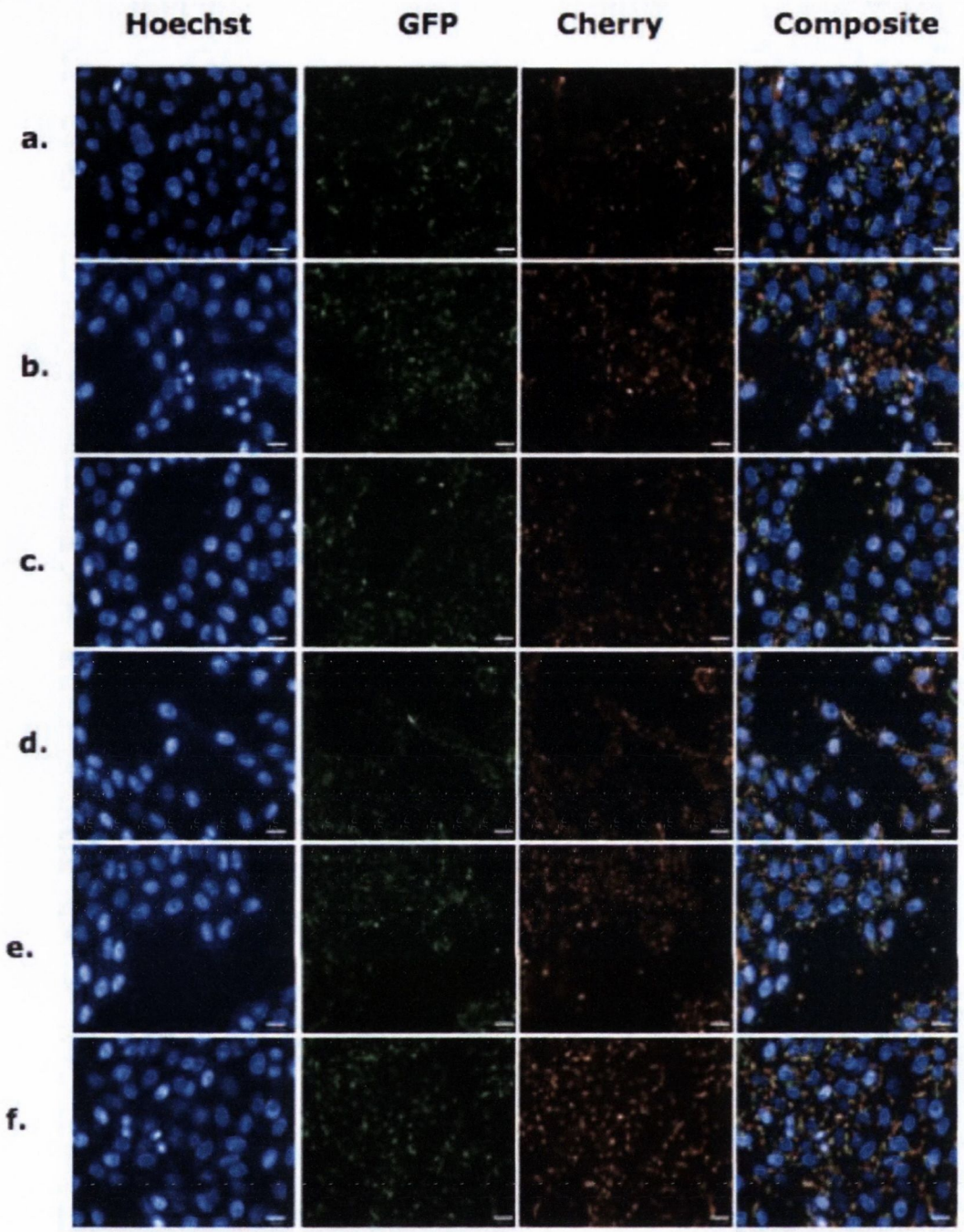

FIG. 3.9. Optimisation of the staining of extracellular bacteria for use in a high-throughput analysis for bacterial invasion using the Olympus IX81 platform. *E. coli* DH5αZ1 harbouring plasmids pML1 and pCM01 were allowed to invade CHO-K1 cells for 30 minutes. Non-adherent or loosely-adherent bacteria were removed and the monolayer containing bacteria was fixed. A range of blocking times and secondary antibody concentrations were tested. (a) No block 1:250 (b) 30 minutes blocking 1:250 (c) 60 minutes blocking 1:250 (d) No block 1:500 (e) 30 minutes blocking 1:500 (f) 60 minutes blocking 1:500. The white bar indicates 20 μm.

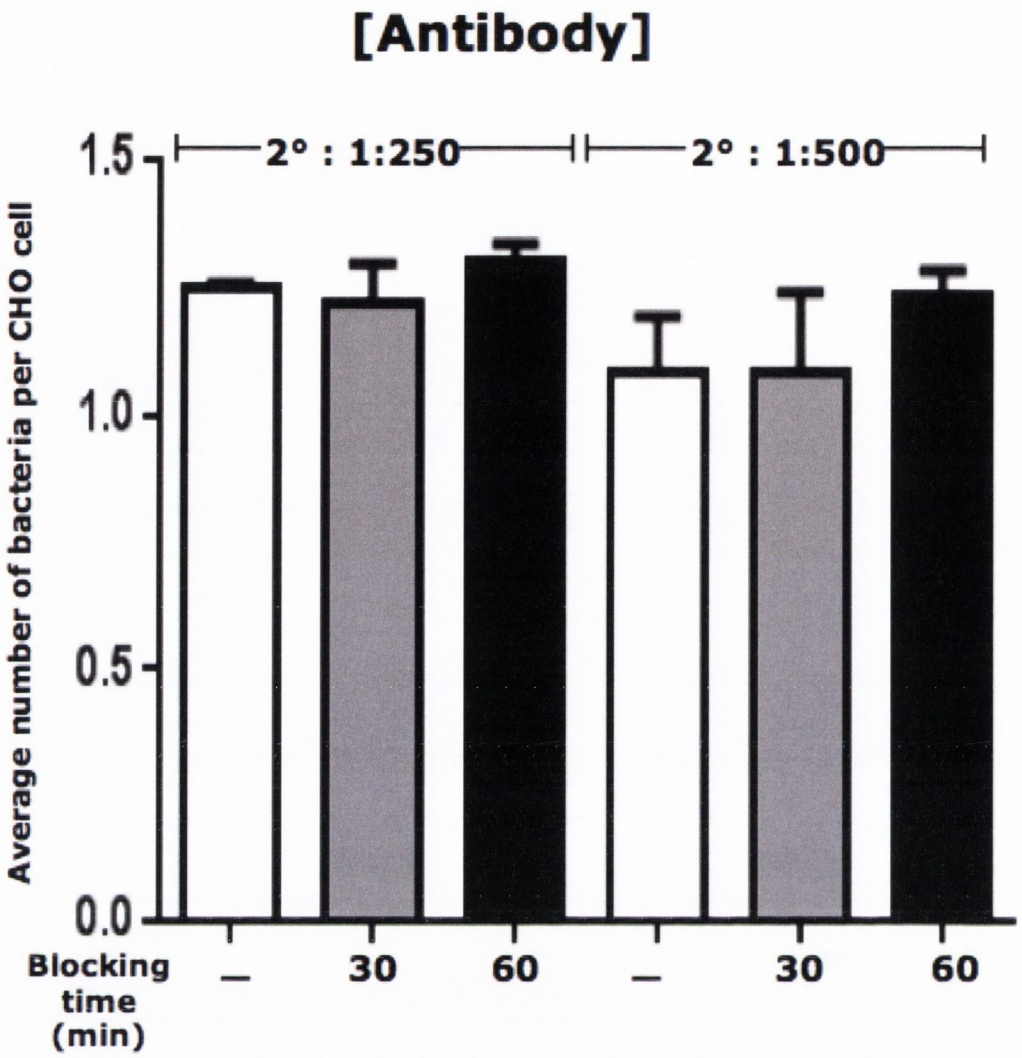

FIG 3.10. Optimisation of the staining of extracellular *Salmonella* in a high throughput assay. The average number of *S.* Typhimurium SL1344 expressing *gfp*+ from plasmid pCM01 adhering to CHO-K1 cells was calculated. A range of staining procedures were tested and standard error bars are shown. – indicates no blocking while some wells were incubated for 30 or 60 minutes of blocking in 0.2% BSA prior to the addition of the primary anti-vesicle antibody. Secondary antibody at a concentration of 1:250 or 1:500 were also tested. $n = 3$. Data were analysed using the one way ANOVA method. A post-test Dunnett test was performed to compare all means to the the wells containing bacteria exposed to the highest concentration of antibody with the lowest blocking time. Statistical significance was determined for $p < 0.05$.

3.3 Discussion

The gentamicin protection assay for analysing bacterial invasion is a well-defined phenotypic assay with several major flaws. The GPA is long and cumbersome, requiring a week or more depending on the doubling time of the mammalian cell line used. In addition to the time required, it is a labour intensive assay, requiring dilutions to at least 10^{-6} per technical replicate for both the initial inoculum and the post-invasion enumeration. On repetition, the assay can yield variable results. Each of these drawbacks makes the GPA an outdated method for measuring cell invasion by bacteria. In order to circumvent the need for the GPA to measure invasion, a high content platform for the analysis of invasion in a faster, more quantitative manner was necessary.

Fluorescent microscopy assays to monitor bacterial invasion of mammalian cells, phagosome maturation, and gene expression *in vivo* have been well documented (154, 227, 247, 324). Fluorescent assays rely on the ability of the microscope to capture and distinguish the different emission wavelengths of fluorescent proteins.

There are many different methods for distinguishing intracellular versus extracellular bacteria in high-throughput assays. Many fluorescently-tagged primary antibodies are commercially available. Of the published results relied on to develop our assay, all used a two-antibody labelling system where the secondary antibody was coupled to a fluorophore. Table 3.10 summarises the major invasion and staining procedures used by Misselwitz *et al.* (247), Mansson *et al.* (227), and Steinberg *et al.* (324) as compared with our techniques.

Table 3.10. Comparison of fluorescent microscopy assays.

	(247)	(227)	(324)	This study
Intracellular detection	GFP	GFP+	Cy3	GFP+
Blocking	None	None	None	None
Primary antibody	anti-*S.* Typhimurium	None	anti-human	anti-vesicle or anti-*S.* Typhimurium
Secondary antibody emission	519 nm	None	506 nm	603 nm
Nuclear stain	DAPI	Hoechst 33342	Hoechst 33342	Hoechst 33342
M.O.I	128	N.A.	N.A.	10-90
Internalisation time (min)	12	5760	15	30

All of the protocols advise using Hoechst or DAPI to stain mammalian cell nucleic acid. Both stains bind to the minor groove of double stranded DNA and emit blue fluorescence. Hoechst and DAPI are relatively inexpensive and can be used at very low concentrations. Misselwitz *et al.* used a FITC labelled secondary antibody with an emission/excitation wavelength of 495/519 nm to distinguish intracellular from extracellular bacteria (247). As GFP+ emits fluorescence at 509 nm, we determined that a FITC labelled antibody would not be sufficient to easily differentiate bacteria that were successful in invasion versus those that remain outside of the cell. Our use of a secondary antibody excitation/emission at 568/603 nm enables us to easily identify green from orange (intracellular from extracellular) bacteria.

While staining procedures between the groups did not vary, the protocols for invasion showed substantial differences. Those developed

by Mansson *et al.* and Steinberg *et al.* can be disregarded as they were working with live animal assays and macrophage phagocytosis, respectively. When compared with Misselwitz *et al.*, we used a much lower M.O.I. For *Salmonella*, we used an M.O.I. of 10 whereas they used an M.O.I. of 130. While adopting an M.O.I. of over 100 would increase the numbers of invasive and adherent bacteria captured in the images, we did observe ~2 invasive bacteria and 1 adherent bacterium per CHO-K1 cell. In addition, it became apparent that when an excess of bacteria was added to the wells, the ability of the primary and secondary antibody to sufficiently stain all bacteria was compromised.

The Misselwitz protocol also differs in bacterial invasion times. The protocol developed in this study allowed bacteria to adhere to and invade the mammalian cell monolayer for up to 30 min while Misselwitz *et al.* stopped the invasion after 12 min. There was no statistically significant difference between *Salmonella* or *E. coli* allowed to invade for 10 - 15 min versus 30 min. An invasion time of 30 min was chosen as the deviation between samples was lower than that for 15 min invasion (± 0.0798 for 30 min versus ± 1.69 for 15 min invasion).

When data generated by the GPA are compared with those gathered by the high-throughput assay, the high-throughput assay is far superior for detecting the number of bacteria per mammalian cell as opposed to the percentage invasion (Table 3.11). It is possible to easily calculate percentage invasion for the HCA by performing a dilution series and enumerating the input number of bacteria and calculating the number of GFP bacteria per well. It is not possible, however, to easily determine anything other than the percentage invasion for the GPA.

Table 3.11. A comparison of the average number of bacteria per CHO-K1 cell using the gentamicin protection assay versus the high-throughput assay.

	GPA	HCA
Average bacteria/CHO-K1	~0.132	3.12

These data indicate the high-throughput assay described in this chapter is a useful tool to quickly and quantitatively monitor the adherence to, and invasion of mammalian cells by bacteria such as *E. coli* and *Salmonella.*

Chapter 4 A Comparison of the PagN proteins of *S.* Typhimurium and *S.* Typhi

4.1 Introduction

Gram-negative bacteria are encased by two separate membranes. The two membranes differ greatly in both structure and function. The inner, cytoplasmic membrane is composed mainly of phospholipids such as phosphatidylethanolamine, phosphatidylglycerol, and cardiolipin (192). The inner leaflet of the outer membrane is composed of similar substances, while the outer leaflet is composed of lipopolysaccharides (192, 327). The outer membrane is also described as being "more leaky" than the inner membrane due to a number of pore-forming proteins (192).

There are two classes of integral membrane proteins consisting of either α-helical bundles or β-pleated sheets (192). These two structural classes not only serve to categorise membrane proteins but also defines their location (192). Transmembrane α-helical proteins are typically embedded in the inner membrane while proteins consisting of β-sheets are confined to the LPS-based outer membrane (192). Roughly one half of the outer membrane consists of protein. This includes integral membrane proteins and lipoproteins attached to the membrane via N-terminally anchored lipids (192). Though comparatively recalcitrant to biochemical analyses, as of December 2014, 332 bacterial outer membrane protein structures have been solved (RCSB Protein Data Bank).

The non-polar core of the lipid bilayer imposes physical constraints on the number of possible designs for stable β-sheets (349). Due to these constraints, all transmembrane proteins must fold into a structure that is roughly cylindrical across the bilayer. This structure exposes

predominantly non-polar sidechains to the membrane. Transmembrane β-strands are laterally hydrogen bonded in a circular pattern. These interstrand hydrogen bonds are the dominant stabilising interaction (31). As a result of the hydrogen bonding interactions, β-barrels make very stable structures that do not readily unfold (144, 287). The first solved crystal structure of an outer membrane protein was the porin of *Rhodobacter capsulatus* (348). The crystal structure of this porin confirmed previous predictions that outer membrane proteins form β-barrels.

There are several general structural features common to β-barrel proteins. They generally consist of an even number of β-strands with the amino- and carboxy-termini located in the periplasm. The number of anti-parallel β-strands may range from 8 to 22 (192, 309, 327, 352) and their tilts range from 20 to 45° (352). These strands are connected by tight periplasmic turns and longer extracellular loops. Much of the sequence variability attributed to outer membrane proteins is found in the loop regions (309). The predicted size for periplasmic turns ranges from 1 to 12 amino acids while the lowest number predicted to be feasible for loop formation is 5 (192, 345). The length of the transmembrane portion of the β-strands varies between 6 and 25 amino acid residues long with an average length of 12.3 residues (192). The tilt of the β-strands is generally higher in longer sequences, therefore the minimum number of residues required to span the membrane is greater.

The primary amino acid composition of the β-sheets gives rise to an amphipathic barrel. Residues facing the bilayer are mostly hydrophobic while those exposed to the channel interior are polar. The size and hydrophobicity of the protein channel varies between β-barrels. For example porins such as OmpC from *E. coli* and *S.* Typhimurium have water-filled, hydrophilic channels while the membrane adhesin OpcA of *Neisseria meningitidis* has a closed channel (276). A feature seen amongst most β-barrels is the ring of aromatic residues found at the

interface between the sheet and loop domains and the sheets and turns (192, 309, 327, 352). This aromatic girdle is thought to bridge the polar and non-polar environments present at the protein/bilayer interface.

Recent work undertaken by Ghosh *et al.* in 2011, identified an adhesin and invasin necessary for *Salmonella* Typhi invasion of epithelial cells which they named T2544. They were able to identify this protein as a potent immunogen (129). Deletion of the *t2544* gene led to a decrease in bacterial adhesion and invasion of colonic epithelial cells (129). Protein-protein BLAST alignment showed that the T2544 protein is >98% identical to the already known PagN protein of *Salmonella* Typhimurium. The purpose of this study was to predict the structure of T2544 (termed $PagN_{STY}$) and determine how this protein functions as compared with the homologous adhesin and invasin of *S.* Typhimurium ($PagN_{STM}$). The questions deemed most relevant in this study were:

- What is the predicted topology of $PagN_{STY}$?
- Do the PagN proteins of *S.* Typhimurium and *S.* Typhi display similar levels of erythrocyte adherence?
- Can the $PagN_{STY}$ protein promote adherence to and invasion of epithelial cells?

4.1.1 Statistical Analyses Utilised

All data presented within all graphs in this chapter reflect the mean plus or minus the standard error. When the number of strains tested reached three or more, a one way analysis of variance test was used. The Dunnett post-test analysis was used to compare all means to a control mean as indicated in the text. Statistical significance was described for values where $p < 0.05$.

4.2 Results

4.2.1 Optimisation of an anti-PagN peptide antibody for Western immunoblotting

An antibody was required to detect PagN expressed exogenously in *E. coli*. Eurogentec (Belgium) generated an anti-PagN antibody via immunization of a rabbit with a peptide coupled to KLH (keyhole limpet haemolysin). The peptide sequence, AGDEHTAYDADTKAA, which is located in the exposed loop 4 of the protein (from both *S.* Typhi and Typhimurium) was chosen for immunization. As this peptide is surface exposed and located at the C-terminus, the generated antibody would be able to recognise full-length PagN protein. The antibody was screened at three different concentrations: 1:100, 1:1,000, or 1:10,000 against lysates from *E. coli* that had been induced or uninduced for expression of PagN. An anti-MBP antibody was used as a loading control (Fig. 4.1). The western immunoblots were exposed for 20 seconds (for 1:100 and 1:1,000 concentrations) or 5 min (for 1:10,000 concentration). Expression of PagN was easily detected in the lysates containing induced PagN protein at both 1:100 and 1:1,000 antibody concentrations. Due to the sequence specificity, there is a lack of cross-reactivity of the anti-PagN antibody with other proteins present in the bacterial lysates. Although the 1:10,000 dilution of anti-PagN antibody was able to detect expression of the PagN protein after exposure for 5 min, the band shown in Fig. 4.1 is less bright than those displayed for the 1:100 and 1:1000 dilutions. A concentration of 1:1,000 was chosen for use in subsequent detection of PagN to ensure sensitivity, whilst being parsimonious with the quantity of antibody used.

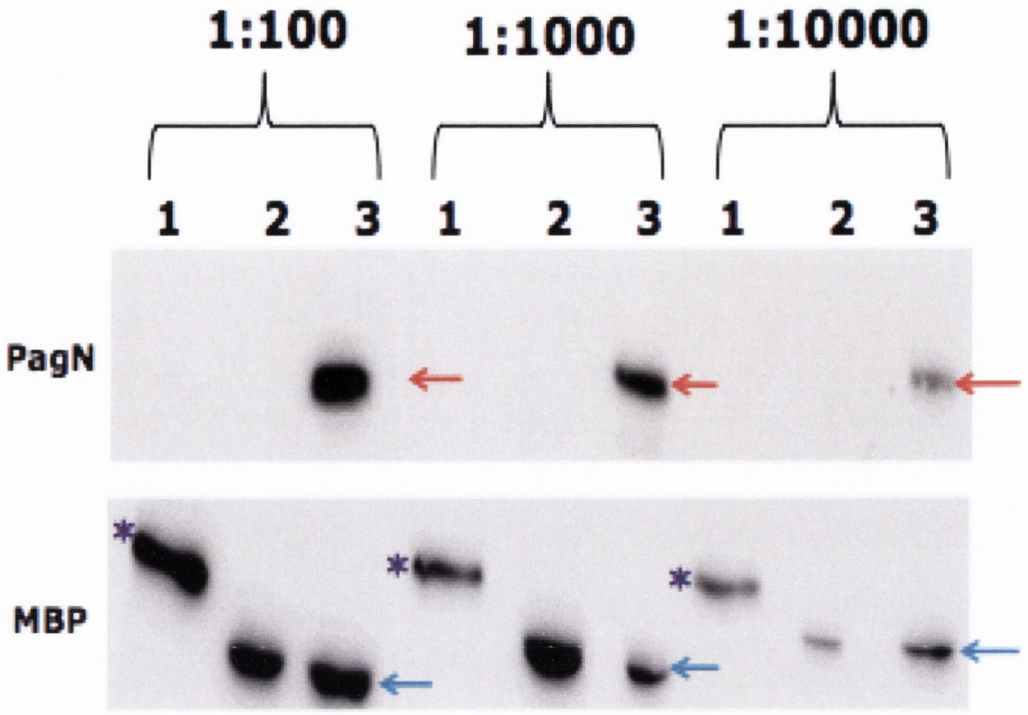

FIG 4.1. Western Immunoblot detection of uninduced and induced PagN expression using differing concentrations of antibody. A western immunoblot was performed using whole cell lysates of E. coli DH5α bacteria expressing PagN protein from plasmid pML1. A band was seen at ~26 kDa corresponding to full length PagN protein. Antibody concentrations of 1:1,000 and 1:10,000 were tested. The red arrows indicate PagN protein. In each panel, lane number 1 refers to the protein ladder, lane 2 to uninduced bacteria, and lane 3 to induced PagN expressing bacteria. The ~42 kDa maltose binding protein (MBP) was used as a loading control (blue arrows). The purple asterisk in lane 1 indicates an MBP-fusion protein of a higher molecular weight.

4.2.2 Comparative analysis of $PagN_{STM}$ and $PagN_{STY}$

4.2.2.1 Bioinformatic analysis of the PagN proteins of *S.* Typhimurium and *S.* Typhi

Protein-protein BLAST (www.ncbi.nlm.nih.gov/BLAST) analysis of the $PagN_{STM}$ primary sequence indicated that the protein is 98% similar to $PagN_{STY}$ (Fig. 4.2). Differences between the proteins included two amino acid substitutions in the surface exposed extracellular loops 1 and 2, and two amino acid substitutions in transmembrane portions of the proteins. Clustal Omega alignment of the two PagN proteins indicated that the two proteins share 98.3% similarity. The online programme PRED-TMBB indicated that $PagN_{STY}$ is an outer-membrane β-barrel protein as the sequence scored a value of 2.882 which is lower than the threshold value of 2.965 (12). Ghosh *et al.* demonstrated that $PagN_{STY}$ is capable of binding the glycoprotein laminin (129). Previous studies demonstrated that $PagN_{STM}$ likely binds to a heparan sulphate proteoglycan (204). It is possible that the proteins are able to bind to both laminin and heparan sulphate. It is also conceivable that differences in the amino acid composition the extracellular loops specify affinity to either laminin or heparan sulphate.

Score	Expect	Method	Identities	Positives	Gaps
480 bits(1235)	8e-170	Compositional matrix adjust.	235/239(98%)	237/239(99%)	0/239(0%)

```
PagN_STY   1    MKNFFAVCIIPLVVTWSATASAKEGIYITGKAGTSVVNVYGINSTFSQEEIVNGHATLPD
                MKNFFAVCIIPLVV WSATASAKEGIYITGKAGTSVVNVYGINSTFSQ+EIVNGHATLPD
PagN_STM   1    MKNFFAVCIIPLVVAWSATASAKEGIYITGKAGTSVVNVYGINSTFSQDEIVNGHATLPD

PagN_STY   61   RTKGVFGGGVAIGYDFYDPFQLPVRLELDTTFRGETDAKGGQDIIAFGQPVHINVKNQVR
                RTKGVFGGGVAIGYDFYDPFQLPVRLELDTTFRGETDAKGGQDIIAFG PVHINVKNQVR
PagN_STM   61   RTKGVFGGGVAIGYDFYDPFQLPVRLELDTTFRGETDAKGGQDIIAFGDPVHINVKNQVR

PagN_STY   121  MTTYIVNGYYDFHNSTAFTPYISAGVGLAHVKLSNNTIPVGFGINETLSASKNNFAWGAG
                MTTY+VNGYYDFHNSTAFTPYISAGVGLAHVKLSNNTIPVGFGINETLSASKNNFAWGAG
PagN_STM   121  MTTYMVNGYYDFHNSTAFTPYISAGVGLAHVKLSNNTIPVGFGINETLSASKNNFAWGAG

PagN_STY   181  IGAKYAVTDNIMIDASYKYINAGKVSISKNHYAGDEHTAYDADTKAASNDFMLGITYAF
                IGAKYAVTDNIMIDASYKYINAGKVSISKNHYAGDEHTAYDADTKAASNDFMLGITYAF
PagN_STM   181  IGAKYAVTDNIMIDASYKYINAGKVSISKNHYAGDEHTAYDADTKAASNDFMLGITYAF
```

FIG. 4.2. Protein BLAST alignment of the extracellular loops of the PagN protein from *S.* Typhimurium ($PagN_{STM}$) and PagN from *S.* Typhi ($PagN_{STY}$). Conserved amino acid residues are depicted in white with black background while differences are shown in black lettering with a white background. Numbering refers to the amino acid residues of the mature protein.

4.2.2.2 PagN$_{STY}$ is predicted to adopt a β-barrel conformation

The *pagN$_{STY}$* ORF consists of 720 bp corresponding to 239 amino acids. Analysis and comparison of the primary sequence revealed the presence of a putative amino-terminal signal peptide. The proposed signal peptide, 22 residues in length, displays features typical of bacterial proteins translocated across the inner membrane via the Sec secretion system. This prediction was supported by sequence similarity between PagN$_{STY}$ and the *S.* Typhimurium adhesin. The mature PagN$_{STM}$ protein starts with an identical Lys residue at the amino-terminal end of the protein, which is preceded by identical alanine residues at positions –1 and –3 relative to the start of the mature protein.

The presence of the predicted signal sequence was strengthened by sequence analysis using the SignalP 4.1 program (23). The program agreed with predictions that the first 22 amino acids of the primary sequence form a signal sequence with a cleavage site immediately after the twenty-second residue, an Alanine (data shown in Appendix 1). These data demonstrate that PagN$_{STY}$ has a signal sequence identical to that of PagN$_{STM}$, suggesting that it is also translocated across the inner membrane via the Sec secretion system.

The secondary structure of the mature 217-residue PagN protein was predicted using the web-based structural modeling program Phyre2 (186). Phyre2 predicted the structure of PagN$_{STY}$ with 100% confidence using the nuclear magnetic resonance (NMR) solved structure of opc60 protein found in *Neisseria gonorrhoeae*.

The PagN$_{STY}$ protein was predicted to contain 8 amphipathic β-sheets separated by alternating short (2 – 6 residues) turns or long (26 – 29 residues) loops. Characteristic of β-barrel proteins, each β-sheet consists of alternating hydrophobic residues (192). Transmembrane β-strands are rich in glycines and aromatic residues such as tryptophan and tyrosine are found in two rings that contact the lipid bilayer (192, 309, 327, 352). Many of the β-sheets of PagN$_{STY}$ are flanked by aromatic

residues, creating such a girdle. Based on these observations, PagN is likely to adopt a β-barrel conformation in the outer membrane consisting of 8 anti-parallel β-sheets, connected by 4 long, flexible, surface-exposed loops and 3 short periplasmic turns. The predicted surface-exposed loops were found to contain a large number of charged residues. A model of $PagN_{STY}$ is predicted in Fig. 4.3 highlighting the main secondary structural features.

4.2.2.3 Construction of a *pagN*$_{STY}$ expressing plasmid

The *pagN* gene of *S.* Typhi strain BRD948 was amplified by PCR using primers T2544fwd and T2544rev. *Bam*HI and *Nco*I restriction digest sites were engineered at either end of the *pagN* gene. The plasmid vector pTrc99a was chosen as it contains the IPTG inducible P_{trc} promoter. pTrc99a was digested with *Bam*HI and *Nco*I restriction endonucleases and agarose gel purified. The PCR product was then ligated into plasmid pTrc99a to create plasmid pSP1. The pSP1 plasmid was transformed into chemically competent *E. coli* XL1 Blue cells and the bacteria were grown on LB agar plates containing carbenicillin. Plasmid extractions were performed on several overnight cultures of bacteria isolated from the antibiotic plates and subsequently digested using *Bam*HI and *Nco*I. The digests were electrophoresed through a 1% agarose gel. Putative clones displaying two bands, one at ~720 nucleotides and one at ~4 kilobases, corresponding to the size of the amplified insert and the plasmid vector, respectively, were retained. The inserts of 3 clones were sequenced. One clone, termed pSP1, contained a sequence identical to *pagN*$_{STY}$. A map of plasmid pSP1 can be seen in Fig. 4.4.

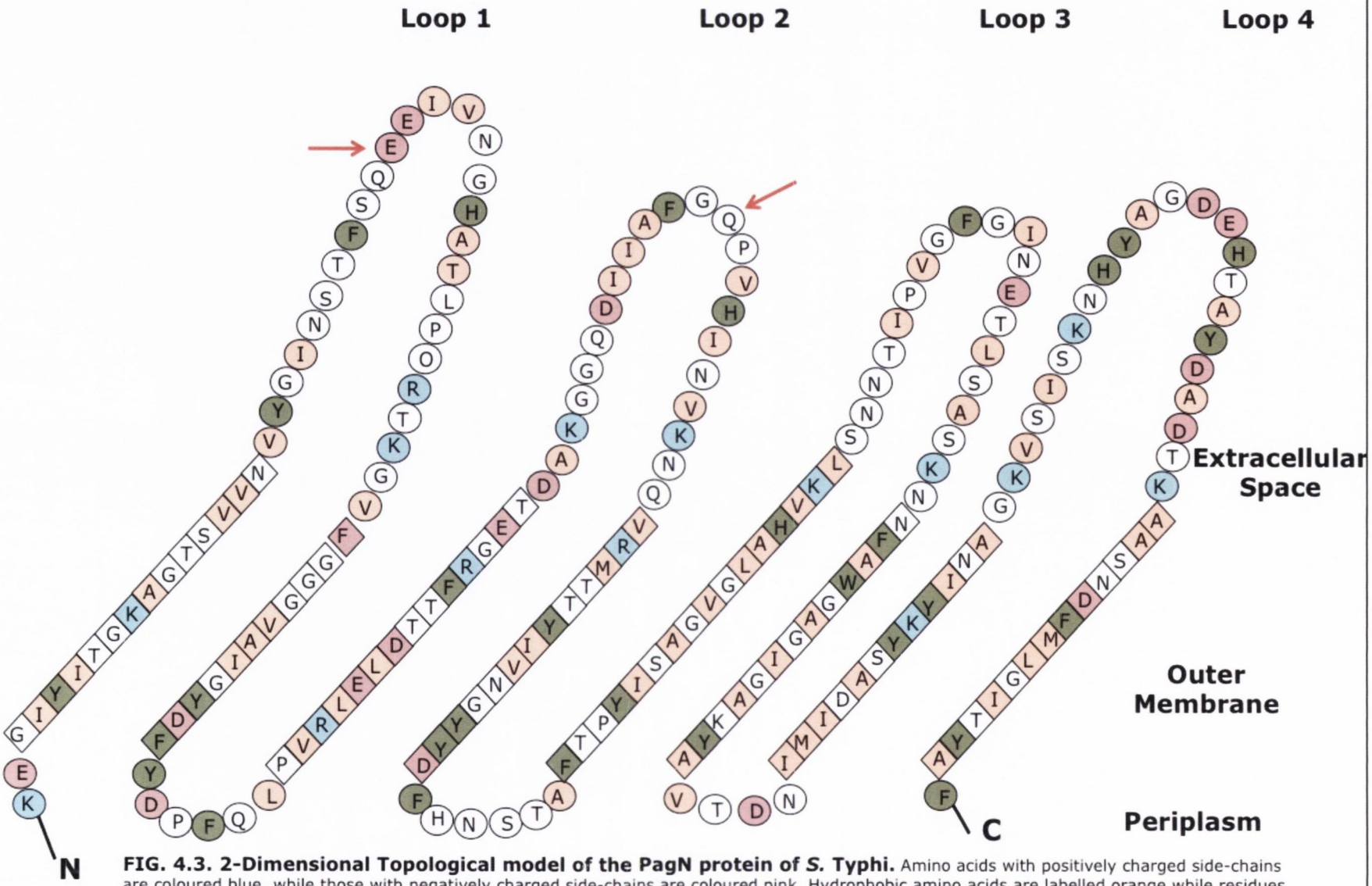

FIG. 4.3. 2-Dimensional Topological model of the PagN protein of *S.* Typhi. Amino acids with positively charged side-chains are coloured blue, while those with negatively charged side-chains are coloured pink. Hydrophobic amino acids are labelled orange while residues with aromatic side-chains are green. The red arrows indicate surface-exposed amino acids that differ between $PagN_{STM}$ and $PagN_{STY}$. The diamonds indicate transmembrane residues while the circles are residues located outside of the membrane.

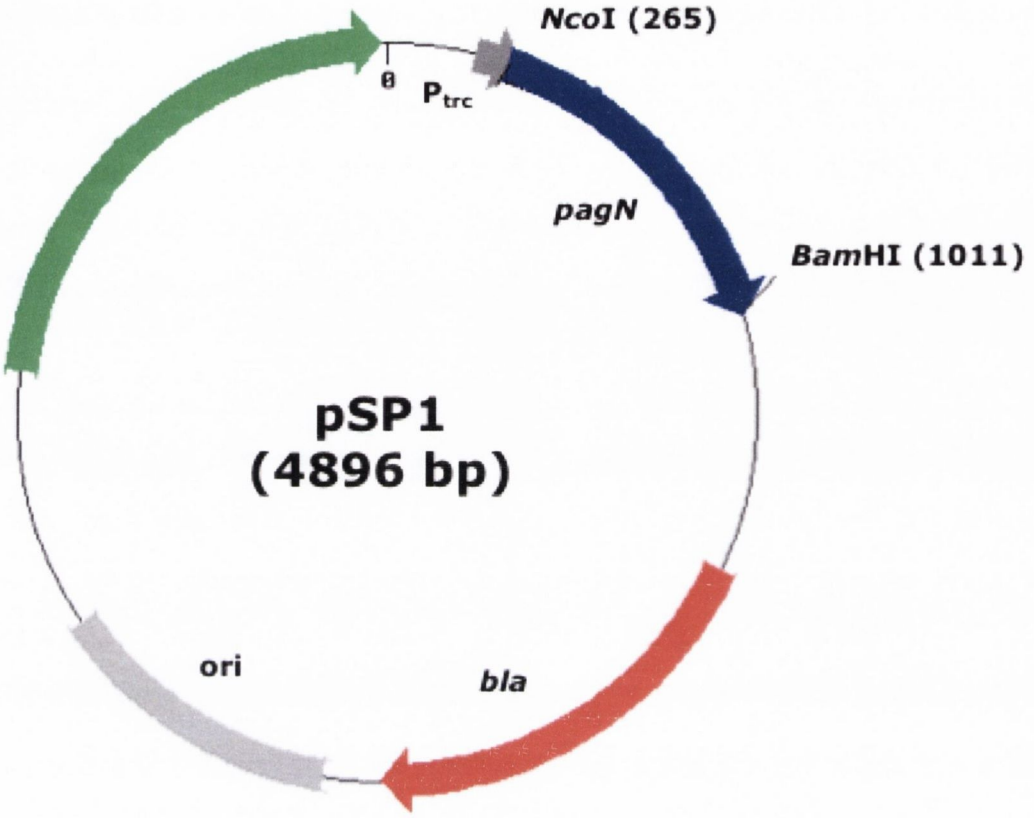

FIG. 4.4. Map of the plasmid pSP1. The positions of the *pagN* and *bla* genes are indicated as is the P_{trc} promoter for IPTG-inducible expression. The origin of replication is indicated, which gives rise to a copy number of ~25 plasmids/cell while the *bla* gene encodes resistance to ampicillin.

4.2.2.4 The anti-PagN antibody recognizes both $PagN_{STM}$ and $PagN_{STY}$

The anti-PagN antibody was raised against a peptide fragment of the exposed fourth loop of the protein. This region of the protein is conserved between $PagN_{STM}$ and $PagN_{STY}$. It was hypothesised that the antibody would recognize both PagN proteins.

Once putative $PagN_{STY}$ expressing plasmids were sequenced, it was important to determine whether full length PagN protein was produced from plasmid pSP1. A western immunoblot of whole cell lysates of both $PagN_{STM}$ and $PagN_{STY}$ was performed (Fig. 4.5 (a)). For both lysates, a band corresponding to the PagN protein was seen, and this band was absent from lysates containing the empty vector plasmid. Both proteins were expressed to approximately equal levels.

PagN promotes agglutination of erythrocytes as well as invasion of mammalian cells through interaction of the bacterial loops with receptors located on the cell surface. The proper association of the protein with the outer membrane is crucial to all PagN-promoted phenotypes. A Western immunoblot was performed on a preparation of outer membrane proteins using sarcosyl enrichment. Bands corresponding to the ~26 kDa PagN protein were seen in the lysates from bacteria harbouring plasmids pSP1 or pML1, and were absent from the lysate of bacteria harbouring the vector plasmid (Fig. 4.5 (b)).

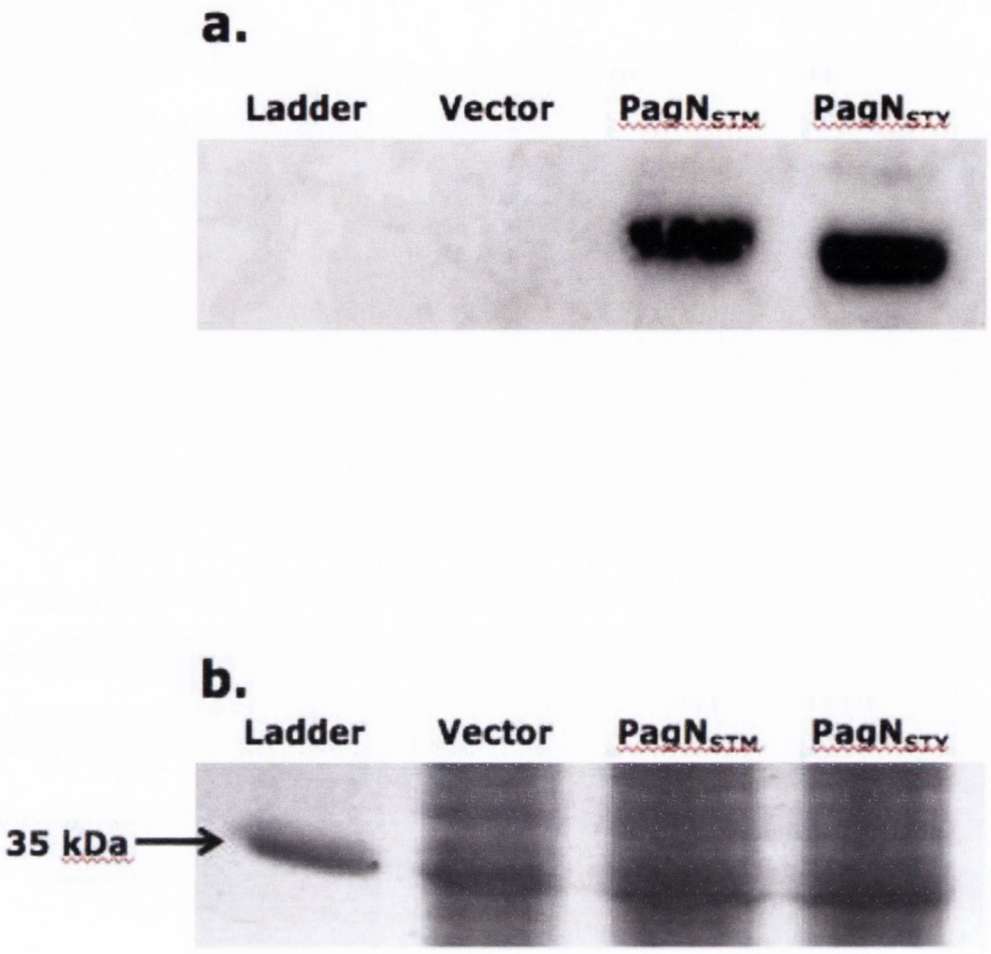

FIG. 4.5. Western immunoblot displaying PagN$_{STM}$ and PagN$_{STY}$ expression from plasmids pML1 and pSP1. Whole cell lysates of bacteria were prepared and transferred to a PVDF membrane. Anti-PagN antibody was used to detect PagN expression from plasmids pML1 and pSP1, respectively and the results are shown in panel a. An SDS gel stained using Coomassie stain was used to show equal loading in all lanes.

4.2.2.5 $PagN_{STM}$ and $PagN_{STY}$ agglutinate human erythrocytes

$PagN_{STM}$ is capable of binding to and agglutinating human erythrocytes in a heat-sensitive manner (205). The $PagN_{STY}$ protein differs from that of *S.* Typhimurium by only two surface exposed changes. Despite these sequence differences, $PagN_{STY}$ may also agglutinate human erythrocytes. To test this hypothesis, a microtitre haemagglutination (HA) assay was performed as described in Section 2.4.1. *E. coli* K-12 strain XL-1 containing the *pagN*$_{STM}$ expression-vector pML1, the *pagN*$_{STY}$ expression-vector, pSP1, or the empty vector control, pTrc99a, were incubated with human erythrocytes overnight. The expression of both PagN proteins conferred upon recombinant *E. coli* the ability to agglutinate erythrocytes. Using 1 % blood donated by a type O^+ human female, a bacterial HA titre of 16 was displayed by PagN-expressing *E. coli*, which was higher than that promoted by E. *coli* expressing the vector plasmid (HA titre = 2).

4.2.2.6 Interaction of PagN with CHO-K1 epithelial cells

4.2.2.6.1 PagN-mediated invasion of CHO-K1 cells monitored through the GPA

CHO-K1 cells are easily cultured and are readily invaded by strains of pathogenic *S.* Typhimurium (83) and *E. coli* (111).

To investigate if PagN could promote adhesion to and invasion of CHO-K1 cell monlayers, cell association and invasion assays, as described in the Section 2.4.3.1, were performed. *E. coli* DH5α carrying the pML1 plasmid were compared with those harbouring the pSP1 plasmid. $PagN_{STM}$ expressed exogenously in *E. coli* has been shown to promote strong invasion of CHO-K1 epithelial cells (203, 204).

When $PagN_{STM}$ was over expressed in *E. coli* K-12 strain DH5α, more than 28% of the inoculum bound to the CHO-K1 cells, while ~12%

of bacteria were successful in invasion (Fig. 4.6). *E. coli* expressing $PagN_{STY}$, showed similar levels of adhesion (18%); however, there was a significant decrease in the level of invasion (5%, $p < 0.05$) compared to $PagN_{STM}$ (Fig. 4.6). These data indicate that $PagN_{STY}$ and $PagN_{STM}$, whilst both were capable of adhering to the CHO-K1 cell monolayer, may differ in their ability to promote invasion.

4.2.2.6.2 PagN-mediated invasion of CHO-K1 cells analysed using the HCA

The major drawbacks of the GPA in the detection of bacterial interaction with mammalian cells have already been discussed in Chapter 3. A high-throughput invasion assay was also performed using CHO-K1 cells to compare $PagN_{STM}$ and $PagN_{STY}$ mediated invasion. 12 fields per well (4 wells per strain) were imaged using the Olympus IX81 microscope (Fig. 4.7). In this assay, CHO-K1 cells were stained blue using the DNA stain Hoechst; both intracellular and extracellular bacteria express GFP, while extracellular bacteria were distinguished using the Alexa Fluor 568 antibody and are orange. An average of 2.0 – 3.5 invasive bacteria per CHO-K1 cell were seen for both $PagN_{STM}$ and $PagN_{STY}$ while ~0.1 bacterium per CHO was seen for bacteria harbouring the vector plasmid.

Similar trends were seen for bacteria adhering to the mammalian cells. Between 1.9 – 2.8 bacteria per CHO-K1 cell were seen for the PagN expressing bacteria while less than 1 bacterium per CHO was visualised for the bacteria harbouring the vector plasmid. The data shown in Fig. 4.8 indicate the average number of intracellular (a) or extracellular (b) bacteria per CHO-K1 cell. Bacteria expressing $PagN_{STY}$ showed an average of 91% adherence and 83% invasion of CHO-K1

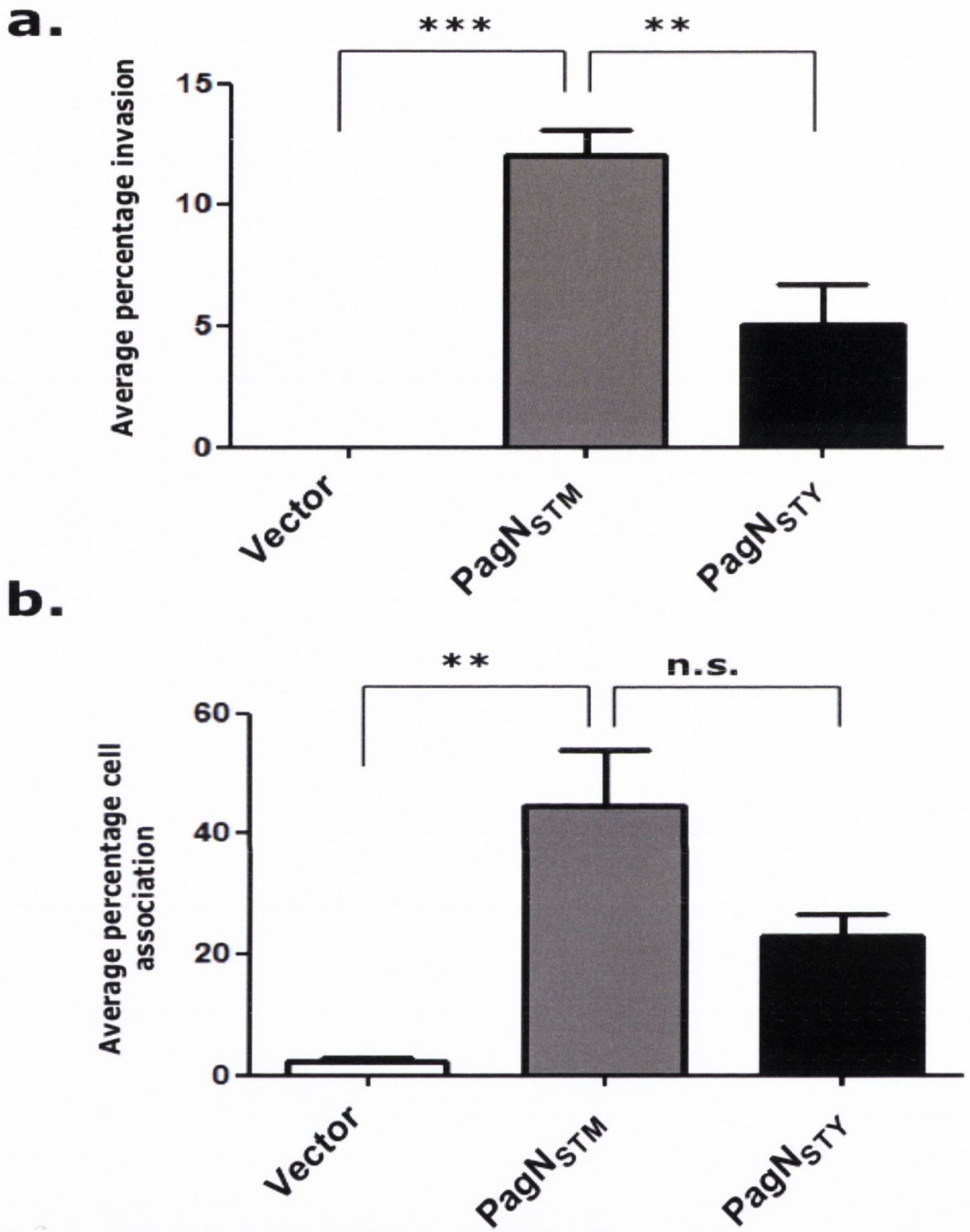

FIG 4.6. Comparison of CHO-K1 cell adhesion and invasion mediated by the PagN proteins of *S.* Typhimurium and Typhi. Gentamicin invasion and cell-association assays were performed as described in Section 2.4.3.1. The assay was performed in triplicate and the data presented in panel a indicate the average percentage of bacterial invasion while the data presented in panel b indicate the average bacterial cell association. ** denotes $p < 0.01$, *** denotes $p < 0.0001$. Data were analysed using the one way analysis of variance with the Dunnett post test to compare all means to the bacteria expressing $PagN_{STM}$.

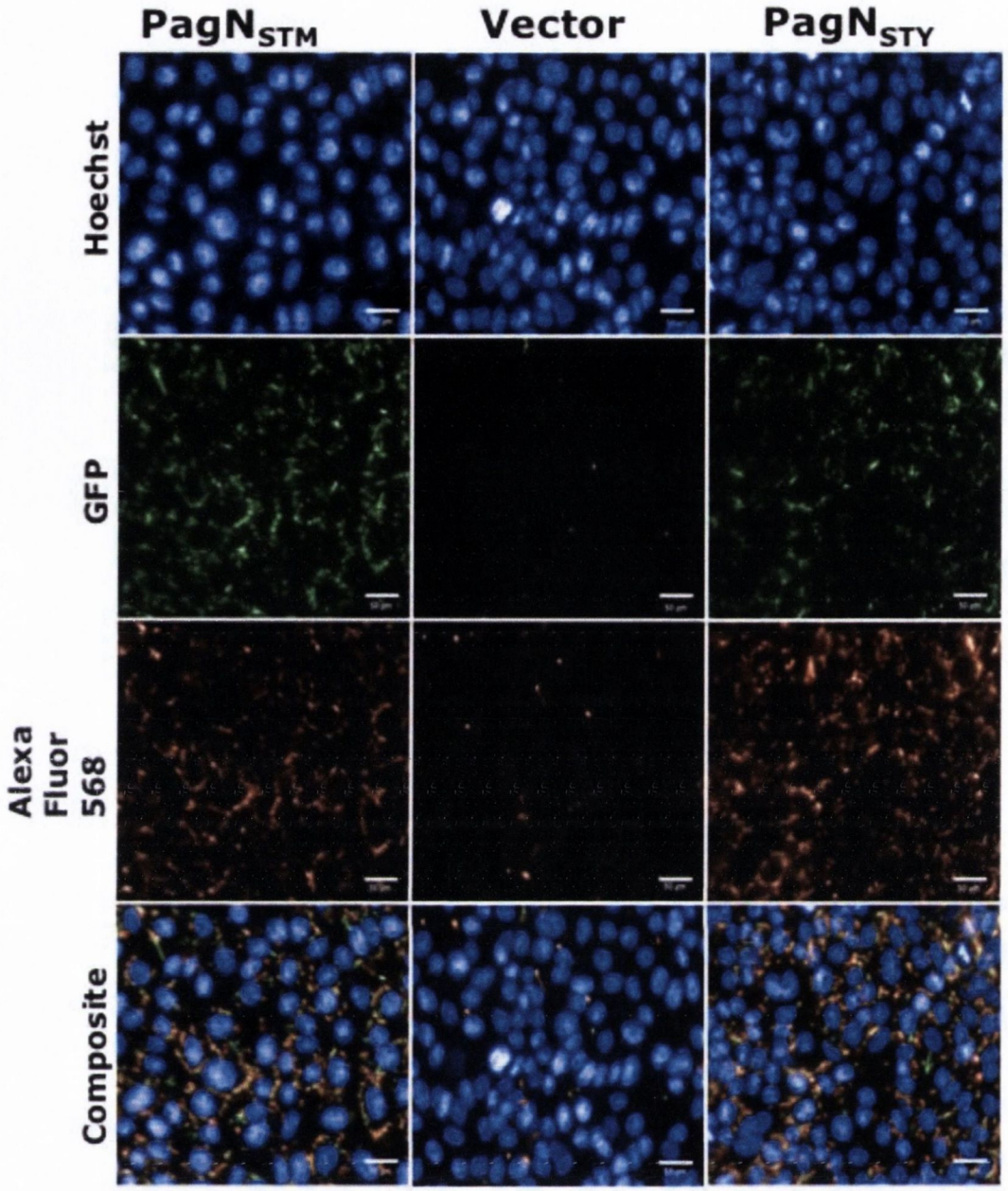

Fig. 4.7. Images generated of PagN-mediated invasion of CHO-K1 cells. A high-throughput assay of invasion was performed and stained as described in Section 2.4.3.2. Images were generated using the Olympus IX81 microscope. Mammalian cells are stained with Hoechst. Bacteria express GFP, and extracellular bacteria were stained orange using a rabbit polyclonal anti-vesicle antibody and a fluorophore coupled donkey anti-rabbit secondary antibody. The white bar indicates 50 μm.

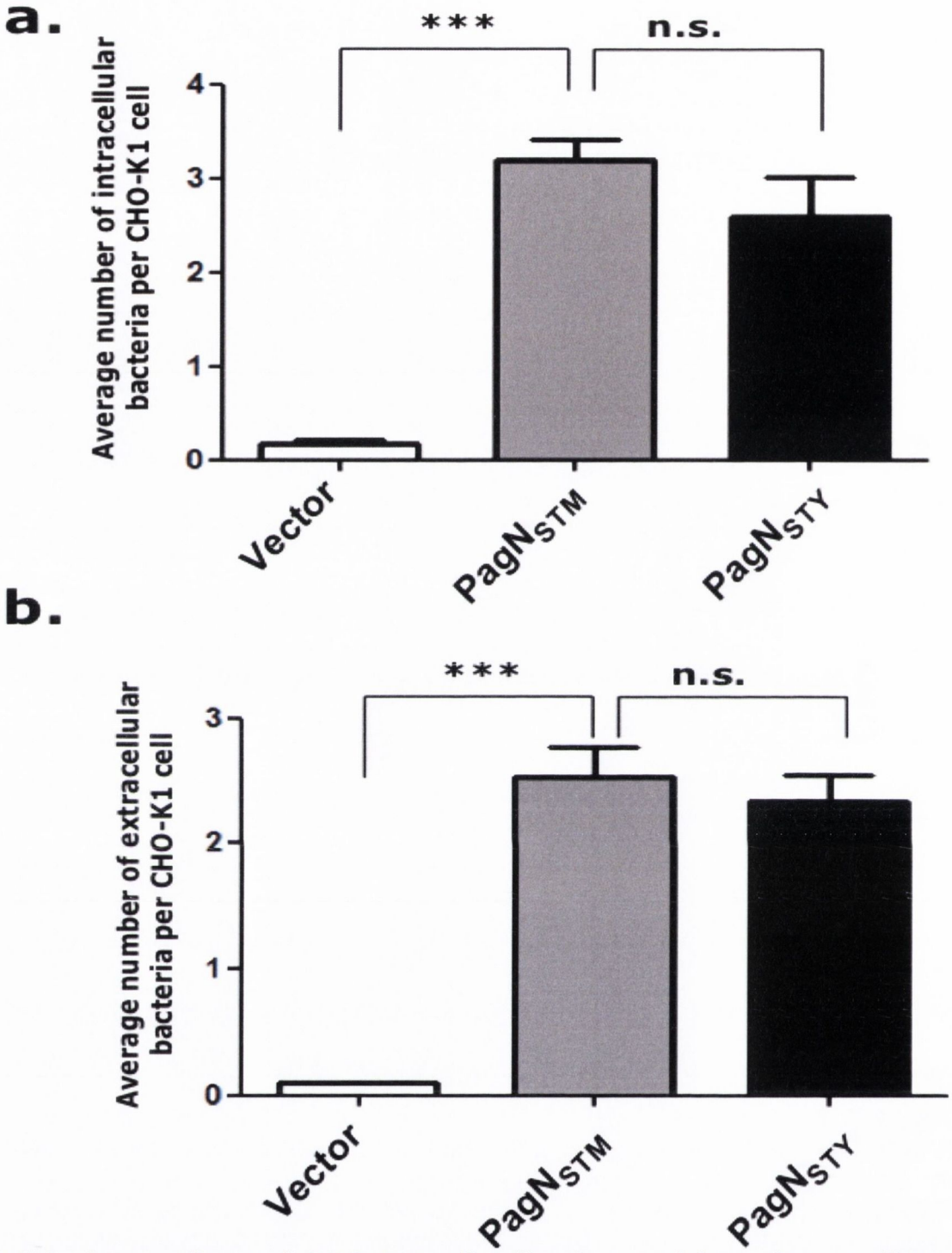

FIG 4.8. Comparison of CHO-K1 cell adhesion and invasion mediated by the PagN proteins of *S.* Typhimurium and Typhi in a high-throughput manner. A high-throughput invasion assay was performed and stained as described in Section 2.4.3.2. An average of 12 fields per well were imaged and the data are displayed as the average number of intracellular (panel a) or extracellular (panel b) bacteria per CHO-K1 cell. *** denotes $p < 0.001$. Data were analysed using the one way analysis of variance with the Dunnett post test to compare all means to the bacteria expressing $PagN_{STM}$.

cells when compared relative to that mediated by $PagN_{STM}$ (p = 0.923 for adhesion and p = 0.483 for invasion). Data were analysed using the one way analysis of variance with the Dunnett post test to compare all means to the bacteria expressing $PagN_{STM}$.

4.2.2.7 Interaction of PagN with HT-29 enterocytes

While CHO-K1 cells are a valuable resource for determining bacterial invasion of epithelial cells, they are not of human origin, and are, therefore, not ideal for determination of the *Salmonella* or *Salmonella*-specific effector mediated invasion. The HT-29 colorectal adenocarcinoma cell line was selected as a more relevant cell line for investigating PagN-mediated invasion.

4.2.2.7.1 Monitoring of PagN-interaction with colonic epithelial cells through the GPA

Association with and invasion of HT-29 cells by *E. coli* DH5α carrying either the pML1 plasmid or the pSP1 plasmid was assessed by the GPA. $PagN_{STM}$ expressed exogenously in *E. coli* has been shown to promote invasion of and adhesion to HT-29 cells (203, 205).

When $PagN_{STM}$ was over expressed in *E. coli* K-12 strain DH5α, ~17% of the inoculum associated with the HT-29 cells, while ~1% of bacteria were successful in invasion. *E. coli* expressing $PagN_{STY}$, showed similar levels of cell association (28%) and invasion (~1%) (Fig. 4.9); however, there was no significant difference in the levels of adhesion or invasion mediated by the two PagN proteins. A high level of cell association was also seen for bacteria harbouring the vector plasmids (~7%) indicating that either the bacteria are able to adhere to the HT-29 cell monolayer independent of the expression of PagN

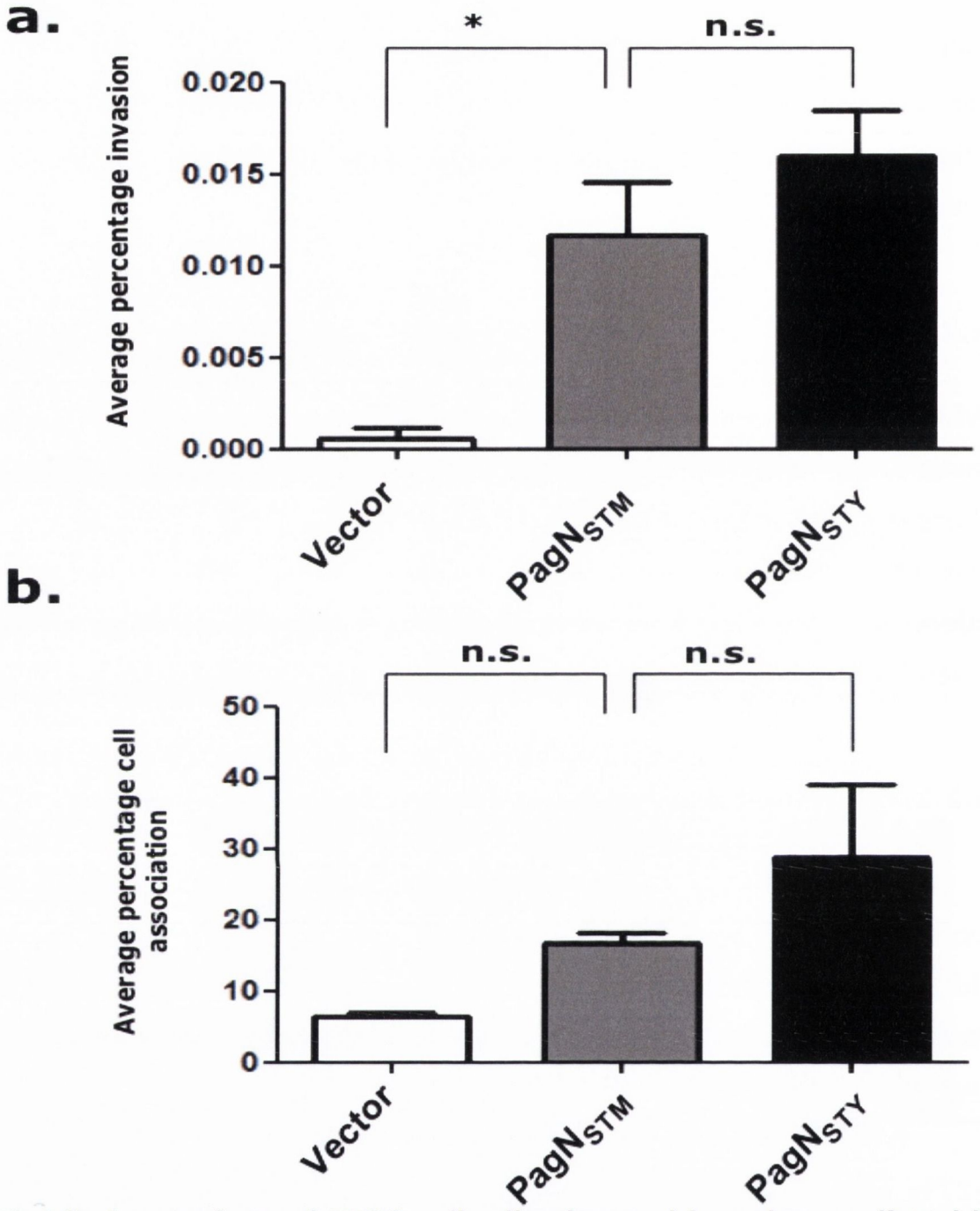

FIG 4.9. Comparison of HT29 cell adhesion and invasion mediated by the PagN proteins of *S.* Typhimurium and Typhi. Gentamicin invasion and cell-association assays were performed as described in the Section 2.4.3.1 with *E. coli* DH5α expressing $PagN_{STM}$ and $PagN_{STY}$ from plasmids pML1 or pSP1, respectively. The assay was performed in triplicate and panel a depicts the average percentage of bacterial invasion while the data shown in panel b indicate the average percentage cell association. There was no statistically significant difference in invasion or adhesion mediated by $PagN_{STY}$ when compared with that promoted by $PagN_{STM}$. * denotes $p < 0.05$. Data were analysed using the one way analysis of variance with the Dunnett post test to compare all means to the bacteria expressing $PagN_{STM}$.

protein, possibly through the expression of Type-1 fimbriae, or that the vector plasmid expresses other proteins that are able to mediate attachment to human epithelial cells.

These data indicate that while $PagN_{STY}$ and $PagN_{STM}$ differ in their abilities to promote invasion of the CHO-K1 cell monolayer, there are no differences in PagN-mediated invasion of the clinically relevant colonic cell line, HT-29.

4.2.2.7.2 Observation of PagN-interaction with HT-29 epithelial cells using the HCA

A high-throughput invasion assay was also performed using HT-29 cells to compare $PagN_{STM}$ and $PagN_{STY}$ mediated invasion. The images generated by the Olympus IX81 microscope are displayed in Fig. 4.10. Low levels of bacterial association were seen in this assay. An average of between 0.5 and 0.7 bacteria per HT-29 cell were seen for both $PagN_{STM}$ and $PagN_{STY}$ expressing bacteria while 0.1 bacteria per HT-29 cell were seen for vector-expressing bacteria (Fig. 4.11). There was, however, a significant decrease in cell association for $PagN_{STY}$-expressing bacteria when compared with those expressing $PagN_{STM}$ ($p < 0.05$, as measured using the one way analysis of variance with the Dunnett post test to compare all means to the bacteria expressing $PagN_{STM}$). This significance was not seen using the GPA due to its cumbersome technique. The HCA is a far more sensitive technique, which allowed the slight, but significant, differences in cell association promoted by the PagN proteins to be elucidated

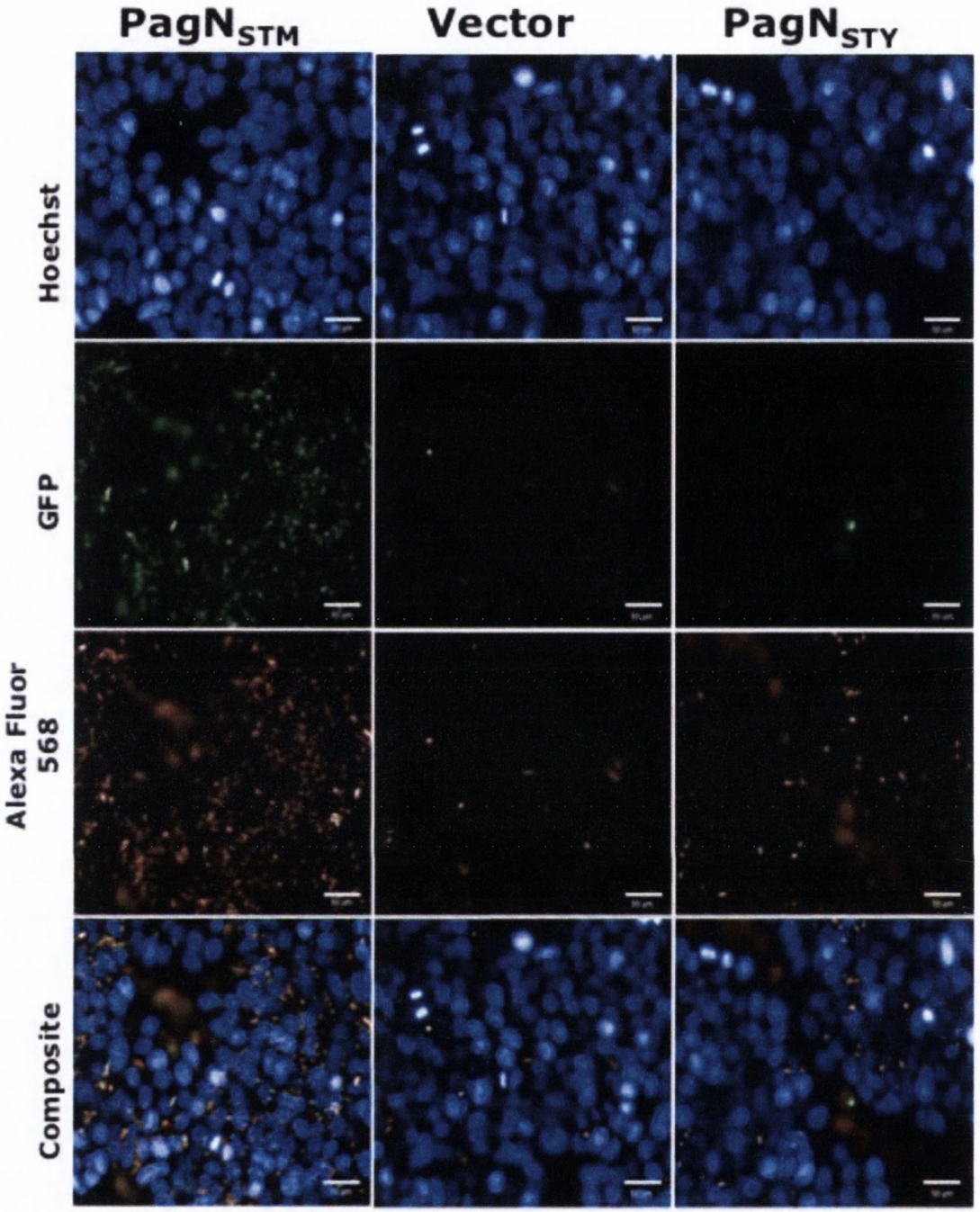

Fig. 4.10. Comparison of PagN-mediated invasion of HT-29 enterocytes in a high-throughput manner. A high-throughput assay of invasion was performed and stained as described in Section 2.4.3.2. Images were generated using the Olympus IX81 microscope. Mammalian cells are stained with Hoechst. Bacteria express GFP, and extracellular bacteria were stained orange using a rabbit polyclonal anti-vesicle antibody and a fluorophore coupled donkey anti-rabbit secondary antibody. The white bar indicates 50 μm.

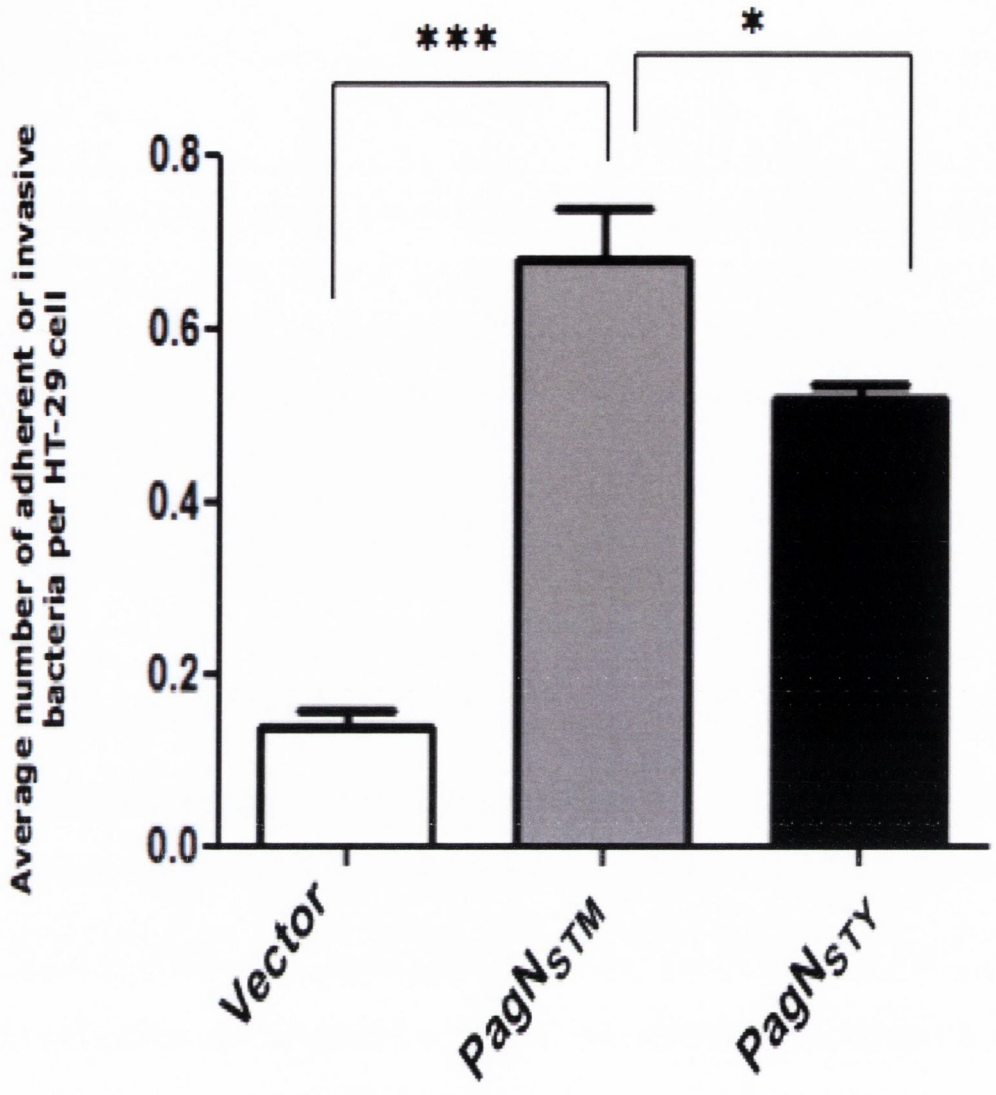

Fig. 4.11. Comparison of the interaction of the PagN protein of *S.* Typhimurium and Typhi with HT-29 cells in a high-throughput manner. A high-throughput fluorescent invasion assay was performed as described in Section 2.4.3.2. with *E. coli* DH5αZ1 expressing $PagN_{STM}$ and $PagN_{STY}$ from plasmids pML1 or pSP1, respectively. The assay was performed in triplicate and the average percentage of cell association relative to $PagN_{STM}$ is displayed. There was no statistically significant difference in cell association mediated by $PagN_{STY}$ when compared with that promoted by $PagN_{STM}$. * denotes $p < 0.05$, *** denotes $p < 0.001$. Data were analysed using the one way analysis of variance with the Dunnett post test to compare all means to the bacteria expressing $PagN_{STM}$.

4.3 Discussion

Despite an overall high level of sequence similarity between the PagN proteins of *S.* Typhimurium and *S.* Typhi, some important differences have been identified. Discrepancies between the amino-acid sequences of the two proteins can be found, as well as differences in the predicted protein structure and the receptor to which PagN binds (129, 203, 205, 357). The *pagN*$_{STM}$ gene has been well characterised and the conditions under which it is expressed have been elucidated (66, 160-162, 205). However, the PagN$_{STY}$ protein is largely uncharacterised. This study was conducted to further describe and compare PagN$_{STY}$ at the protein level with the PagN$_{STM}$ adhesin.

Much of the characterisation of PagN$_{STY}$ to date has been carried out by Ghosh *et al.* Using a computational analysis suggested by Freeman *et al.*, the Ghosh group predicted the PagN$_{STY}$ topology to be composed of 9 β-strands forming a barrel in the outer membrane with residues 30 – 42 and 75 – 97 forming two large extracellular loops (129). The Ghosh *et al.* topology prediction for PagN$_{STY}$ contradicts the structure predicted by the three online programmes utilised by this study (Fig. 4.12) (129). It is possible that the online programmes utilised in this study were false in their predictions; however, Ghosh *et al.* have indicated that there are 9 β-strands forming the transmembrane barrel of the protein. This means the N- and C-termini of the protein are located extracellularly and periplasmically, respectively. One of the major characteristics of β-barrel proteins is their even number of anti-parallel β-strands traversing the membrane bilayer (309). The topology generated by Ghosh *et al.* lacks this defining characteristic.

In addition to the concerns regarding Ghosh *et al.*'s predicted β-strand number and topology, they have only named two large extracellular loops despite having annotated four exposed loops. Their expected extracellular loops 3 and 4 are somewhat consistent with

Ghosh *et al.*

MKNFFAVCIIPLVVTWSATASA KEGIYITGKAGTS
VVNVYGINSTFSQDEEIVNGHATLPDRTKGVFGGG
VAIGYDFYDPFQLPVRLELDTTFRGETDAKGGQDII
AFGQPVHINVKNQVRMTTYIVNGYYDFHNSTAFTP
YISAGVGLAHVKLSNNTIPVGFGINETLSASKNNFA
WGAGIGAKYAVTDNIMIDASYKYINAGKVSISKNH
YAGDEHTAYDADTKAASNDFMLGITYAF

This study

MKNFFAVCIIPLVVTWSATASA KEGIYITGKAGTS
VVNVYGINSTFSQDEEIVNGHATLPDRTKGVFGGG
VAIGYDFYDPFQLPVRLELDTTFRGETDAKGGQDII
AFGQPVHINVKNQVRMTTYIVNGYYDFHNSTAFTP
YISAGVGLAHVKLSNNTIPVGFGINETLSASKNNFA
WGAGIGAKYAVTDNIMIDASYKYINAGKVSISKNH
YAGDEHTAYDADTKAASNDFMLGITYAF

FIG. 4.12. Comparison of the secondary structure predictions of the PagN$_{STY}$ protein. The box surrounds the signal sequence. Residues coloured red are predicted to be extracellular while those coloured blue are periplasmic. Transmembrane β-strands are underlined.

those predicted in this study, though the exact start and end points of the loops and transmembrane portions are variable. Ghosh *et al.* have suggested an extra 4 amino acid residues reside extracellularly in the exposed loop 4 of the protein (129). The predicted loop 2 of the protein is also somewhat consistent with that predicted by this study; the only difference lies in the proposed start of the extracellularly located amino acid residues. However, the predictions for Loop 1 of the protein are, very different to those proposed by this study. The structure proposed by Ghosh *et al.*, only contains 15 amino acid residues, which is quite small for an exposed loop (we have attributed 28 to loop 1) (129). Ghosh *et al.* proposed the N-terminus $PagN_{STY}$ protein is exposed on the extracellular side of the membrane (129). This would mean that many of the amino acids this study has annotated as part of the exposed loop 1 of the protein are buried in the outer membrane.

The high prediction confidence displayed by the online secondary structure prediction tools (203) lend credence to the topology predicted in this study as the true secondary structure of the $PagN_{STY}$ protein.

The ability of *Salmonella* to bind to, and enter host intestinal cells is central to its pathogenesis. Once *Salmonella* enter the small bowel, they must cross the intestinal mucous layer, after which they can attach to and invade the intestinal epithelia. *Salmonella* attach to the host cell using capsular proteins and fimbrial projections; fimbrial adhesins such as Type 1 fimbriae, curli (or tafi) fimbriae, Pef fimbriae, and Std fimbriae are all used by the bacterium to aid in adherence. Each type of fimbriae binds to a different cell surface receptor such as the extracellular matrix protein laminin, fibronectin, the Lewis X blood group antigen, and other receptors expressed in the cecal mucosa (19, 53-55, 65, 82, 200). Once initial attachment has taken place, the bacterium moves to a state of initmate contact before it begins to mobilise the T3SS-1 and an arsenal of effector proteins to produce a response in the host cell and bring about invasion. The T3SS injects the effector proteins into the host cell

thereby initiating phagocytosis by an otherwise non-phagocytic cell (Section 1.5.6.1).

Bacteria such as *Salmonella* use shorter, afimbrial adhesins to facilitate the transition between initial and intimate contact. Salmonellae have a varied collection of adhesins and invasins thought to aid in this transition. $PagN_{STM}$ has already been characterised as an adhesin and invasin (204, 205). This study sought to characterise the newly annotated $PagN_{STY}$ protein in terms of adhesion and invasion to several different mammalian cell types in both a quantitative and high-throughput manner.

Data from cell association and invasion assays indicate that $PagN_{STY}$ is also an adhesin and invasin. PagN conferred upon recombinant *E. coli* the ability to adhere to and invade both human (HT-29) and non-human (CHO-K1) epithelial cells. Expression of $PagN_{STY}$ in the poorly adhesive *E. coli* K-12 strain DH5α promoted ~29% cell association with an HT-29 monolayer, as compared with ~17% cell association for $PagN_{STM}$ expressing bacteria. Low-level invasion was also promoted; however, there was no significant difference in invasion or association mediated by $PagN_{STY}$ when compared with that of the $PagN_{STM}$ protein. When levels of $PagN_{STY}$-mediated cell association seen using the high-throughput assay are measured against cell association promoted by $PagN_{STM}$, there was a significant decrease in cell association mediated by the $PagN_{STY}$ protein. . It's possible that the decrease seen in the HCA is due to a more sensitive system of measurement. The GPA is a much utilised assay, however, it can be variable and is a more coarse and inelegant system of measurement.

Ghosh *et al.* also inspected cell association and invasion promoted by $PagN_{STY}$ (129). They determined that $PagN_{STM}$, when naturally expressed in *S.* Typhimurium LT2, did not promote the PagN-associated phenotypes seen here (129). In their assay, Ghosh *et al.* grew strains of *Salmonella* in L-broth to mid-log phase prior to invasion (129). As previously discussed, the conditions under which *pagN* is expressed

have been elucidated (66, 160-162, 194, 205). Maximal expression of *pagN* is not reached until early stationary phase (194). Growth in MOPS minimal media at a pH of 5.8 will also induce maximal *pagN* expression (66, 160-162, 205). As Ghosh *et al.* did not grow the *S.* Typhimurium strains in *pagN*-inducing media, it is unlikely that they were able to distinguish the true contribution of $PagN_{STM}$ to bacterial association and invasion.

In comparison to levels of association observed with HT-29 cells, $PagN_{STY}$ promoted lower levels of association with CHO-K1 cells (23% association), though invasion levels were raised (<1% invasion for HT-29 cells versus 5% invasion for CHO-K1 cells). There was a significant difference in invasion mediated by the two PagN proteins when analyzed using the GPA ($p < 0.05$). When compared using the high-throughput invasion assay, ~3.2 invasive bacteria/CHO-K1 cell and ~2.7 invasive bacteria/CHO-K1 cell were seen for bacteria expressing $PagN_{STM}$ and $PagN_{STY}$, respectively. Bacteria expressing $PagN_{STY}$ showed 83.3% of $PagN_{STM}$ levels of invasion. There was less of a noticeable difference in adhesion levels when the two PagN proteins are compared (90% of $PagN_{STM}$-levels of adhesion). There were no significant differences in CHO-K1 cell invasion or adhesion between bacteria carrying the PagN-expressing plasmids as measured by the HCA.

The discrepancies between cell association and invasion of CHO-K1 cells as compared to that of HT-29 cells suggest that while HT-29 cells display greater levels of the $PagN_{STY}$ receptor than CHO-K1 cells, bacteria expressing the PagN protein from *S.* Typhi are better able to invade the hamster-derived cell-line. The inconsistencies seen in $PagN_{STY}$-mediated cell association and invasion of HT-29 cells may be due to the production of bacteriocidal peptides such as defensins (72, 73, 294, 295). Ovary cells such as CHO-K1 cells do not produce defensins, and as such, are more readily invaded. Studies with HT-29 cells and T84 cells, a colorectal carcinoma derived from a 72 year old male, have revealed that differences between human colon carcinoma

cell lines significantly influence the levels of invasion and the mechanisms available for *S.* Typhimurium to enter into host cells (278); it is therefore not surprising that bacteria display disparate levels of invasion for cell lines from different host animals. Ghosh *et al.* characterised the $PagN_{STY}$ receptor as the extracellular matrix component, laminin, while previous studies by Lambert *et al.* described the $PagN_{STM}$ receptor as a heparan-sulphate proteoglycan (129, 204). It is possible that the differences in cell-association and invasion levels displayed by bacteria expressing the proteins are due to differences in expression levels of the receptor molecules on the surface of target cells. Future work comparing the two proteins should involve determination of $PagN_{STY}$-mediated interactions with heparan-sulphate proteoglycans, as well as characterisation of $PagN_{STM}$-interactions with laminin.

The vast array of data presented in this chapter predicts $PagN_{STY}$ as a β-barrel protein with four large extracellular loops, three short periplasmic turns, and an N-terminal signal sequence targetting it to the outer membrane using the Sec translocation machinery. Confirmation of the structure of $PagN_{STY}$ should be estabilished in future work through the crystallisation of the protein in its native form. $PagN_{STY}$ is also an adhesin and invasin comparable to the already characterised $PagN_{STM}$ protein. Using the gentamicin protection assay and a high-throughput fluorescent assay of invasion, $PagN_{STY}$ was shown to promote adhesion to and subsequent invasion of cultured epithelial cells in a clinically relevant cell type. Future work should include generation of mutant *S.* Typhi Ty2 strains lacking the *t2544/pagN* gene and repeated cell association and invasion assays using the parental and mutant strains of *S.* Typhi.

Chapter 5 A Structural and Functional analysis of the PagN protein of *Salmonella enterica*

5.1 Introduction

Once enteric bacteria such as *Salmonella* and *E. coli* have reached the intestinal lumen, the pathogen needs to establish initial contact with the epithelium to interact with target cells such as M cells in Peyer's patches. These bacteria may employ all or some of an arsenal of secretion systems, adhesins, fimbriae, and effector proteins to adhere to and invade the gut epithelial layer. Intimate attachment between the eukaryotic cells and bacteria is a prerequisite for the translocation activity of the *Salmonella* SPI-1 T3SS; however, attachment is initally mediated by fimbriae and adhesins. PagN is one such adhesin. The protein interacts with unknown receptors on the cell surface to promote attachment to the epithelial cell monolayer and induce bacterial uptake (204, 205). PagN was first identified in 1994 by Belden *et al.* as they identified and characterised the PhoP regulon of *S.* Typhimurium 14028s (22). Douglas Heithoff *et al.*, using *in vitro* expression technology (IVET), were able to identify >100 unique genes in *S.* Typhimurium 14028s as specifically expressed during infection of BALB/c mice (160) including the *pagN* gene, which they termed *iviVI-A*. In 1998, Conner *et al.* identified PagN mutants as less competitive when mutant deletions were mixed with the parental strain of *S.* Typhimurium 14028s and intraperitoneally injected into BALB/c mice (66). Heithoff *et al.* also identified the *pagN* gene as being highly up-regulated in cultured RAW 264.7 murine macrophages and human epithelial cells such as HEp-2 (larynx carcinoma) and Henle-407 (embryonic small intestine) cell lines (161). In addition to the IVET screens used by Heithoff *et al.*, *S.*

Typhimurium strain 4/74 lacking a functional *pagN* gene was shown to be attenuated in chickens, pigs, and cattle using transposon-directed insertion-site sequencing (TraDIS) (50).

Previous structure/function relationship studies have indicated that the PagN protein adopts a β-barrel outer membrane conformation (205). β-barrel proteins, such as OmpA, are structurally arranged in such a way as to insert the β-sheets into the lipid bilayer of the outer membrane and present large hydrophilic loops to the external environment (192, 327, 352). PagN possesses four large surface exposed loops (205), and it is likely that one of these loops interacts with a receptor located on the surface of epithelial cells. The *E. coli* proteins Tia and Hek are well-characterised adhesins and invasins (101, 103, 225). Tia has been shown to be necessary for invasion by Enterotoxigenic *E. coli* and sufficient to promote invasion by a non-invasive *E. coli* K-12 strain (225); while Hek plays a role in the primary attachment of neonatal-meningitic *E. coli* to epithelial cells (103). PagN, Tia, and Hek are similar proteins (62% identical, Fig. 5.1) and are expected to interact with similar receptors on the cell surface. Work in our lab has shown that the second extracellular loop of the Hek protein is necessary for all Hek-mediated phenotypes (101, 253). In 2009, data were published by Lambert and Smith to determine whether the second extracellular loop of PagN is a requirement for all PagN-promoted phenotypes (204). It was shown that contrary to the Hek protein, all four loops are necessary to produce all PagN-mediated phenotypes (204). A topological model (Fig. 5.2.) depicts the extent of each of the PagN truncates.

It was suggested that the previous loop-deletion mutants created were aggressive and although it was shown that the truncated proteins were able to insert in the outer membrane, it is possible that the loop-deletion proteins were unable to fully integrate and form a structurally sound β-barrel.

FIG. 5.1. Comparison of loop2 of the Hek and Tia proteins of *E. coli* with the PagN protein of *Salmonella*. Loop 2 of the Hek protein was aligned with the corresponding sequences of Tia and PagN. The amino acid numbers refer to the mature proteins. Identical residues are shaded black whilst semi-conserved are shaded grey. Image taken from (208).

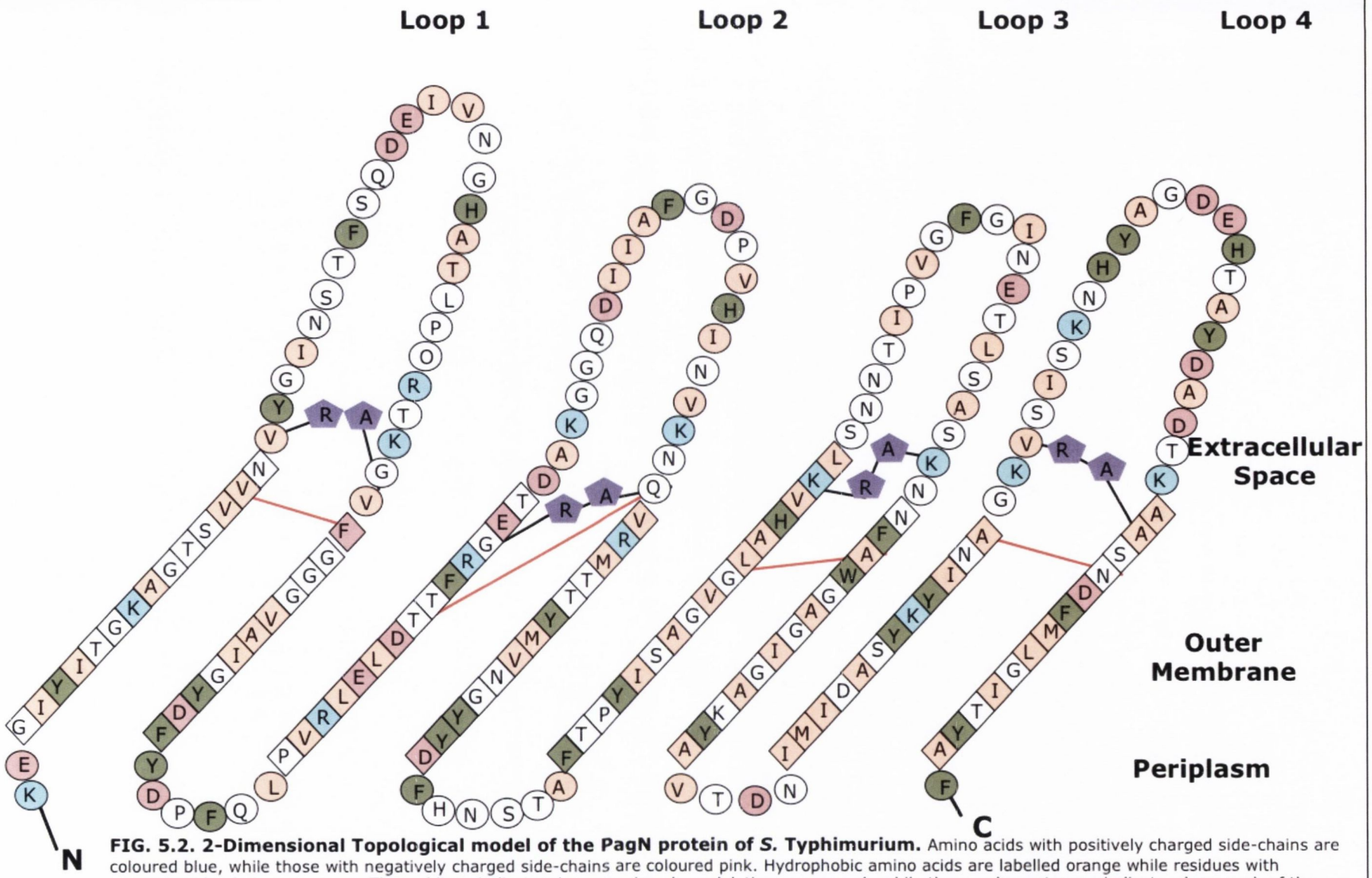

FIG. 5.2. 2-Dimensional Topological model of the PagN protein of *S.* Typhimurium. Amino acids with positively charged side-chains are coloured blue, while those with negatively charged side-chains are coloured pink. Hydrophobic amino acids are labelled orange while residues with aromatic side-chains are green. The red lines indicate where previous loop-deletions were made while the purple pentagons indicate where each of the loop-deletions created in this study were formed. The diamonds indicate transmembrane residues while the circles are located outside of the membrane.

The purpose of this study was to determine how the structure of the PagN relates to its functions. The questions deemed most relevant in this study were:

- Are all four extracellular loops of the PagN protein necessary for PagN-mediated invasion?
- Does PagN promote autoaggregation when expressed from the same promoter as the *hek* gene?
- Do the conserved charged residues between the Hek and PagN proteins affect PagN promoted phenotypes?
- What effect does PagN have on *Salmonella* adhesion to and invasion of mammalian cells?

5.1.1 Statistical Analyses Utilised

All data presented within all graphs in this chapter reflect the mean plus or minus the standard error. When the number of strains tested reached three or more, a one way analysis of variance test was used. The Dunnett post-test analysis was used to compare all means to a control mean as indicated in the text. Statistical significance was described for values where $p < 0.05$.

5.2 Results

5.2.1 Expression of *pagN* from a constitutive expression plasmid

5.2.1.1 Construction of pSP8

Originally, the *pagN* gene was cloned under the control of an IPTG inducible promoter to yield plasmid pML1 (203, 205). Experiments performed with bacteria harbouring pML1 are long. In order to circumvent the need for the extended period of growth, a constitutive expression plasmid where the *pagN* gene was under the control of an *E. coli* promoter was created. The promoter chosen was the P_{hek} of the *hek* gene as it consistently led to high levels of expression of the Hek protein (103). Furthermore, it was hypothesised that expression of PagN from this promoter would make subsequent experimental data directly comparable to that of a Hek control. Several strategies were attempted in order to clone the *pagN* gene under the constitutive P_{hek} promoter.

1. The *pagN* gene was amplified without its start codon and inserted into pHek6, which had been amplified using inverse PCR to exclude the *hek* gene. This did not yield any PagN-expressing clones.
2. Next, the P_{hek} promoter was amplified by PCR to create an *Nco*I restriction site prior to the start of the *hek* gene and ligated to a promoter-less *pagN* gene expressed in pML4. Unfortunately, as the DNA at the promoter is extremely AT rich, a reverse primer capable of faithfully binding to the DNA could not be created.
3. Finally, pHek6 was mutated to contain a new *Nco*I site at the start codon, this created plasmid pHekN. The *pagN* gene was digested from pML4 using *Nco*I and *Bam*HI and ligated to the pHekN backbone, which had been previously digested with the same

restriction endonucleases to create pSP8. Several clones were tested for insertion of the *pagN* gene.

It was expected when pSP8 was digested with *Hind*III and *Bam*HI it would yield two fragments; the first at 2.9 kbp and the second at 819 bp. When pHekN was digested, it yielded fragments at 2.9 kbp and 860 bp, and pML4 (the plasmid from which the *pagN* gene was purified) yielded fragments at 2.9 kbp and 720 bp. Putative samples were sequenced and found to contain the *pagN* gene under the control of the consitutively active P_{hek} promoter. Figure 5.3 outlines the construction of pSP8 and shows an agarose gel of plasmids pSP8, pHekN, and pML4 after digestion with *Hind*III and *Bam*HI.

5.2.1.2 Full length PagN is produced by pSP8

Once the constitutive expression plasmid was created, a Western immunoblot was necessary to determine whether full length PagN was produced by bacteria harbouring this plasmid. PagN-production by pSP8 was compared with production by the inducible pML1 plasmid via Western immunoblotting (Fig. 5.4). The anti-PagN peptide antibody (Eurogentec) was used at a concentration of 1:1000. *E. coli* express a multitude of other proteins including maltose binding protein (MBP). MBP can be found in whole-cell lysates of bacteria and is a useful loading control. Protein of the correct predicted size (~26 kDa) was detected for the constitutive expression PagN.

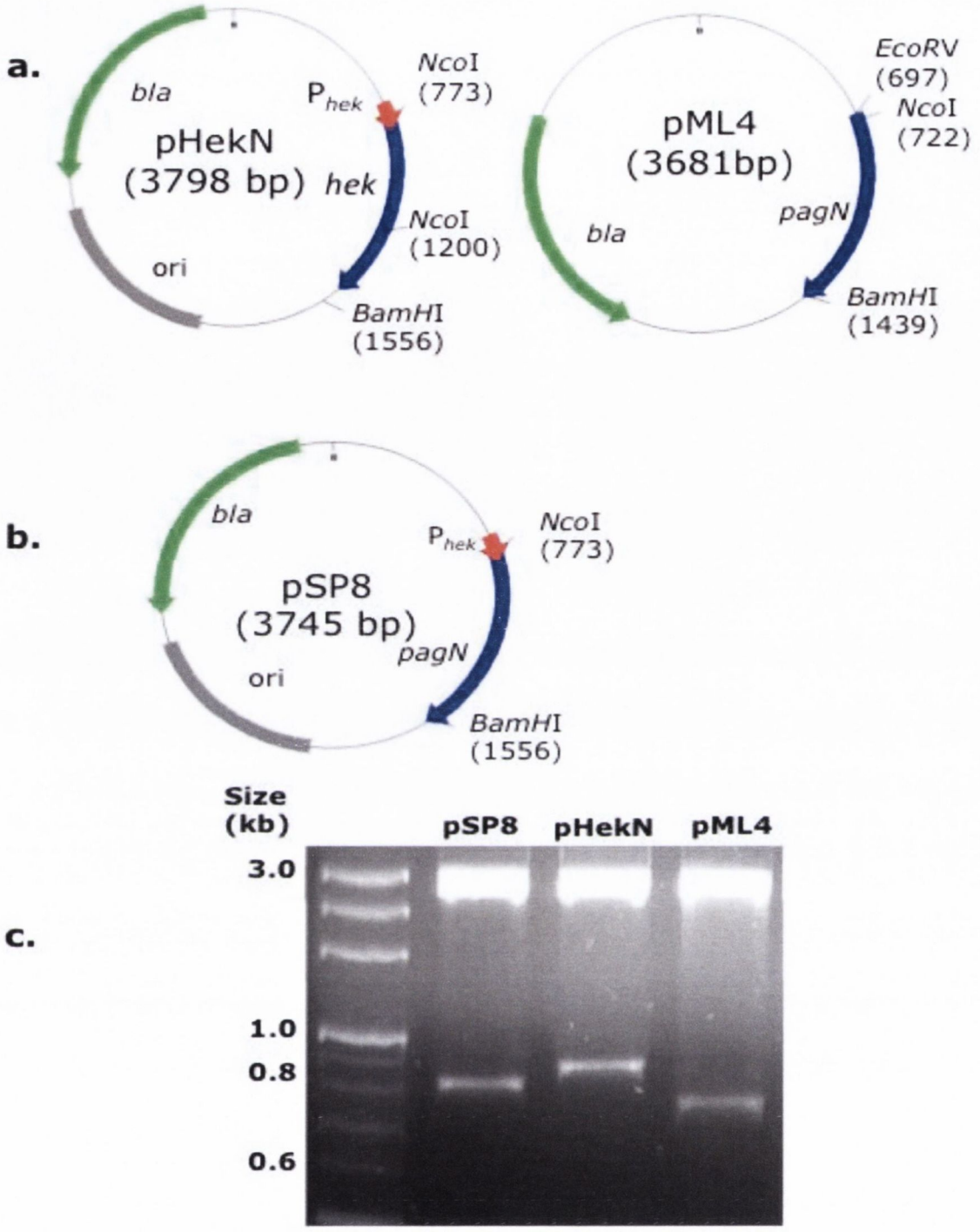

FIG. 5.3. Creation of a *pagN* constitutive expression plasmid. An *Nco*I restriction site was created in plasmid pHek6 using site-directed mutagenesis to create plasmid pHekN. A promoter-less *pagN* gene was isolated from pML4 after digestion with *Nco*I and *BamH*I (panel a). The *pagN* gene was ligated with the pHekN backbone to give rise to plasmid pSP8 in which the *pagN* gene is under the control of the P_{hek} promoter (panel b). Putative clones were digested with *BamH*III and *Hind*III. Panel c displays a 2% agarose gel showing a digestion of pSP8, pHekN, and pML4. A 2.9 kb band corresponding to the plasmid backbone was expected for each. A second band at 816 bp, 860 bp, and 720 bp was expected for pSP8, pHekN, and pML4, respectively.

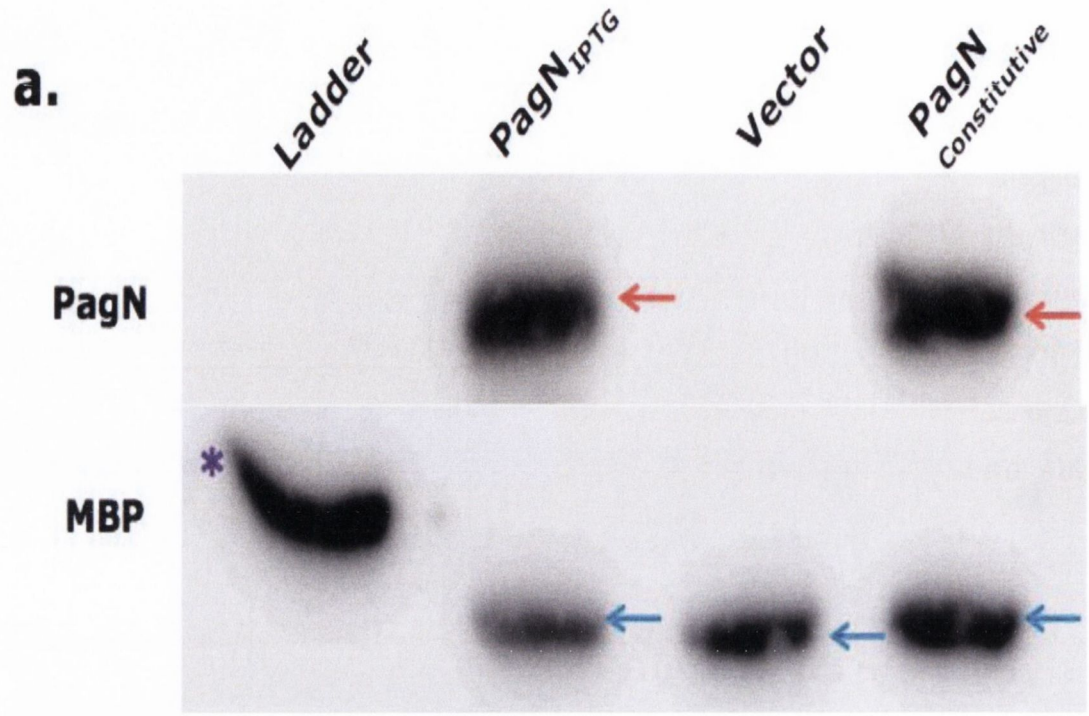

FIG. 5.4. Expression of PagN protein from the inducible pML1 plasmid and the constitutive expression plasmid pSP8 in *E. coli*. Panel a displays a Western immunoblot performed using whole cell lysates of *E. coli* XL-1 Blue cells expressing *pagN* from either the IPTG-inducible pML1 plasmid or the constitutie expression plasmid pSP8. The red arrows indicate PagN protein. The pTrc99a vector control is displayed in lane 3, while the protein ladder is displayed in lane 1. The ~42 kDa maltose binding protein (MBP) was used as a loading control (blue arrows). The purple asterisk in lane 1 indicates an MBP-fusion protein of a higher molecular weight.

5.2.1.3 PagN expressed from pSP8 does not promote autoaggregation

Liquid cultures of *E. coli* K-12 harbouring the pHek6 plasmid, containing the *hek* gene were observed to clear rapidly when allowed to stand at room-temperature (103). Bacteria began to settle out of solution and to clump together at the bottom of the culture tube. The rapid bacterial settling was termed autoaggregation and is an easily assayed Hek-promoted phenotype. Autoaggreggation was not displayed by PagN-expressing bacteria (203), however it was suggested that perhaps the autoaggregation associated with the Hek protein was due in part to the expression of the *hek* gene by the P_{hek} promoter. In the pSP8 plasmid, the *pagN* gene is under the control of the P_{hek} promoter, indicating that PagN produced by this plasmid may promote autoaggregation.

The OD_{600nm} of overnight cultures of bacteria were measured, bacteria were harvested by centrifugation, and resuspended to 4 OD_{600nm} units/ml. Autoaggregation rates were calculated by monitoring change in the OD_{600nm} of settling overnight cultures every 30 min over the course of 3 hours. Vector (pBSKII)-containing *E. coli* XL-1 Blue were used as a negative control, as they autoaggregate at a rate of 0.0132 OD_{600nm} units per minute. *E. coli* XL-1 Blue containing pHek6 were used as a positive control as they autoaggregate at a rate of 0.136 OD_{600nm} units per minute. *E. coli* expressing PagN from plasmid pSP8 displayed an autoaggregation rate of 0.00595 OD_{600nm} units per minute. These data indicate that although *pagN* was expressed from the *hek* promoter, the protein was unable to promote similar interactions between bacteria. In Fig. 5.5, the autoaggreggation of Hek, vector, and PagN expressing bacteria is shown over a time course.

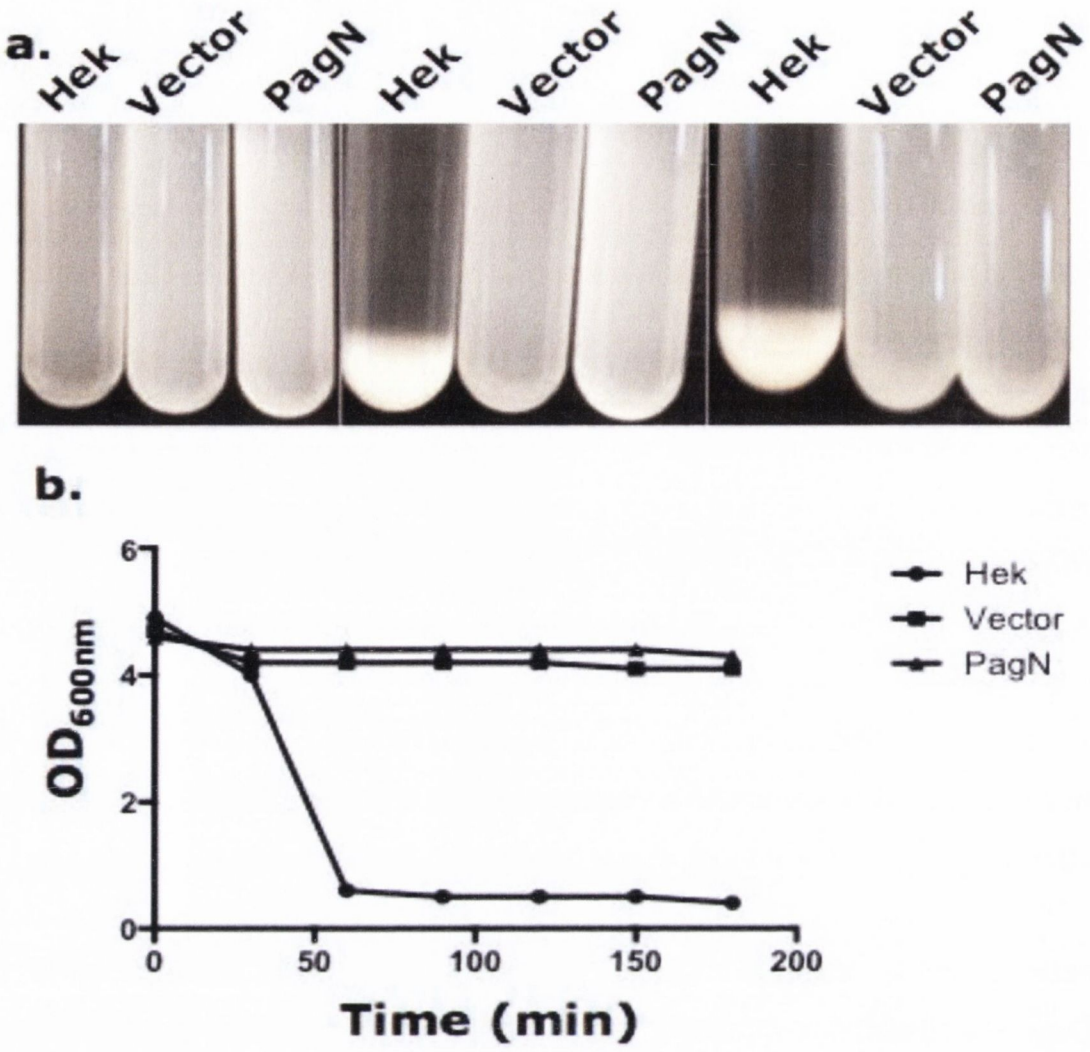

FIG. 5.5. Autoaggregation of *E. coli* expressing the Hek or PagN proteins. The OD_{600nm} of *E. coli* XL-1 expressing Hek, PagN, or the vector plasmid (from plasmids pHek6, pBSKII, and pSP8, respectively) were monitored over the course of 3 hours. At 0 minutes incubation, the khan tubes containing the bacterial suspensions was opaque (panel a); however, a rapid clearing was seen for bacteria expressing the Hek protein (panel a). This clearing was not seen for bacteria expressing the vector plasmid (panel a) or PagN protein (panel a). There was a steep drop in the optical density for cultures expressing Hek (panel b, circles), and again, this was not displayed for bacteria expressing the PagN protein (panel b, triangles) or the vector plasmid (panel b, squares).

5.2.1.4 PagN expressed from pSP8 does not mediate invasion of CHO-K1 cells

The purpose of the creation of pSP8 was to dramatically decrease the amount of time needed for bacterial growth and protein expression prior to the start of invasion and cell association experiments. Strains of *E. coli* K-12 harbouring pHek6 plasmids are grown overnight and can be used in experiments immediately after as the P_{hek} promoter induces constitutive expression. In order to determine whether PagN produced from the pSP8 plasmid was able to promote invasion of CHO-K1 cells, a standard gentamicin assay was performed. These data established that PagN produced by plasmid pML1 was internalised in significantly greater numbers than the constitutive expression strain harbouring plasmid pSP8 (Fig. 5.6). Data from triplicate wells revealed that levels of invasion mediated by the constitutive expression PagN protein were reduced by 96%, to the same level seen by bacteria harbouring the empty vector plasmid ($p < 0.001$, as measured using the one way analysis of variance with the Dunnett post-test to compare all means to the bacteria expressing PagN expressed from plasmid pML1). The significant decrease in invasion mediated by PagN expressed from pSP8 is interesting. The plasmid was sequenced, confirming the correct sequence of the *hek* promoter as well as the sequence of the *pagN* gene. In addition to the correct sequence, a Western immunoblot of the outer membrane confirmed that PagN protein was produced and trafficked to the outer membrane, indicating that there should have been no difference between PagN produced by pML1 when compared with that manufactured by pSP8. There are no major differences in the vector backbone of the plasmids (pTRC99a for pML1 and pBluescript II SK for pSP8), indicating that the differences must lie in either the protein expression, or perhaps in the copy number of the plasmid.

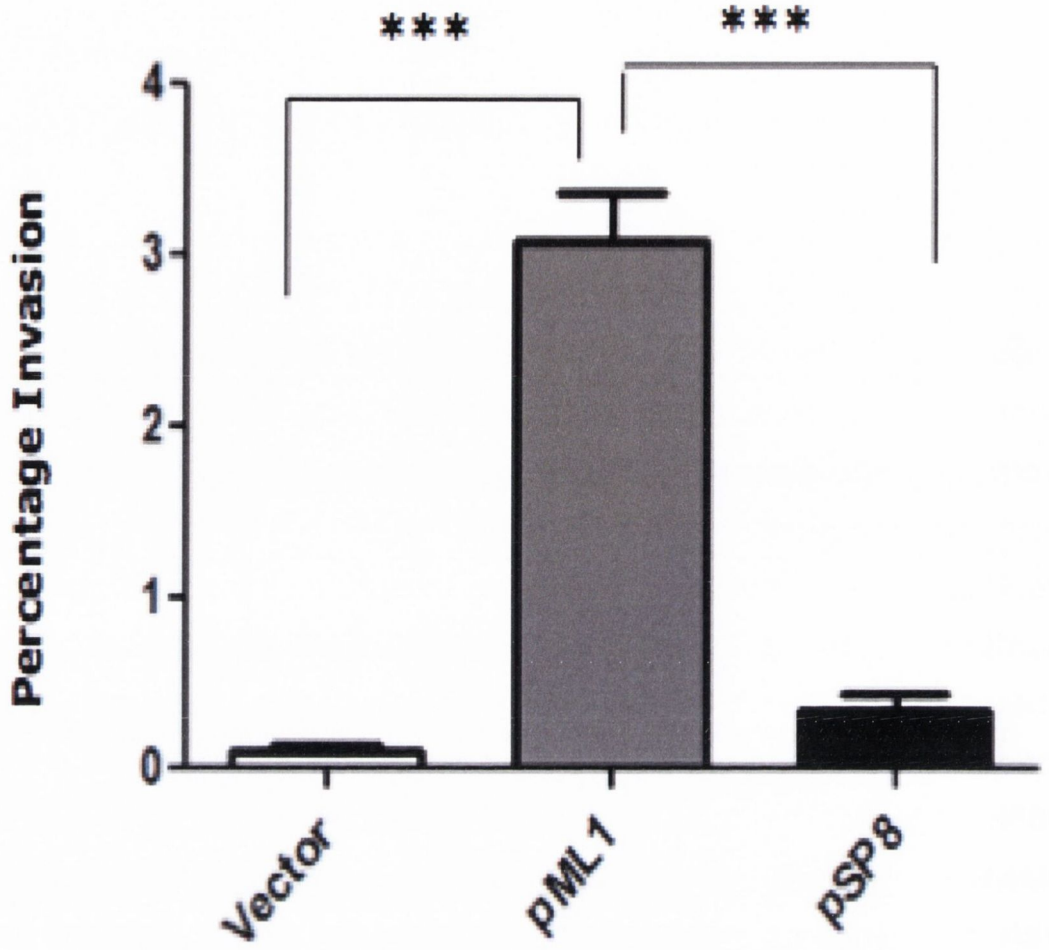

FIG. 5.6. *E. coli* invasion of CHO-K1 cells via inducible or constitutive expression of PagN protein. A gentamicin protection assay was performed as described in Section 2.3.4.1. *E. coli* DH5αZ1 expressing *pagN* from the IPTG-inducible pML1 plasmid or the constitutive expression pSP8 plasmid were incubated with CHO-K1 cell monolayers. External bacteria were killed using gentamicin and the internalised bacteria were enumerated. The average percentage invasion is depicted. There was a highly statistically significant difference seen for bacteria harbouring the empty vector plasmid or the pSP8 plasmid as compared with the invasion of bacteria harbouring the pML1 plasmid. *** denotes $p < 0.001$. Data were analysed using the one way analysis of variance with the Dunnett post test to compare all means to the bacteria expressing PagN expressed from plasmid pML1.

5.2.2 Structure/Function analysis of the PagN protein

5.2.2.1 A Comparison of PagN loop-deletion mutants

5.2.2.1.1 Expression of PagN loop-deletion mutants

As described in Section 5.1, the homologous Tia and Hek invasins of *E. coli* utilise a single extracellular loop to mediate their functions. Interestingly, the PagN protein seemed to deviate from this trend as it was shown to require all four extracellular loops to mediate invasion (204). It was important to confirm whether PagN protein was produced from each plasmid used by Lambert *et al.* (204). A Western immunoblot of whole cell lysates of full-length PagN and PagNΔloops was performed (Fig. 5.7). For each lysate, a band corresponding to the PagN protein was seen; this band was absent from lysates containing the empty vector plasmid, and from the lysate containing the loop four deletion mutant. The loop four deletion contains the peptide sequence that was used in the anti-PagN peptide antibody; deletion of the fourth extracellular loop abolished the ability of the antibody to detect the truncated PagN protein. The 42 kDa maltose binding protein (MBP) was used as a loading control.

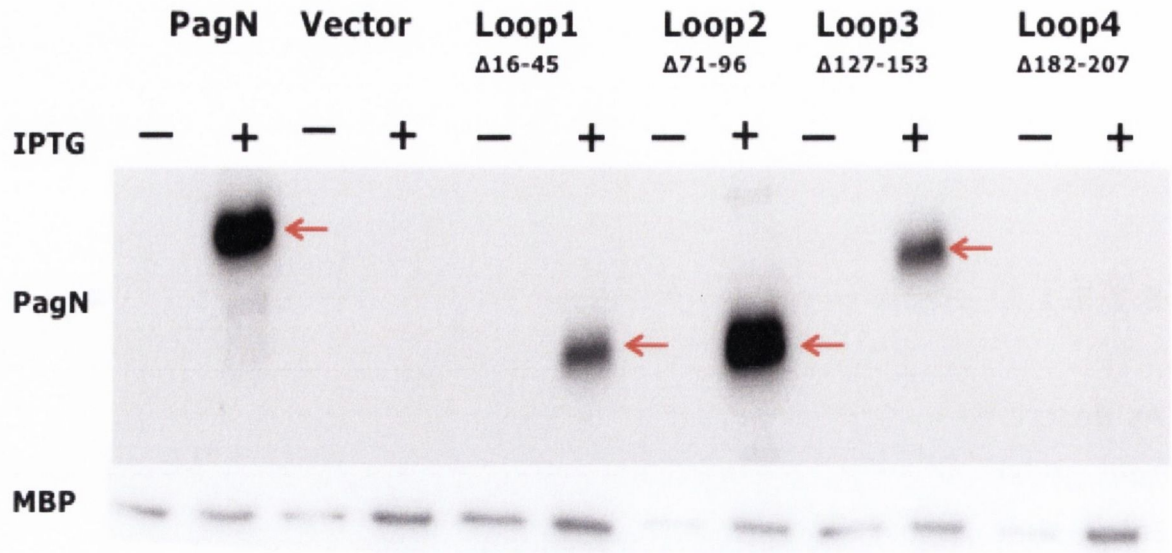

FIG. 5.7. Expression of full length PagN and PagN truncates in *E. coli*. A Western immunoblot was performed using whole cell lysates of *E. coli* XL-1 Blue cells expressing wild-type *pagN* or PagN loop-deletion mutants from plasmids pML1 and pΔLoop1-4, respectively. The pTrc99a vector control is also displayed. The Loop4 deletion mutant could not be detected via immunoblotting as the anti-PagN antibody recognises a peptide sequence located on the exposed loop4 of the protein. The red arrows indicate PagN protein. + indicates the addition of IPTG while – indicates no IPTG was added. The 42 kDa maltose binding protein (MBP) was used as a loading control.

5.2.2.1.2 Interaction of PagN with mammalian epithelial cells

To investigate if the removal of the extracellular loops of PagN affected the adhesion to and invasion of CHO-K1 monolayers a high-throughput invasion assay was performed as described in Section 2.4.3.2. *E. coli* DH5αZ1 carrying the pML1 plasmid were compared with those harbouring the loop-deletion plasmids. PagN expressed exogenously in *E. coli* has been shown to promote strong invasion of CHO-K1 epithelial cells ((204, 205), Section 4.2.2.6.1/2). 12 fields per well (4 wells per strain) were imaged using the Olympus IX81 microscope (Fig. 5.8.). An average of 6.3 – 6.7 invasive bacteria per CHO-K1 cell were seen for full-length PagN while less than 1 bacterium per CHO was seen for bacteria harbouring the vector plasmid or any of the PagN loop-deletion plasmids. Similar trends were seen for bacteria adhering to the mammalian cells; between 3.3 – 3.5 bacteria per CHO-K1 cell were seen for the PagN expressing bacteria while less than 1 bacterium per cell was visualised for the vector and loop-deletion plasmids. The data shown in Fig. 5.9 indicates the average number of intracellular (panel a) or extracellular (panel b) bacteria per CHO-K1 cell. Deletion of each of the loops decreased invasion or adhesion by 95 to 99 percent as compared with wild-type PagN. There was a highly statistically significant difference between full-length PagN-mediated adhesion to and invasion of CHO-K1 cells and that mediated by any of the loop-deletion mutants ($p < 0.0001$, tested by one-way ANOVA method and Dunnett post-test to compare all means to full-length PagN). These data were in agreement with that generated by Lambert *et al.* (204). Using the previously created loop-deletion constructs, the PagN protein requires all four extracellular loops to interact with CHO-K1 cells.

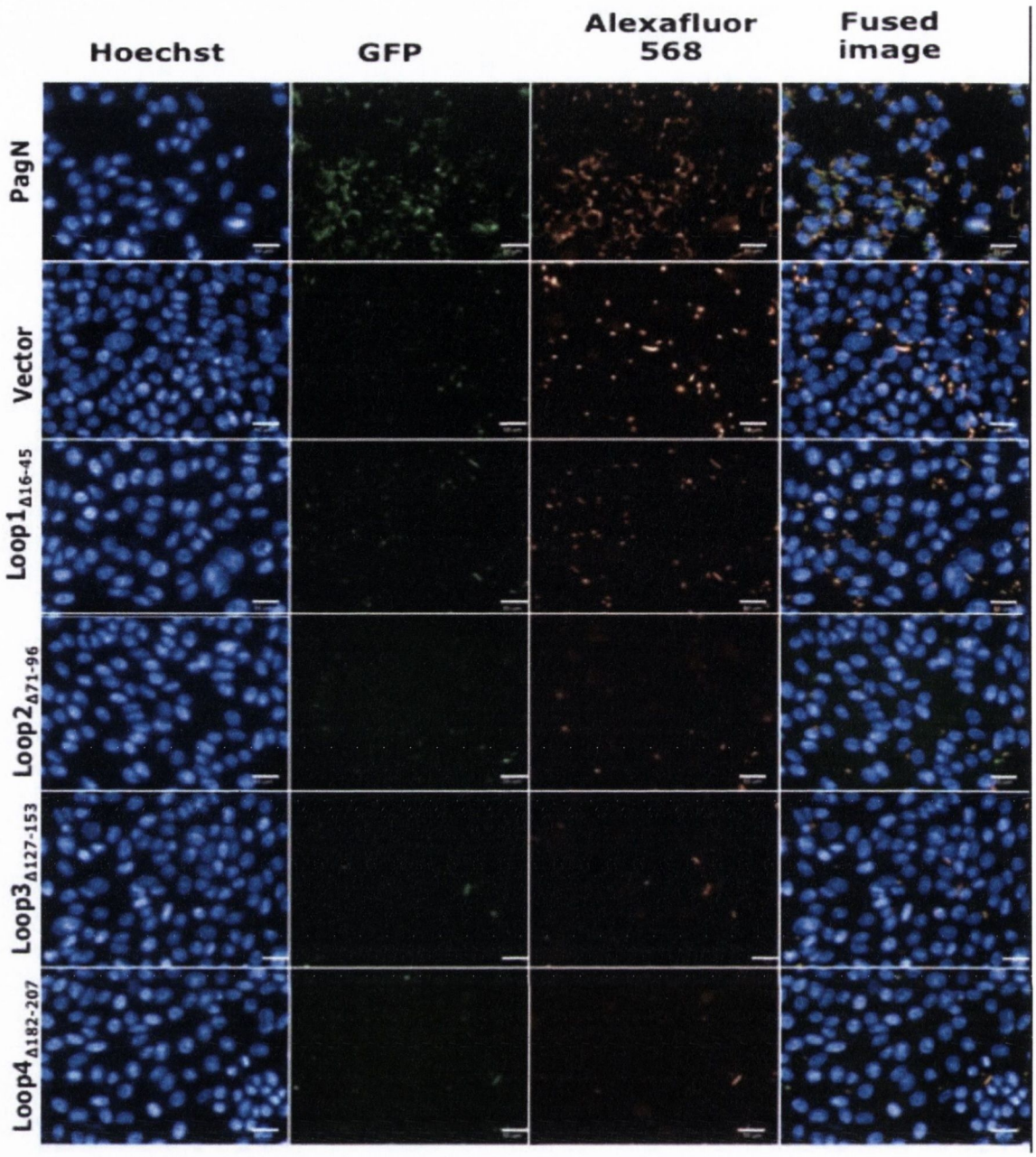

FIG 5.8. Images of PagN-mediated invasion of CHO-K1 epithelial cells. A high-throughput fluorescent invasion assay was performed as described in Section 2.3.4.2. to determine whether all four extracellular loops of the PagN protein are necessary to mediate adhesion to and invasion of CHO-K1 cells. *E. coli* DH5αZ1 expressed PagN from plasmid pML1 and the mutant PagN proteins from plasmids pLoop1$_{\Delta 16\text{-}45}$, pLoop2$_{\Delta 71\text{-}96}$, pLoop3$_{\Delta 127\text{-}153}$, and pLoop4$_{\Delta 182\text{-}207}$, respectively or harboured an empty vector plasmid. Mammalian cells were stained with hoechst, bacteria express GFP, and extracellular bacteria were distinguished using an Alexafluor 568 nm antibody. The white bar indicates 50 μm.

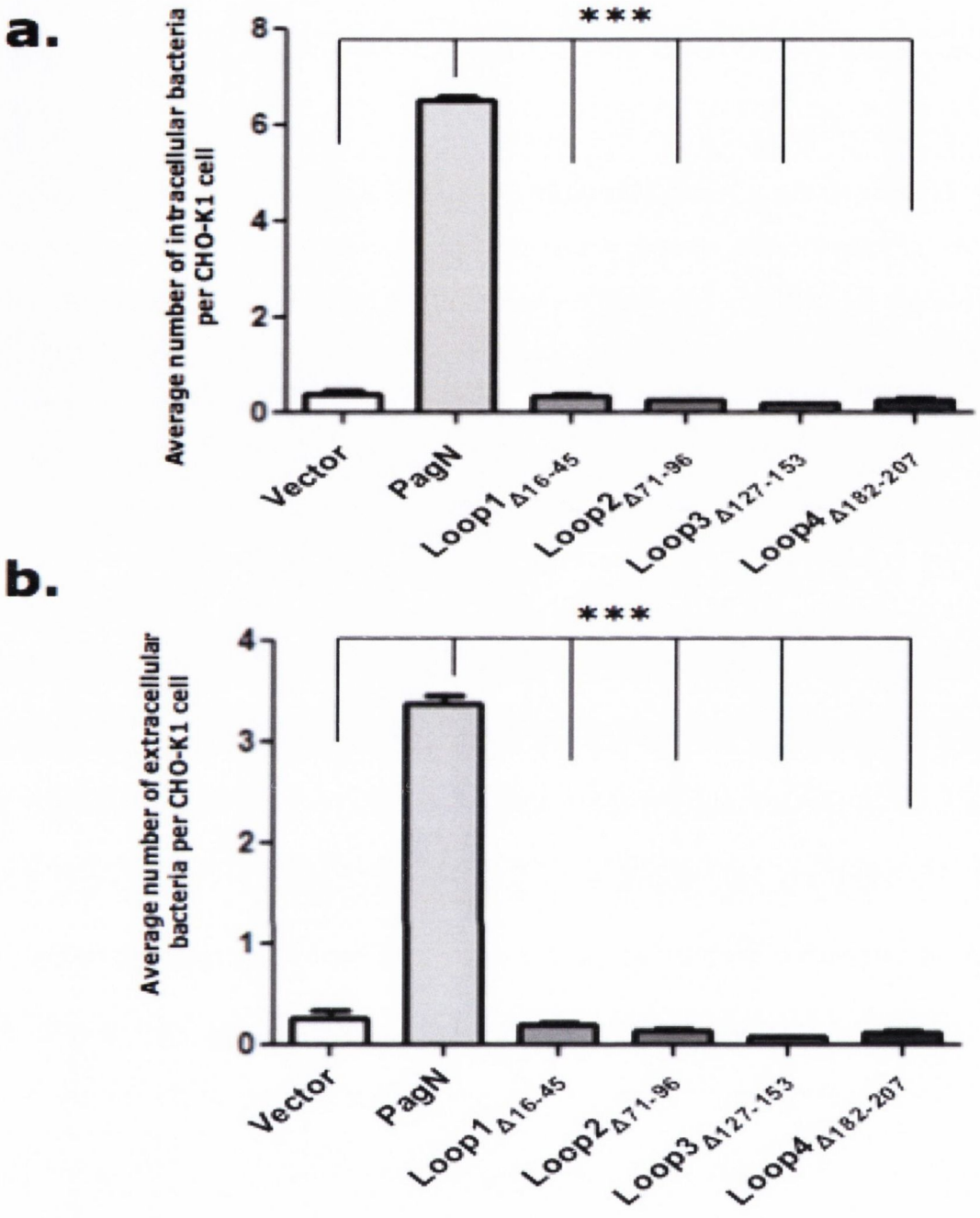

FIG 5.9. PagN-mediated invasion of CHO-K1 epithelial cells. A high-throughput fluorescent invasion assay was performed as described in Section 2.4.3.2. to confirm whether all four extracellular loops of the PagN protein are necessary to mediate adhesion to and invasion of CHO-K1 cells. *E. coli* DH5αZ1 expressed PagN from plasmid pML1 and the mutant PagN proteins from plasmids pLoop1$_{\Delta 16\text{-}45}$, pLoop2$_{\Delta 71\text{-}96}$, pLoop3$_{\Delta 127\text{-}153}$, and pLoop4$_{\Delta 182\text{-}207}$, respectively. The assay was performed in triplicate and the average number of intracellular (panel a) or extracellular (panel b) bacteria per CHO-K1 cell is displayed. There was an extremely statistically significant difference in invasion mediated by full-length PagN when compared with that promoted by the PagN-truncates (*** indicates $p < 0.0001$). Data were analysed using the one way analysis of variance with the Dunnett post test to compare all means to the bacteria expressing full-length PagN protein.

5.2.2.2 Interaction of PagN with HT-29 enterocytes

A high-throughput invasion assay was also performed using HT-29 cells to compare PagN-mediated invasion of a more infection relevant cell line. The images generated by the Olympus IX81 microscope are displayed in Fig. 5.10. There was a highly significant difference between full-length PagN-mediated adhesion to and invasion of HT-29 cells and that mediated by any of the loop-deletion mutants ($p < 0.0001$) (Fig. 5.11(a) and 5.11(b)). A 95 to 99 percent decrease in adhesion was also seen for the PagN-loop deletion mutants. While these data indicate that PagN absolutely requires all four extracellular loops to mediate interactions with receptors on the surface of mammalian epithelial cells, it is possible that the truncations affected the stability of the protein in the outer membrane, thus abrogating its function. Therefore, less aggressive loop-deletion mutants were engineered to test this theory.

5.2.2.2.1 Creation of new *pagN* loop-deletion mutants

A series of new, less drastic loop-deletion mutant ORFs were constructed based on the PagN expression vector, pML1. Inverse PCR, using divergent primers which flank the region to be deleted (Table. 2.3), were used to generate a linear fragment lacking the DNA sequence corresponding to a particular loop. Re-ligation of this linear DNA produced an expression vector capable of expressing a mutant PagN protein lacking one of the four loop sections. In order to retain a correctly folded protein, the individual loops were replaced with Arginine - Alanine di-amino acid sequence. Arginine was chosen for its turn-promoting properties (292) and Ala as it has a short side chain. In

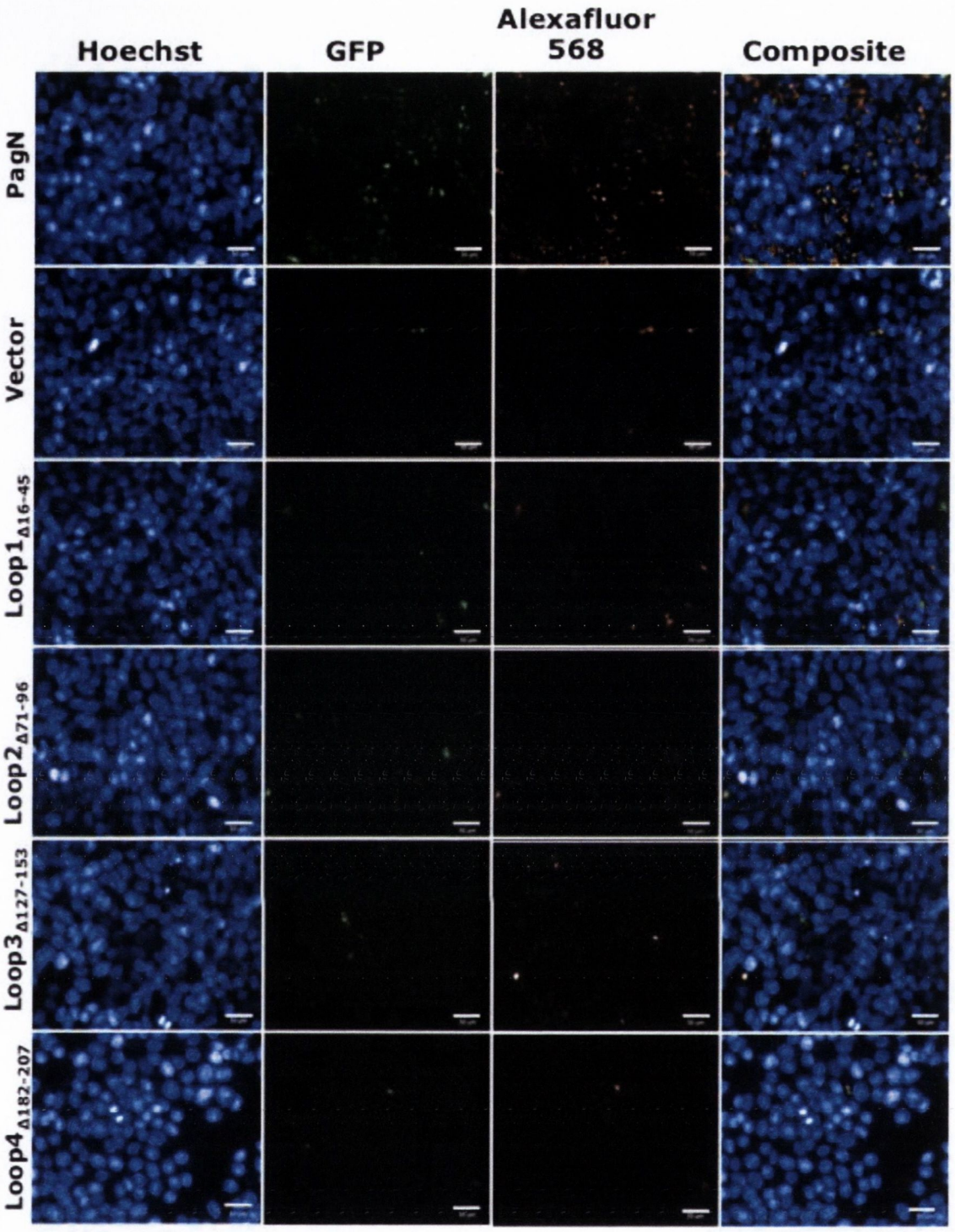

FIG 5.10. Images of PagN-mediated invasion of human HT-29 cells. A high-throughput fluorescent invasion assay was performed as described in Section 2.2.4.2. to determine whether all four extracellular loops of the PagN protein are necessary to mediate adhesion to and invasion of HT-29 cells. *E. coli* DH5αZ1 expressed the vector plasmid, or PagN from plasmid pML1 and the mutant PagN proteins from plasmids pLoop1$_{\Delta 16\text{-}45}$, pLoop2$_{\Delta 71\text{-}96}$, pLoop3$_{\Delta 127\text{-}153}$, and pLoop4$_{\Delta 182\text{-}207}$, respectively. Mammalian cells were stained with Hoechst, bacteria express GFP, and extracellular bacteria were distinguished using an Alexafluor 568 nm antibody. The white bar indicates 50 μm.

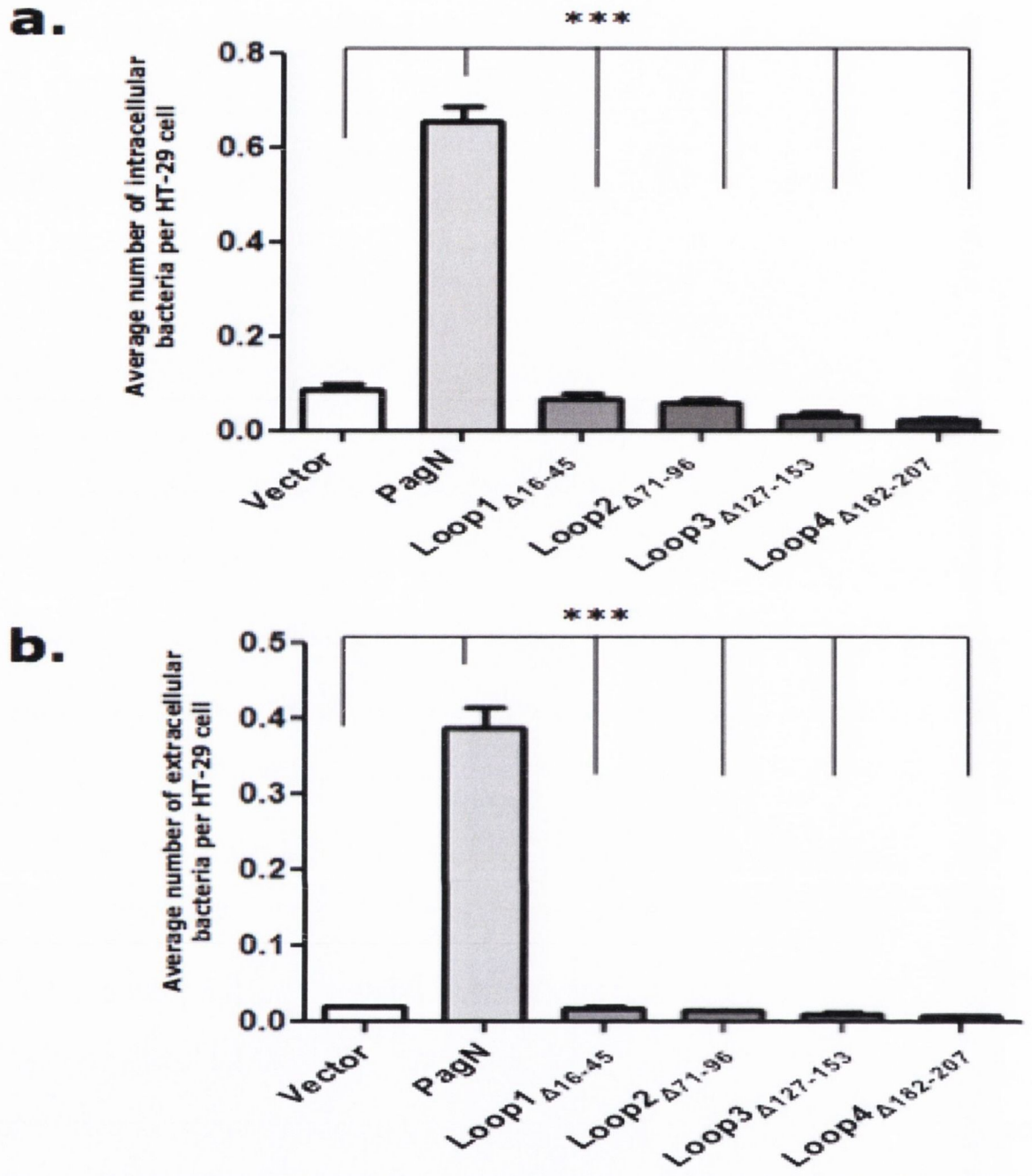

5.11. Interaction of PagN protein with HT-29 colonic epithelial cells. A high-throughput fluorescent invasion assay was performed as described in Section 2.4.3.2. to confirm whether all four extracellular loops of the PagN protein are necessary to mediate adhesion to and invasion of HT-29 cells. *E. coli* DH5αZ1 expressed PagN from plasmid pML1 and the mutant PagN proteins from plasmids pLoop1$_{\Delta 16\text{-}45}$, pLoop2$_{\Delta 71\text{-}96}$, pLoop3$_{\Delta 127\text{-}153}$, and pLoop4$_{\Delta 182\text{-}207}$, respectively. The assay was performed in triplicate and the average number of intracellular (panel a) or extracellular (panel b) is displayed. There was an extremely statistically significant difference in both adhesion and invasion mediated by full-length PagN when compared with that promoted by the PagN-truncates. *** denotes $p < 0.0001$. Data were analysed using the one way analysis of variance with the Dunnett post test to compare all means to the bacteria expressing full-length PagN protein.

this manner, four expression vectors were constructed each one lacking the DNA coding for one of the four predicted loop domains. The structure of putative mutant plasmids was confirmed by diagnostic endonuclease digests. Each plasmid was sequenced to confirm the DNA sequence of the insert and they were designated ploop1$_{\Delta 18\text{-}42}$, ploop2$_{\Delta 74\text{-}96}$, ploop3$_{\Delta 131\text{-}150}$, and ploop4$_{\Delta 184\text{-}205}$. The extent of each loop deletion is shown in the topological model depicted in Fig. 5.2.

5.2.2.2.2 Expression of PagN loop-deletion mutants

Once putative PagN-loop deletion-expressing plasmids were sequenced, it was important to determine whether PagN protein was produced from each plasmid. A western immunoblot of whole cell lysates of full-length PagN and PagNΔloops was performed (Fig. 5.12 (a)). For each lysate, a band corresponding to the PagN protein was seen, and this band was absent from lysates containing the empty vector plasmid, and from the lysate containing the loop four deletion mutant. An SDS gel was prepared in tandem with the Western immunoblot and was subsequently stained using Coomassie stain to demonstrate equal loading in all lanes (Fig. 5.12(b)).

5.2.2.2.3 Interaction of PagN with CHO-K1 cells

To investigate if the removal of the extracellular loops of PagN affected the adhesion to and invasion of CHO-K1 monlayers a high-throughput invasion assay was performed as described in Section 2.3.4.2. *E. coli* DH5αZ1 carrying the pML1 plasmid were compared with those harbouring the new loop-deletion plasmids. Images generated using the Olympus IX81 microscope are displayed in Fig. 5.13. An average of 2.8 – 3.6 invasive bacteria per CHO-K1 cell were seen for full-length PagN while less than 1 bacterium per cell was seen for bacteria

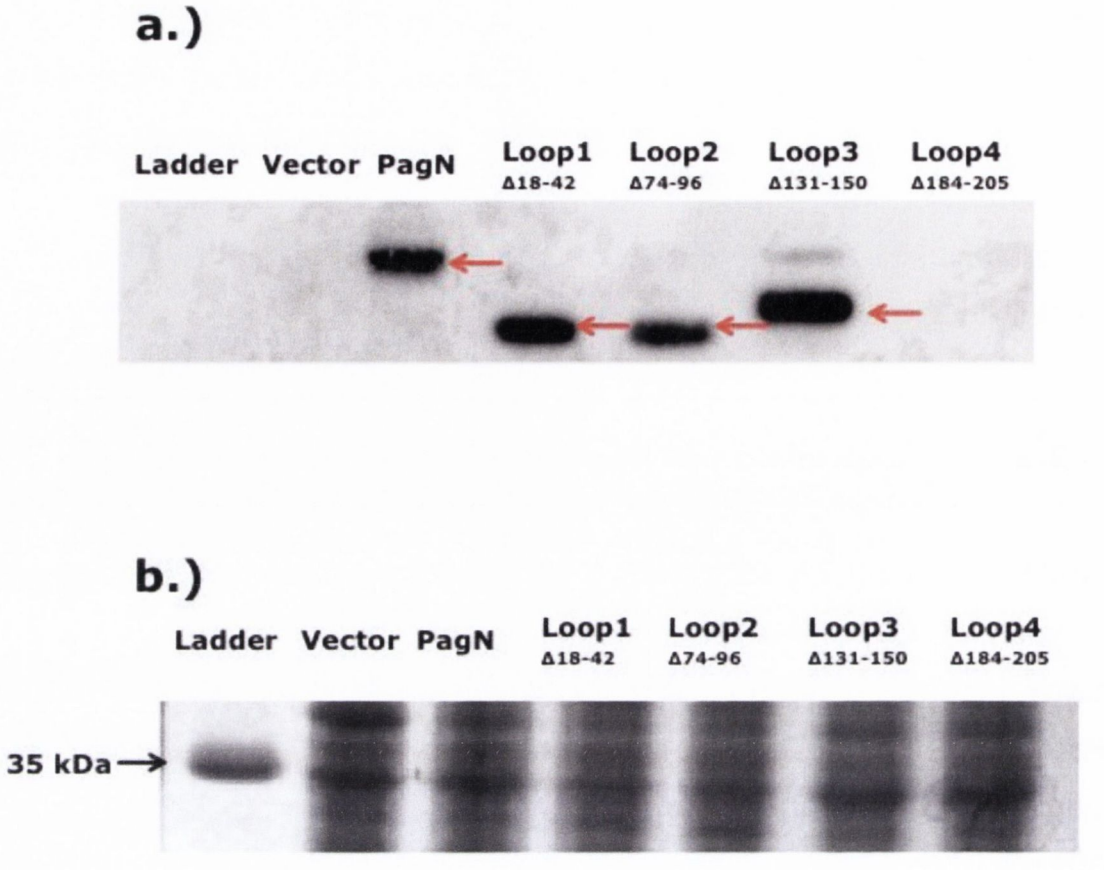

FIG. 5.12. Expression of full length PagN and PagN truncates in *E. coli*. A Western immunoblot was performed using whole cell lysates of *E. coli* XL-1 Blue cells expressing wild-type *pagN* or PagN loop-deletion mutants from plasmids pML1 and pΔLoop1-4, respectively (panel a). The pTrc99a vector control are also displayed, though they could not be detected by the anti-PagN antibody. The Loop4 deletion mutant could not be detected via immunoblotting as the anti-PagN antibody recognises a peptide sequence located on the exposed loop4 of the protein. The red arrows indicate PagN protein. An SDS gel stained with Coomassie stain is depicted in panel b to show equal loading.

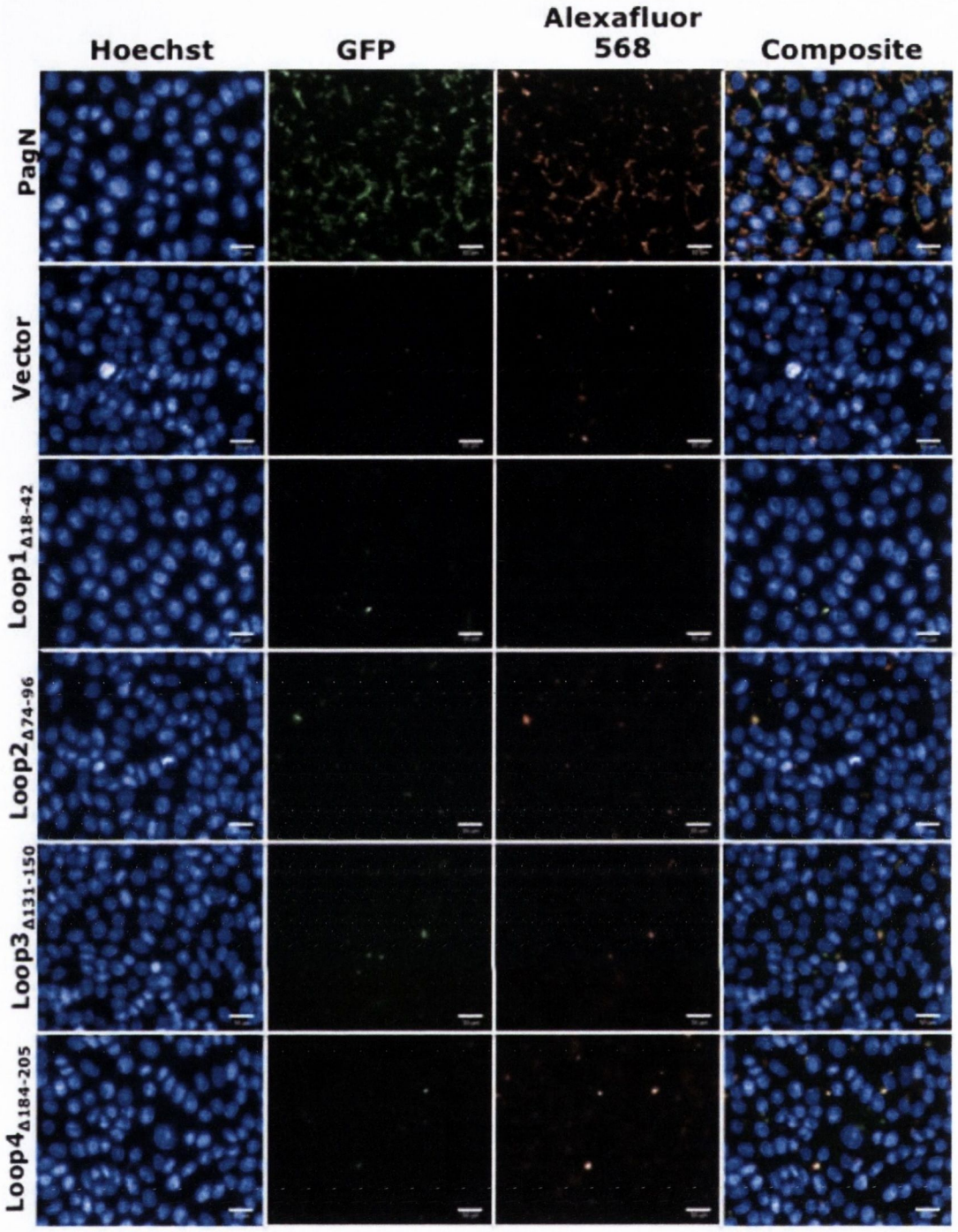

FIG 5.13. Images of PagN-mediated invasion of CHO-K1 epithelial cells. A high-throughput fluorescent invasion assay was performed as described in Section 2.3.4.2. to determine whether all four extracellular loops of the PagN protein are necessary to mediate adhesion to and invasion of CHO-K1 cells. *E. coli* DH5αZ1 expressed PagN from plasmid pML1 and the mutant PagN proteins from plasmids pLoop1$_{\Delta 18\text{-}42}$, pLoop2$_{\Delta 74\text{-}96}$, pLoop3$_{\Delta 131\text{-}150}$, and pLoop4$_{\Delta 184\text{-}207}$, respectively or the empty vector plasmid. Mammalian cells were stained with Hoechst, bacteria express GFP, and extracellular bacteria were distinguished using an Alexafluor 568 nm antibody. The white bar indicates 50 μm.

harbouring the vector plasmid or any of the PagN loop-deletion plasmids. Similar trends were seen for bacteria adhering to the mammalian cells; between 2.0 – 2.8 bacteria per CHO-K1 cell were seen for the PagN expressing bacteria while less than 1 bacterium per CHO was visualised for the vector and loop-deletion-expressing bacteria. The data shown in Fig. 5.14 indicates the average number of intracellular (panel a) or extracellular (panel b) bacteria per CHO-K1 cell. Deletion of each of the loops decreased the invasion by 86 to 91 percent as compared with wild-type PagN. There was a highly statistically significant difference between full-length PagN-mediated adhesion to and invasion of CHO-K1 cells and that mediated by any of the loop-deletion mutants ($p < 0.0001$). These data reflect those presented in Section 5.2.2.1.2. PagN absolutely requires all four loops for adherence to and invasion of CHO-K1 cells.

5.2.2.2.4 Interaction of PagN with HT-29 cells

A high-throughput invasion assay was also performed using HT-29 cells to compare PagN-mediated invasion of a more infection relevant cell line. The Olympus IX81 was used to collect the images in Fig. 5.15. There was an average decrease in cell association of 86 to 92 percent as compared with wild-type PagN (Fig. 5.16.). There was a highly significant difference between full-length PagN-mediated invasion of HT-29 cells and that mediated by any of the loop-deletion mutants ($p < 0.0001$). These data agree with previously published data regarding the necessity of the extracellular loops of PagN (204) and establish that for PagN-mediated adhesion to and invasion of epithelial cells, all four loops are absolutely required. The abolition of invasion upon loss of any one loop suggests that either the PagN loops may have a more stabilising, structural role as compared with other un-structured β-barrel surface-

exposed loops, or each of the loops may play a role in interacting with the PagN receptor molecule.

5.2.3 The requirement for selected, conserved residues within loop two

5.2.3.1 Single amino acid substitutions in loop two

In the previous sections, it was reported that all of the loops of PagN are of equal importance with regards to the promotion of invasion of epithelial cells. Comparison of the primary sequence of PagN, Hek and Tia reveal that there are several identical residues in the amino acid sequence predicted to form loop 2 of the proteins (205). This would suggest that these residues may be involved in the function of the protein. Many of these residues are charged amino acids and may participate in receptor binding. To investigate the contribution of selected residues, namely Arg 71, Asp 75, Lys 77 and Asp 81, site-directed mutagenesis was performed on the plasmid pML1 by Lambert (203).

To confirm the expression of all four mutant proteins, whole cell lysates of *E. coli* DH5α containing each of the four mutant expression vectors and the parental construct, pML1, were extracted, separated by SDS-PAGE, transferred to a PVDF membrane and analysed by Western immunoblotting using anti-PagN peptide antiserum. Proteins were detected for all four mutants (Fig. 5.17). The 42 kDa maltose binding protein was used as a loading control. An MBP-fusion protein of a higher molecular weight is displayed in the lane containing the ladder.

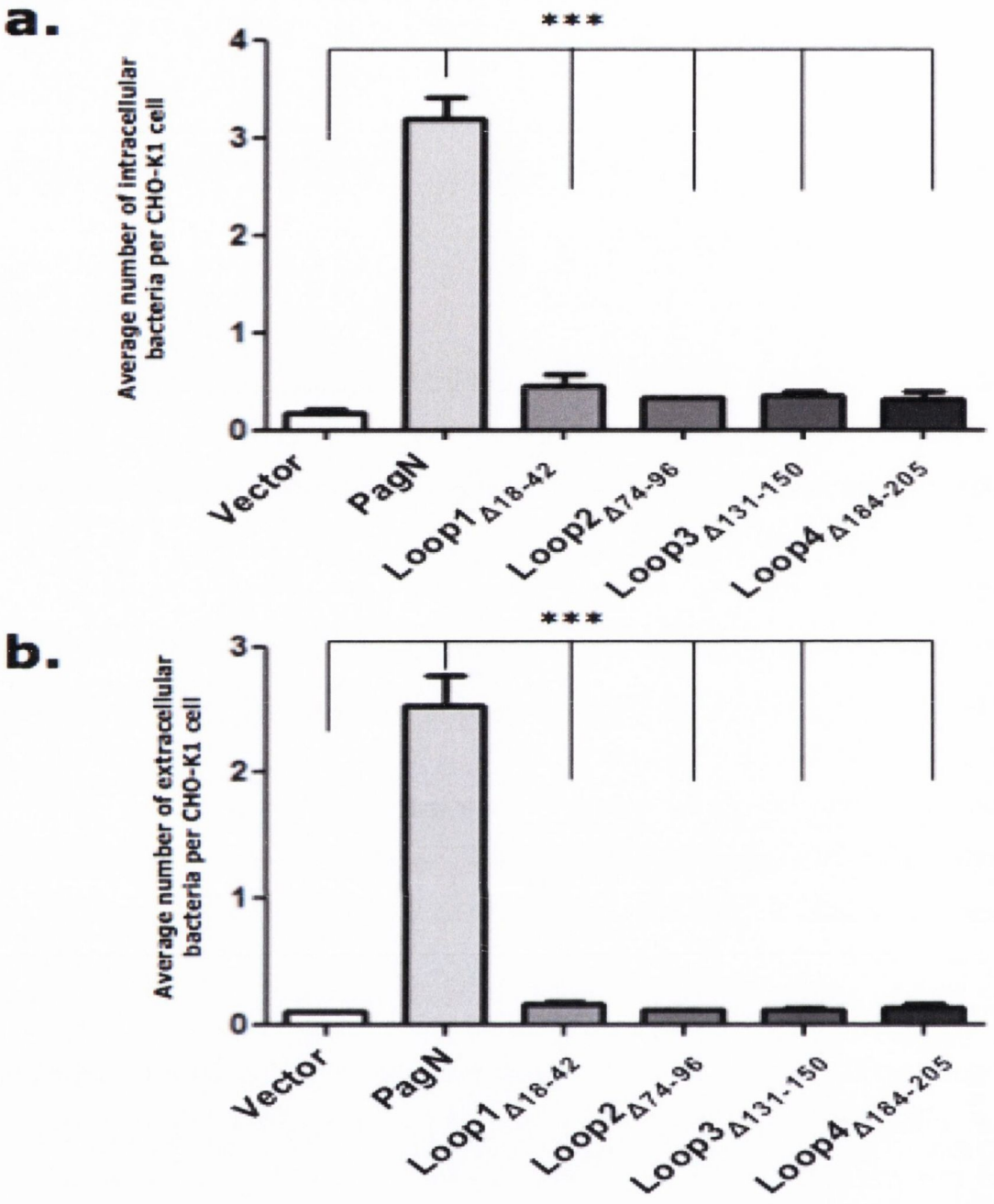

FIG 5.14. PagN-mediated invasion of CHO-K1 epithelial cells. A high-throughput fluorescent invasion assay was performed as described in Section 2.4.3.2. to determine whether all four extracellular loops of the PagN protein are necessary to mediate adhesion to and invasion of CHO-K1 cells. *E. coli* DH5αZ1 expressed PagN from plasmid pML1 and the mutant PagN proteins from plasmids pLoop1$_{\Delta 18\text{-}42}$, pLoop2$_{\Delta 74\text{-}96}$, pLoop3$_{\Delta 131\text{-}150}$, and pLoop4$_{\Delta 184\text{-}205}$, respectively. The assay was performed in triplicate and the average number of intracellular (panel a) or extracellular (panel b) bacteria per CHO-K1 cell is displayed. There was a highly statistically significant difference in invasion mediated by full-length PagN when compared with that promoted by the PagN-truncates. *** denotes $p < 0.0001$. Data were analysed using the one way analysis of variance with the Dunnett post test to compare all means to the bacteria expressing full-length PagN protein.

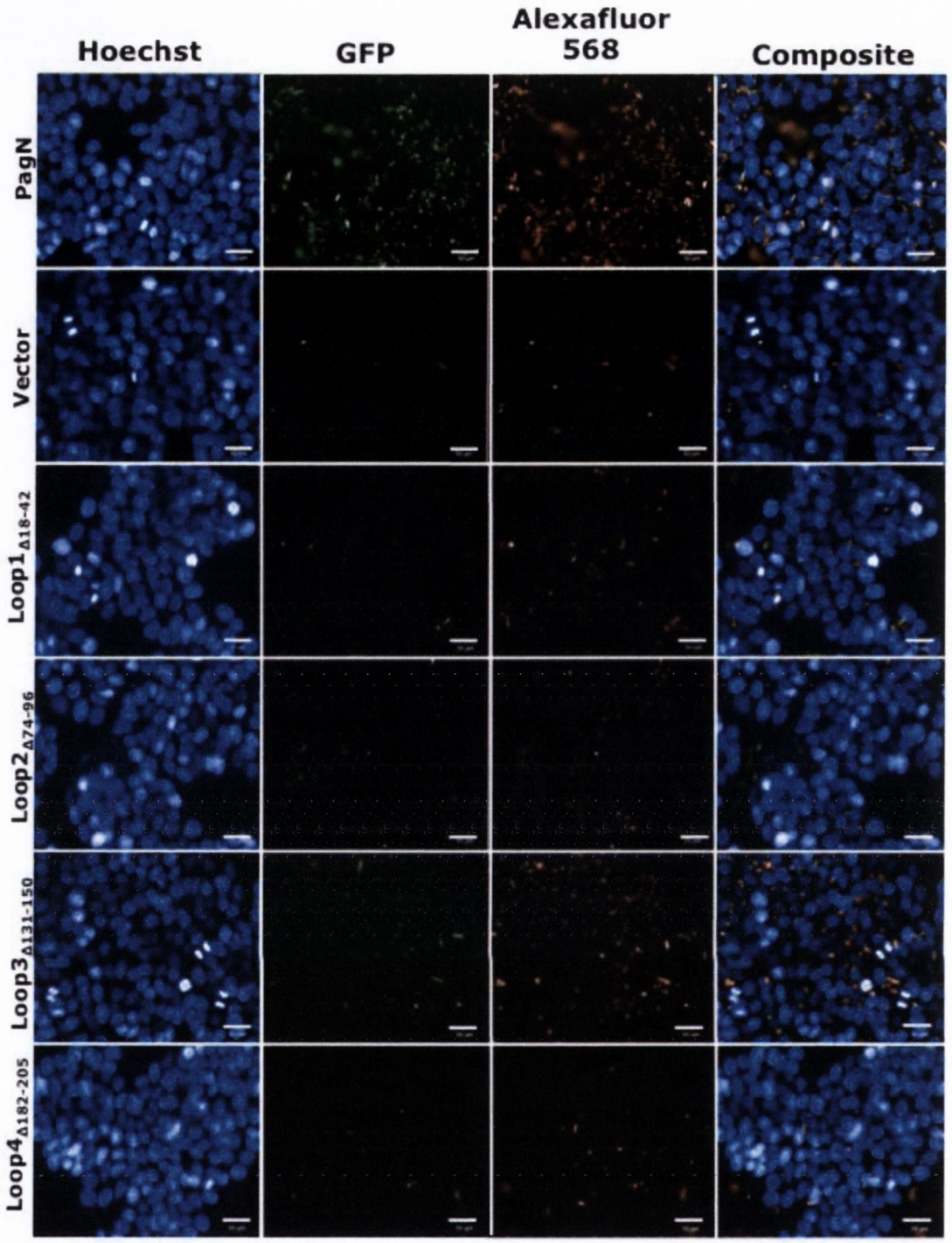

FIG 5.15. Images of PagN-mediated invasion of human HT-29 cells. A high-throughput fluorescent invasion assay was performed as described in the Section 2.3.4.2 to determine whether all four extracellular loops of the PagN protein are necessary to mediate adhesion to and invasion of HT-29 cells. *E. coli* DH5αZ1 expressed the vector plasmid or PagN from plasmid pML1 and the mutant PagN proteins from plasmids pLoop1$_{\Delta 16\text{-}45}$, pLoop2$_{\Delta 74\text{-}96}$, pLoop3$_{\Delta 131\text{-}150}$, and pLoop4$_{\Delta 182\text{-}205}$, respectively. Mammalian cells were stained with Hoechst, bacteria express GFP, and extracellular bacteria were distinguished using a rabbit polyclonal anti-vesicle antibody and an Alexafluor 568 nm coupled anti-rabbit antibody. The white bar indicates 50 μm.

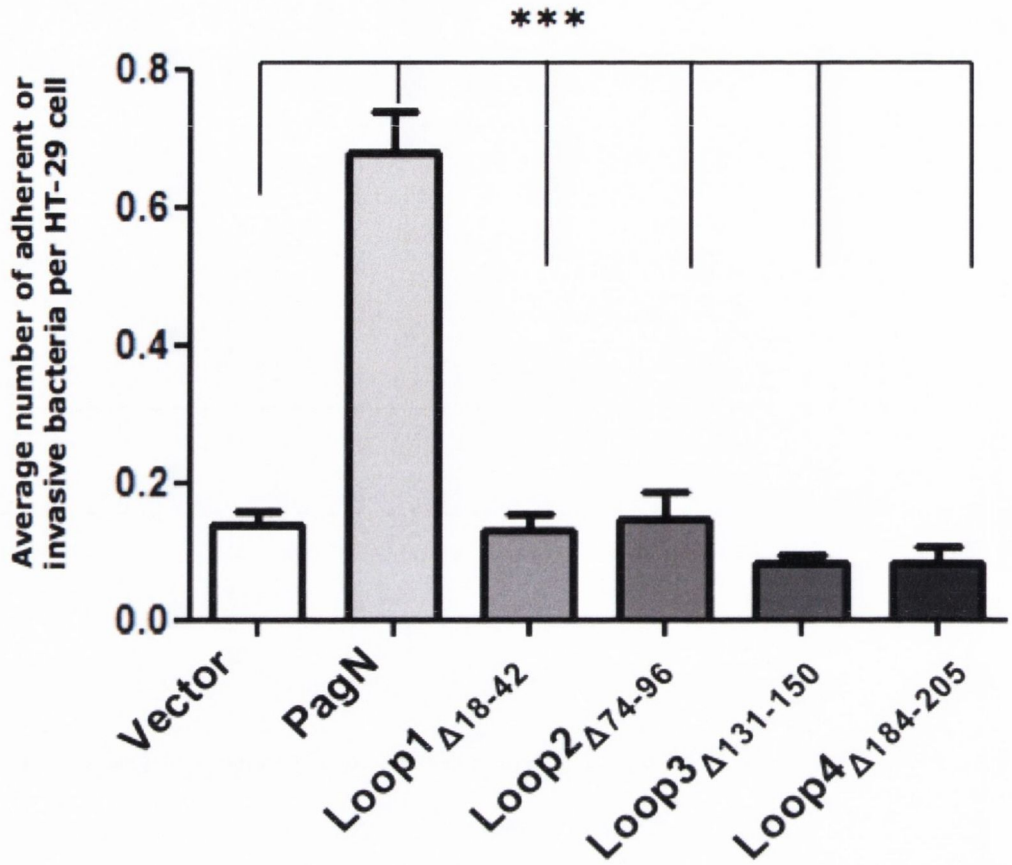

FIG 5.16. PagN-mediated invasion of HT-29 enterocytes. A high-throughput fluorescent invasion assay was performed as described in Section 2.4.3.2. to determine whether all four extracellular loops of the PagN protein are necessary to mediate invasion into HT-29 colonic epithelial cells. *E. coli* DH5αZ1 expressed PagN from plasmid pML1 and the mutant PagN proteins from plasmids pLoop1$_{\Delta 18\text{-}42}$, pLoop2$_{\Delta 74\text{-}96}$, pLoop3$_{\Delta 131\text{-}150}$, and pLoop4$_{\Delta 184\text{-}205}$, respectively. The assay was performed in triplicate and the average number of adherent or invasive bacteria per HT-29 cell. There was a highly statistically significant difference in cell association mediated by full-length PagN when compared with that promoted by the PagN-truncates. *** denotes $p < 0.0001$. Data were analysed using the one way analysis of variance with the Dunnett post test to compare all means to the bacteria expressing full-length PagN protein.

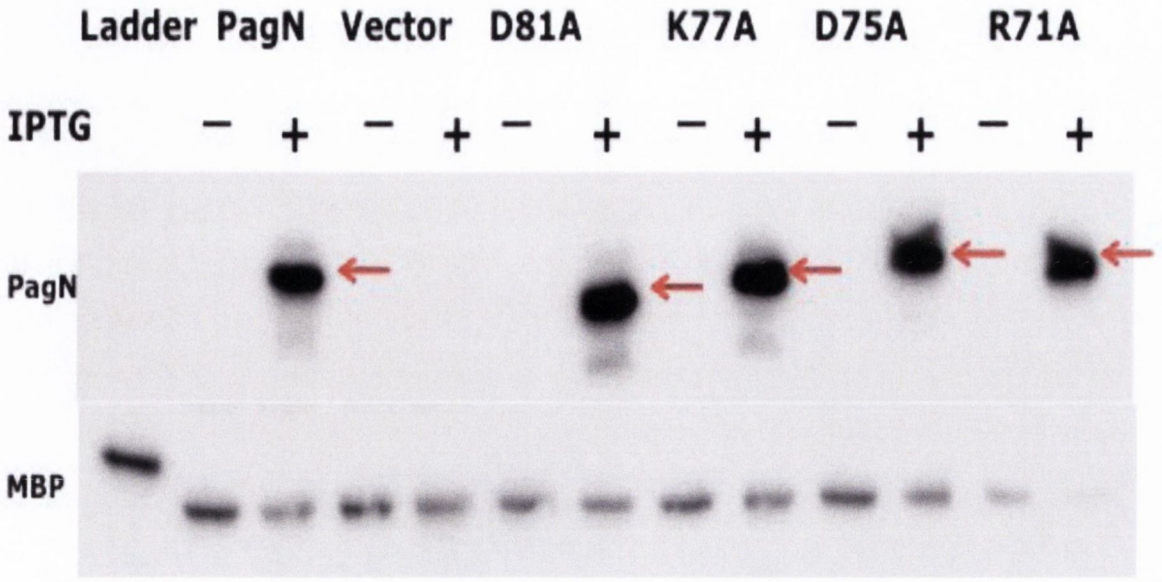

FIG. 5.17. Expression of full length PagN and PagN site-directed mutants in *E. coli*. A Western immunoblot was performed using whole cell lysates of *E. coli* XL-1 Blue cells expressing wild-type PagN or the PagN site-directed mutants from plasmids pML1 and pR71A, pD75A, pK77A, and pD81A. The pTrc99a vector control is displayed in lane 3. The red arrows indicate the 26 kDa PagN protein. + indicates the addition of IPTG while – indicates no IPTG added. The 42 kDa maltose binding protein (MBP) was used as a loading control. An MBP-fusion protein of a higher molecular weight can be seen in the lane containing the protein ladder.

5.2.3.2 Single amino acid substitutions within loop 2 affect PagN-mediated invasion of CHO-K1 epithelial cells

It has previously been reported that the second extracellular loop of the homologous Hek protein is necessary for Hek-promoted invasion of epithelial cells (101). There are several conserved charged amino-acid residues in the second extracellular loop of PagN, raising the possibility that one or all of these charged amino acids interacts with receptors on the mammalian cell surface. In order to test this hypothesis, a high-throughput invasion assay using *E. coli* DH5αZ1 expressing each of the amino-acid substitute proteins and CHO-K1 cells was performed (Fig. 5.18). Invasion levels seen by bacteria harbouring these mutant plasmids (Fig. 5.19(a)) were quite different to those seen by Lambert in 2009 (204). Mutation of any of the amino acid residues in Loop 2 of the protein had no effect on invasion levels when compared to invasion mediated by the wild-type PagN protein using the one-way ANOVA method and Dunnett post-test. Although, bacteria expressing the R71A mutant protein displayed an increase in adhesion to CHO-K1 cells ($p < 0.05$). This was not seen for any other mutant, indicating that R71 may block the ability of other amino acid residues to promote binding to the mammalian cell receptor. The high-throughput assay also revealed no significant effects of the Lys 77 (K77A) or Asp 81 (D81A) mutations on PagN-mediated invasion. While the K77A and D81A mutations displayed no significant effect on PagN-mediated invasion, there was a 9 and 26 percent decrease in invasion promoted by these proteins with respect to wild-type which was in agreement with observations by Lambert (203). Interestingly, bacteria expressing any of the site-directed mutant proteins, aside from the K77A mutation, appeared to be more able to easily adhere to the CHO-K1 cell monolayer when compared with wild-type levels of adhesion.

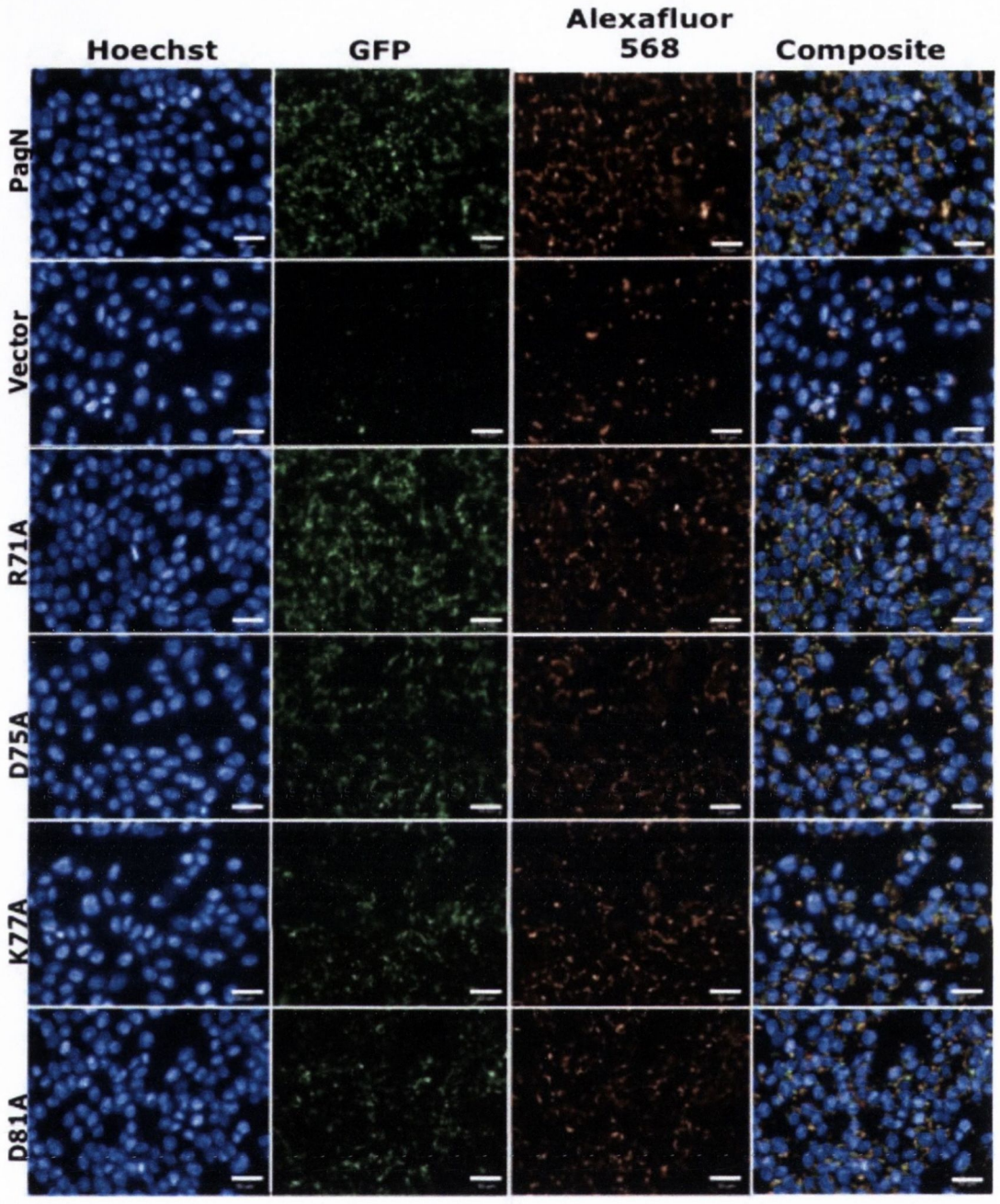

FIG 5.18. Images of PagN-mediated invasion of CHO-K1 epithelial cells. A high-throughput fluorescent invasion assay was performed as described in Section 2.3.4.2. to determine whether all four extracellular loops of the PagN protein are necessary to mediate adhesion to and invasion of CHO-K1 cells. *E. coli* DH5αZ1 expressed the empty vector plasmid or PagN from plasmid pML1 and the mutant PagN proteins from plasmids pR71A, pD75A, pK77A, and pD81A, respectively. Mammalian cells were stained with Hoechst, bacteria express GFP, and extracellular bacteria were distinguished using an Alexafluor 568 nm antibody. The white bar indicates 50 μm.

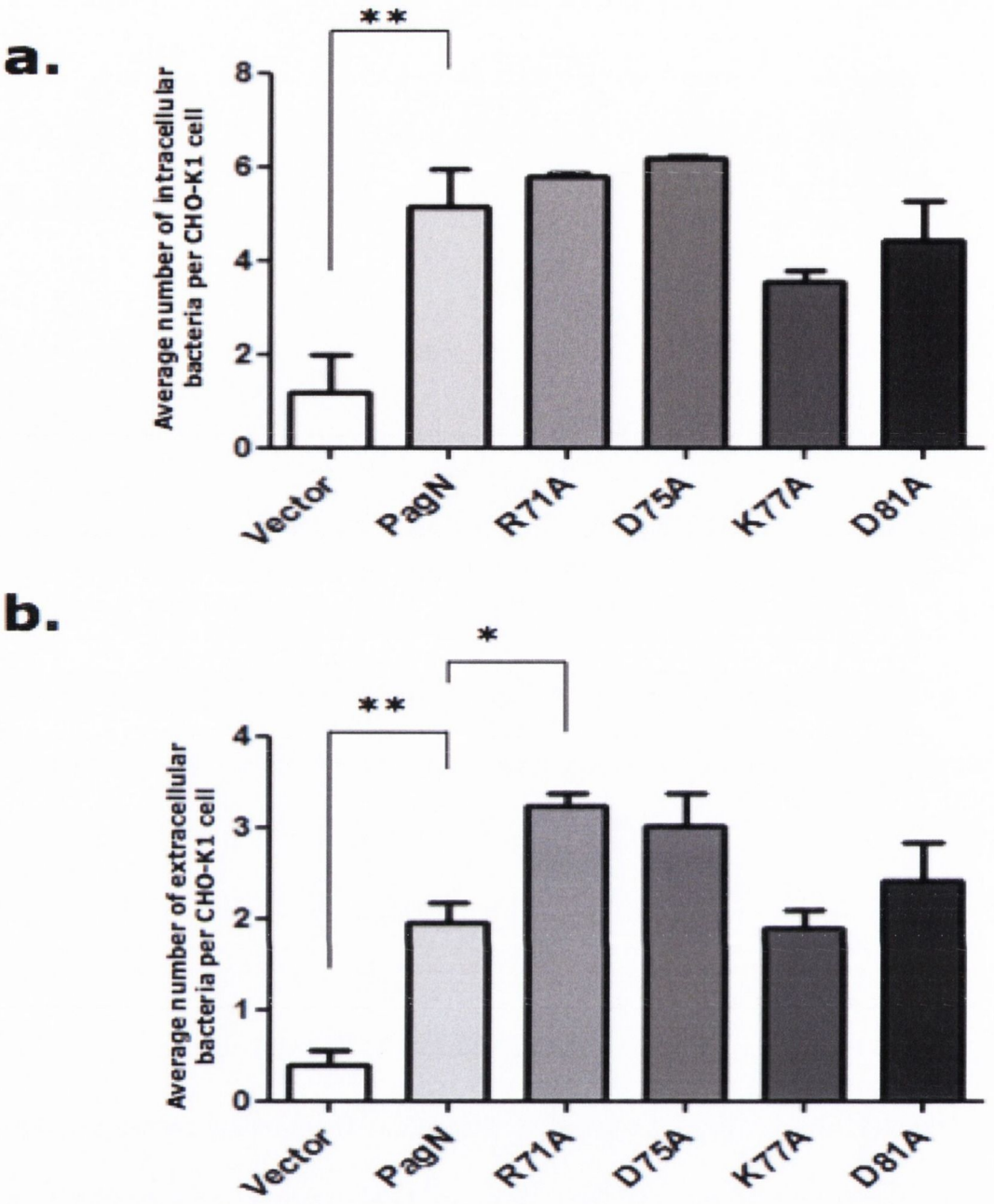

5.19. Analysis of the effect of single amino acid substitutions of loop2 of PagN protein on CHO-K1 cell adhesion and invasion. A high-throughput fluorescent invasion assay was performed as described in Section 2.4.3.2. to determine whether any or all of the conserved charged amino acid residues of Loop two of PagN are necessary to mediate adhesion to and invasion of CHO-K1 cells. *E. coli* DH5αZ1 expressed PagN from plasmid pML1 and the mutant PagN proteins from plasmids pR71A, pD75A, pK77A, and pD81A, respectively. The assay was performed in triplicate and the average number of intracellular (panel a) or extracellular (panel b) bacteria per CHO-K1 cell is displayed. * denotes $p < 0.05$, ** denotes $p < 0.01$. Data were analysed using the one way analysis of variance with the Dunnett post test to compare all means to the bacteria expressing wild-type PagN protein.

5.2.3.3 Single amino acid substitutions within loop two do not affect PagN-mediated invasion of HT-29 epithelial cells

As with the PagN loop deletion mutants, it was important to determine whether the same trends were seen when bacteria were exposed to the HT-29 colonic cell line. Another high-throughput invasion assay was performed using *E. coli* DH5αZ1 expressing each of the amino-acid substitute proteins (Fig. 5.20). For each of the mutants tested, there was no significant difference seen in bacterial invasion (Fig. 5.21(a)). The bacteria expressing the D75A mutant protein exhibited a significant decrease in adhesion to the HT-29 cell monolayer when compared with adhesion mediated by the wild-type PagN protein ($p < 0.05$, Fig. 5.21(b)).

The differences between CHO-K1 cell association/invasion and that of bacteria exposed to HT-29 cells is possibly due to differences in receptor concentrations between the two cell lines. In addition to differing concentrations of cell surface receptors, HT-29 cells produce a number of antibacterial peptides; these peptides may contribute to the reduction in cell association/invasion to levels in which it is difficult to discern small changes in the associated mutant phenotype. Table 5.1 displays a summary of the structure/function relationship of PagN with invasion of two separate mammalian cell lines.

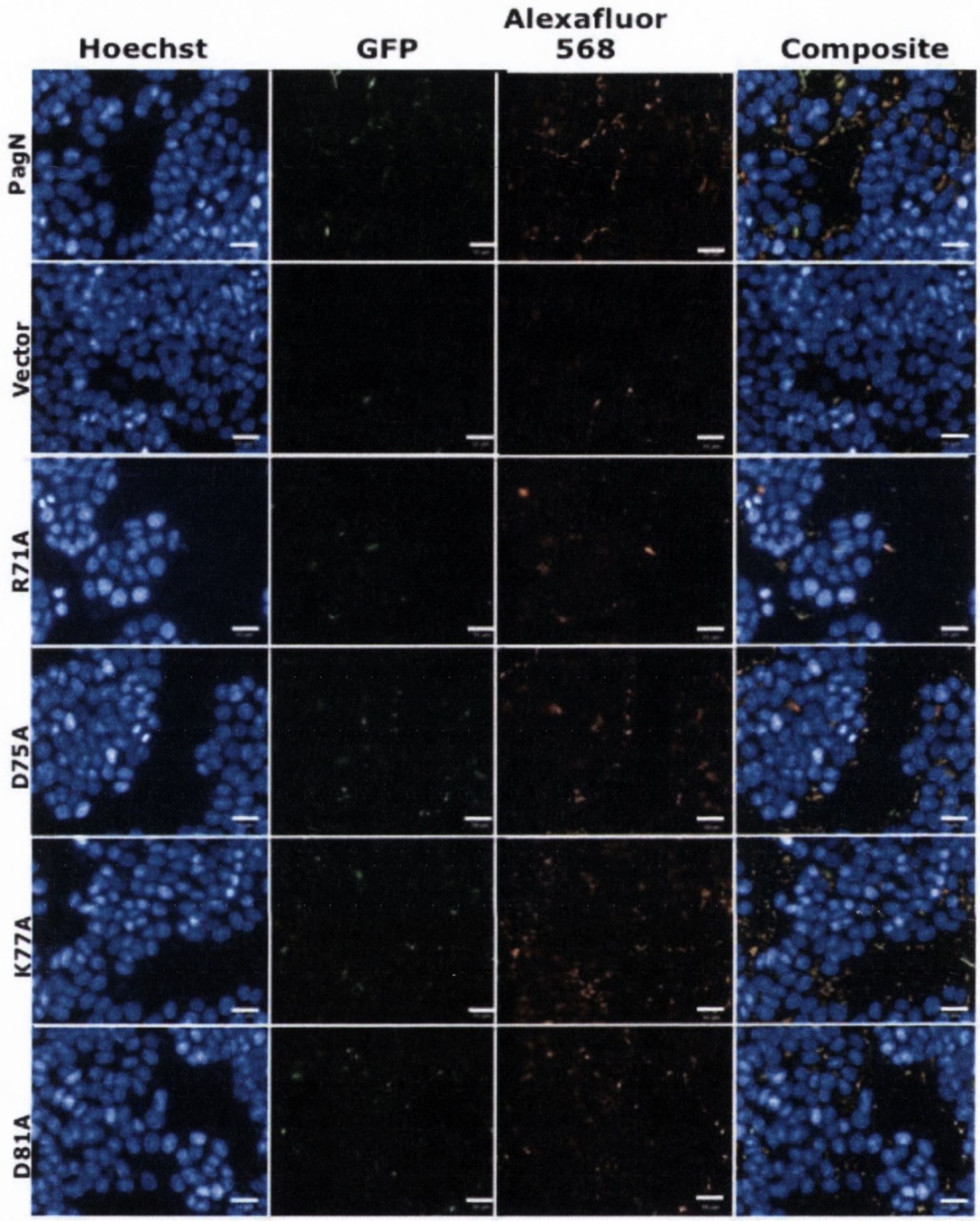

FIG 5.20. Images of PagN-mediated invasion of human HT-29 cells. A high-throughput fluorescent invasion assay was performed as described in Section 2.4.3.2. to determine whether all four extracellular loops of the PagN protein are necessary to mediate adhesion to and invasion of HT-29 cells. *E. coli* DH5αZ1 expressed PagN from plasmid pML1 and the mutant PagN proteins from plasmids pR71A, pD75A, pK77A, and pD81A, respectively. Mammalian cells were stained with Hoechst, bacteria express GFP, and extracellular bacteria were distinguished using a rabbit polyclonal anti-vesicle antibody and an Alexafluor 568 nm coupled anti-rabbit antibody. The white bar indicates 50 μm.

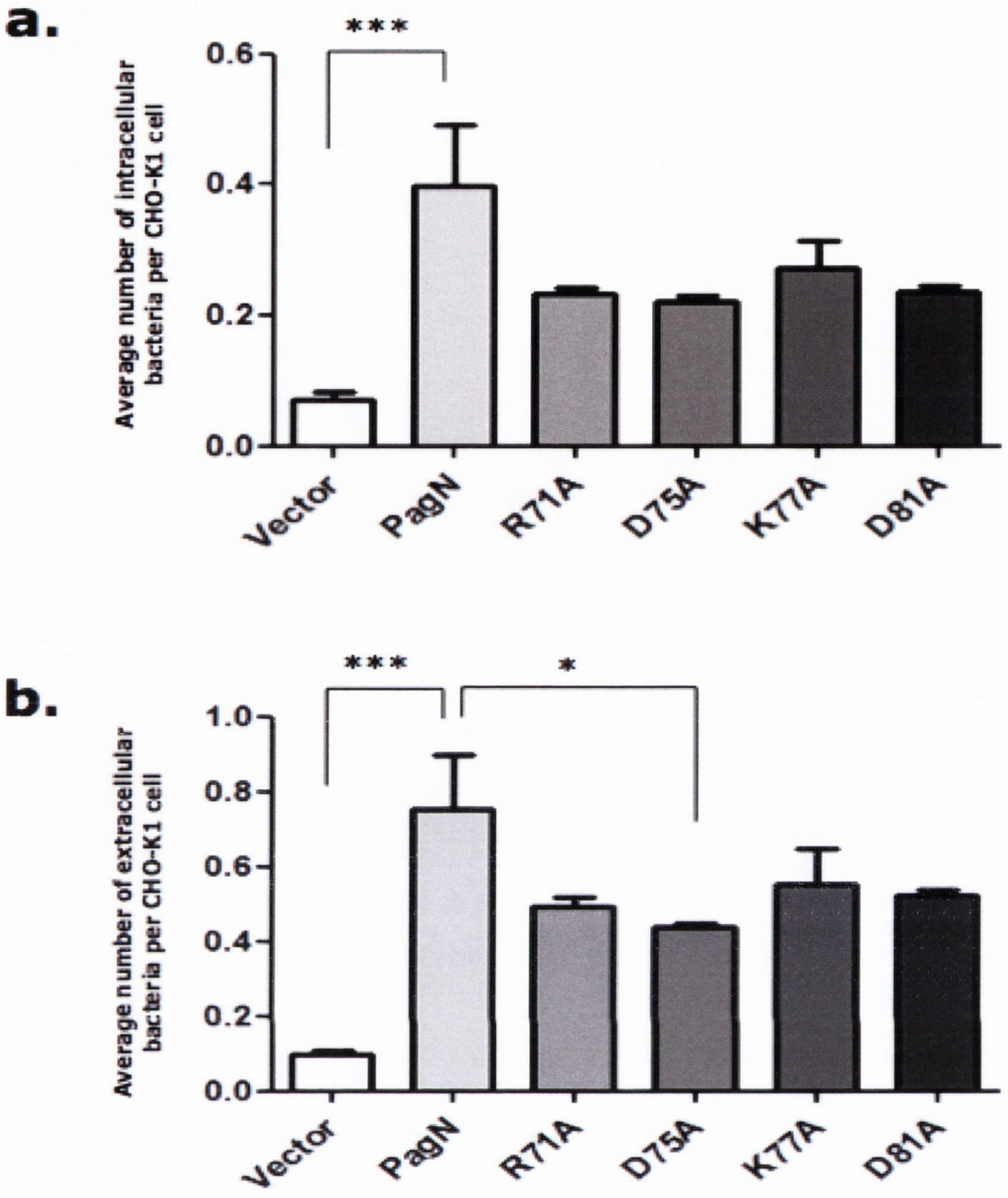

FIG. 5.21. Interaction of PagN site-directed mutants with human colonic HT-29 cells. A high-throughput fluorescent invasion assay was performed as described in Section 2.4.3.2. to determine whether any or all of the conserved charged amino acid residues of Loop two of PagN are necessary to mediate adhesion to and invasion of HT-29 cells. *E. coli* DH5αZ1 expressed PagN from plasmid pML1 and the mutant PagN proteins from plasmids pR71A, pD75A, pK77A, and pD81A, respectively. The assay was performed in triplicate and the average number of intracellular (panel a) or extracellular (panel b) bacteria per HT-29 cell is displayed. * denotes $p < 0.05$, *** denotes $p < 0.0001$. Data were analysed using the one way analysis of variance with the Dunnett post test to compare all means to the bacteria expressing wild-type PagN protein.

Table 5.1. Comparison of PagN mutants in mammalian cell association and invasion

PagN-mutant	CHO-K1 Invasion	CHO-K1 Association	HT-29 Invasion	HT-29 Association	Source
$Loop1_{\Delta 16-45}$	- 95%	-95%	- 82%	- 90%	(205)
$Loop1_{\Delta 18-42}$	- 86%	-94%	n.t.	- 86%	This study
$Loop2_{\Delta 71-96}$	- 97%	-96%	- 84%	- 92%	(205)
$Loop2_{\Delta 74-96}$	- 90%	-96%	n.t.	- 83%	This study
$Loop3_{\Delta 127-153}$	- 98%	-99%	- 92%	- 96%	(205)
$Loop3_{\Delta 131-150}$	- 89%	-96%	n.t.	- 92%	This study
$Loop4_{\Delta 182-207}$	- 96%	-97%	- 94%	- 97%	(205)
$Loop4_{\Delta 184-205}$	- 91%	-95%	n.t.	- 92%	This study
R71A	n.s.	+71%	n.t.	n.s.	(203)
D75A	n.s.	n.s.	n.t.	- 39%	(203)
K77A	n.s.	n.s.	n.s.	n.s.	(203)
D81A	n.s.	n.s.	n.s.	n.s.	(203)

n.t. indicates samples not tested. n.s. indicates results that are not significant.

5.2.4 Quantitative cell association and invasion assays of PagN-expressing *Salmonella*

5.2.4.1 Interaction of *Salmonella* with human HT-29 cells

Although the data presented in the previous sections demonstrate that PagN does promote *E. coli* adhesion to and invasion of mammalian cell lines such as CHO-K1 and HT-29 cells, it is a *Salmonella*-specific protein, and its role in *Salmonella* adhesion and invasion should be determined. Gentamicin protection assays were first performed to determine the role of PagN in mediating interactions with HT-29 cells. In this assay, the *Salmonella* Typhimurium SL1344 derivative named ML5 was used as a negative control for invasion. ML5 lacks the *invA* gene, which abrogates functionality of the SPI-1 encoded T3SS apparatus. ML6, an *S.* Typhimurium SL1344 derivative lacking a functional *pagN* gene, was used to determine the contribution of PagN to *Salmonella* adhesion and invasion. Overnight cultures of *S.* Typhimurium SL1344 and the SL1344 derivatives were incubated with HT-29 cell monolayers and the percentage invasion and cell association were calculated. The data in Fig. 5.22(a) depicts the average percentage invasion. There was a significant decrease in invasion seen by ML5 (SL1344Δ*invA*) bacteria (-88% invasion, $p < 0.05$, tested by one-way ANOVA method and Dunnett post-test to compare all means to wild-type SL1344 bacteria). A functional SPI-1 secretion system is necessary for bacteria to efficiently inject effector proteins and cause actin cytoskeletal rearrangements, thereby facilitating bacterial uptake (Discussed in Section 1.5.6.1). There was also a moderate decrease in invasion seen by the PagN-deficient ML6 bacteria (-59%, $p < 0.05$). As expected, there was no significant decrease in bacterial adhesion upon

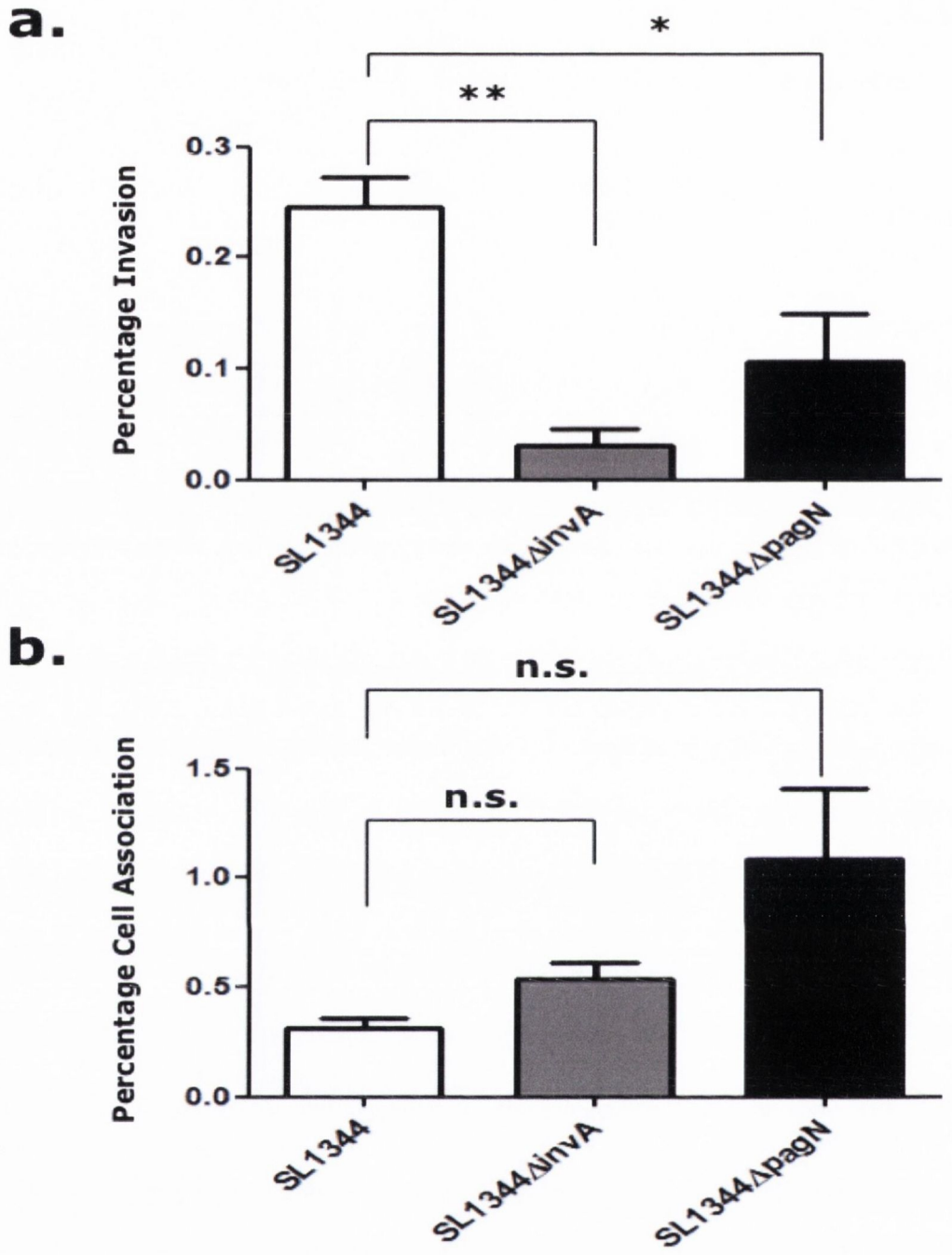

5.22. Analysis of the interaction of PagN-deficient *Salmonella* with HT-29 cells. A gentamicin protection (invasion) assay was performed as described in Section 2.4.3.1. to determine the role of PagN in mediating *Salmonella* attachment to and invasion of the human colonic cancer cell line HT-29. *Salmonella* SL1344 was used as a positive control while the SPI-1 mutant strain SL1344Δ*invA* was used as a negative control for invasion. The strain SL1344Δ*pagN* lacks a functional *pagN* gene. The assay was performed in triplicate and the average percentage invasion (panel a) and cell association (panel b) is displayed. * denotes $p < 0.05$, ** denotes $p < 0.01$. Data were analysed using the one way analysis of variance with the Dunnett post test to compare all means to wild-type SL1344 bacteria.

deletion of the SPI-1 secretion system (+81%, $p = 0.100$). SPI-1 is not necessary for bacterial adhesion. The genes encoding the system are not up-regulated until the bacteria have formed an intimate attachment to the epithelial cell monolayer. There was, however, a statistically significant increase in bacterial cell association upon removal of the *pagN* gene (+271%, $p < 0.05$). This is interesting, as previous studies have shown that PagN is necessary to mediate efficient adhesion to and invasion of HT-29 cells (205, 357). The major difference, however was in the overnight cultivation of bacteria; in the Lambert *et al.* paper, bacteria were grown overnight in minimal media at pH 5.8 (MM5.8), in this assay, overnight cultures were grown in L-broth (205, 357). The PagN protein is expressed maximally in PhoP-inducing media, such as MM5.8 (49).

In order to corroborate the findings of Lambert *et al.*, a high-throughput invasion assay was performed. Strains of *S.* Typhimurium SL1344 and its derivatives harbouring the GFP-producing pCM01 plasmid were grown overnight in either L-broth or MM5.8 and allowed to invade the HT-29 cell monolayer before fixation, staining, and imaging using the Olympus IX81 microscope. The images gathered using the Olympus microscope can be seen in Figure 5.23.

There was no difference in invasion seen between the wild-type strain of *Salmonella* and either mutant strain (Fig. 5.24). The *invA* gene is maximally up-regulated in late log phase/early stationary phase, and during oxygen limiting conditions (194). As the cultures were grown overnight in L-broth with shaking, they were in late-stationary phase, at which time expression of the *invA* gene/SPI-1 secretion system is minimal (194). Bacteria were also grown in MM5.8, a known PhoP-inducing media. The expression of *invA* is also minimal in MM5.8, indicating that the effect of deletion of a functional SPI-1 T3SS would be negligible. Expression of the *pagN* gene, however, is

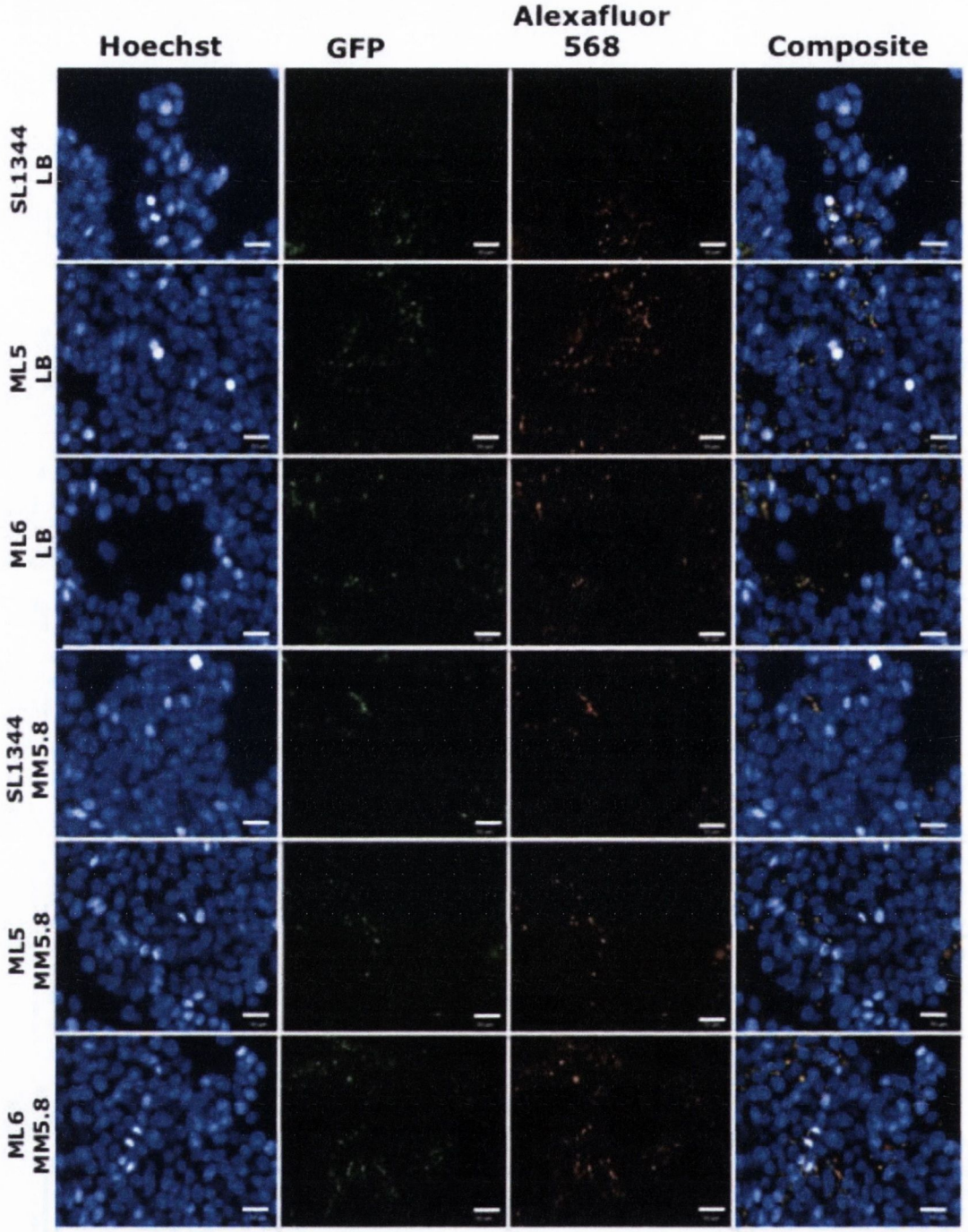

FIG 5.23. Images of PagN-promoted invasion of *Salmonella* into human HT-29 cells. A high-throughput invasion assay was performed as described in Section 2.4.3.2. to determine the role of PagN in mediating *Salmonella* attachment to and invasion of the human colonic cancer cell line HT-29. Bacteria were grown overnight in either L-broth or in minimal media pH 5.8 (MM5.8). *Salmonella* SL1344 was used as a positive control while the SPI-1 mutant strain SL1344Δ*invA* was used as a negative control for invasion. The strain SL1344Δ*pagN* lacks a functional *pagN* gene. Mammalian cells were stained with Hoechst, bacteria express GFP, and extracellular bacteria were distinguished using an Alexafluor 568 nm secondary antibody. The white bar indicates 50 μm.

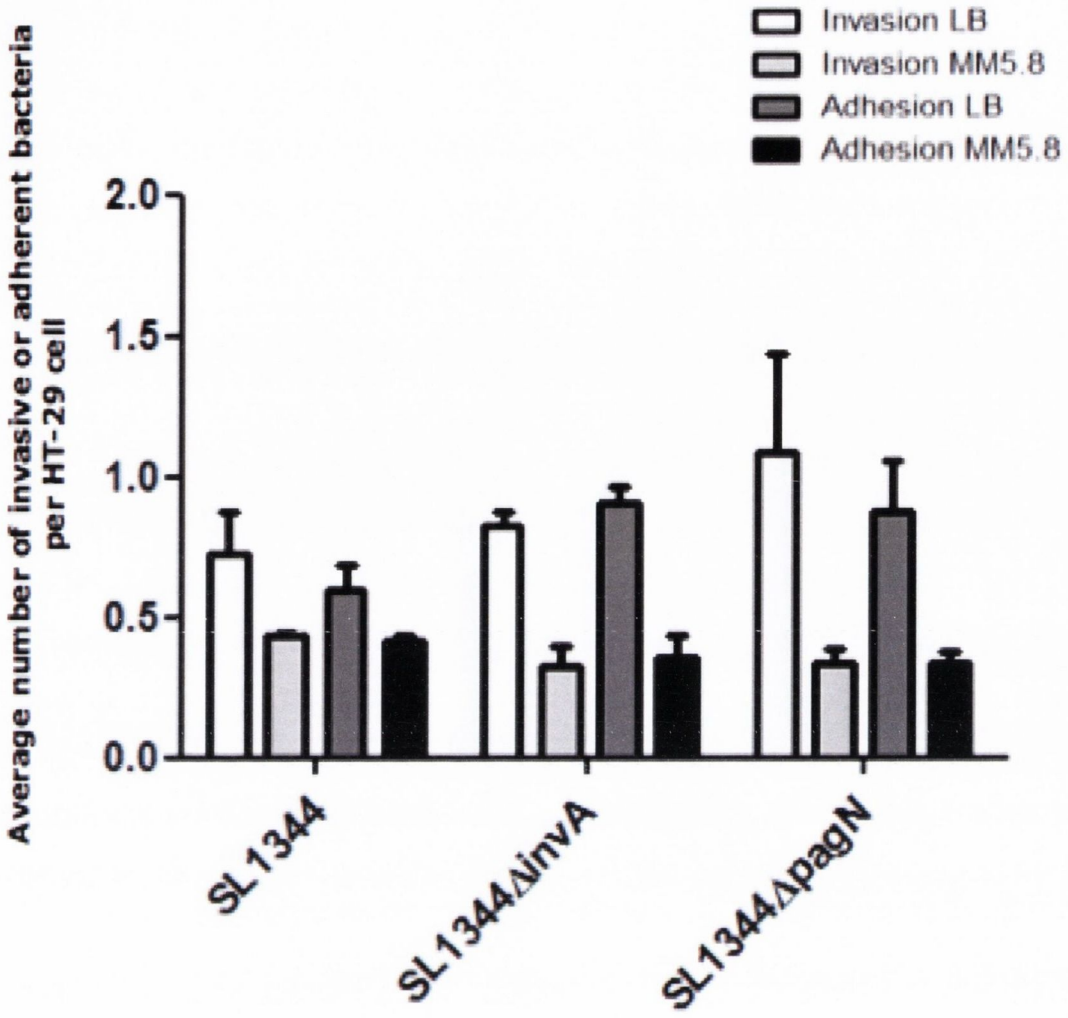

5.24. Analysis of the effect of PagN protein on *S.* Typhimurium SL1344 invasion and adhesion of HT-29 colonic epithelium. A high-throughput invasion assay was performed as described in Section 2.4.3.2. to determine the role of PagN in mediating *Salmonella* attachment to and invasion of the human colonic cancer cell line HT-29. Bacteria were grown overnight in either L-broth or in minimal media pH 5.8 (MM5.8). *Salmonella* SL1344 was used as a positive control while the SPI-1 mutant strain SL1344Δ*invA* was used as a negative control for invasion. The strain SL1344Δ*pagN* lacks a functional *pagN* gene. The assay was performed in triplicate and the average number of invasive (L-broth – white bars, MM5.8 – black bars) or adherent (L-broth – dark grey bars, MM5.8 – light grey bars) bacteria per HT-29 cell is displayed. Separate one-way ANOVA tests with the Dunnett post-test were performed to compare the means of bacterial invasion to the invasion (or adhesion) seen by wild-type SL1344 bacteria after growth in LB or MM5.8.

maximal in early stationary phase (194). The gene is also up-regulated in SPI-2 inducing media, as well as under limiting Mg^{2+}-concentrations because the *pagN* gene is regulated by the PhoP-PhoQ two-component system which recognises SPI-2 inducing conditions and low-Mg^{2+}-concentrations (137, 194).

5.2.4.2 Interaction of *Salmonella* with CHO-K1 cells

The contribution of PagN to the invasion of CHO-K1 cells by *S.* Typhimurium strain SL1344 was determined. Invasion promoted by *S.* Typhimurium strain SL1344, the *invA*/SPI-1 T3SS mutant, ML5, and the *pagN* mutant derivative, ML6, were tested with non-polarised cells in a gentamicin protection invasion assay. In this assay, bacteria were grown overnight in MM5.8 as this has been shown to induce expression of the *pagN* gene (49, 194, 205). The data presented in Fig. 5.25(a) established that the *pagN* mutant strain, ML6, was internalised in greater numbers than the wild-type SL1344 strain, there was a significant difference in invasion of the CHO-K1 cell monolayer ($p < 0.05$, tested by one-way ANOVA method and Dunnett post-test to compare all means to wild-type SL1344 grown in LB or in MM5.8). Invasion of the PagN-deficient SL1344 strain increased by 74% relative to the wild-type strain. There was also no changes in invasion mediated by the SPI-1 deficient strain, however, it has been established in the previous section that the *invA* gene is not expressed under the PhoP-inducing conditions used. There was no significant difference in cell association mediated by wild-type *S.* Typhimurium SL1344 and its mutant derivatives (Fig. 5.25(b)). Bacteria grown overnight in minimal media are exposed to nutrient limitation and to prolonged exposure to an acidic pH (pH 5.8). It's possible that the

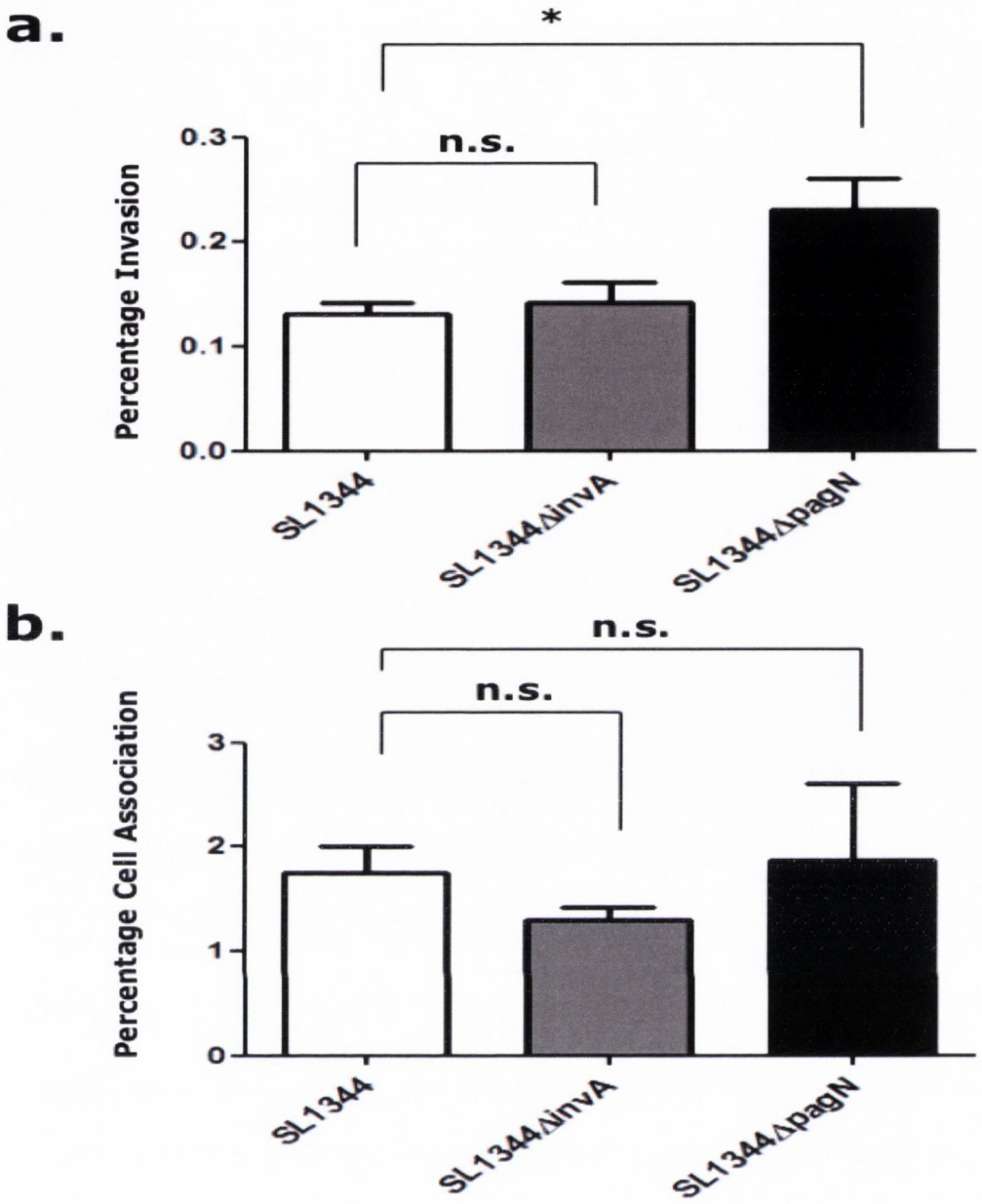

5.25. Analysis of the effect of PagN protein on *S.* Typhimurium SL1344 invasion and adhesion to CHO-K1 cells by GPA. A gentamicin protection assay was performed as described in Section 2.4.3.1. to determine the role of PagN in mediating *Salmonella* attachment to and invasion of the CHO-K1 cell line. Bacteria were grown overnight in minimal media pH 5.8 (MM5.8). *Salmonella* SL1344 was used as a positive control while the SPI-1 mutant strain SL1344Δ*invA* was used as a negative control for invasion. The strain SL1344Δ*pagN* lacks a functional *pagN* gene. The assay was performed in triplicate and the average percentage invasion (panel a) and cell association (panel b) is displayed. * indicates $p < 0.05$. Data were analysed using the one way analysis of variance with the Dunnett post test to compare all means to wild-type SL1344 bacteria.

exposure to long growth in MM5.8 inhibits the ability of the bacteria to invade the mammalian cell monolayer. Differences may become more apparent if bacteria are grown overnight in L-broth, harvested by centrifugation, washed, and finally sub-inoculated in MM5.8 and grown to early stationary phase to induce maximal expression of the *pagN* gene.

A high-throughput invasion assay was also performed to compare bacterial invasion and adhesion to CHO-K1 cells after growth overnight in either L-broth or MM5.8. The images generated by the assay are displayed in Figure 5.26. There was a decrease in invasion seen for the *invA* mutant after growth in L-broth ($p < 0.05$, Fig. 5.27). There was also a significant decrease in adhesion seen for both the *invA* and the *pagN* mutants after growth in L-broth ($p < 0.05$).

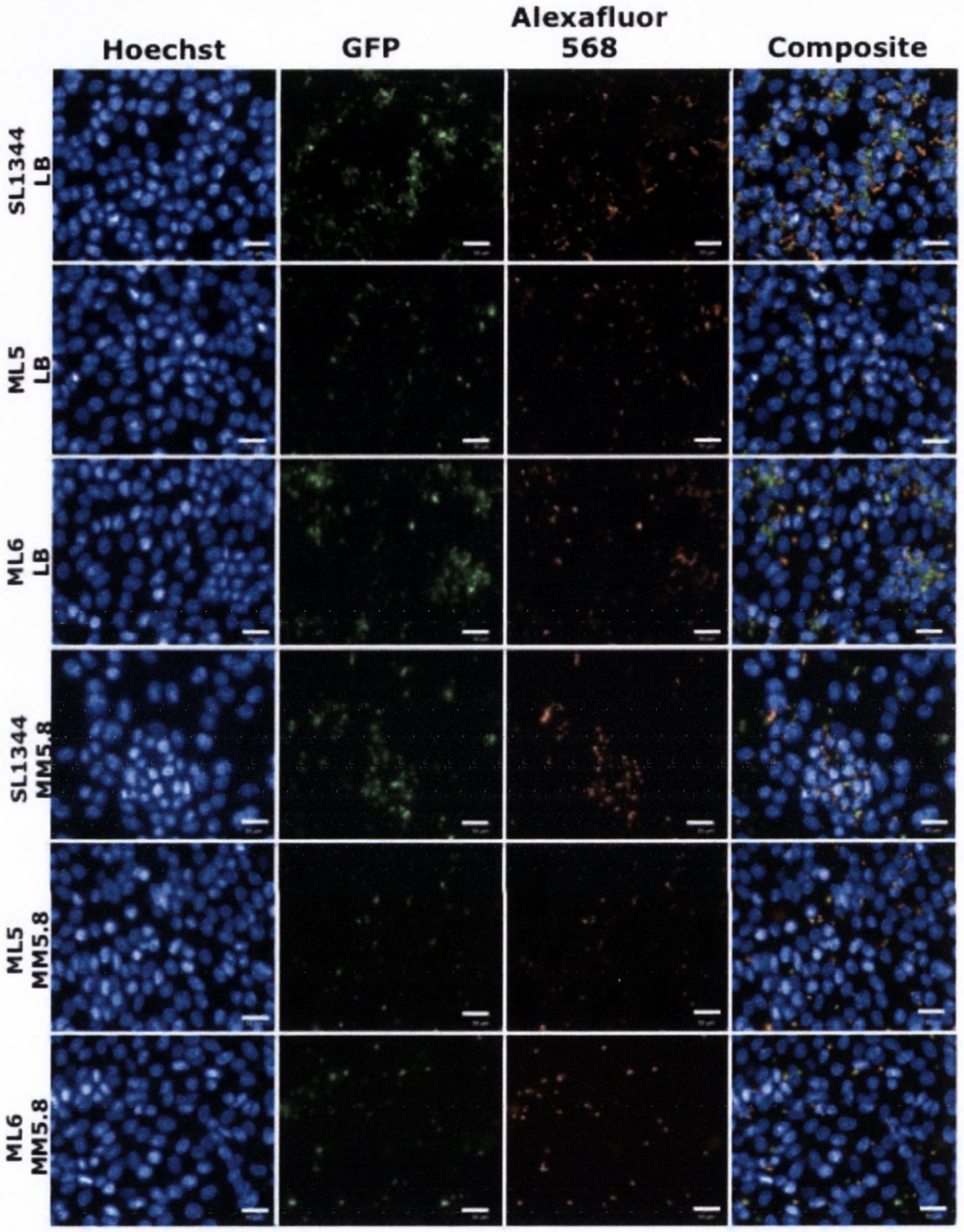

FIG 5.26. Images of PagN-promoted invasion of *Salmonella* into CHO-K1 cells. A high-throughput invasion assay was performed as described in Section 2.4.3.2. to determine the role of PagN in mediating *Salmonella* attachment to and invasion of CHO-K1 cells. Bacteria were grown overnight in either L-broth or in minimal media pH 5.8 (MM5.8). *Salmonella* SL1344 was used as a positive control while the SPI-1 mutant strain SL1344Δ*invA* was used as a negative control for invasion. The strain SL1344Δ*pagN* lacks a functional *pagN* gene. Mammalian cells were stained with Hoechst, bacteria express GFP, and extracellular bacteria were distinguished using an Alexafluor 568 nm secondary antibody. The white bar indicates 50 μm.

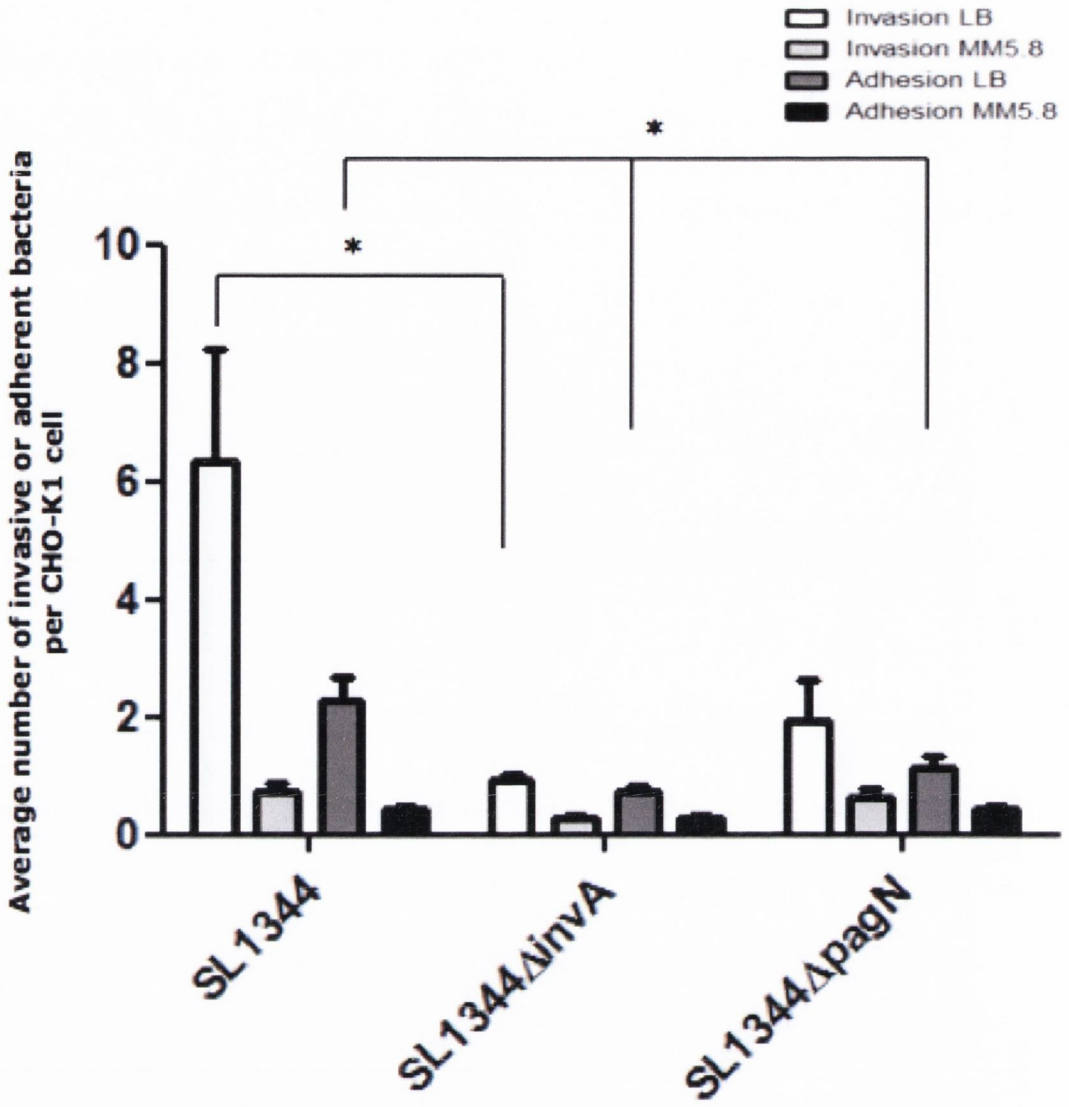

5.27. Analysis of the effect PagN protein on *S.* Typhimurium SL1344 invasion and adhesion of CHO-K1 cells by HCA. A high-throughput invasion assay was performed as described in Section 2.4.3.2 to determine the role of PagN in mediating *Salmonella* attachment to and invasion of the CHO-K1 cell line. Bacteria were grown overnight in either L-broth or in minimal media pH 5.8 (MM5.8). *Salmonella* SL1344 was used as a positive control while the SPI-1 mutant strain SL1344Δ*invA* was used as a negative control for invasion. The strain SL1344Δ*pagN* lacks a functional *pagN* gene. The assay was performed in triplicate and the average number of intracellular (L-broth – white bars, MM5.8 – black bars) or extracellular (L-broth – dark grey bars, MM5.8 – light grey bars) bacteria per CHO-K1 cell is displayed. * denotes $p < 0.05$. Separate one-way ANOVA tests with the Dunnett post-test were performed to compare the means of bacterial invasion to the invasion (or adhesion) seen by wild-type SL1344 bacteria after growth in LB or MM5.8.

5.3 Discussion

Previous studies have asserted that all four extracellular loops of the PagN protein are necessary for maximal protein function (204), however, Lambert *et al.* created PagN mutants in which the loop was removed directly at the interface of the membrane and extracellular space. The predicted loop 2 of the homologous proteins Hek and Tia are established as contributing maximally to protein function (101, 225). As PagN shares ~54% homology with both Tia and Hek, it was suggested that the aggressive loop-deletions may affect the ability of the protein to mediate functions such as adhesion and invasion, and the second extracellular loop of the protein may play a larger role than previously suggested. To confirm the role of the loops of the PagN protein, the four extracellular loops were deleted further from the interface between the membrane and extracellular space. A series of mutant PagN expression vectors were constructed based on the IPTG-inducible pML1 vector. Each plasmid encoded a mutant PagN protein lacking a single loop. All four proteins could be expressed in *E. coli* K-12 and reached their native location as determined by western immunoblotting.

Investigation of the contribution of each of the four loops confirmed that all four are required for a functional protein. Deletion of any one of the loops completely abrogated the ability of the protein to promote adhesion to and invasion of both CHO-K1 and HT-29 epithelial cells. It's possible that several important residues within each of the loops act cooperatively to promote mammalian cell interactions. Deletion of any one of the loops would remove the integral amino acid residues and thus diminish PagN-promoted phenotypes. Site-directed mutagenesis of each of the charged residues in the extracellular loops would help determine whether specific amino acids play a role in mediating adhesion and invasion. All four extracellular loops may also

play a structural role in stabilising the protein. Structural studies including the crystallization of the protein would determine whether the loops play a central role in the structural integrity of the PagN protein.

For the Tia and Hek proteins, the second extracellular loop of the protein has been shown to promote adhesion/invasion of mammalian cells, bacterial autoaggregation, and interactions with erythrocytes (101, 103, 225, 253). Within loop two of both proteins, there are several highly conserved amino acid residues including two basic and two acidic charged residues.

The contribution of these charged amino acids to the function of PagN was investigated. Mutagenesis of the Arg at position 71 or Asp at position 75, led to a moderate, and statistically significant, increase in PagN-mediated invasion of CHO-K1 cells. Proteoglycans are suspected to be the mammalian receptor recognised by PagN to initiate bacterial adhesion and begin the uptake process. Proteoglycans are negatively charged (288). Mutation of D75 to Alanine may increase the net positive charge of the protein thereby increasing the binding capabilities of PagN. The large side-chains of the R71 and D75 residues may contribute to steric hindrance by blocking the ability of other amino acid residues to interact with proteoglycans displayed on the cell surface. Mutation of either of these residues increased bacterial adhesion/invasion as it removed the barriers blocking the PagN recognised receptor from the necessary amino acids. Mutating residues K77 and D81 to Alanine decreased PagN-mediated invasion, while increasing adhesion to CHO-K1 cells. Their absence did not reduce the ability of the protein to mediate attachment to its receptor, though it did decrease the ability of the protein to promote invasion indicating that K77 and D81 may be involved in promoting invasion rather than adhesion. The distinct phenotype associated with mutating each residue reflects the complex structure of the PagN protein. Mutation of any one of the conserved, charged amino acids within Loop two of PagN affected bacterial adhesion/invasion of CHO-K1 cells, indicating that they all play a role in

PagN-mediated phenotypes. When the mutant PagN-proteins were tested for their ability to promote adhesion to and invasion of the more clinically relevant HT-29 cell line, a different trend was seen. Each of the mutations caused a decrease in both adhesion and invasion with the exception of the D75A mutation which showed a small but statistically insignificant increase in invasion. There was an overall decrease in the number of PagN-expressing bacteria interacting with HT-29 cells. Colonic epithelial cells such as the HT-29 cell line may display lower amounts of the receptor recognised by the PagN protein. Proteoglycans are less expressed on the surface of non-confluent HT-29 cells (163). In addition to the decrease in cell-surface receptors, HT-29 cells have been shown to produce antimicrobial peptides such as defensins (298, 302). There is the potential for more PagN and mutant PagN-expressing bacteria to adhere to and invade the cells only to be killed by antimicrobial peptides prior to the fixation, staining, and visualisation of the high-throughput assay.

Although expression of PagN via a high copy-number expression vector in *E. coli* has allowed us to begin to characterise the protein, it is naturally expressed in *Salmonella* spp. and it is necessary to determine the role of the protein in its natural host. *S.* Typhimurium SL1344 *pagN*-deletion mutants were previously created by Lambert *et al.* (203, 205). The data presented in the previous sections indicate that the PagN protein is not required for adhesion to and invasion of non-polarised epithelial cells such as CHO-K1 and HT-29 cells. Despite the GPA and HCA presenting similar results, other groups have shown that the PagN protein is important for *Salmonella* survival within a host and for bacterial invasion (66, 160, 205, 357). It is possible that the conditions tested in this study were not optimal for *pagN* expression, and thus the true potential for the protein was not seen. Charles *et al.* and Kroger *et al.* have shown that the *pagN* gene is maximally up-regulated by PhoP under PhoP-inducing conditions and during early stationary phase (49, 194). The conditions tested in this study included growth in PhoP-

inducing media, however, as the bacteria were grown overnight to late stationary phase, it is possible that they were experiencing stresses such as severe nutrient limitation. *S.* Typhimurium SL1344 also lacks the gene for the TetR repressor protein. When the bacteria harbour the pCM01 plasmid, the *gfp+* gene is constitutively expressed. Growth curves and viable counts were performed for *S.* Typhimurium SL1344 harbouring the pCM01 plasmid grown in L-broth. Although no fitness defect was seen in these conditions, it is possible that there is a fitness defect for strains grown in MM5.8. This would contribute to the decrease in bacterial adhesion and invasion seen.

In conclusion, although the PagN protein has previously been shown to be involved in adhesion to and invasion of mammalian cells, more in depth studies are needed to further elucidate the structure/function relationship of the PagN protein.

Chapter 6 Identification of the PagN Receptor

6.1 Introduction

The surface of mammalian cells is decorated with proteoglycans. A wide variety of microbial pathogens including viruses, bacteria, and parasites have managed to subvert the cell surface proteoglycans for use in attachment and subsequent cellular entry (27, 52, 147, 215, 270). There are two major families of proteoglycans, the syndecans and glypicans (288). Syndecans are a type-I transmembrane proteoglycans, while the glypicans are linked to membrane lipids via a glycosylphosphatidylinositol (GPI) anchor (27, 288). Glypicans, thus, do not traverse the lipid bilayer. Proteoglycans contain long chains of glycosaminoglycans (GAGs) composed of disaccharide repeats of heparan sulphate (HS), chondroitin sulphate (CS), dermatan sulphate (DS), and heparin (H). Glypicans are expressed on the cells of the central nervous system and during embryonic development leading to the hypothesis that bacteria using the more widely expressed syndecans as receptors (27). Syndecans are so named from the Greek 'syndein' meaning to bind together as they were first thought to link the extracellular matrix (ECM) to the actin cytoskeleton (300).

There are four different classes of syndecans (syndecan-1 through syndecan-4). Syndecan-1, the prototypical syndecan, was first identified as a developmentally-regulated type-I transmembrane protein involved in binding ECM components to epithelial cells (191, 283, 299). Syndecan-1 is expressed on the basolateral and epithelial surface of epithelial and plasma cells while Syndecan-4 is expressed ubiquitously on the focal adhesions of all adherent cells (27). Syndecan-1 and syndecan-4 contain long HS and CS chains linked to a core protein

traversing the cell membrane through a uniform tetrasaccharaide linker, GlcA-Gal-Gal-Xyl-Ser (130). The GAG chains begin biosynthesis in the Golgi apparatus and through a series of incomplete sequential enzymatic modifications including sulphation, acetylation, deacetylation and epimerisation, end with heterogeneous disaccharide chains linked to the core protein. The initial steps linking GAG attachment to proteoglycans involves the biosynthesis of the tetrasaccharide linker region through the transfer of xylose from UDP-xylose to the hydroxyl group of a specific serine residue on the core protein (Fig. 6.1) (27, 130). All higher organisms, including humans, possess two xylosyltransferase genes, *xylt-1* and *xylt-2* (131, 132, 251, 252, 274, 351). Human Xylosyltransferase-I (XT-I) was the first to be discovered and purified in 2000 by Kuhn *et al.* (199). Since then, Xylosyltransferase-II (XT-II) cDNA has been isolated and expressed in CHO-K1 cells (71, 274). The amino acid sequences of XT-I and XT-II share 55% overall sequence identity with several highly homologous regions with 80% identical amino acids (131).

Expression of *xylt-1* and *xylt-2* in tissue samples has been characterised previously (71, 274). In both of these studies, *xylt-2* was found to be expressed in most cell types tested (71, 274). *xylt-1*, however, was minimally expressed in all but the mouse kidneys and testis (274) and breast tissue (71). XT-I was not expressed at all in HeLa cells or the K562 bone marrow cell line (71). In both of these studies colonic cells were not tested for xylosyltransferase expression.

Previous studies have indicated that PagN is unable to promote adherence to and invasion of the mutant CHO-K1 cell line pgsA-745. pgsA745 cells lack *xylt-1*, though there is some discrepancy as to whether they also completely lack *xylt-2* (71, 274). This study attempted to recreate this phenomenon in the human colonic epithelial HT-29 cell line using an siRNA to knockdown XT-II expression due to its presence in a greater variety of cell types.

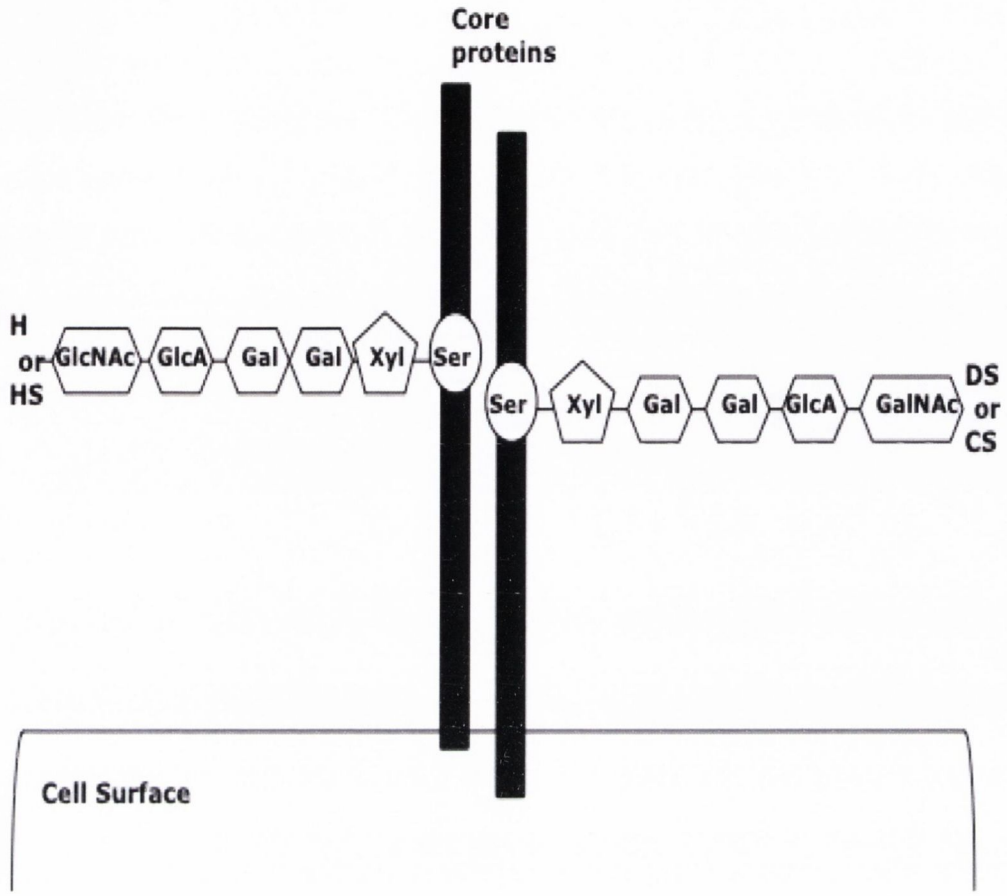

FIG. 6.1. Biosynthesis of glycosaminoglycans. The glycosaminoglycan chains of proteoglycans are synthesised in the Golgi apparatus through the transfer of monosaccharides catalysed by specific glycosyltransferases. The biosynthesis of the common tetrasaccharaide linker (Xyl-Gal-Gal-GlcA) is initiated by the transfer of xylose from UDP-xylose to a specific serine residue in the core protein by xylosyltransferase-I or xylosyltransferase-II. The fifth sugar in the chain is either N-acetylgalactosamine (found in dermatan sulphate (DS) or chondroitin sulphate (CS) chains) or N-acetylglucosamine (found in heparan sulphate (HS) or heparin (H) chains). Ser: serine, Xyl: xylose, Gal: galactose, GlcA: glucuronic acid, GalNAc: N-acetylgalactosamine, GlcNAc: N-acetylglucosamine.

6.1.1 Statistical Analyses Utilised

All data presented within all graphs in this chapter reflect the mean plus or minus the standard error. When the number of strains tested reached three or more, a one way analysis of variance test was used. The Dunnett post-test analysis was used to compare all means to a control mean as indicated in the text. Statistical significance was described for values where $p < 0.05$.

6.2 Results

6.2.1 Optimisation of the qRT-PCR reaction

In order to confidently determine whether the siRNA was effective in knocking down XT-II expression, the qRT-PCR reaction conditions were optimised. A confluent monolayer of cells was disrupted and the total RNA was extracted as described in Section 2.2.6.2. cDNA was synthesised (Section 2.2.6.3) and used in a qRT-PCR standard curve reaction. DNA template concentrations of 100 fg, 10 fg, 1 fg, 0.1 fg or 0.01 fg were amplified with either 0.5 µM or 0.8 µM of the forward and reverse primers (Table 2.3) to obtain a PCR efficiency of 90 – 110 % (Figs. 6.2 and 6.3). The glyceraldehyde-3-phosphate dehydrogenase (GAPDH) housekeeping gene was used as a reference.

6.2.2 Optimisation of the siRNA knockdown of *xylt-2*

Once the conditions for the qRT-PCR were optimised and *xylt-2* expression had been confirmed, siRNA knockdown of the gene expression could begin. Confluent monolayers of cells were disrupted and reverse transfections were performed as described in Section 2.2.6.1 using a final concentration of 10 nM of siRNA or scrambled siRNA. Cells were incubated for 24, 48, or 72 hours with the siRNA or scrambled siRNA after which time the total RNA was extracted and converted to cDNA (Section 2.2.6.2/3). Several wells were also left untreated to determine the basal level of *xylt-2* expression. A relative quantification of gene expression was performed using qRT-PCR as described in Section 2.2.6.4. The house-keeping gene *GAPDH* (in

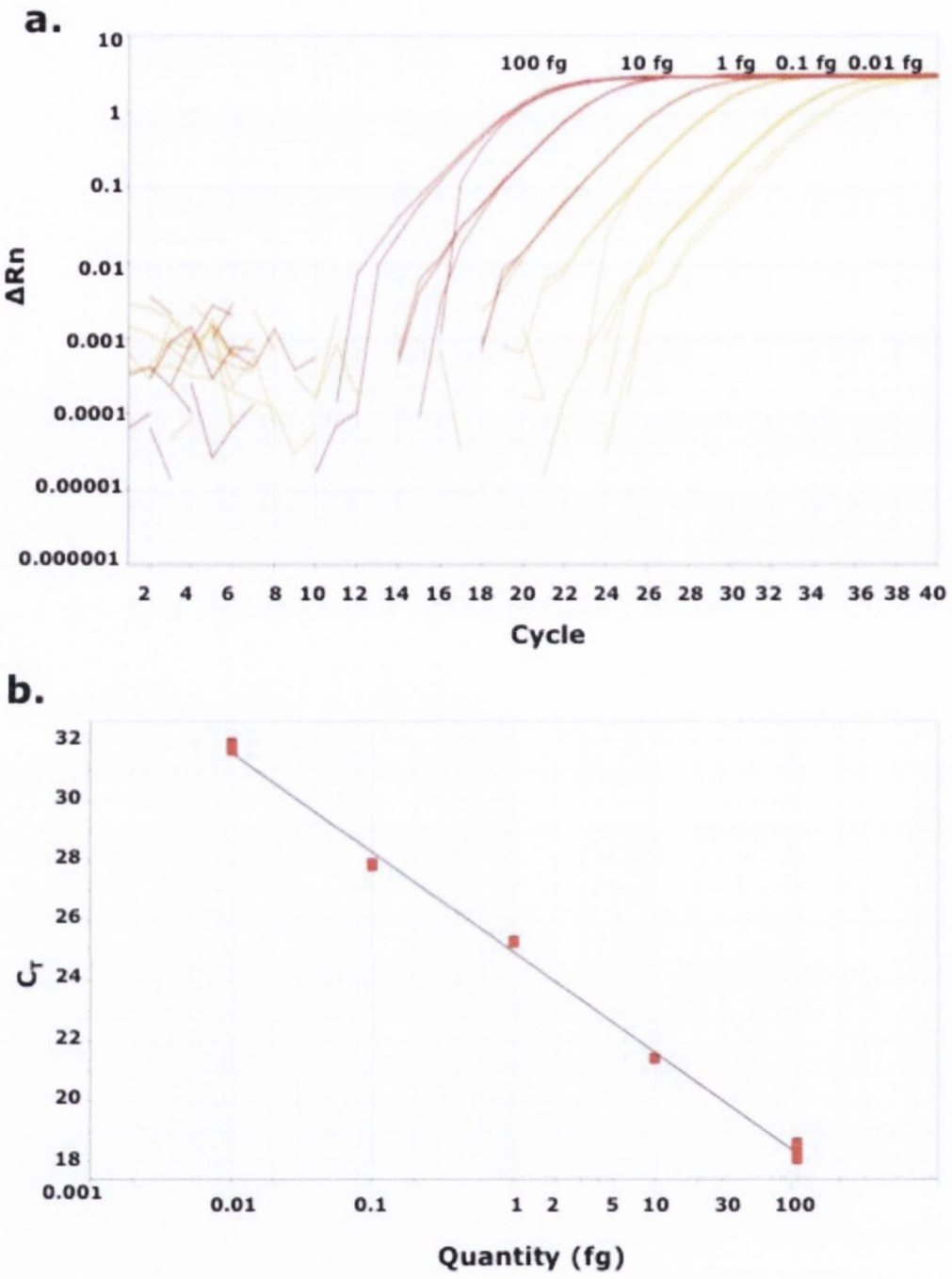

FIG. 6.2. Standard curve and amplification plot of the *GAPDH* gene in human HT-29 cells using qRT-PCR. Total RNA was extracted from the human colonic epithelial cell line HT-29 and converted to cDNA as described in Sections 2.2.6.2 to 2.2.6.4. The cDNA was amplified with primers GAPDHfwd and GAPDHRev using PCR and the DNA fragment was purified. A standard curve was performed in triplicate using 0.5 µM primers. Panel a displays the amplification plot, the numbers indicate the amount of DNA added in fg. Panel b displays the standard curve. The efficiency was 99.5% with a slope of -3.3 and an R^2 value of 0.996.

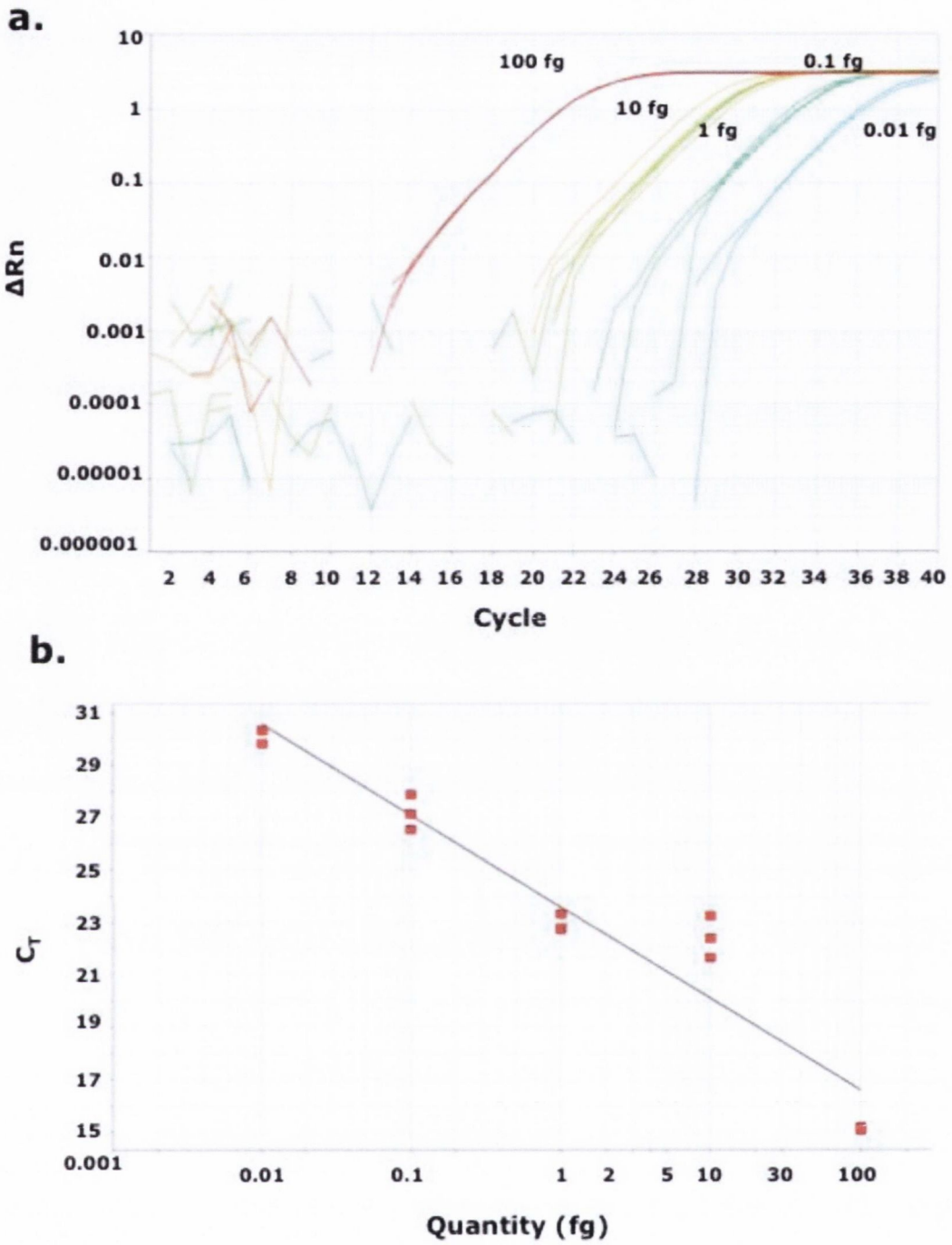

FIG. 6.3. Standard curve and amplification plot of the *xylt-2* gene in human HT-29 cells using qRT-PCR. Total RNA was extracted from the human colonic epithelial cell line HT-29 and converted to cDNA as described in Sections 2.2.6.2 to 2.2.6.4. The cDNA was amplified with primers XYLT2fwd and XYLT2Rev using PCR and the DNA fragment was purified. A standard curve was performed in triplicate using 0.8 µM primers. Panel a displays the amplification plot. The red lines indicate 100 fg DNA, the yellow lines display 10 fg DNA, the lime green lines 1 fg DNA, the teal lines 0.1 fg DNA, and the blue lines 0.01 fg DNA. Panel b displays the standard curve. The efficiency was 93.1% with a slope of -3.5 and an R^2 value of 0.921.

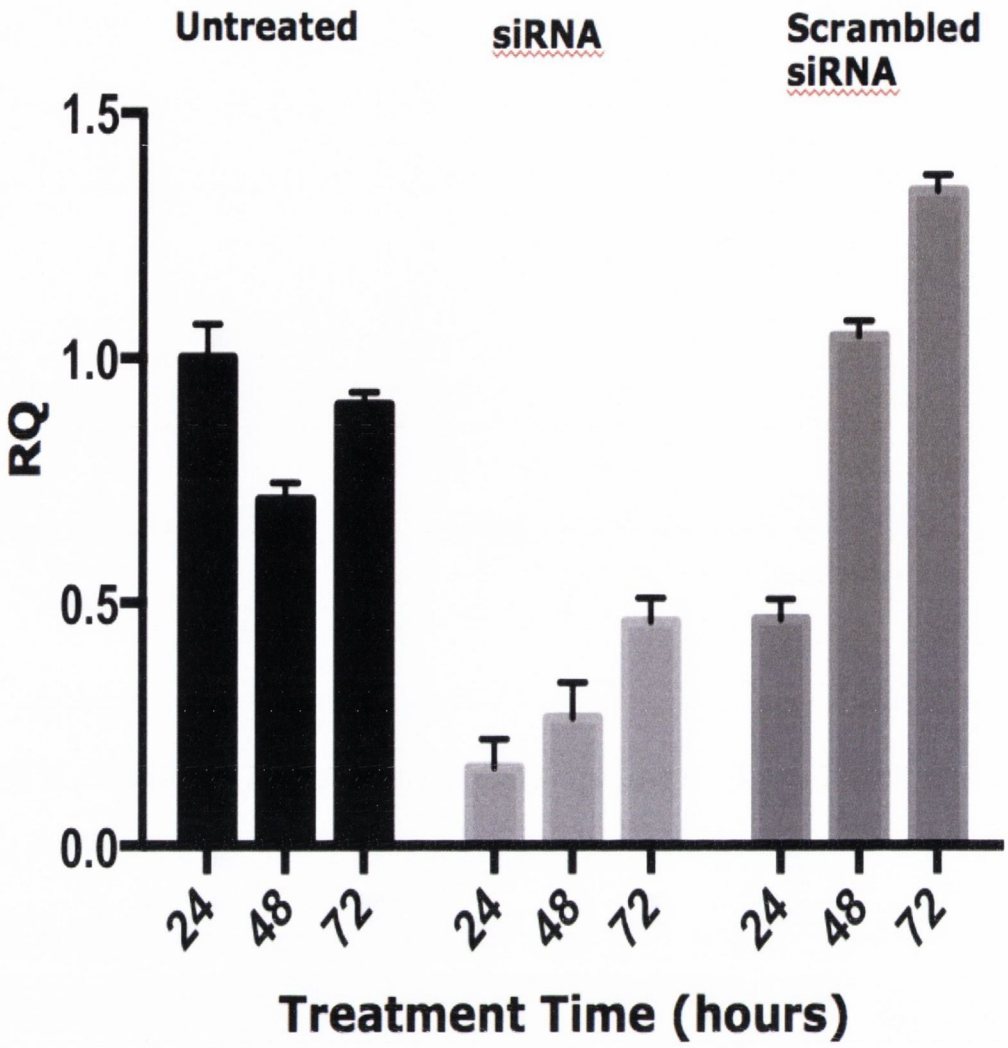

FIG. 6.4. siRNA knockdown of *xylt-2* in human HT-29 cells over time. HT-29 colonic epithelial cells were either treated with 10 nM siRNA, 10 nM scrambled siRNA, or left untreated. Total RNA was extracted from the cells after 24, 48, and 72 hours of treatment and converted to cDNA as described in Sections 2.2.6.2 to 2.2.6.4. qRT-PCR was performed to determine the expression of the *xylt-2* gene relative to the housekeeping gene *GAPDH* in untreated cells after 24 hours.

untreated cells after 24 hours) was used as the reference sample. After 24 hours, expression of *xylt-2* had decreased by 90% (Fig. 6.4). Expression of *xylt-2* also decreased in cells treated with the scrambled siRNA indicating that the transfection itself altered expression of the *xylt-2* gene. Expression of *xylt-2* returned to normal in the cells treated with the scrambled siRNA after 48 hours. The expression level also rose to levels above normal after 72 hours incubation. After 48 hours expression levels of *xylt-2* in the untreated cells decreased relative to the 24 hour incubation. Expression levels of *xylt-2* in the siRNA treated cells stayed between 10 – 50 % of the level seen in the untreated cells. An incubation period of 48 hours was selected to allow the *xylt-2* expression level in the scrambled siRNA treated cells to return to normal.

6.2.3 Knockdown of XT-II does not affect PagN-mediated invasion

Previous studies have indicated that PagN expressing bacteria are unable to effectively invade CHO-K1 cells lacking cell-surface proteoglycans. The mutant CHO-K1 cell line pgsA-745 does not produce any glycosaminoglycan chains (99, 100). Previous studies have found that invasion of this cell line by bacteria expressing PagN or the Hek and Tia invasins of *E. coli* was completely abolished (203). I sought to replicate these findings in the colonic epithelial HT-29 cell line using siRNA knockdown of *xylt-2* gene expression and testing of bacterial invasion using a high-throughput invasion assay. Reverse transfections were performed in 96 well plates as described in Section 2.2.6.1 using 2 nmol of siRNA or scrambled siRNA per well. After 48 hours, the total RNA was extracted from 6 wells, pooled (Section 2.2.6.2) and converted to cDNA (Section 2.2.6.3). The cDNA was used in a qRT-PCR reaction to confirm knockdown of *xylt-2* expression (Fig. 6.5). After confirming the decrease in *xylt-2* expression, a high-throughput assay was performed

as described in Section 2.4.3.2. *E. coli* DH5αZ1 expressing PagN, as well as GFP, were incubated with HT-29 cells that had been treated with either the siRNA or scrambled siRNA. The Olympus IX81 was used to collect the images in Fig. 6.6. There were no differences in PagN-mediated invasion of HT-29 cells exposed to the scrambled versus validated siRNA (Fig. 6.7). There was, however, a significant increase in bacterial adhesion to the siRNA treated cells when compared with those treated with the scrambled siRNA. These data indicate that a decrease in *xylt-2* in HT-29 cells was not enough to completely abrogate PagN-promoted adhesion and invasion. It is possible that removal of the GAG chains allows PagN to adhere to its true, and hitherto unknown, target.

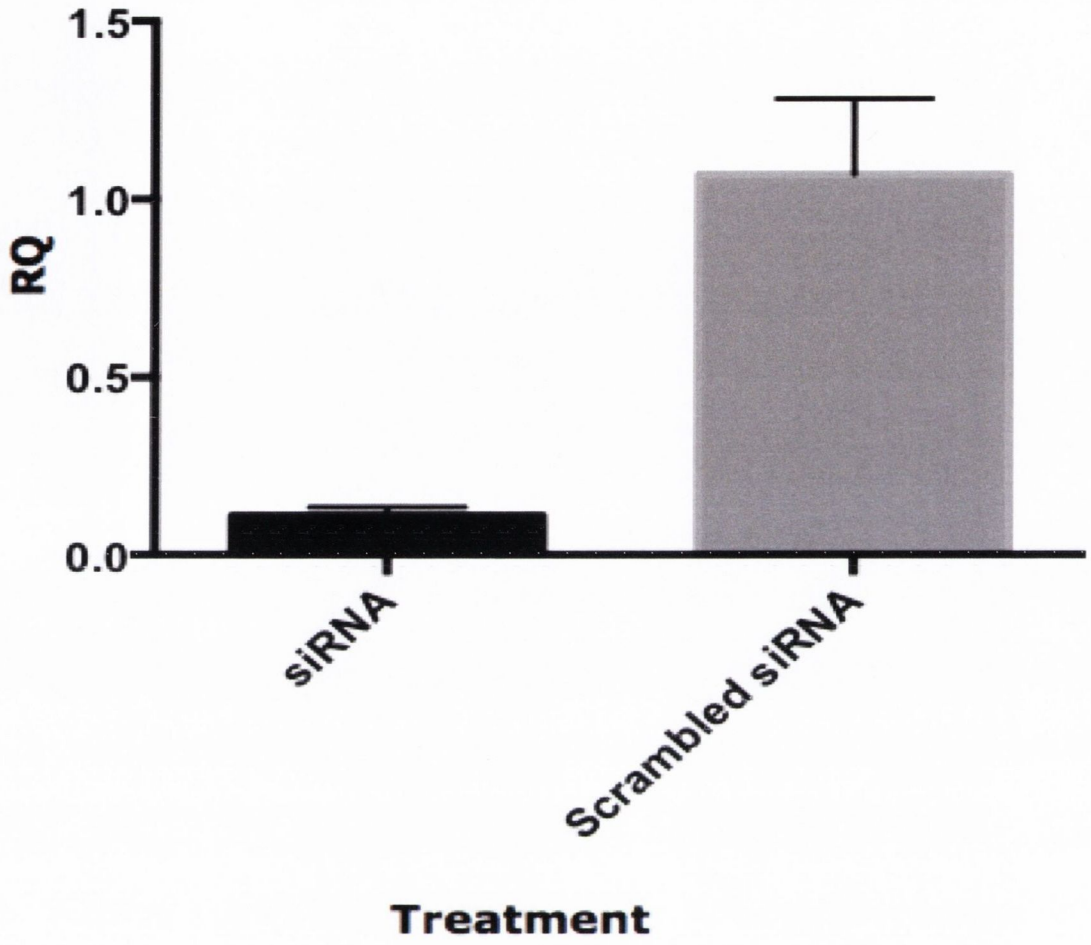

FIG. 6.5. siRNA knockdown of *xylt-2* in human HT-29 cells prior to use in an HCA. HT-29 colonic epithelial cells were either treated with 10 nM siRNA, 10 nM scrambled siRNA prior to use in a high throughput invasion assay. Total RNA was extracted from the cells after 48 hours of treatment and converted to cDNA as described in Sections 2.2.6.2 to 2.2.6.4. qRT-PCR was performed to determine the expression of the *xylt-2* gene relative to the housekeeping gene *GAPDH* in cells treated with the scrambled siRNA. There was a 89 % decrease in XT-II expression.

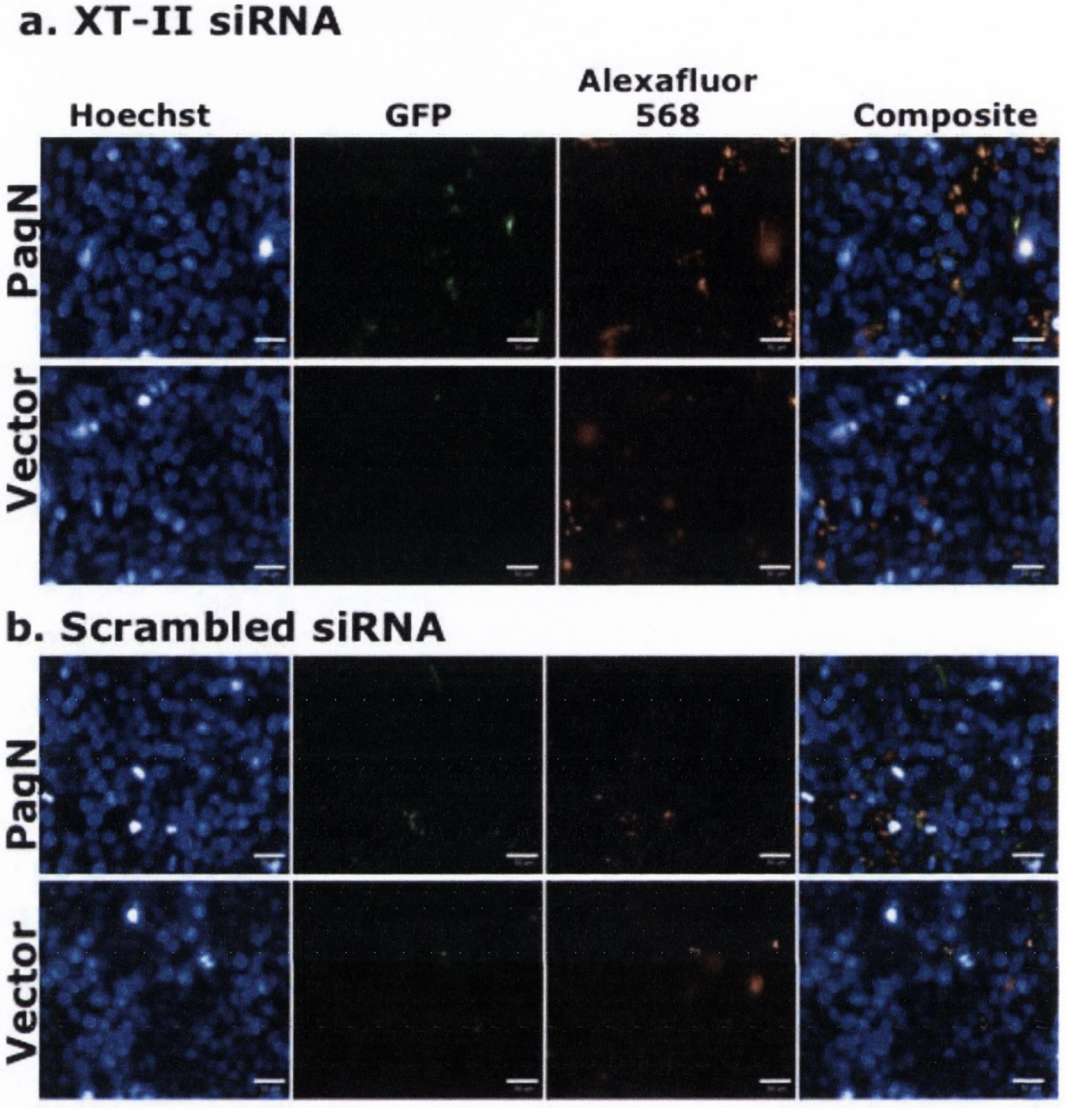

FIG 6.6. Images of PagN-mediated invasion of XT-II deficient human HT-29 cells. A high-throughput fluorescent invasion assay was performed as described in Section 2.2.4.2. to determine whether reduction of *xylt-2* expression affected PagN-mediated adhesion and invasion of HT-29 cells. Bacteria were allowed to invade cells treated with the siRNA (panel a) or a scrambled siRNA (panel b). *E. coli* DH5αZ1 expressed PagN from plasmid pML1 or harboured the vector plasmid. Mammalian cells were stained with Hoechst, bacteria express GFP, and extracellular bacteria were distinguished using an Alexafluor 568 nm antibody. The white bar indicates 50 μm.

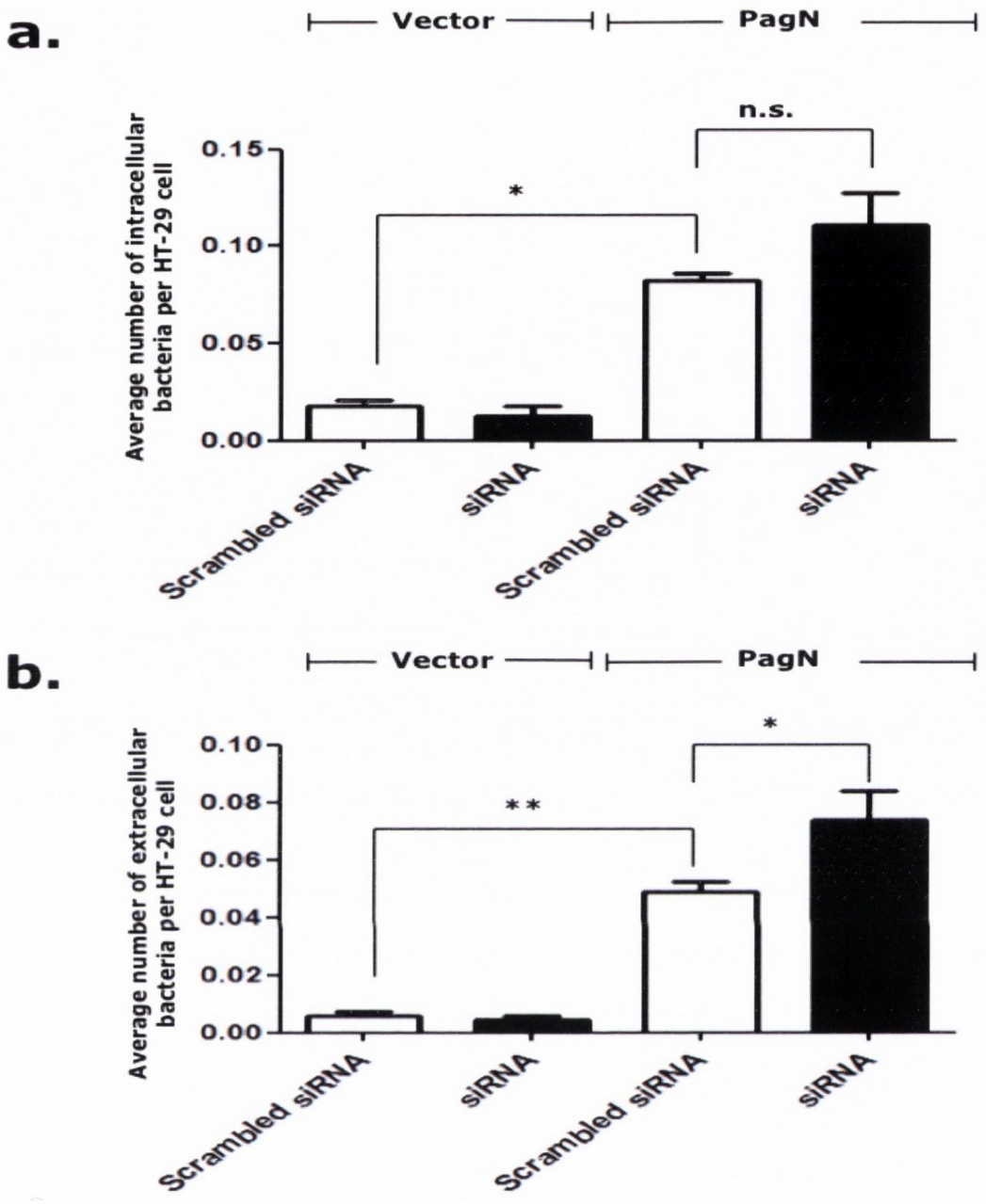

FIG 6.7. PagN-mediated adhesion and invasion of XT-II deficient HT-29 cells. A high-throughput fluorescent invasion assay of HT-29 cells deficient in xylosyltransferase-II was performed as described in Section 2.4.3.2. to determine whether PagN bound to glycosaminoglycans. *E. coli* DH5αZ1 expressed PagN from plasmid pML1 or the vector plasmid. The assay was performed in triplicate and the average number of intracellular (panel a) or extracellular (panel b) bacteria are displayed. * denotes $p < 0.05$, ** indicates $p < 0.01$. Data were analysed using the one way analysis of variance with the Dunnett post test to compare all means to the bacteria expressing wild-type PagN protein that were exposed to cells treated with the scrambled siRNA.

6.3 Discussion

Previous studies have indicated that PagN-expressing bacteria are unable to effectively adhere to and invade the glycosaminoglycan deficient pgsA-745 cell line (203). In the XT deficient pgsA-745 cells, expression of the human *xylt-1* gene and both the human and mouse *xylt-2* genes can restore the biosynthesis of GAGs such as CS and HS. The data presented in Section 6.2.3 demonstrate either XT-I is present in HT-29 cells and can compensate for the lack of XT-II in the production of GAGs, or the level of *xylt-2* expression in the siRNA treated cells produces enough GAGs to allow PagN-mediated invasion. Previous studies have not characterised the predominant xylosyltransferases found in colonic epithelial cells, therefore it is possible that *xylt-1* is expressed in HT-29 cells and that it can compensate for the siRNA-mediated loss of *xylt-2*. Future studies should characterise the predominant xylosyltransferases of HT-29 cells prior to siRNA knockdown methodology.

Biotinylated fibroblast growth factor 2 (FGF-2) binds to cell surface heparan sulphate proteoglycans, and can be used to determine the level of heparan sulphate through flow cytometry. In future studies, the level of HSPGs expressed on the cell surface should be measured prior to high content assays.

Previous studies have indicated proteoglycans expressing heparan sulphate as a potential receptor molecule (203, 204). The CHO-K1 mutant cell line pgsD-677 lacks *N*-Acetylglucosaminyl transferase and does not produce any heparan sulphate, though it does express threefold-higher levels of chondroitin sulphate (216). Studies involving this cell line would provide a better indicator as to the effect of heparan sulphate on PagN-mediated invasion. Once studies involving the pgsD-677 cell line are completed, siRNA knockdown of the human syndecan-

1 and syndecan-4, which express highly heparan sulphated glycosaminoglycans, could be performed.

Chapter 7 General Discussion

The PagN protein has recently been implicated as a potential vaccine candidate in the fight against the global burden of *Salmonella* infection (129, 357). It is important to determine the molecular characteristics of PagN and to elucidate the mechanisms by which it promotes adhesion to and invasion of the gut epithelial layer. Previous studies have characterised the regulation of the *pagN* gene and begun to determine the relationship between the structure and function of the PagN protein (203-205, 357). This study was conceived to further resolve the complex relationship between *Salmonella* and its host.

High-throughput invasion assays using fluorescent microscopy have become widely-used in recent years (217, 227, 246, 324), and they are an excellent method for studying the interactions of bacteria with mammalian cells. The development and optimisation of a high-throughput invasion assay has allowed for an in-depth analysis of the role of each of the extracellular loops of PagN, as well as the effect of individual amino acid substitutions within loop two of the protein on its ability to interact with mammalian cells.

In addition to the functional analysis of PagN, a comparison was also undertaken with the 98.3 % similar *S.* Typhi $PagN_{STY}$. This study predicted $PagN_{STY}$ to form an 8-stranded β-barrel protein within the outer membrane of bacteria. Four large loops were predicted to be exposed to the extracellular matrix, while three short turns were predicted to be located in the periplasm of bacteria. An N-terminal signal sequence located within the first 20 amino-acid residues directs protein export using the Sec-dependent transport machinery. These findings were in conflict with those expressed by Ghosh *et al.* (129). High-throughput invasion assays were also performed to compare adhesion and invasion mediated by these two proteins. There were no significant differences in cell association or invasion of CHO-K1 or HT-29 cells indicating that the

observed differences in the peptide sequences did not affect amino-acid residues necessary for PagN-promoted phenotypes.

Previous studies have implicated all four extracellular loops of $PagN_{STM}$ as being necessary to mediate adherence to and invasion of epithelial cells (204). Each of the loops was deleted at the membrane-surface interface. This study sought to create less aggressive loop-deletions in order to corroborate those results seen by Lambert *et al.* (204). Bacteria expressing the new loop-deletion mutants displayed the same adhesion/invasion defects as those previously tested (Section 5.2.2.2.3/4), indicating that PagN requires all four extracellular loops for invasion. It is possible that the loops play a role in maintaining the structure and stability of the protein once it has been inserted into the outer membrane. Protein crystallography to determine the true structure of the protein would aid in understanding the structure/function relationship.

In addition to the loop-deletion mutants created, site-directed mutagenesis was performed on the conserved, charged amino-acid residues found in the exposed loop two of the protein. Of the four residues tested, only the R71A mutant displayed a significant change in both adhesion and invasion of CHO-K1 cells. While bacteria expressing this mutant form of PagN displayed an increase in adhesion and invasion of CHO-K1 cells, bacteria expressing the Hek protein mutated at the same residue displayed a decrease in both adhesion and invasion (253). In the Hek protein, it is possible that the conserved arginine residue plays a role in mediating invasion while it plays a different role in the PagN protein. As Hek requires only loop two of the protein to mediate invasion, many of the charged amino-acid residues may play a larger role in mediating attachment to and invasion of mammalian cells. PagN, however, requires all four extracellular loops for invasion. In addition to playing a role in stabilising the protein, several charged amino-acid residues dispersed throughout all four extracellular loops may be involved in mediating PagN-associated phenotypes. Future work should

include site-directed mutagenesis on several different exposed, charged amino-acid residues located throughout the four exposed extracellular loops to determine their involvement in adhesion and invasion.

As discussed in Section 5.2.4, PagN, as expressed in its natural host, did not appear to play a role in mediating attachment to and invasion of epithelial cells such as CHO-K1 and HT-29 cells. However, there are several parameters that must be re-tested before the effectiveness of PagN as an adhesin/invasin can be discounted. Firstly, the M.O.I. chosen for *S.* Typhimurium strains was 10 bacteria per mammalian cell while that chosen for *E. coli* strains expressing PagN exogenously from a plasmid was 90 bacteria per cell. High levels of adhesion and invasion were seen for strains of PagN-expressing *E. coli* (up to 9.0 bacteria per cell). The same was not seen for *S.* Typhimurium SL1344 (up to 3.0 bacteria per cell). Using high-throughput assays, the Hardt laboratory in Switzerland have demonstrated high levels of *Salmonella* invasion using an M.O.I. of ~100 – 130 (246, 247). In future, the dose-dependent high-throughput assay should be repeated with higher M.O.I. levels from 1 to 1000.

S. Typhimurium SL1344 and SL1344 mutant derivatives were grown in PhoP-inducing media to promote transcriptional activation of the *pagN* gene prior to invasion. It is possible that prolonged growth in nutrient-limiting, acidic media affected the ability of the bacteria to invade a mammalian cell monolayer. In order to determine whether this influenced the data generated in Section 5.2.4, high-throughput invasion assays should be repeated with several modifications. Overnight cultures of *S.* Typhimurium should be grown in L-broth, harvested, washed thrice in MM5.8, and sub-inoculated and grown in MM5.8 prior to the start of the assay. If the overnight growth in MM5.8 did play a role in dampening invasion, the shorter incubation period should abolish this effect.

S. Typhimurium SL1344 does not possess the *tetR* gene encoding the TetR repressor protein. When plasmid pCM01 was transformed into

E. coli XL-1 Blue strains, which also lack the *tetR* gene, they appeared form long strings of aberrantly growing bacteria unable to correctly divide. While this was not seen for *S.* Typhimurium SL1344 pCM01 when viewed under a microscope, it is possible that the lack of a repressor protein and constitutive activation of the *gfp* gene affected the ability of the bacteria to effectively invade epithelial cells. Mansson *et al.* were able to effectively integrate the $P_{LtetO-1}$ *gfp-cmR* fragment into the chromosomal *cobS* locus of *E. coli* CFT073 (227). Using the Datsenko and Wanner method for gene inactivation, the tet-controlled *gfp* gene as well as the *tetR* repressor gene could be incorporated into the homologous *cobS* locus in *S.* Typhimurium SL1344 (79). This would add two additional points of regulation. First, the number of copies of the *gfp* gene would decrease from 15 seen for plasmid pCM01 to 1 seen for the chromosome. Second, the addition of the *tetR* gene would allow bacteria to block expression of the *gfp* gene until the addition of ATc. The higher M.O.I., decreased period of growth in MM5.8, and control of *gfp* expression should increase the overall invasion of *Salmonella* strains and allow the structure/function relationship of PagN to be further clarified.

In addition to the structure/function relationship studies, further work is needed to determine the receptor to which PagN binds. siRNA knockdown of *xylt-2* in HT-29 cells did not completely abolish PagN-mediated invasion of these cells. As discussed in Section 6.3, expression of the alternate xylosyltransferase, *xylt-1*, has not been examined in this cell line. Future work should include a characterisation of *xylt-1* expression. If high levels of *xylt-1* are seen in HT-29 cells, then it may play the role of predominant xylosyltransferase in which case XT-II may be functionally redundant and display lower levels of expression. siRNA knockdown of *xylt-1* expression followed by high-throughput invasion assays would determine whether XT-I was responsible for GAG biosynthesis. Flow cytomentry using biotinylated FGF-2 post-siRNA knockdown would determine the level of HSPGs displayed on the cell surface and provide further evidence as to whether XT-I or XT-II plays

the major role in GAG biosynthesis in colonic epithelial cells. Previous studies have implicated HSPGs as the PagN cell-surface receptor (204). Syndecan-1 and Syndecan-4 are the predominant HSPGs expressed on the epithelium (27). siRNA knockdown of these two receptors followed by quantification using qRT-PCR and high-throughput invasion assays would help to further elicudate the PagN receptor molecule.

While further work is necessary to fully characterise the nature of the interaction between PagN and HSPGs, the loop-deletions, site-directed mutagenesis, and development of the high-throughput fluorescent assay for invasion have allowed for a greater understanding of processes involved in the functionality of the PagN protein.

Chapter 8 Bibliography

1. **Ahmer, B. M., J. van Reeuwijk, C. D. Timmers, P. J. Valentine, and F. Heffron.** 1998. *Salmonella typhimurium* encodes an SdiA homolog, a putative quorum sensor of the LuxR family, that regulates genes on the virulence plasmid. J Bacteriol **180:**1185-1193.
2. **Akbar, S., L. M. Schechter, C. P. Lostroh, and C. A. Lee.** 2003. AraC/XylS family members, HilD and HilC, directly activate virulence gene expression independently of HilA in *Salmonella typhimurium*. Mol Microbiol **47:**715-728.
3. **Akeda, Y., and J. E. Galan.** 2005. Chaperone release and unfolding of substrates in type III secretion. Nature **437:**911-915.
4. **Alekshun, M. N., and S. B. Levy.** 1997. Regulation of chromosomally mediated multiple antibiotic resistance: the mar regulon. Antimicrob Agents Ch **41:**2067-2075.
5. **Alpuche-Aranda, C. M., E. L. Racoosin, J. A. Swanson, and S. I. Miller.** 1994. *Salmonella* stimulate macrophage macropinocytosis and persist within spacious phagosomes. The J Exp Med **179:**601-608.
6. **Alpuche Aranda, C. M., J. A. Swanson, W. P. Loomis, and S. I. Miller.** 1992. *Salmonella typhimurium* activates virulence gene transcription within acidified macrophage phagosomes. P Natl Acad Sci USA **89:**10079-10083.
7. **Altier, C.** 2005. Genetic and environmental control of *salmonella* invasion. J Microbiol **43 Spec No:**85-92.
8. **Amann, E. B., B. Ochs, and K. J. Abel.** 1988. Tightly regulated *tac* promoter vectors useful for the expression of fused and unfused proteins in *Escherichia coli* Gene **69:**301-316.
9. **Amavisit, P., D. Lightfoot, G. F. Browning, and P. F. Markham.** 2003. Variation between pathogenic serovars within *Salmonella* pathogenicity islands. J Bacteriol **185:**3624-3635.
10. **Bader, M. W., W. W. Navarre, W. Shiau, H. Nikaido, J. G. Frye, M. McClelland, F. C. Fang, and S. I. Miller.** 2003. Regulation of *Salmonella typhimurium* virulence gene expression by cationic antimicrobial peptides. Mol Microbiol **50:**219-230.
11. **Bader, M. W., S. Sanowar, M. E. Daley, A. R. Schneider, U. Cho, W. Xu, R. E. Klevit, H. Le Moual, and S. I. Miller.** 2005. Recognition of antimicrobial peptides by a bacterial sensor kinase. Cell **122:**461-472.
12. **Bagos, P. G., T. D. Liakopoulos, I. C. Spyropoulos, and S. J. Hamodrakas.** 2004. PRED-TMBB: a web server for predicting the topology of beta-barrel outer membrane proteins. Nucleic Acids Res **32:**W400-404.
13. **Bajaj, V., C. Hwang, and C. A. Lee.** 1995. *hilA* is a novel *ompR/toxR* family member that activates the expression of

Salmonella typhimurium invasion genes. Mol Microbiol **18:**715-727.

14. **Bajaj, V., R. L. Lucas, C. Hwang, and C. A. Lee.** 1996. Co-ordinate regulation of *Salmonella typhimurium* invasion genes by environmental and regulatory factors is mediated by control of *hilA* expression. Mol Microbiol **22:**703-714.
15. **Bakshi, C. S., V. P. Singh, M. W. Wood, P. W. Jones, T. S. Wallis, and E. E. Galyov.** 2000. Identification of SopE2, a *Salmonella* secreted protein which is highly homologous to SopE and involved in bacterial invasion of epithelial cells. J Bacteriol **182:**2341-2344.
16. **Barlag, B., and M. Hensel.** 2015. The Giant Adhesin SiiE of *Salmonella enterica*. Molecules **20:**1134-1150.
17. **Baumler, A. J., and F. Heffron.** 1995. Identification and sequence analysis of *lpfABCDE*, a putative fimbrial operon of *Salmonella typhimurium*. J Bacteriol **177:**2087-2097.
18. **Baumler, A. J., R. M. Tsolis, and F. Heffron.** 1996. Contribution of fimbrial operons to attachment to and invasion of epithelial cell lines by *Salmonella typhimurium*. Infect Immun **64:**1862-1865.
19. **Baumler, A. J., R. M. Tsolis, and F. Heffron.** 1996. The *lpf* fimbrial operon mediates adhesion of *Salmonella typhimurium* to murine Peyer's patches. P Natl Acad Sci USA **93:**279-283.
20. **Baumler, A. J., R. M. Tsolis, P. J. Valentine, T. A. Ficht, and F. Heffron.** 1997. Synergistic *effect* of mutations in *invA* and *lpfC* on the ability of *Salmonella* typhimurium to cause murine typhoid. Infect Immun **65:**2254-2259.
21. **Bearson, B. L., L. Wilson, and J. W. Foster.** 1998. A low pH-inducible, PhoPQ-dependent acid tolerance response protects *Salmonella typhimurium* against inorganic acid stress. J Bacteriol **180:**2409-2417.
22. **Belden, W. J., and S. I. Miller.** 1994. Further characterization of the PhoP regulon: identification of new PhoP-activated virulence loci. Infect Immun **62:**5095-5101.
23. **Bendtsen, J. D., H. Nielsen, G. von Heijne, and S. Brunak.** 2004. Improved prediction of signal peptides: SignalP 3.0. J Mol Biol **340:**783-795.
24. **Benz, I., and M. A. Schmidt.** 1992. AIDA-I, the adhesin involved in diffuse adherence of the diarrhoeagenic *Escherichia coli* strain 2787 (O126:H27), is synthesized via a precursor molecule. Mol Microbiol **6:**1539-1546.
25. **Berens, C., S. Lochner, S. Lober, I. Usai, A. Schmidt, L. Drueppel, W. Hillen, and P. Gmeiner.** 2006. Subtype selective tetracycline agonists and their application for a two-stage regulatory system. Chembiochem **7:**1320-1324.
26. **Bernal-Bayard, J., E. Cardenal-Munoz, and F. Ramos-Morales.** 2010. The *Salmonella* type III secretion effector,

salmonella leucine-rich repeat protein (SlrP), targets the human chaperone ERdj3. J Biol Chem **285:**16360-16368.

27. **Bernfield, M., M. Gotte, P. W. Park, O. Reizes, M. L. Fitzgerald, J. Lincecum, and M. Zako.** 1999. Functions of cell surface heparan sulfate proteoglycans. Annu Rev Biochem **68:**729-777.
28. **Bernstein, E., A. A. Caudy, S. M. Hammond, and G. J. Hannon.** 2001. Role for a bidentate ribonuclease in the initiation step of RNA interference. Nature **409:**363-366.
29. **Bijlsma, J. J., and E. A. Groisman.** 2005. The PhoP/PhoQ system controls the intramacrophage type three secretion system of *Salmonella enterica*. Mol Microbiol **57:**85-96.
30. **Billy, E., V. Brondani, H. Zhang, U. Muller, and W. Filipowicz.** 2001. Specific interference with gene expression induced by long, double-stranded RNA in mouse embryonal teratocarcinoma cell lines. P Natl Acad Sci USA **98:**14428-14433.
31. **Bishop, C. M., W. F. Walkenhorst, and W. C. Wimley.** 2001. Folding of beta-sheets in membranes: specificity and promiscuity in peptide model systems. J Mol Biol **309:**975-988.
32. **Biswas, R., R. K. Agarwal, K. N. Bhilegaonkar, A. Kumar, P. Nambiar, S. Rawat, and M. Singh.** 2011. Cloning and sequencing of biofilm-associated protein (*bapA*) gene and its occurrence in different serotypes of *Salmonella*. Lett Appl Microbiol **52:**138-143.
33. **Blanc-Potard, A. B., and E. A. Groisman.** 1997. The *Salmonella selC* locus contains a pathogenicity island mediating intramacrophage survival. EMBO J **16:**5376-5385.
34. **Boddicker, J. D., B. M. Knosp, and B. D. Jones.** 2003. Transcription of the *Salmonella* invasion gene activator, *hilA*, requires HilD activation in the absence of negative regulators. J Bacteriol **185:**525-533.
35. **Bontorin, G., S. Renaud, A. Garenne, L. Alvado, G. Le Masson, and J. Tomas.** 2007. A real-time closed-loop setup for hybrid neural networks. Conference proceedings : ... Annual International Conference of the IEEE Engineering in Medicine and Biology Society. IEEE Engineering in Medicine and Biology Society. Conference **2007:**3004-3007.
36. **Botelho, R. J., M. Teruel, R. Dierckman, R. Anderson, A. Wells, J. D. York, T. Meyer, and S. Grinstein.** 2000. Localized biphasic changes in phosphatidylinositol-4,5-bisphosphate at sites of phagocytosis. J Cell Biol **151:**1353-1368.
37. **Boyle, E. C., N. F. Brown, and B. B. Finlay.** 2006. *Salmonella enterica* serovar Typhimurium effectors SopB, SopE, SopE2 and SipA disrupt tight junction structure and function. Cell Microbiol **8:**1946-1957.

38. **Bronstein, P. A., E. A. Miao, and S. I. Miller.** 2000. InvB is a type III secretion chaperone specific for SspA. J Bacteriol **182:**6638-6644.
39. **Browne, S. H., M. L. Lesnick, and D. G. Guiney.** 2002. Genetic requirements for *Salmonella*-induced cytopathology in human monocyte-derived macrophages. Infect Immun **70:**7126-7135.
40. **Brumell, J. H., and S. Grinstein.** 2004. *Salmonella* redirects phagosomal maturation. Curr Opin Microbiol **7:**78-84.
41. **Buchwald, G., A. Friebel, J. E. Galan, W. D. Hardt, A. Wittinghofer, and K. Scheffzek.** 2002. Structural basis for the reversible activation of a Rho protein by the bacterial toxin SopE. EMBO J **21:**3286-3295.
42. **Bustamante, V. H., L. C. Martinez, F. J. Santana, L. A. Knodler, O. Steele-Mortimer, and J. L. Puente.** 2008. HilD-mediated transcriptional cross-talk between SPI-1 and SPI-2. P Natl Acad Sci USA **105:**14591-14596.
43. **Butler, T., A. Islam, I. Kabir, and P. K. Jones.** 1991. Patterns of morbidity and mortality in typhoid fever dependent on age and gender: review of 552 hospitalized patients with diarrhea. Rev Infect Dis **13:**85-90.
44. **Cantalupo, G., P. Alifano, V. Roberti, C. B. Bruni, and C. Bucci.** 2001. Rab-interacting lysosomal protein (RILP): the Rab7 effector required for transport to lysosomes. EMBO J **20:**683-693.
45. **Castelli, M. E., E. Garcia Vescovi, and F. C. Soncini.** 2000. The phosphatase activity is the target for Mg2+ regulation of the sensor protein PhoQ in *Salmonella*. J Biol Chem **275:**22948-22954.
46. **Catron, D. M., M. D. Sylvester, Y. Lange, M. Kadekoppala, B. D. Jones, D. M. Monack, S. Falkow, and K. Haldar.** 2002. The *Salmonella*-containing vacuole is a major site of intracellular cholesterol accumulation and recruits the GPI-anchored protein CD55. Cell Microbiol **4:**315-328.
47. **Chamnongpol, S., M. Cromie, and E. A. Groisman.** 2003. Mg2+ sensing by the Mg2+ sensor PhoQ of *Salmonella enterica*. J Mol Biol **325:**795-807.
48. **Chang, J., J. Chen, and D. Zhou.** 2005. Delineation and characterization of the actin nucleation and effector translocation activities of *Salmonella* SipC. Mol Microbiol **55:**1379-1389.
49. **Charles, R. C., J. B. Harris, M. R. Chase, L. M. Lebrun, A. Sheikh, R. C. LaRocque, T. Logvinenko, S. M. Rollins, A. Tarique, E. L. Hohmann, I. Rosenberg, B. Krastins, D. A. Sarracino, F. Qadri, S. B. Calderwood, and E. T. Ryan.** 2009. Comparative proteomic analysis of the PhoP regulon in *Salmonella enterica* serovar Typhi versus Typhimurium. PloS one **4:**e6994.
50. **Chaudhuri, R. R., E. Morgan, S. E. Peters, S. J. Pleasance, D. L. Hudson, H. M. Davies, J. Wang, P. M. van Diemen, A. M. Buckley, A. J. Bowen, G. D. Pullinger, D. J. Turner, G. C.**

Langridge, A. K. Turner, J. Parkhill, I. G. Charles, D. J. Maskell, and M. P. Stevens. 2013. Comprehensive assignment of roles for *Salmonella typhimurium* genes in intestinal colonization of food-producing animals. PLoS genetics **9:**e1003456.

51. **Chaveroche, M. K., J. M. Ghigo, and C. d'Enfert.** 2000. A rapid method for efficient gene replacement in the filamentous fungus *Aspergillus nidulans*. Nucleic Acids Res **28:**E97.
52. **Chen, T., R. J. Belland, J. Wilson, and J. Swanson.** 1995. Adherence of pilus- Opa+ gonococci to epithelial cells in vitro involves heparan sulfate. The J Exp Med **182:**511-517.
53. **Chessa, D., C. W. Dorsey, M. Winter, and A. J. Baumler.** 2008. Binding specificity of Salmonella plasmid-encoded fimbriae assessed by glycomics. J Biol Chem **283:**8118-8124.
54. **Chessa, D., M. G. Winter, M. Jakomin, and A. J. Baumler.** 2009. *Salmonella enterica* serotype Typhimurium Std fimbriae bind terminal alpha(1,2)fucose residues in the cecal mucosa. Mol Microbiol **71:**864-875.
55. **Chessa, D., M. G. Winter, S. P. Nuccio, C. Tukel, and A. J. Baumler.** 2008. RosE represses Std fimbrial expression in *Salmonella enterica* serotype Typhimurium. Mol Microbiol **68:**573-587.
56. **Chomczynski, P., and N. Sacchi.** 1987. Single-step method of RNA isolation by acid guanidinium thiocyanate-phenol-chloroform extraction. Anal Biochem **162:**156-159.
57. **Chu, C., S. F. Hong, C. Tsai, W. S. Lin, T. P. Liu, and J. T. Ou.** 1999. Comparative physical and genetic maps of the virulence plasmids of *Salmonella enterica* serovars Typhimurium, Enteritidis, Choleraesuis, and Dublin. Infect Immun **67:**2611-2614.
58. **Cirillo, D. M., R. H. Valdivia, D. M. Monack, and S. Falkow.** 1998. Macrophage-dependent induction of the *Salmonella* pathogenicity island 2 type III secretion system and its role in intracellular survival. Mol Microbiol **30:**175-188.
59. **Clegg, S., B. K. Purcell, and J. Pruckler.** 1987. Characterization of genes encoding type 1 fimbriae of *Klebsiella pneumoniae*, *Salmonella typhimurium*, and *Serratia marcescens*. Infect Immun **55:**281-287.
60. **Cloeckaert, A., and S. Schwarz.** 2001. Molecular characterization, spread and evolution of multidrug resistance in *Salmonella enterica* typhimurium DT104. Vet Res **32:**301-310.
61. **Coburn, B., I. Sekirov, and B. B. Finlay.** 2007. Type III secretion systems and disease. Clin Microbiol Rev **20:**535-549.
62. **Cohen, S. P., S. B. Levy, J. Foulds, and J. L. Rosner.** 1993. Salicylate induction of antibiotic resistance in *Escherichia coli*: activation of the *mar* operon and a *mar*-independent pathway. J Bacteriol **175:**7856-7862.

63. **Collazo, C. M., and J. E. Galan.** 1996. Requirement for exported proteins in secretion through the invasion-associated type III system of *Salmonella typhimurium*. Infect Immun **64:**3524-3531.
64. **Collinson, S. K., S. C. Clouthier, J. L. Doran, P. A. Banser, and W. W. Kay.** 1996. *Salmonella enteritidis agfBAC* operon encoding thin, aggregative fimbriae. J Bacteriol **178:**662-667.
65. **Collinson, S. K., P. C. Doig, J. L. Doran, S. Clouthier, T. J. Trust, and W. W. Kay.** 1993. Thin, aggregative fimbriae mediate binding of *Salmonella enteritidis* to fibronectin. J Bacteriol **175:**12-18.
66. **Conner, C. P., D. M. Heithoff, S. M. Julio, R. L. Sinsheimer, and M. J. Mahan.** 1998. Differential patterns of acquired virulence genes distinguish *Salmonella* strains. P Natl Acad Sci USA **95:**4641-4645.
67. **Crago, A. M., and V. Koronakis.** 1999. Binding of extracellular matrix laminin to *Escherichia coli* expressing the *Salmonella* outer membrane proteins Rck and PagC. FEMS Microbiol Lett **176:**495-501.
68. **Criss, A. K., and J. E. Casanova.** 2003. Coordinate regulation of *Salmonella enterica* serovar Typhimurium invasion of epithelial cells by the Arp2/3 complex and Rho GTPases. Infect Immun **71:**2885-2891.
69. **Crump, J. A., S. P. Luby, and E. D. Mintz.** 2004. The global burden of typhoid fever. B World Health Organ **82:**346-353.
70. **Cuellar-Mata, P., N. Jabado, J. Liu, W. Furuya, B. B. Finlay, P. Gros, and S. Grinstein.** 2002. Nramp1 modifies the fusion of *Salmonella typhimurium*-containing vacuoles with cellular endomembranes in macrophages. J Biol Chem **277:**2258-2265.
71. **Cuellar, K., H. Chuong, S. M. Hubbell, and M. E. Hinsdale.** 2007. Biosynthesis of chondroitin and heparan sulfate in chinese hamster ovary cells depends on xylosyltransferase II. J Biol Chem **282:**5195-5200.
72. **Cunliffe, R. N.** 2003. Alpha-defensins in the gastrointestinal tract. Mol Immunol **40:**463-467.
73. **Cunliffe, R. N., and Y. R. Mahida.** 2004. Expression and regulation of antimicrobial peptides in the gastrointestinal tract. J Leukocyte Biol **75:**49-58.
74. **Curtiss, R., 3rd, and S. M. Kelly.** 1987. *Salmonella typhimurium* deletion mutants lacking adenylate cyclase and cyclic AMP receptor protein are avirulent and immunogenic. Infect Immun **55:**3035-3043.
75. **Dai, S., P. D. Sarmiere, O. Wiggan, J. R. Bamburg, and D. Zhou.** 2004. Efficient *Salmonella* entry requires activity cycles of host ADF and cofilin. Cell Microbiol **6:**459-471.
76. **Darwin, K. H., and V. L. Miller.** 1999. InvF is required for expression of genes encoding proteins secreted by the SPI1 type

III secretion apparatus in *Salmonella typhimurium*. J Bacteriol **181:**4949-4954.

77. **Darwin, K. H., and V. L. Miller.** 1999. Molecular basis of the interaction of *Salmonella* with the intestinal mucosa. Clin Microbiol Rev **12:**405-428.
78. **Datsenko, K. A., and B. L. Wanner.** 2000. One-step inactivation of chromosomal genes in *Escherichia coli* K-12 using PCR products. P Natl Acad Sci USA **97:**6640-6645.
79. **Datsenko, K. A., and B. L. Wanner.** 2000. One-step inactivation of chromosomal genes in *Escherichia coli* K-12 using PCR products. P Natl Acad Sci USA **97:**6640-6645.
80. **Davies, D. G., M. R. Parsek, J. P. Pearson, B. H. Iglewski, J. W. Costerton, and E. P. Greenberg.** 1998. The involvement of cell-to-cell signals in the development of a bacterial biofilm. Science **280:**295-298.
81. **Deighan, P., A. Free, and C. J. Dorman.** 2000. A role for the *Escherichia coli* H-NS-like protein StpA in OmpF porin expression through modulation of micF RNA stability. Mol Microbiol **38:**126-139.
82. **Dibb-Fuller, M. P., E. Allen-Vercoe, C. J. Thorns, and M. J. Woodward.** 1999. Fimbriae- and flagella-mediated association with and invasion of cultured epithelial cells by *Salmonella enteritidis*. Microbiology **145 (Pt 5):**1023-1031.
83. **Dinjus, U., I. Hanel, W. Rabsch, and R. Helmuth.** 1998. Studies of the presence of the virulence factors, adhesion, invasion, intracellular multiplication and toxin formation in salmonellas of different origin. Zbl Bakt Int J Med M **287:**387-398.
84. **Dorman, C. J., S. Chatfield, C. F. Higgins, C. Hayward, and G. Dougan.** 1989. Characterization of porin and *ompR* mutants of a virulent strain of *Salmonella typhimurium*: *ompR* mutants are attenuated *in vivo*. Infect Immun **57:**2136-2140.
85. **Dorsey, C. W., M. C. Laarakker, A. D. Humphries, E. H. Weening, and A. J. Baumler.** 2005. *Salmonella enterica* serotype Typhimurium MisL is an intestinal colonization factor that binds fibronectin. Mol Microbiol **57:**196-211.
86. **Dower, W. J., J. F. Miller, and C. W. Ragsdale.** 1988. High efficiency transformation of *E. coli* by high voltage electroporation. Nucleic Acids Res **16:**6127-6145.
87. **Drecktrah, D., L. A. Knodler, D. Howe, and O. Steele-Mortimer.** 2007. *Salmonella* trafficking is defined by continuous dynamic interactions with the endolysosomal system. Traffic **8:**212-225.
88. **Duguid, J. P., and R. R. Gillies.** 1958. Fimbriae and haemagglutinating activity in *Salmonella*, *Klebsiella*, *Proteus*, and *Chromobacterium*. J Pathol Bacteriol **75:**519-520.
89. **Ehrbar, K., A. Friebel, S. I. Miller, and W. D. Hardt.** 2003. Role of the *Salmonella* pathogenicity island 1 (SPI-1) protein InvB in

type III secretion of SopE and SopE2, two *Salmonella* effector proteins encoded outside of SPI-1. J Bacteriol **185:**6950-6967.

90. **Eichelberg, K., *and* J. E. Galan.** 1999. Differential regulation of *Salmonella* typhimurium type III secreted proteins by pathogenicity island 1 (SPI-1)-encoded transcriptional activators InvF and HilA. Infect Immun **67:**4099-4105.
91. **Elbashir, S. M., J. Harborth, W. Lendeckel, A. Yalcin, K. Weber, and T. Tuschl.** 2001. Duplexes of 21-nucleotide RNAs mediate RNA interference in cultured mammalian cells. Nature **411:**494-498.
92. **Elbashir, S. M., W. Lendeckel, and T. Tuschl.** 2001. RNA interference is mediated by 21- and 22-nucleotide RNAs. Gene Dev **15:**188-200.
93. **Ellermeier, C. D., J. R. Ellermeier, and J. M. Slauch.** 2005. HilD, HilC and RtsA constitute a feed forward loop that controls expression of the SPI1 type three secretion system regulator hilA in *Salmonella enterica* serovar Typhimurium. Mol Microbiol **57:**691-705.
94. **Ellermeier, C. D., and J. M. Slauch.** 2003. RtsA and RtsB coordinately regulate expression of the invasion and flagellar genes in *Salmonella enterica* serovar Typhimurium. J Bacteriol **185:**5096-5108.
95. **Ellermeier, J. R., and J. M. Slauch.** 2007. Adaptation to the host environment: regulation of the SPI1 type III secretion system in *Salmonella enterica* serovar Typhimurium. Curr Opin Microbiol **10:**24-29.
96. **Elsinghorst, E. A.** 1994. Measurement of invasion by gentamicin resistance. Method Enzymol **236:**405-420.
97. **Engler, M. J., and C. C. Richardson.** 1982. The Enzymes, vol. 5. Academic Press, San Diego.
98. **Erdem, B., S. Ercis, G. Hascelik, D. Gur, S. Gedikoglu, A. D. Aysev, B. Sumerkan, M. Tatman-Otkun, and I. Tuncer.** 2005. Antimicrobial resistance patterns and serotype distribution among *Salmonella enterica* strains in Turkey, 2000-2002. Eur J Clin Microbiol **24:**220-225.
99. **Esko, J. D., A. Elgavish, T. Prasthofer, W. H. Taylor, and J. L. Weinke.** 1986. Sulfate transport-deficient mutants of Chinese hamster ovary cells. Sulfation of glycosaminoglycans dependent on cysteine. J Biol Chem **261:**15725-15733.
100. **Esko, J. D., T. E. Stewart, and W. H. Taylor.** 1985. Animal cell mutants defective in glycosaminoglycan biosynthesis. P Natl Acad Sci USA **82:**3197-3201.
101. **Fagan, R. P., M. A. Lambert, and S. G. Smith.** 2008. The *hek* outer membrane protein of *Escherichia coli* strain RS218 binds to proteoglycan and utilizes a single extracellular loop for adherence, invasion, and autoaggregation. Infect Immun **76:**1135-1142.

102. **Fagan, R. P., and S. G. Smith.** 2007. The Hek outer membrane protein of *Escherichia coli* is an auto-aggregating adhesin and invasin. FEMS Microbiol Lett.
103. **Fagan, R. P., and S. G. Smith.** 2007. The Hek outer membrane protein of Escherichia coli is an auto-aggregating adhesin and invasin.FEMS Microbiol Lett **269:**248-255.
104. **Fang, F. C., S. J. Libby, N. A. Buchmeier, P. C. Loewen, J. Switala, J. Harwood, and D. G. Guiney.** 1992. The alternative sigma factor *katF* (rpoS) regulates *Salmonella* virulence. P Natl Acad Sci USA **89:**11978-11982.
105. **Feldman, M. F., and G. R. Cornelis.** 2003. The multitalented type III chaperones: all you can do with 15 kDa. FEMS Microbiol Lett **219:**151-158.
106. **Fields, P. I., R. V. Swanson, C. G. Haidaris, and F. Heffron.** 1986. Mutants of *Salmonella typhimurium* that cannot survive within the macrophage are avirulent. P Natl Acad Sci USA **83:**5189-5193.
107. **Fierer, J., and D. G. Guiney.** 2001. Diverse virulence traits underlying different clinical outcomes of *Salmonella* infection. J Clin Invest **107:**775-780.
108. **Fink, S. L., and B. T. Cookson.** 2007. Pyroptosis and host cell death responses during Salmonella infection. Cell Microbiol **9:**2562-2570.
109. **Fire, A., S. Xu, M. K. Montgomery, S. A. Kostas, S. E. Driver, and C. C. Mello.** 1998. Potent and specific genetic interference by double-stranded RNA in Caenorhabditis elegans. Nature **391:**806-811.
110. **Fleckenstein, J. M., J. T. Holland, and D. L. Hasty.** 2002. Interaction of an outer membrane protein of enterotoxigenic *Escherichia coli* with cell surface heparan sulfate proteoglycans. Infect Immun **70:**1530-1537.
111. **Fleckenstein, J. M., J. T. Holland, and D. L. Hasty.** 2002. Interaction of an uuter membrane protein of enterotoxigenic *Escherichia coli* with cell surface heparan sulfate proteoglycans. Infect Immun **70:**1530-1537.
112. **Fleckenstein, J. M., D. J. Kopecko, R. L. Warren, and E. A. Elsinghorst.** 1996. Molecular characterization of the *tia* invasion locus from enterotoxigenic *Escherichia coli*. Infect Immun **64:**2256-2265.
113. **Folkesson, A., A. Advani, S. Sukupolvi, J. D. Pfeifer, S. Normark, and S. Lofdahl.** 1999. Multiple insertions of fimbrial operons correlate with the evolution of Salmonella serovars responsible for human disease. Mol Microbiol **33:**612-622.
114. **Folkesson, A., S. Lofdahl, and S. Normark.** 2002. The *Salmonella enterica* subspecies I specific centisome 7 genomic island encodes novel protein families present in bacteria living in close contact with eukaryotic cells. Res Microbiol **153:**537-545.

115. **Fratti, R. A., J. M. Backer, J. Gruenberg, S. Corvera, and V. Deretic.** 2001. Role of phosphatidylinositol 3-kinase and Rab5 effectors in phagosomal biogenesis and mycobacterial phagosome maturation arrest. J Cell Biol **154:**631-644.
116. **Friebel, A., H. Ilchmann, M. Aepfelbacher, K. Ehrbar, W. Machleidt, and W. D. Hardt.** 2001. SopE and SopE2 from Salmonella typhimurium activate different sets of RhoGTPases of the host cell. J Biol Chem **276:**34035-34040.
117. **Friedrich, M. J., N. E. Kinsey, J. Vila, and R. J. Kadner.** 1993. Nucleotide sequence of a 13.9 kb segment of the 90 kb virulence plasmid of *Salmonella typhimurium*: the presence of fimbrial biosynthetic genes. Mol Microbiol **8:**543-558.
118. **Fu, Y., and J. E. Galan.** 1998. Identification of a specific chaperone for SptP, a substrate of the centisome 63 type III secretion system of *Salmonella typhimurium*. J Bacteriol **180:**3393-3399.
119. **Fu, Y., and J. E. Galan.** 1999. A *salmonella* protein antagonizes Rac-1 and Cdc42 to mediate host-cell recovery after bacterial invasion. Nature **401:**293-297.
120. **Fu, Y., and J. E. Galan.** 1998. The *Salmonella typhimurium* tyrosine phosphatase SptP is translocated into host cells and disrupts the actin cytoskeleton. Mol Microbiol **27:**359-368.
121. **Galan, J. E., and R. Curtiss, 3rd.** 1989. Cloning and molecular characterization of genes whose products allow *Salmonella typhimurium* to penetrate tissue culture cells. P Natl Acad Sci USA **86:**6383-6387.
122. **Galan, J. E., and H. Wolf-Watz.** 2006. Protein delivery into eukaryotic cells by type III secretion machines. Nature **444:**567-573.
123. **Galyov, E. E., M. W. Wood, R. Rosqvist, P. B. Mullan, P. R. Watson, S. Hedges, and T. S. Wallis.** 1997. A secreted effector protein of *Salmonella dublin* is translocated into eukaryotic cells and mediates inflammation and fluid secretion in infected ileal mucosa. Mol Microbiol **25:**903-912.
124. **Garcia-del Portillo, F., and B. B. Finlay.** 1995. Targeting of *Salmonella typhimurium* to vesicles containing lysosomal membrane glycoproteins bypasses compartments with mannose 6-phosphate receptors. J Cell Biol **129:**81-97.
125. **Garmendia, J., C. R. Beuzon, J. Ruiz-Albert, and D. W. Holden.** 2003. The roles of SsrA-SsrB and OmpR-EnvZ in the regulation of genes encoding the *Salmonella typhimurium* SPI-2 type III secretion system. Microbiology **149:**2385-2396.
126. **Garvis, S. G., C. R. Beuzon, and D. W. Holden.** 2001. A role for the PhoP/Q regulon in inhibition of fusion between lysosomes and *Salmonella*-containing vacuoles in macrophages. Cell Microbiol **3:**731-744.

127. **Gerlach, R. G., N. Claudio, M. Rohde, D. Jackel, C. Wagner, and M. Hensel.** 2008. Cooperation of *Salmonella* pathogenicity islands 1 and 4 is required to breach epithelial barriers. Cell Microbiol **10:**2364-2376.
128. **Gerlach, R. G., D. Jackel, B. Stecher, C. Wagner, A. Lupas, W. D. Hardt, and M. Hensel.** 2007. *Salmonella* Pathogenicity Island 4 encodes a giant non-fimbrial adhesin and the cognate type 1 secretion system. Cell Microbiol **9:**1834-1850.
129. **Ghosh, S., K. Chakraborty, T. Nagaraja, S. Basak, H. Koley, S. Dutta, U. Mitra, and S. Das.** 2011. An adhesion protein of Salmonella enterica serovar Typhi is required for pathogenesis and potential target for vaccine development. P Natl Acad Sci USA **108:**3348-3353.
130. **Gotting, C., J. Kuhn, and K. Kleesiek.** 2007. Human xylosyltransferases in health and disease. Cell Mol Life Sci **64:**1498-1517.
131. **Gotting, C., J. Kuhn, R. Zahn, T. Brinkmann, and K. Kleesiek.** 2000. Molecular cloning and expression of human UDP-d-Xylose:proteoglycan core protein beta-d-xylosyltransferase and its first isoform XT-II. J Mol Biol **304:**517-528.
132. **Gotting, C., S. Muller, M. Schottler, S. Schon, C. Prante, T. Brinkmann, J. Kuhn, and K. Kleesiek.** 2004. Analysis of the DXD motifs in human xylosyltransferase I required for enzyme activity. J Biol Chem **279:**42566-42573.
133. **Grkovic, S., M. H. Brown, and R. A. Skurray.** 2002. Regulation of bacterial drug export systems. Microbiol Mol Biol Rev **66:**671-701, table of contents.
134. **Groisman, E. A.** 1998. The ins and outs of virulence gene expression: Mg2+ as a regulatory signal. Bioessays **20:**96-101.
135. **Groisman, E. A.** 2001. The pleiotropic two-component regulatory system PhoP-PhoQ. J Bacteriol **183:**1835-1842.
136. **Groisman, E. A., E. Chiao, C. J. Lipps, and F. Heffron.** 1989. *Salmonella typhimurium phoP* virulence gene is a transcriptional regulator. P Natl Acad Sci USA **86:**7077-7081.
137. **Groisman, E. A., and C. Mouslim.** 2006. Sensing by bacterial regulatory systems in host and non-host environments. Nat Rev Microbiol **4:**705-709.
138. **Guiney, D. G.** 2005. The role of host cell death in *Salmonella* infections. Curr Top Microbiol **289:**131-150.
139. **Gulig, P. A.** 1990. Virulence plasmids of *Salmonella typhimurium* and other Salmonellae. Microb Pathogenesis **8:**3-11.
140. **Gulig, P. A., H. Danbara, D. G. Guiney, A. J. Lax, F. Norel, and M. Rhen.** 1993. Molecular analysis of *spv* virulence genes of the *Salmonella* virulence plasmids. Mol Microbiol **7:**825-830.
141. **Gulig, P. A., and T. J. Doyle.** 1993. The *Salmonella typhimurium* virulence plasmid increases the growth rate of salmonellae in mice. Infect Immun **61:**504-511.

142. **Hakansson, S., K. Schesser, C. Persson, E. E. Galyov, R. Rosqvist, F. Homble, and H. Wolf-Watz.** 1996. The YopB protein of *Yersinia pseudotuberculosis* is essential for the translocation of Yop effector proteins across the target cell plasma membrane and displays a contact-dependent membrane disrupting activity. EMBO J **15:**5812-5823.
143. **Hall, A.** 1998. Rho GTPases and the actin cytoskeleton. Science **279:**509-514.
144. **Haltia, T., and E. Freire.** 1995. Forces and factors that contribute to the structural stability of membrane proteins. Biochim Biophys Acta **1228:**1-27.
145. **Hammond, S. M., E. Bernstein, D. Beach, and G. J. Hannon.** 2000. An RNA-directed nuclease mediates post-transcriptional gene silencing in Drosophila cells. Nature **404:**293-296.
146. **Haneda, T., Y. Ishii, H. Shimizu, K. Ohshima, N. Iida, H. Danbara, and N. Okada.** 2012. *Salmonella* type III effector SpvC, a phosphothreonine lyase, contributes to reduction in inflammatory response during intestinal phase of infection. Cell Microbiol **14:**485-499.
147. **Hannah, J. H., F. D. Menozzi, G. Renauld, C. Locht, and M. J. Brennan.** 1994. Sulfated glycoconjugate receptors for the Bordetella pertussis adhesin filamentous hemagglutinin (FHA) and mapping of the heparin-binding domain on FHA. Infect Immun **62:**5010-5019.
148. **Hannon, G. J.** 2002. RNA interference. Nature **418:**244-251.
149. **Hara-Kaonga, B., and T. G. Pistole.** 2004. OmpD but not OmpC is involved in adherence of *Salmonella enterica* serovar Typhimurium to human cells. Can J Microbiol **50:**719-727.
150. **Hardt, W. D., L. M. Chen, K. E. Schuebel, X. R. Bustelo, and J. E. Galan.** 1998. *S. typhimurium* encodes an activator of Rho GTPases that induces membrane ruffling and nuclear responses in host cells. Cell **93:**815-826.
151. **Hardt, W. D., H. Urlaub, and J. E. Galan.** 1998. A substrate of the centisome 63 type III protein secretion system of *Salmonella typhimurium* is encoded by a cryptic bacteriophage. P Natl Acad Sci USA **95:**2574-2579.
152. **Harrison, R. E., C. Bucci, O. V. Vieira, T. A. Schroer, and S. Grinstein.** 2003. Phagosomes fuse with late endosomes and/or lysosomes by extension of membrane protrusions along microtubules: role of Rab7 and RILP. Mol Cell Biol **23:**6494-6506.
153. **Hashim, S., K. Mukherjee, M. Raje, S. K. Basu, and A. Mukhopadhyay.** 2000. Live *Salmonella* modulate expression of Rab proteins to persist in a specialized compartment and escape transport to lysosomes. J Biol Chem **275:**16281-16288.
154. **Hautefort, I., M. J. Proenca, and J. C. Hinton.** 2003. Single-copy green fluorescent protein gene fusions allow accurate

measurement of *Salmonella* gene expression in vitro and during infection of mammalian cells. Appl Environ Microb **69:**7480-7491.

155. **Hayward, R. D., and V. Koronakis.** 1999. Direct nucleation and bundling of actin by the SipC protein of invasive *Salmonella*. Embo J **18:**4926-4934.
156. **Heffernan, E. J., J. Harwood, J. Fierer, and D. Guiney.** 1992. The *Salmonella typhimurium* virulence plasmid complement resistance gene *rck* is homologous to a family of virulence-related outer membrane protein genes, including *pagC* and *ail*. J Bacteriol **174:**84-91.
157. **Heffernan, E. J., S. Reed, J. Hackett, J. Fierer, C. Roudier, and D. Guiney.** 1992. Mechanism of resistance to complement-mediated killing of bacteria encoded by the *Salmonella typhimurium* virulence plasmid gene *rck*. J Clin Invest **90:**953-964.
158. **Heffernan, E. J., L. Wu, J. Louie, S. Okamoto, J. Fierer, and D. G. Guiney.** 1994. Specificity of the complement resistance and cell association phenotypes encoded by the outer membrane protein genes *rck* from *Salmonella typhimurium* and *ail* from *Yersinia enterocolitica*. Infect Immun **62:**5183-5186.
159. **Heffernan, L. F., and J. C. Simpson.** 2014. The trials and tubule-ations of Rab6 involvement in Golgi-to-ER retrograde transport. Biochem Soc T **42:**1453-1459.
160. **Heithoff, D. M., C. P. Conner, P. C. Hanna, S. M. Julio, U. Hentschel, and M. J. Mahan.** 1997. Bacterial infection as assessed by *in vivo* gene expression. P Natl Acad Sci USA **94:**934-939.
161. **Heithoff, D. M., C. P. Conner, U. Hentschel, F. Govantes, P. C. Hanna, and M. J. Mahan.** 1999. Coordinate intracellular expression of *Salmonella* genes induced during infection. J Bacteriol **181:**799-807.
162. **Heithoff, D. M., C. P. Conner, and M. J. Mahan.** 1997. Dissecting the biology of a pathogen during infection. Trends Microbiol **5:**509-513.
163. **Henry-Stanley, M., D. J. Hess, E. Erickson, R. M. Garni, and C. Wells.** 2003. Role of heparan sulfate in interactions of Listeria monocytogenes with enterocytes. Med Microbiol Immun **192:**107-115.
164. **Hensel, M.** 2000. *Salmonella* pathogenicity island 2. Mol Microbiol **36:**1015-1023.
165. **Hensel, M., A. P. Hinsley, T. Nikolaus, G. Sawers, and B. C. Berks.** 1999. The genetic basis of tetrathionate respiration in *Salmonella typhimurium*. Mol Microbiol **32:**275-287.
166. **Hensel, M., T. Nikolaus, and C. Egelseer.** 1999. Molecular and functional analysis indicates a mosaic structure of *Salmonella* pathogenicity island 2. Mol Microbiol **31:**489-498.

167. **Hensel, M., J. E. Shea, C. Gleeson, M. D. Jones, E. Dalton, and D. W. Holden.** 1995. Simultaneous identification of bacterial virulence genes by negative selection. Science **269:**400-403.
168. **Hensel, M., J. E. Shea, B. Raupach, D. Monack, S. Falkow, C. Gleeson, T. Kubo, and D. W. Holden.** 1997. Functional analysis of *ssaJ* and the *ssaK/U* operon, 13 genes encoding components of the type III secretion apparatus of *Salmonella* Pathogenicity Island 2. Mol Microbiol **24:**155-167.
169. **Hernandez, L. D., M. Pypaert, R. A. Flavell, and J. E. Galan.** 2003. A *Salmonella* protein causes macrophage cell death by inducing autophagy. J Cell Biol **163:**1123-1131.
170. **Hersh, D., D. M. Monack, M. R. Smith, N. Ghori, S. Falkow, and A. Zychlinsky.** 1999. The *Salmonella* invasin SipB induces macrophage apoptosis by binding to caspase-1. P Natl Acad Sci USA **96:**2396-2401.
171. **Higashide, W., and D. Zhou.** 2006. The first 45 amino acids of SopA are necessary for InvB binding and SPI-1 secretion. J Bacteriol **188:**2411-2420.
172. **Hisert, K. B., M. MacCoss, M. U. Shiloh, K. H. Darwin, S. Singh, R. A. Jones, S. Ehrt, Z. Zhang, B. L. Gaffney, S. Gandotra, D. W. Holden, D. Murray, and C. Nathan.** 2005. A glutamate-alanine-leucine (EAL) domain protein of *Salmonella* controls bacterial survival in mice, antioxidant defence and killing of macrophages: role of cyclic diGMP. Mol Microbiol **56:**1234-1245.
173. **Hohmann, E. L.** 2001. Nontyphoidal salmonellosis. Clin Infect Dis **32:**263-269.
174. **Hoiczyk, E., and G. Blobel.** 2001. Polymerization of a single protein of the pathogen *Yersinia enterocolitica* into needles punctures eukaryotic cells. P Natl Acad Sci USA **98:**4669-4674.
175. **Hong, K. H., and V. L. Miller.** 1998. Identification of a novel *Salmonella* invasion locus homologous to *Shigella* ipgDE. J Bacteriol **180:**1793-1802.
176. **Hsu, L. C., J. M. Park, K. Zhang, J. L. Luo, S. Maeda, R. J. Kaufman, L. Eckmann, D. G. Guiney, and M. Karin.** 2004. The protein kinase PKR is required for macrophage apoptosis after activation of Toll-like receptor 4. Nature **428:**341-345.
177. **Hueck, C. J.** 1998. Type III protein secretion systems in bacterial pathogens of animals and plants. Microbiol Mol Biol Rev **62:**379-433.
178. **Hueffer, K., and J. E. Galan.** 2004. *Salmonella*-induced macrophage death: multiple mechanisms, different outcomes. Cell Microbiol **6:**1019-1025.
179. **Isberg, R. R., and S. Falkow.** 1985. A single genetic locus encoded by *Yersinia pseudotuberculosis* permits invasion of cultured animal cells by *Escherichia coli* K-12. Nature **317:**262-264.

180. **Jones, B. D., N. Ghori, and S. Falkow.** 1994. *Salmonella typhimurium* initiates murine infection by penetrating and destroying the specialized epithelial M cells of the Peyer's patches. The J Exp Med **180:**15-23.
181. **Jones, G. W., D. K. Rabert, D. M. Svinarich, and H. J. Whitfield.** 1982. Association of adhesive, invasive, and virulent phenotypes of *Salmonella typhimurium* with autonomous 60-megadalton plasmids. Infect Immun **38:**476-486.
182. **Jost, M., F. Simpson, J. M. Kavran, M. A. Lemmon, and S. L. Schmid.** 1998. Phosphatidylinositol-4,5-bisphosphate is required for endocytic coated vesicle formation. Curr Biol **8:**1399-1402.
183. **Kamio, Y., and H. Nikaido.** 1977. Outer membrane of *Salmonella typhimurium*. Identification of proteins exposed on cell surface. Biochim Biophys Acta **464:**589-601.
184. **Kaniga, K., D. Trollinger, and J. E. Galan.** 1995. Identification of two targets of the type III protein secretion system encoded by the *inv* and *spa* loci of *Salmonella typhimurium* that have homology to the Shigella IpaD and IpaA proteins. J Bacteriol **177:**7078-7085.
185. **Kaniga, K., J. Uralil, J. B. Bliska, and J. E. Galan.** 1996. A secreted protein tyrosine phosphatase with modular effector domains in the bacterial pathogen *Salmonella typhimurium*. Mol Microbiol **21:**633-641.
186. **Kelley, L. A., S. Mezulis, C. M. Yates, M. N. Wass, and M. J. Sternberg.** 2015. The Phyre2 web portal for protein modeling, prediction and analysis. Nature protocols **10:**845-858.
187. **Kim, W., and M. G. Surette.** 2006. Coordinated regulation of two independent cell-cell signaling systems and swarmer differentiation in *Salmonella enterica* serovar Typhimurium. J Bacteriol **188:**431-440.
188. **Klumpp, J., and T. M. Fuchs.** 2007. Identification of novel genes in genomic islands that contribute to *Salmonella typhimurium* replication in macrophages. Microbiology **153:**1207-1220.
189. **Knodler, L. A., J. Celli, W. D. Hardt, B. A. Vallance, C. Yip, and B. B. Finlay.** 2002. *Salmonella* effectors within a single pathogenicity island are differentially expressed and translocated by separate type III secretion systems. Mol Microbiol **43:**1089-1103.
190. **Knodler, L. A., B. B. Finlay, and O. Steele-Mortimer.** 2005. The *Salmonella* effector protein SopB protects epithelial cells from apoptosis by sustained activation of Akt. J Biol Chem **280:**9058-9064.
191. **Koda, J. E., and M. Bernfield.** 1984. Heparan sulfate proteoglycans from mouse mammary epithelial cells. Basal extracellular proteoglycan binds specifically to native type I collagen fibrils. J Biol Chem **259:**11763-11770.

192. **Koebnik, R., K. P. Locher, and P. Van Gelder.** 2000. Structure and function of bacterial outer membrane proteins: barrels in a nutshell. Mol Microbiol **37:**239-253.
193. **Kox, L. F., M. M. Wosten, and E. A. Groisman.** 2000. A small protein that mediates the activation of a two-component system by another two-component system. Embo J **19:**1861-1872.
194. **Kroger, C., A. Colgan, S. Srikumar, K. Handler, S. K. Sivasankaran, D. L. Hammarlof, R. Canals, J. E. Grissom, T. Conway, K. Hokamp, and J. C. Hinton.** 2013. An infection-relevant transcriptomic compendium for *Salmonella enterica* serovar Typhimurium. Cell Host Microbe **14:**683-695.
195. **Kubori, T., and J. E. Galan.** 2003. Temporal regulation of *Salmonella* virulence effector function by proteasome-dependent protein degradation. Cell **115:**333-342.
196. **Kubori, T., Y. Matsushima, D. Nakamura, J. Uralil, M. Lara-Tejero, A. Sukhan, J. E. Galan, and S. I. Aizawa.** 1998. Supramolecular structure of the Salmonella typhimurium type III protein secretion system. Science **280:**602-605.
197. **Kubori, T., A. Sukhan, S. I. Aizawa, and J. E. Galan.** 2000. Molecular characterization and assembly of the needle complex of the *Salmonella typhimurium* type III protein secretion system. P Natl Acad Sci USA **97:**10225-10230.
198. **Kuhle, V., and M. Hensel.** 2004. Cellular microbiology of intracellular *Salmonella enterica*: functions of the type III secretion system encoded by *Salmonella* pathogenicity island 2. Cell Mol Life Sci **61:**2812-2826.
199. **Kuhn, J., C. Gotting, M. Schnolzer, T. Kempf, T. Brinkmann, and K. Kleesiek.** 2001. First isolation of human UDP-D-xylose: proteoglycan core protein beta-D-xylosyltransferase secreted from cultured JAR choriocarcinoma cells. J Biol Chem **276:**4940-4947.
200. **Kukkonen, M., T. Raunio, R. Virkola, K. Lahteenmaki, P. H. Makela, P. Klemm, S. Clegg, and T. K. Korhonen.** 1993. Basement membrane carbohydrate as a target for bacterial adhesion: binding of type I fimbriae of Salmonella enterica and *Escherichia coli* to laminin. Mol Microbiol **7:**229-237.
201. **Kurita, A., H. Gotoh, M. Eguchi, N. Okada, S. Matsuura, H. Matsui, H. Danbara, and Y. Kikuchi.** 2003. Intracellular expression of the *Salmonella* plasmid virulence protein, SpvB, causes apoptotic cell death in eukaryotic cells. Microb Pathogenesis **35:**43-48.
202. **Laemmli, U. K.** 1970. Cleavage of structural proteins during the assembly of the head of bacteriophage T4. Nature **227:**680-685.
203. **Lambert, M. A.** 2006. Molecular Characterisation of the *Salmonella*-specific protein PagN. Trinity College, Dublin.

204. **Lambert, M. A., and S. G. Smith.** 2009. The PagN protein mediates invasion via interaction with proteoglycan.FEMS Microbiol Lett **297:**209-216.
205. **Lambert, M. A., and S. G. Smith.** 2008. The PagN protein of *Salmonella enterica* serovar Typhimurium is an adhesin and invasin. BMC Microbiol **8:**142.
206. **Lan, R., P. R. Reeves, and S. Octavia.** 2009. Population structure, origins and evolution of major *Salmonella* enterica clones. Infect Genet Evol : journal of molecular epidemiology and evolutionary genetics in infectious diseases **9:**996-1005.
207. **Lara-Tejero, M., and J. E. Galan.** 2009. *Salmonella enterica* serovar typhimurium pathogenicity island 1-encoded type III secretion system translocases mediate intimate attachment to nonphagocytic cells. Infect Immun **77:**2635-2642.
208. **Latasa, C., A. Roux, A. Toledo-Arana, J. M. Ghigo, C. Gamazo, J. R. Penades, and I. Lasa.** 2005. BapA, a large secreted protein required for biofilm formation and host colonization of *Salmonella enterica* serovar Enteritidis. Mol Microbiol **58:**1322-1339.
209. **Lawley, T. D., K. Chan, L. J. Thompson, C. C. Kim, G. R. Govoni, and D. M. Monack.** 2006. Genome-wide screen for *Salmonella* genes required for long-term systemic infection of the mouse. PLoS Pathog **2:**e11.
210. **Lederer, T., M. Kintrup, M. Takahashi, P. E. Sum, G. A. Ellestad, and W. Hillen.** 1996. Tetracycline analogs affecting binding to Tn10-Encoded Tet repressor trigger the same mechanism of induction. Biochemistry **35:**7439-7446.
211. **Lee, A. K., C. S. Detweiler, and S. Falkow.** 2000. OmpR regulates the two-component system SsrA-ssrB in *Salmonella* pathogenicity island 2. J Bacteriol **182:**771-781.
212. **Lee, C. A., B. D. Jones, and S. Falkow.** 1992. Identification of a *Salmonella typhimurium* invasion locus by selection for hyperinvasive mutants. P Natl Acad Sci USA **89:**1847-1851.
213. **Lee, S. H., and J. E. Galan.** 2004. *Salmonella* type III secretion-associated chaperones confer secretion-pathway specificity. Mol Microbiol **51:**483-495.
214. **Lesnick, M. L., N. E. Reiner, J. Fierer, and D. G. Guiney.** 2001. The *Salmonella spvB* virulence gene encodes an enzyme that ADP-ribosylates actin and destabilizes the cytoskeleton of eukaryotic cells. Mol Microbiol **39:**1464-1470.
215. **Liang, O. D., F. Ascencio, L. A. Fransson, and T. Wadstrom.** 1992. Binding of heparan sulfate to *Staphylococcus aureus*. Infect Immun **60:**899-906.
216. **Lidholt, K., J. L. Weinke, C. S. Kiser, F. N. Lugemwa, K. J. Bame, S. Cheifetz, J. Massague, U. Lindahl, and J. D. Esko.** 1992. A single mutation affects both N-acetylglucosaminyltransferase and glucuronosyltransferase

activities in a Chinese hamster ovary cell mutant defective in heparan sulfate biosynthesis. P Natl Acad Sci USA **89:**2267-2271.

217. **Loetscher, Y., A. Wieser, J. Lengefeld, P. Kaiser, S. Schubert, M. Heikenwalder, W. D. Hardt, and B. Stecher.** 2012. *Salmonella* transiently reside in luminal neutrophils in the inflamed gut. PloS one **7:**e34812.
218. **Lopez-Garrido, J., and J. Casadesus.** 2012. Crosstalk between virulence loci: regulation of *Salmonella enterica* pathogenicity island 1 (SPI-1) by products of the *std* fimbrial operon. PloS one **7:**e30499.
219. **Lucas, R. L., C. P. Lostroh, C. C. DiRusso, M. P. Spector, B. L. Wanner, and C. A. Lee.** 2000. Multiple factors independently regulate *hilA* and invasion gene expression in *Salmonella enterica* serovar typhimurium. J Bacteriol **182:**1872-1882.
220. **Lutz, R., and H. Bujard.** 1997. Independent and tight regulation of transcriptional units in *Escherichia coli* via the LacR/O, the TetR/O and AraC/I1-I2 regulatory elements. Nucleic Acids Res **25:**1203-1210.
221. **Ma, D., D. N. Cook, M. Alberti, N. G. Pon, H. Nikaido, and J. E. Hearst.** 1995. Genes acrA and acrB encode a stress-induced efflux system of *Escherichia coli*. Mol Microbiol **16:**45-55.
222. **Maddocks, O. D., A. J. Short, M. S. Donnenberg, S. Bader, and D. J. Harrison.** 2009. Attaching and effacing *Escherichia coli* downregulate DNA mismatch repair protein in vitro and are associated with colorectal adenocarcinomas in humans. PloS one **4:**e5517.
223. **Main-Hester, K. L., K. M. Colpitts, G. A. Thomas, F. C. Fang, and S. J. Libby.** 2008. Coordinate regulation of *Salmonella* pathogenicity island 1 (SPI1) and SPI4 in *Salmonella enterica* serovar Typhimurium. Infect Immun **76:**1024-1035.
224. **Majowicz, S. E., J. Musto, E. Scallan, F. J. Angulo, M. Kirk, S. J. O'Brien, T. F. Jones, A. Fazil, R. M. Hoekstra, and S. International Collaboration on Enteric Disease 'Burden of Illness.** 2010. The global burden of nontyphoidal *Salmonella* gastroenteritis. Clin Infect Dis **50:**882-889.
225. **Mammarappallil, J. G., and E. A. Elsinghorst.** 2000. Epithelial cell adherence mediated by the enterotoxigenic *Escherichia coli* Tia protein. Infect Immun **68:**6595-6601.
226. **Mandel, M., and A. Higa.** 1970. Calcium-dependent bacteriophage DNA infection. J Mol Biol **53:**159-162.
227. **Mansson, L. E., K. Melican, J. Boekel, R. M. Sandoval, I. Hautefort, G. A. Tanner, B. A. Molitoris, and A. Richter-Dahlfors.** 2007. Real-time studies of the progression of bacterial infections and immediate tissue responses in live animals. Cell Microbiol **9:**413-424.

228. **Marcus, S. L., J. H. Brumell, C. G. Pfeifer, and B. B. Finlay.** 2000. *Salmonella* pathogenicity islands: big virulence in small packages. Microbes Infect **2:**145-156.
229. **Marlovits, T. C., T. Kubori, A. Sukhan, D. R. Thomas, J. E. Galan, and V. M. Unger.** 2004. Structural insights into the assembly of the type III secretion needle complex. Science **306:**1040-1042.
230. **Marshall, D. G., F. Bowe, C. Hale, G. Dougan, and C. J. Dorman.** 2000. DNA topology and adaptation of *Salmonella typhimurium* to an intracellular environment. Philos T Roy Soc B **355:**565-574.
231. **Marshall, D. G., B. J. Sheehan, and C. J. Dorman.** 1999. A role for the leucine-responsive regulatory protein and integration host factor in the regulation of the *Salmonella* plasmid virulence (spv) locus in *Salmonella typhimurium*. Mol Microbiol **34:**134-145.
232. **Martin-Orozco, N., N. Touret, M. L. Zaharik, E. Park, R. Kopelman, S. Miller, B. B. Finlay, P. Gros, and S. Grinstein.** 2006. Visualization of vacuolar acidification-induced transcription of genes of pathogens inside macrophages. Mol Biol Cell **17:**498-510.
233. **Martinez, J., A. Patkaniowska, H. Urlaub, R. Luhrmann, and T. Tuschl.** 2002. Single-stranded antisense siRNAs guide target RNA cleavage in RNAi. Cell **110:**563-574.
234. **Matsui, H., C. M. Bacot, W. A. Garlington, T. J. Doyle, S. Roberts, and P. A. Gulig.** 2001. Virulence plasmid-borne spvB and *spvC* genes can replace the 90-kilobase plasmid in conferring virulence to *Salmonella enterica* serovar Typhimurium in subcutaneously inoculated mice. J Bacteriol **183:**4652-4658.
235. **Mazurkiewicz, P., J. Thomas, J. A. Thompson, M. Liu, L. Arbibe, P. Sansonetti, and D. W. Holden.** 2008. SpvC is a *Salmonella* effector with phosphothreonine lyase activity on host mitogen-activated protein kinases. Mol Microbiol **67:**1371-1383.
236. **McClelland, M., K. E. Sanderson, J. Spieth, S. W. Clifton, P. Latreille, L. Courtney, S. Porwollik, J. Ali, M. Dante, F. Du, S. Hou, D. Layman, S. Leonard, C. Nguyen, K. Scott, A. Holmes, N. Grewal, E. Mulvaney, E. Ryan, H. Sun, L. Florea, W. Miller, T. Stoneking, M. Nhan, R. Waterston, and R. K. Wilson.** 2001. Complete genome sequence of *Salmonella enterica* serovar Typhimurium LT2. Nature **413:**852-856.
237. **McGhie, E. J., R. D. Hayward, and V. Koronakis.** 2004. Control of actin turnover by a *Salmonella* invasion protein. Mol Cell **13:**497-510.
238. **McGhie, E. J., R. D. Hayward, and V. Koronakis.** 2001. Cooperation between actin-binding proteins of invasive *Salmonella*: SipA potentiates SipC nucleation and bundling of actin. Embo J **20:**2131-2139.

239. **Mecsas, J., R. Welch, J. W. Erickson, and C. A. Gross.** 1995. Identification and characterization of an outer membrane protein, OmpX, in *Escherichia coli* that is homologous to a family of outer membrane proteins including Ail of *Yersinia enterocolitica*. J Bacteriol **177:**799-804.
240. **Meresse, S., O. Steele-Mortimer, B. B. Finlay, and J. P. Gorvel.** 1999. The rab7 GTPase controls the maturation of *Salmonella typhimurium*-containing vacuoles in HeLa cells. EMBO J **18:**4394-4403.
241. **Meyer, P. N., M. R. Wilmes-Riesenberg, C. Stathopoulos, and R. Curtiss, 3rd.** 1998. Virulence of a *Salmonella typhimurium* OmpD mutant. Infect Immun **66:**387-390.
242. **Miao, E. A., J. A. Freeman, and S. I. Miller.** 2002. Transcription of the SsrAB regulon is repressed by alkaline pH and is independent of PhoPQ and magnesium concentration. J Bacteriol **184:**1493-1497.
243. **Miller, S. I., A. M. Kukral, and J. J. Mekalanos.** 1989. A two-component regulatory system (*phoP phoQ*) controls *Salmonella typhimurium* virulence. P Natl Acad Sci USA **86:**5054-5058.
244. **Miller, V. L., J. B. Bliska, and S. Falkow.** 1990. Nucleotide sequence of the *Yersinia enterocolitica ail* gene and characterization of the Ail protein product. J Bacteriol **172:**1062-1069.
245. **Miller, V. L., and J. J. Mekalanos.** 1984. Synthesis of cholera toxin is positively regulated at the transcriptional level by toxR. P Natl Acad Sci USA **81:**3471-3475.
246. **Misselwitz, B., N. Barrett, S. Kreibich, P. Vonaesch, D. Andritschke, S. Rout, K. Weidner, M. Sormaz, P. Songhet, P. Horvath, M. Chabria, V. Vogel, D. M. Spori, P. Jenny, and W. D. Hardt.** 2012. Near surface swimming of *Salmonella* Typhimurium explains target-site selection and cooperative invasion. PLoS pathogens **8:**e1002810.
247. **Misselwitz, B., S. K. Kreibich, S. Rout, B. Stecher, B. Periaswamy, and W. D. Hardt.** 2011. *Salmonella enterica* serovar Typhimurium binds to HeLa cells via Fim-mediated reversible adhesion and irreversible type three secretion system 1-mediated docking. Infect Immun **79:**330-341.
248. **Monack, D. M., C. S. Detweiler, and S. Falkow.** 2001. *Salmonella* pathogenicity island 2-dependent macrophage death is mediated in part by the host cysteine protease caspase-1. Cell Microbiol **3:**825-837.
249. **Montagne, M., A. Martel, and H. Le Moual.** 2001. Characterization of the catalytic activities of the PhoQ histidine protein kinase of *Salmonella enterica* serovar Typhimurium. J Bacteriol **183:**1787-1791.
250. **Morgan, E., J. D. Campbell, S. C. Rowe, J. Bispham, M. P. Stevens, A. J. Bowen, P. A. Barrow, D. J. Maskell, and T. S.**

Wallis. 2004. Identification of host-specific colonization factors of *Salmonella enterica* serovar Typhimurium. Mol Microbiol **54:**994-1010.

251. **Muller, S., J. Disse, M. Schottler, S. Schon, C. Prante, T. Brinkmann, J. Kuhn, K. Kleesiek, and C. Gotting.** 2006. Human xylosyltransferase I and N-terminal truncated forms: functional characterization of the core enzyme. Biochem J **394:**163-171.
252. **Muller, S., M. Schottler, S. Schon, C. Prante, T. Brinkmann, J. Kuhn, C. Gotting, and K. Kleesiek.** 2005. Human xylosyltransferase I: functional and biochemical characterization of cysteine residues required for enzymic activity. Biochem J **386:**227-236.
253. **Murphy, C.** 2014. Structural and Functional Analysis of the Hek adhesin and invasin of *Escherichia coli*. Trinity College, Dublin.
254. **Napoli, C., C. Lemieux, and R. Jorgensen.** 1990. Introduction of a Chimeric Chalcone Synthase Gene into Petunia Results in Reversible Co-Suppression of Homologous Genes in trans. Plant cell **2:**279-289.
255. **Navarre, W. W., T. A. Halsey, D. Walthers, J. Frye, M. McClelland, J. L. Potter, L. J. Kenney, J. S. Gunn, F. C. Fang, and S. J. Libby.** 2005. Co-regulation of *Salmonella enterica* genes required for virulence and resistance to antimicrobial peptides by SlyA and PhoP/PhoQ. Mol Microbiol **56:**492-508.
256. **Neidhardt, F. C., P. L. Bloch, and D. F. Smith.** 1974. Culture medium for enterobacteria. J Bacteriol **119:**736-747.
257. **Nickerson, C. A., and R. Curtiss, 3rd.** 1997. Role of sigma factor RpoS in initial stages of *Salmonella typhimurium* infection. Infect Immun **65:**1814-1823.
258. **Norte, V. A., M. R. Stapleton, and J. Green.** 2003. PhoP-responsive expression of the *Salmonella enterica* serovar Typhimurium *slyA* gene. J Bacteriol **185:**3508-3514.
259. **Nunez-Hernandez, C., A. Tierrez, A. D. Ortega, M. G. Pucciarelli, M. Godoy, B. Eisman, J. Casadesus, and F. Garcia-del Portillo.** 2013. Genome expression analysis of nonproliferating intracellular *Salmonella enterica* serovar Typhimurium unravels an acid pH-dependent PhoP-PhoQ response essential for dormancy. Infect Immun **81:**154-165.
260. **Nykanen, A., B. Haley, and P. D. Zamore.** 2001. ATP requirements and small interfering RNA structure in the RNA interference pathway. Cell **107:**309-321.
261. **O'Byrne, C. P., and C. J. Dorman.** 1994. The spv virulence operon of *Salmonella typhimurium* LT2 is regulated negatively by the cyclic AMP (cAMP)-cAMP receptor protein system. J Bacteriol **176:**905-912.
262. **O'Byrne, C. P., and C. J. Dorman.** 1994. Transcription of the *Salmonella typhimurium* spv virulence locus is regulated

negatively by the nucleoid-associated protein H-NS.FEMS Microbiol Lett **121:**99-105.

263. **Ochman, H., F. C. Soncini, F. Solomon, and E. A. Groisman.** 1996. Identification of a pathogenicity island required for *Salmonella* survival in host cells. P Natl Acad Sci USA **93:**7800-7804.
264. **Ohl, M. E., and S. I. Miller.** 2001. *Salmonella*: a model for bacterial pathogenesis. Annu Rev Med **52:**259-274.
265. **Okada, N., Y. Oi, M. Takeda-Shitaka, K. Kanou, H. Umeyama, T. Haneda, T. Miki, S. Hosoya, and H. Danbara.** 2007. Identification of amino acid residues of *Salmonella* SlyA that are critical for transcriptional regulation. Microbiology **153:**548-560.
266. **Paddison, P. J., A. A. Caudy, and G. J. Hannon.** 2002. Stable suppression of gene expression by RNAi in mammalian cells. P Natl Acad Sci USA **99:**1443-1448.
267. **Parkhill, J., G. Dougan, K. D. James, N. R. Thomson, D. Pickard, J. Wain, C. Churcher, K. L. Mungall, S. D. Bentley, M. T. Holden, M. Sebaihia, S. Baker, D. Basham, K. Brooks, T. Chillingworth, P. Connerton, A. Cronin, P. Davis, R. M. Davies, L. Dowd, N. White, J. Farrar, T. Feltwell, N. Hamlin, A. Haque, T. T. Hien, S. Holroyd, K. Jagels, A. Krogh, T. S. Larsen, S. Leather, S. Moule, P. O'Gaora, C. Parry, M. Quail, K. Rutherford, M. Simmonds, J. Skelton, K. Stevens, S. Whitehead, and B. G. Barrell.** 2001. Complete genome sequence of a multiple drug resistant *Salmonella enterica* serovar Typhi CT18. Nature **413:**848-852.
268. **Parry, C. M., T. T. Hien, G. Dougan, N. J. White, and J. J. Farrar.** 2002. Typhoid fever. New Engl J Med **347:**1770-1782.
269. **Patel, J. C., and J. E. Galan.** 2006. Differential activation and function of Rho GTPases during *Salmonella*-host cell interactions. J Cell Biol **175:**453-463.
270. **Patel, M., M. Yanagishita, G. Roderiquez, D. C. Bou-Habib, T. Oravecz, V. C. Hascall, and M. A. Norcross.** 1993. Cell-surface heparan sulfate proteoglycan mediates HIV-1 infection of T-cell lines. AIDS Res Hum Retrov **9:**167-174.
271. **Pattni, K., M. Jepson, H. Stenmark, and G. Banting.** 2001. A PtdIns(3)P-specific probe cycles on and off host cell membranes during *Salmonella* invasion of mammalian cells. Curr Biol **11:**1636-1642.
272. **Peters, J. E., T. E. Thate, and N. L. Craig.** 2003. Definition of the *Escherichia coli* MC4100 genome by use of a DNA array. J Bact **185:**2017-2021.
273. **Pettersson, J., R. Nordfelth, E. Dubinina, T. Bergman, M. Gustafsson, K. E. Magnusson, and H. Wolf-Watz.** 1996. Modulation of virulence factor expression by pathogen target cell contact. Science **273:**1231-1233.

274. **Ponighaus, C., M. Ambrosius, J. C. Casanova, C. Prante, J. Kuhn, J. D. Esko, K. Kleesiek, and C. Gotting.** 2007. Human xylosyltransferase II is involved in the biosynthesis of the uniform tetrasaccharide linkage region in chondroitin sulfate and heparan sulfate proteoglycans. J Biol Chem **282:**5201-5206.
275. **Porwollik, S., and M. McClelland.** 2003. Lateral gene transfer in *Salmonella*. Microbes Infect **5:**977-989.
276. **Prince, S. M., C. Feron, D. Janssens, Y. Lobet, M. Achtman, B. Kusecek, P. A. Bullough, and J. P. Derrick.** 2001. Expression, refolding and crystallization of the OpcA invasin from *Neisseria meningitidis*. Acta Crystallogr D **57:**1164-1166.
277. **Prost, L. R., M. E. Daley, V. Le Sage, M. W. Bader, H. Le Moual, R. E. Klevit, and S. I. Miller.** 2007. Activation of the bacterial sensor kinase PhoQ by acidic pH. Mol Cell **26:**165-174.
278. **Raffatellu, M., R. P. Wilson, D. Chessa, H. Andrews-Polymenis, Q. T. Tran, S. Lawhon, S. Khare, L. G. Adams, and A. J. Baumler.** 2005. SipA, SopA, SopB, SopD, and SopE2 contribute to *Salmonella enterica* serotype Typhimurium invasion of epithelial cells. Infect Immun **73:**146-154.
279. **Raiborg, C., K. G. Bache, D. J. Gillooly, I. H. Madshus, E. Stang, and H. Stenmark.** 2002. Hrs sorts ubiquitinated proteins into clathrin-coated microdomains of early endosomes. Nat Cell Biol **4:**394-398.
280. **Raiborg, C., and H. Stenmark.** 2002. Hrs and endocytic sorting of ubiquitinated membrane proteins. Cell Struct Funct **27:**403-408.
281. **Rajashekar, R., D. Liebl, A. Seitz, and M. Hensel.** 2008. Dynamic remodeling of the endosomal system during formation of *Salmonella*-induced filaments by intracellular *Salmonella enterica*. Traffic **9:**2100-2116.
282. **Rang, C., J. E. Galen, J. B. Kaper, and L. Chao.** 2003. Fitness cost of the green fluorescent protein in gastrointestinal bacteria. Can J Microbiol **49:**531-537.
283. **Rapraeger, A. C., and M. Bernfield.** 1983. Heparan sulfate proteoglycans from mouse mammary epithelial cells. A putative membrane proteoglycan associates quantitatively with lipid vesicles. J Biol Chem **258:**3632-3636.
284. **Rathman, M., M. D. Sjaastad, and S. Falkow.** 1996. Acidification of phagosomes containing *Salmonella typhimurium* in murine macrophages. Infect Immun **64:**2765-2773.
285. **Rhen, M., P. Riikonen, and S. Taira.** 1993. Transcriptional regulation of *Salmonella enterica* virulence plasmid genes in cultured macrophages. Mol Microbiol **10:**45-56.
286. **Roberts, R. L., M. A. Barbieri, J. Ullrich, and P. D. Stahl.** 2000. Dynamics of rab5 activation in endocytosis and phagocytosis. J Leukoc Biol **68:**627-632.

287. **Rosenbusch, J. P.** 1999. Folding patterns of membrane proteins: diversity and the limitations of their prediction. Novartis Foundation symposium **225:**207-213; discussion 213-204.
288. **Rostand, K. S., and J. D. Esko.** 1997. Microbial adherence to and invasion through proteoglycans. Infect Immun **65:**1-8.
289. **Rotger, R., and J. Casadesus.** 1999. The virulence plasmids of *Salmonella*. Int Microbiol **2:**177-184.
290. **Rudolph, M. G., C. Weise, S. Mirold, B. Hillenbrand, B. Bader, A. Wittinghofer, and W. D. Hardt.** 1999. Biochemical analysis of SopE from *Salmonella typhimurium*, a highly efficient guanosine nucleotide exchange factor for RhoGTPases. J Biol Chem **274:**30501-30509.
291. **Ruiz-Albert, J., R. Mundy, X. J. Yu, C. R. Beuzon, and D. W. Holden.** 2003. SseA is a chaperone for the SseB and SseD translocon components of the *Salmonella* pathogenicity-island-2-encoded type III secretion system. Microbiology **149:**1103-1111.
292. **Saaf, A., M. Hermansson, and G. von Heijne.** 2000. Formation of cytoplasmic turns between two closely spaced transmembrane helices during membrane protein integration into the ER membrane. J Mol Biol **301:**191-197.
293. **Saiki, R. K., D. H. Gelfand, S. Stoffel, S. J. Scharf, R. Higuchi, G. T. Horn, K. B. Mullis, and H. A. Erlich.** 1988. Primer-directed enzymatic amplification of DNA with a thermostable DNA polymerase. Science **239:**487-491.
294. **Salzman, N. H., M. M. Chou, H. de Jong, L. Liu, E. M. Porter, and Y. Paterson.** 2003. Enteric salmonella infection inhibits Paneth cell antimicrobial peptide expression. Infect Immun **71:**1109-1115.
295. **Salzman, N. H., D. Ghosh, K. M. Huttner, Y. Paterson, and C. L. Bevins.** 2003. Protection against enteric salmonellosis in transgenic mice expressing a human intestinal defensin. Nature **422:**522-526.
296. **Santiviago, C. A., C. S. Toro, A. A. Hidalgo, P. Youderian, and G. C. Mora.** 2003. Global regulation of the *Salmonella enterica* serovar Typhimurium major porin, OmpD. J Bacteriol **185:**5901-5905.
297. **Santos, R. L., R. M. Tsolis, A. J. Baumler, R. Smith, 3rd, and L. G. Adams.** 2001. *Salmonella enterica* serovar Typhimurium induces cell death in bovine monocyte-derived macrophages by early sipB-dependent and delayed sipB-independent mechanisms. Infect Immun **69:**2293-2301.
298. **Sarker, P., K. Swindells, C. W. Douglas, S. MacNeil, S. Rimmer, and L. Swanson.** 2014. Forster resonance energy transfer confirms the bacterial-induced conformational transition in highly-branched poly(N-isopropyl acrylamide with vancomycin end groups on binding to *Staphylococcus aureus*. Soft matter **10:**5824-5835.

299. **Saunders, S., and M. Bernfield.** 1988. Cell surface proteoglycan binds mouse mammary epithelial cells to fibronectin and behaves as a receptor for interstitial matrix. J Cell Biol **106:**423-430.
300. **Saunders, S., M. Jalkanen, S. O'Farrell, and M. Bernfield.** 1989. Molecular cloning of syndecan, an integral membrane proteoglycan. J Cell Biol **108:**1547-1556.
301. **Scallan, E., R. M. Hoekstra, F. J. Angulo, R. V. Tauxe, M. A. Widdowson, S. L. Roy, J. L. Jones, and P. M. Griffin.** 2011. Foodborne illness acquired in the United States--major pathogens. Emerg Infect Dis **17:**7-15.
302. **Schauber, J., R. A. Dorschner, K. Yamasaki, B. Brouha, and R. L. Gallo.** 2006. Control of the innate epithelial antimicrobial response is cell-type specific and dependent on relevant microenvironmental stimuli. Immunology **118:**509-519.
303. **Schechter, L. M., S. M. Damrauer, and C. A. Lee.** 1999. Two AraC/XylS family members can independently counteract the effect of repressing sequences upstream of the *hilA* promoter. Mol Microbiol **32:**629-642.
304. **Scherer, C. A., E. Cooper, and S. I. Miller.** 2000. The *Salmonella* type III secretion translocon protein SspC is inserted into the epithelial cell plasma membrane upon infection. Mol Microbiol **37:**1133-1145.
305. **Schesser, K., E. Frithz-Lindsten, and H. Wolf-Watz.** 1996. Delineation and mutational analysis of the *Yersinia pseudotuberculosis* YopE domains which mediate translocation across bacterial and eukaryotic cellular membranes. J Bacteriol **178:**7227-7233.
306. **Shea, J. E., M. Hensel, C. Gleeson, and D. W. Holden.** 1996. Identification of a virulence locus encoding a second type III secretion system in *Salmonella typhimurium*. P Natl Acad Sci USA **93:**2593-2597.
307. **Shi, J., G. Scita, and J. E. Casanova.** 2005. WAVE2 signaling mediates invasion of polarized epithelial cells by *Salmonella typhimurium*. J Biol Chem **280:**29849-29855.
308. **Shi, Y., T. Latifi, M. J. Cromie, and E. A. Groisman.** 2004. Transcriptional control of the antimicrobial peptide resistance ugtL gene by the *Salmonella* PhoP and SlyA regulatory proteins. J Biol Chem **279:**38618-38625.
309. **Shulz, G. E.** 2000. b-Barrel membrane proteins. Curr Opin Struc Biol **10:**443-447.
310. **Singh SP, Miller S, Williams YU, Rudd KE, and N. H.** 1996. Immunochemical structure of the OmpD porin from *Salmonella typhimurium*. Microbiology **142:**3201-3210.
311. **Singh, S. P., Y. Upshaw, T. Abdullah, S. R. Singh, and P. E. Klebba.** 1992. Structural relatedness of enteric bacterial porins assessed with monoclonal antibodies to *Salmonella typhimurium* OmpD and OmpC. J Bacteriol **174:**1965-1973.

312. **Smith, A. C., J. T. Cirulis, J. E. Casanova, M. A. Scidmore, and J. H. Brumell.** 2005. Interaction of the Salmonella-containing vacuole with the endocytic recycling system. J Biol Chem **280:**24634-24641.
313. **Snavely, M. D., S. A. Gravina, T. T. Cheung, C. G. Miller, and M. E. Maguire.** 1991. Magnesium transport in *Salmonella typhimurium*. Regulation of mgtA and mgtB expression. J Biol Chem **266:**824-829.
314. **Snavely, M. D., C. G. Miller, and M. E. Maguire.** 1991. The *mgtB* Mg2+ transport locus of *Salmonella typhimurium* encodes a P-type ATPase. J Biol Chem **266:**815-823.
315. **Solano, C., B. Garcia, J. Valle, C. Berasain, J. M. Ghigo, C. Gamazo, and I. Lasa.** 2002. Genetic analysis of *Salmonella enteritidis* biofilm formation: critical role of cellulose. Mol Microbiol **43:**793-808.
316. **Soncini, F. C., E. G. Vescovi, and E. A. Groisman.** 1995. Transcriptional autoregulation of the *Salmonella typhimurium* phoPQ operon. J Bacteriol **177:**4364-4371.
317. **Sorg, J. A., N. C. Miller, and O. Schneewind.** 2005. Substrate recognition of type III secretion machines--testing the RNA signal hypothesis. Cell Microbiol **7:**1217-1225.
318. **Sory, M. P., A. Boland, I. Lambermont, and G. R. Cornelis.** 1995. Identification of the YopE and YopH domains required for secretion and internalization into the cytosol of macrophages, using the *cyaA* gene fusion approach. P Natl Acad Sci USA **92:**11998-12002.
319. **Spoering, A. L., and K. Lewis.** 2001. Biofilms and planktonic cells of *Pseudomonas aeruginosa* have similar resistance to killing by antimicrobials. J Bacteriol **183:**6746-6751.
320. **Stanier, R. Y., J. L. Ingraham, M. L. Wheelis, and P. R. Painter.** 1987. The enteric group and related eubacteria, Fifth ed, vol. 19. Macmillan Education.
321. **Stebbins, C. E., and J. E. Galan.** 2001. Structural mimicry in bacterial virulence. Nature **412:**701-705.
322. **Steele-Mortimer, O., S. Meresse, J. P. Gorvel, B. H. Toh, and B. B. Finlay.** 1999. Biogenesis of *Salmonella typhimurium*-containing vacuoles in epithelial cells involves interactions with the early endocytic pathway. Cell Microbiol **1:**33-49.
323. **Steinberg, B. E., L. Glass, A. Shrier, and G. Bub.** 2006. The role of heterogeneities and intercellular coupling in wave propagation in cardiac tissue. Philos T Roy Soc A **364:**1299-1311.
324. **Steinberg, B. E., C. C. Scott, and S. Grinstein.** 2007. High-throughput assays of phagocytosis, phagosome maturation, and bacterial invasion. Am J Physiol Cell Ph **292:**C945-952.
325. **Stender, S., A. Friebel, S. Linder, M. Rohde, S. Mirold, and W. D. Hardt.** 2000. Identification of SopE2 from *Salmonella*

typhimurium, a conserved guanine nucleotide exchange factor for Cdc42 of the host cell. Mol Microbiol **36:**1206-1221.

326. **Stuart, B. M., and R. L. Pullen.** 1946. Typhoid; clinical analysis of 360 cases. Archives of internal medicine **78:**629-661.
327. **Tamm, L. K., H. Hong, and B. Liang.** 2004. Folding and assembly of beta-barrel membrane proteins. Biochim Biophys Acta **1666:**250-263.
328. **Tardy, F., F. Homble, C. Neyt, R. Wattiez, G. R. Cornelis, J. M. Ruysschaert, and V. Cabiaux.** 1999. *Yersinia enterocolitica* type III secretion-translocation system: channel formation by secreted Yops. Embo J **18:**6793-6799.
329. **Terebiznik, M. R., O. V. Vieira, S. L. Marcus, A. Slade, C. M. Yip, W. S. Trimble, T. Meyer, B. B. Finlay, and S. Grinstein.** 2002. Elimination of host cell PtdIns(4,5)P(2) by bacterial SigD promotes membrane fission during invasion by Salmonella. Nat Cell Biol **4:**766-773.
330. **Testerman, T. L., A. Vazquez-Torres, Y. Xu, J. Jones-Carson, S. J. Libby, and F. C. Fang.** 2002. The alternative sigma factor sigmaE controls antioxidant defences required for *Salmonella* virulence and stationary-phase survival. Mol Microbiol **43:**771-782.
331. **Tezcan-Merdol, D., T. Nyman, U. Lindberg, F. Haag, F. Koch-Nolte, and M. Rhen.** 2001. Actin is ADP-ribosylated by the *Salmonella enterica* virulence-associated protein SpvB. Mol Microbiol **39:**606-619.
332. **Thijs, I. M., S. C. De Keersmaecker, A. Fadda, K. Engelen, H. Zhao, M. McClelland, K. Marchal, and J. Vanderleyden.** 2007. Delineation of the *Salmonella enterica* serovar Typhimurium HilA regulon through genome-wide location and transcript analysis. J Bacteriol **189:**4587-4596.
333. **Tindall, B. J., P. A. Grimont, G. M. Garrity, and J. P. Euzeby.** 2005. Nomenclature and taxonomy of the genus *Salmonella*. Int J Syst Evol Micr **55:**521-524.
334. **Trask, O. J., D. Nickischer, A. Burton, R. G. Williams, R. A. Kandasamy, P. A. Johnston, and P. A. Johnston.** 2009. High-throughput automated confocal microscopy imaging screen of a kinase-focused library to identify p38 mitogen-activated protein kinase inhibitors using the GE InCell 3000 analyzer. Method Mol Cell Biol **565:**159-186.
335. **Tsolis, R. M., S. M. Townsend, E. A. Miao, S. I. Miller, T. A. Ficht, L. G. Adams, and A. J. Baumler.** 1999. Identification of a putative *Salmonella enterica* serotype typhimurium host range factor with homology to IpaH and YopM by signature-tagged mutagenesis. Infect Immun **67:**6385-6393.
336. **Tu, X., T. Latifi, A. Bougdour, S. Gottesman, and E. A. Groisman.** 2006. The PhoP/PhoQ two-component system

stabilizes the alternative sigma factor RpoS in *Salmonella enterica*. P Natl Acad Sci USA **103:**13503-13508.

337. **Tucker, S. C., and J. E. Galan.** 2000. Complex function for SicA, a *Salmonella enterica* serovar Typhimurium type III secretion-associated chaperone. J Bacteriol **182:**2262-2268.
338. **Uchiya, K., M. A. Barbieri, K. Funato, A. H. Shah, P. D. Stahl, and E. A. Groisman.** 1999. A Salmonella virulence protein that inhibits cellular trafficking. EMBO J **18:**3924-3933.
339. **Unsworth, K. E., M. Way, M. McNiven, L. Machesky, and D. W. Holden.** 2004. Analysis of the mechanisms of *Salmonella*-induced actin assembly during invasion of host cells and intracellular replication. Cell Microbiol **6:**1041-1055.
340. **van der Velden, A. W., S. W. Lindgren, M. J. Worley, and F. Heffron.** 2000. *Salmonella* pathogenicity island 1-independent induction of apoptosis in infected macrophages by *Salmonella enterica* serotype typhimurium. Infect Immun **68:**5702-5709.
341. **Vandenbosch, J. L., D. K. Rabert, D. R. Kurlandsky, and G. W. Jones.** 1989. Sequence analysis of rsk, a portion of the 95-kilobase plasmid of *Salmonella typhimurium* associated with resistance to the bactericidal activity of serum. Infect Immun **57:**850-857.
342. **Vaudaux, P., and F. A. Waldvogel.** 1979. Gentamicin antibacterial activity in the presence of human polymorphonuclear leukocytes. Antimicrob Agents Ch **16:**743-749.
343. **Vieira, O. V., C. Bucci, R. E. Harrison, W. S. Trimble, L. Lanzetti, J. Gruenberg, A. D. Schreiber, P. D. Stahl, and S. Grinstein.** 2003. Modulation of Rab5 and Rab7 recruitment to phagosomes by phosphatidylinositol 3-kinase. Mol Cell Biol **23:**2501-2514.
344. **Wagner, C., M. Polke, R. G. Gerlach, D. Linke, Y. D. Stierhof, H. Schwarz, and M. Hensel.** 2011. Functional dissection of SiiE, a giant non-fimbrial adhesin of *Salmonella enterica*. Cell Microbiol **13:**1286-1301.
345. **Waldispuhl, J., B. Berger, P. Clote, and J. M. Steyaert.** 2006. Predicting transmembrane beta-barrels and interstrand residue interactions from sequence. Proteins **65:**61-74.
346. **Waterman, S. R., and D. W. Holden.** 2003. Functions and effectors of the *Salmonella* pathogenicity island 2 type III secretion system. Cell Microbiol **5:**501-511.
347. **Weill, F. X., F. Guesnier, V. Guibert, M. Timinouni, M. Demartin, L. Polomack, and P. A. Grimont.** 2006. Multidrug resistance in *Salmonella enterica* serotype Typhimurium from humans in France (1993 to 2003). J Clin Microbiol **44:**700-708.
348. **Weiss, M. S., A. Kreusch, E. Schiltz, U. Nestel, W. Welte, J. Weckesser, and G. E. Schulz.** 1991. The structure of porin from Rhodobacter capsulatus at 1.8 A resolution. FEBS Lett **280:**379-382.

349. **White, S. H., and W. C. Wimley.** 1999. Membrane protein folding and stability: physical principles. Annu Rev Bioph Biom **28:**319-365.
350. **Wille, T., C. Wagner, W. Mittelstadt, K. Blank, E. Sommer, G. Malengo, D. Dohler, A. Lange, V. Sourjik, M. Hensel, and R. G. Gerlach.** 2014. SiiA and SiiB are novel type I secretion system subunits controlling SPI4-mediated adhesion of *Salmonella enterica*. Cell Microbiol **16:**161-178.
351. **Wilson, I. B.** 2004. The never-ending story of peptide O-xylosyltransferase. Cell Mol Life Sci **61:**794-809.
352. **Wimley, W. C.** 2003. The versatile beta-barrel membrane protein. Curr Opin Struc Biol **13:**404-411.
353. **Wong, K. K., M. McClelland, L. C. Stillwell, E. C. Sisk, S. J. Thurston, and J. D. Saffer.** 1998. Identification and sequence analysis of a 27-kilobase chromosomal fragment containing a *Salmonella* pathogenicity island located at 92 minutes on the chromosome map of *Salmonella enterica* serovar Typhimurium LT2. Infect Immun **66:**3365-3371.
354. **Wood, M. W., M. A. Jones, P. R. Watson, S. Hedges, T. S. Wallis, and E. E. Galyov.** 1998. Identification of a pathogenicity island required for *Salmonella* enteropathogenicity. Mol Microbiol **29:**883-891.
355. **Wood, M. W., R. Rosqvist, P. B. Mullan, M. H. Edwards, and E. E. Galyov.** 1996. SopE, a secreted protein of *Salmonella dublin*, is translocated into the target eukaryotic cell via a sip-dependent mechanism and promotes bacterial entry. Mol Microbiol **22:**327-338.
356. **Wulff-Strobel, C. R., A. W. Williams, and S. C. Straley.** 2002. LcrQ and SycH function together at the Ysc type III secretion system in *Yersinia pestis* to impose a hierarchy of secretion. Mol Microbiol **43:**411-423.
357. **Yang, J., Y. Deng, H. Chu, Y. Cong, J. Zhao, D. Pohl, B. Misselwitz, M. Fried, N. Dai, and M. Fox.** 2013. Prevalence and presentation of lactose intolerance and effects on dairy product intake in healthy subjects and patients with irritable bowel syndrome. Clin Gastroenterol H **11:**262-268 e261.
358. **Yang, Y., C. Wan, H. Xu, Z. P. Aguilar, Q. Tan, F. Xu, W. Lai, Y. Xiong, and H. Wei.** 2013. Identification of an outer membrane protein of *Salmonella enterica* serovar Typhimurium as a potential vaccine candidate for Salmonellosis in mice. Microbes Infect **15:**388-398.
359. **Yrlid, U., and M. J. Wick.** 2002. Antigen presentation capacity and cytokine production by murine splenic dendritic cell subsets upon *Salmonella* encounter. J Immunol **169:**108-116.
360. **Zhou, D., L. M. Chen, L. Hernandez, S. B. Shears, and J. E. Galan.** 2001. A *Salmonella* inositol polyphosphatase acts in conjunction with other bacterial effectors to promote host cell actin

cytoskeleton rearrangements and bacterial internalization. Mol Microbiol **39:**248-259.

361. **Zhou, D., M. S. Mooseker, and J. E. Galan.** 1999. An invasion-associated *Salmonella* protein modulates the actin-bundling activity of plastin. P Natl Acad Sci USA **96:**10176-10181.
362. **Zhou, D., M. S. Mooseker, and J. E. Galan.** 1999. Role of the *S. typhimurium* actin-binding protein SipA in bacterial internalization. Science **283:**2092-2095.
363. **Zhou, D., M. S. Mooseker, and J. E. Galan.** 1999. Role of the *Salmonella typhimurium* actin-binding protein SipA in bacterial internalization. Science **283:**2092-2095.
364. **Zogaj, X., M. Nimtz, M. Rohde, W. Bokranz, and U. Romling.** 2001. The multicellular morphotypes of *Salmonella typhimurium* and *Escherichia coli* produce cellulose as the second component of the extracellular matrix. Mol Microbiol **39:**1452-1463.
365. **Zurawski, D. V., and M. A. Stein.** 2003. SseA acts as the chaperone for the SseB component of the *Salmonella* Pathogenicity Island 2 translocon. Mol Microbiol **47:**1341-1351.
366. **Zwir, I., D. Shin, A. Kato, K. Nishino, T. Latifi, F. Solomon, J. M. Hare, H. Huang, and E. A. Groisman.** 2005. Dissecting the PhoP regulatory network of *Escherichia coli* and *Salmonella enterica*. P Natl Acad Sci USA **102:**2862-2867.

Appendix I

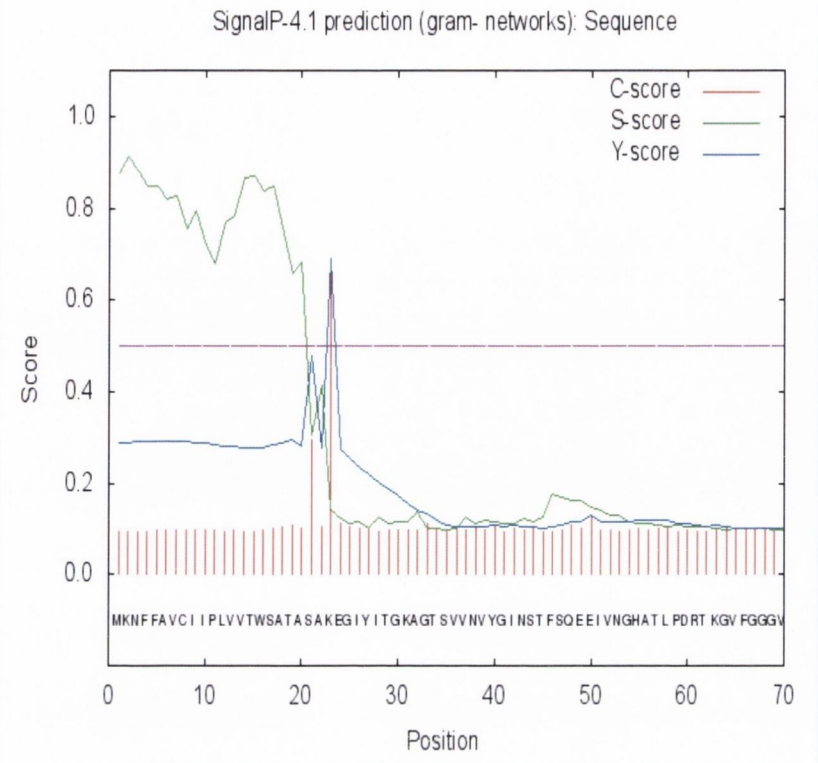


```
# Measure  Position  Value    Cutoff   signal peptide?
  max. C    23       0.672
  max. Y    23       0.689
  max. S     2       0.913
  mean S     1-22    0.762
       D     1-22    0.724   0.570    YES
Name=Sequence   SP='YES' Cleavage site between pos. 22 and 23: ASA-KE D=0.724 D-cutoff=0.570 Networks=SignalP-noTM
```

The role of the *Salmonella* PagN protein in adhesion and invasion.
Samantha Paré

Salmonella, an important genus of Gram-negative enteric bacteria, is the causative agent of many different diseases including Typhoid Fever and Gastroenteritis. *Salmonella* utilises multiple methods of invading mammalian cells, the best characterised is the Type Three Secretion System (T3SS). In addition to the T3SS, *Salmonella* express a multitude of fimbrial and non-fimbrial adhesins to facilitate attachment to and invasion of the epithelial layer lining the intestinal mucosa.

A high-throughput fluorescent assay was developed and optimised for use in determining bacterial adherence to and invasion of mammalian cells. Bacteria were rendered fluorescent using GFP expressed from plasmid pCM01. Mammalian cells and extracellular bacteria were distinguished using nucleic acid dyes and antibody labelling.

Previously, our laboratory has characterised the PagN outer membrane protein of *Salmonella* Typhimurium. PagN was discovered in *S.* Typhi in 2011 and implicated as a bacterial adhesin and potential vaccine candidate (129). The structure of the *S.* Typhi PagN ($PagN_{STY}$) was determined and its function compared with that of the *S.* Typhimurium protein ($PagN_{STM}$).

The four extracellular loops of the PagN protein have been demonstrated as necessary to mediate invasion of epithelial cells (204). These mutants were tested for their adherence to and invasion of CHO-K1 and HT-29 epithelial cells in a high-throughput manner. Deletion of any one of the extracellular loops led to a complete abolishment of association with either cell type. The loop-deletions were created at the membrane-surface interface, and this may affect the ability of the protein to mediate attachment. New, smaller loop-deletion mutants were created to further determine the role they play in mediating invasion of epithelial cells. Again, each of these loop-deletion mutants was unable to promote adherence to or invasion of the CHO-K1 and HT-29 cell lines.

As PagN shares significant sequence homology with the Hek protein, and research has indicated that specific charged residues in Loop two of Hek are involved in invasion (101), the conserved residues in PagN (R71, D75, K77, and D81) were mutated to a neutral alanine residue. High-throughput invasion assays were performed to determine the ability of the mutant forms of PagN to promote adhesion and invasion of CHO-K1 and HT-29 cells. The R71A mutant showed a statistically significant increase in both adhesion and invasion of CHO-K1 cells, and this was not seen for HT-29 cells. There was no statistically significant difference seen for any of the other mutant forms of the protein.

Deletion of the *pagN* gene in *S.* Typhimurium has been shown to affect bacterial adhesion/invasion (160, 205, 259, 357). Strains of wild-type *S.* Typhimurium and strains lacking the *pagN* gene were tested for adherence to and invasion of CHO-K1 and HT-29 cells. Bacteria grown in L-broth did not show any difference in adhesion/invasion of either cell line upon the loss of *pagN.* The *pagN* gene is under the control of the PhoP/Q two-component system. Bacteria were grown overnight in PhoP-inducing media and the high-throughput assay was repeated. Again, no differences were seen in cell association or invasion of either cell line.

Finally, PagN interacts with heparan sulphate proteoglycans expressed on the surface of mammalian cells (204). In human cells, there are two xylosyltransferases, XT-I and XT-II, present to catalyse the rate-limiting step in proteoglycan biosynthesis. XT-II is expressed in many different cell-types while XT-I is less expressed. siRNA knockdown methodology was used to decrease expression of *xylt-2* in the human HT-29 colonic cell line. A high-throughput assay was performed to investigate PagN-mediated invasion of these cells.